

AD-756 893

COMPOSITE WING FOR TRANSONIC IMPROVE-  
MENT. VOLUME III. STRUCTURAL RELI-  
ABILITY STUDIES

Sherrell D. Manning, et al

General Dynamics

Prepared for:

Air Force Flight Dynamics Laboratory

March 1972

DISTRIBUTED BY:

**NTIS**

National Technical Information Service  
U. S. DEPARTMENT OF COMMERCE  
5285 Port Royal Road, Springfield Va. 22151

✓  
AFFDL-TR-71-24

Volume III

AD 706393

# COMPOSITE WING FOR TRANSONIC IMPROVEMENT

VOLUME III - STRUCTURAL RELIABILITY STUDY

S. D. Manning  
G. H. Lemon  
M. E. Waddoups

Convair Aerospace Division of General Dynamics  
Fort Worth Operation

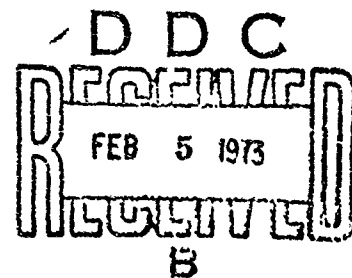
R. T. Achard  
Air Force Flight Dynamics Laboratory

TECHNICAL REPORT AFFDL-TR-71-24

November 1972

Approved for public release;  
distribution unlimited

Reproduced by  
NATIONAL TECHNICAL  
INFORMATION SERVICE  
U S Department of Commerce  
Springfield VA 22151



Air Force Flight Dynamics Laboratory  
Air Force Systems Command  
Wright-Patterson Air Force Base, Ohio

AFFDL-TR-71-24  
Volume III

COMPOSITE WING FOR TRANSONIC IMPROVEMENT

Volume III - Structural Reliability Studies

S. D. Manning  
G. H. Lemon  
M. E. Waddoups  
R. T. Achard

Approved for public release;  
distribution unlimited

## F O R E W O R D

General Dynamics, Convair Aerospace Division, has been involved in a program to provide technical support leading to a composite wing for an aircraft transonic improvement program. The data derived from this program provide an aeroelastic design of a complex stiffness-critical wing, the evaluation of advanced preliminary static and dynamic wing design/analysis procedures, and evaluation of the reliability characteristics of critical structural components utilizing composite materials.

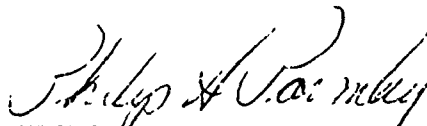
The work was performed under Air Force Contract F33615-70-C-1242, "Composite Wing for Transonic Improvement Program - Aeroelastic Analysis and Reliability Program," under the sponsorship of the Air Force Flight Dynamics Laboratory, Structures Division, Air Force Systems Command, Wright-Patterson Air Force Base, Ohio. The work was initiated by Mr. P. A. Parmley. Mr. R. T. Achard was the Air Force Project Engineer, and Mr. M. E. Waddoups was the program manager for General Dynamics.

This final report is divided into three volumes as follows:

- o Volume I - Composite Wing Aeroelastic Response Study
- o Volume II - Advanced Analysis Evaluation
- o Volume III - Structural Reliability Study

The work reported in this volume, Volume III, concerns the reliability of a bonded joint. The design, analysis, and test methods have been developed and evaluated. The significant parameters affecting the reliability of a bonded joint are presented.

This technical report has been reviewed and is approved.



---

Philip A. Parmley  
Chief, Advanced Composites Branch  
Structures Division  
Air Force Flight Dynamics Laboratory



# TABLE OF CONTENTS

<u>Section</u>		<u>Page</u>
I	INTRODUCTION	1
	1.1 Objective	1
	1.2 Scope and Methodology	1
	1.3 Importance of Joints	3
	1.4 Fatigue-Life Predictions	3
	1.5 Random Fatigue Parameters	4
	1.6 Load History Effects	5
	1.6.1 Metals	5
	1.6.2 Composites	7
	1.7 Fly-It-In-The-Lab Approach	7
	1.8 Report Organization	8
II	TEST PLAN	9
	2.1 Test Objective	9
	2.2 Test Systems	9
III	SPECIMEN DESIGN, FABRICATION AND INSPECTION	17
	3.1 Specimen Design Details	17
	3.1.1 Description	17
	3.1.2 Design Criteria	20
	3.1.3 Acceptance Tests	20
	3.1.4 Material Mechanical Properties	20
	3.2 Fabrication Technique	27
	3.3 Inspection	27
	3.3.1 Fluorescent and Ultrasonic	27
	3.3.2 Warpage	27
IV	RANDOM FATIGUE AND LOAD SPECTRUM	35
	4.1 General Description of Procedure	35
	4.2 Service History Description	36

## TABLE OF CONTENTS (Continued)

<u>Section</u>	<u>Page</u>
4.3 Load History Simulation for Random Fatigue Tests	39
4.3.1 Description of Input Data	39
4.3.2 Application of Input Data	47
4.3.3 Statistical Analysis of Load Simulation	48
4.3.4 Test Tape	53
4.4 Specimen Load Calibration	55
V TEST PROGRAM EXECUTION	57
5.1 Introduction	57
5.2 Constant Amplitude Tests	57
5.2.1 Tension-Tension	57
5.2.2 Tension-Compression	60
5.2.3 Lug Problem	60
5.3 Static Tests	62
5.4 Random Load Tests	62
5.4.1 One-Fifth Scale Specimens	65
5.4.2 One-Half Scale Specimens	68
VI EVALUATION OF TEST RESULTS	71
6.1 Fatigue Analysis for One-Fifth Scale Specimen	71
6.1.1 Procedure Used	71
6.1.2 Fatigue Life Computations Using Miner's Rule	74
6.1.3 Effectiveness of Miner's Rule	74
6.2 Evaluation of the Random Fatigue Data	77
6.3 Residual Strength Characterization	79
6.4 Residual Strength-Lifetime Distribution Based Upon Propagation of Initial Flaws	87
6.5 Random Fatigue Data Evaluation	92

## TABLE OF CONTENTS (Continued)

<u>Section</u>	<u>Page</u>
6.5.1 One-Fifth Scale Wearout Data	92
6.5.2 Scale Effects	96
6.6 Joint Failure Modes	101
6.7 Effect of Sample Size	102
6.8 Effect of Residual Strength and Fatigue Life Variability on Required Design Safety Factors	106
VII RELIABILITY ASPECTS OF BONDED JOINTS	111
7.1 Introduction	111
7.2 Strength-Time Relationship	111
7.3 Residual Strength Function	112
7.3.1 Maximum-Likelihood Estimators	113
7.3.2 Estimation of Scale Parameter When the Shape Parameter is Known	114
7.4 Safe-Life Estimates	115
7.4.1 Individual Components	115
7.4.2 Safe-Life Estimation for a Fleet	116
VIII CONCLUSIONS AND RECOMMENDATIONS	119
8.1 Introduction	119
8.2 Conclusions	119
8.3 Recommendations	121
APPENDIX I - Details of the Spectrum Simu- lation Technique	123
APPENDIX II - Warpage Problem	139
APPENDIX III - Glossary of Technical Terms	159
APPENDIX IV - Photographs of 1/5-Scale Specimen Failures	177
APPENDIX V - Photographs of 1/2-Scale Specimen Failures	203
APPENDIX VI - Statistical Properties of the Weibull Distribution	209
APPENDIX VII - Least-of-Two Statistical Analysis	213

TABLE OF CONTENTS (Continued)

<u>Section</u>	<u>Page</u>
REFERENCES	217

# LIST OF ILLUSTRATIONS

<u>Figure</u>		<u>Page</u>
1	Effect of the Loading Sequence on Fatigue Life	6
2	Closed Loop Fatigue Test Schematic	14
3	Closed Loop Test System (Test Tape, Varian 620/i Computer, Servo Amplifiers)	15
4	Closed Loop Test System (Servo Valve, Hydraulic Ram, Load Cell, Test Fixture and Test Specimen)	15
5	One-Fifth Scale Fatigue Specimen - Boron-to-Titanium Double Scarf Adhesive Bonded Joint	18
6	One-Half Scale Fatigue Specimen - Boron-to-Titanium Double Scarf Adhesive Bonded Joint	19
7	Boron-Epoxy [0 <sub>2</sub> /±45] Design Ultimate Interaction Diagram, R.T.	28
8	Fabrication-Test-Recycling Procedure	29
9	Uncured 1/2 Scale Specimen In Tool With Bleeder Cloth Between Specimen and Tool	30
10	One-Half Scale Specimen Ready for Curing	30
11	One-Fifth Scale Dial Gauge Surface Measurement Locations	32
12	Mission Profile	38
13	Exceedance Curve Mission Segment 1 (Climb-Cruise)	40
14	Exceedance Curve Mission Segment 2 (TFR)	41
15	Exceedance Curve Mission Segment 3 (Air-to-Ground)	42
16	Exceedance Curve Mission Segment 4 (TFR)	43

# LIST OF ILLUSTRATIONS (Continued)

<u>Figure</u>		<u>Page</u>
17	Exceedance Curve Mission Segment 5 (Air-to-Air)	44
18	Exceedance Curve Mission Segment 6 (Cruise-T&G)	45
19	Comparison of Load Simulation Composite Cumulative Exceedances Versus Actual Exceedances	50
20	Random Load Statistics	50
21	Composite Exceedance Correlation and Sample Random Load/Time Signal From Test Tape	54
22	Setup for Constant Amplitude Tension- Tension Strain Survey	58
23	Tension-Compression Constant Amplitude Setup With Center Support Shown Removed	58
24	Broken Lug for Specimen K994567	61
25	Broken Lug for Specimen K012482	61
26	Setup for Static Strain Survey	63
27	Typical 1/5-Scale Specimen Static Test Failures	63
28	Setup for 1/2 Scale Specimen Tests	68
29	Composite Cumulative Exceedances Versus $\Delta B.M.$	72
30	Load Versus Cycles to Failure	72
31	Equivalent Random Load Cycle	76
32	Stress Ratio (R) Variation for Random Load Test Tape	76

## LIST OF ILLUSTRATIONS (Continued)

<u>Figure</u>		<u>Page</u>
33	Probability of Failure Versus Residual Strength Plot on Weibull Paper for 1/5 Scale Static and 10% Lifetime	84
34	Probability of Failure Versus Residual Strength and/or Lifetime Plot on Weibull Paper for 1/5 Scale 50% Lifetime and Fatigue to Failure	84
35	Probability of Failure Versus Residual Strength and/or Lifetime Plot on Weibull Paper for 1/2 Scale 10% Lifetime and Fatigue to Failure	84
36	Residual Strength Distributions	94
37	Factors $f_{90}$ for a 90% - Confidence Lower Bound for the Weibull Shape Parameter	94
38	Factors $f_{90}$ for a 90% - Confidence Lower Bound for the Weibull Scale Parameter	103
39	Factors $f_{90}$ for a 90% - Confidence Lower Bound for the Weibull Scale Parameter - Shape Parameter Known	103
40	Coefficient of Variation for Weibull Distribution	109
41	Service Fatigue Life Distribution	117
42	Fleet Reliability as a Function of Individual Component Reliability	117
43	Fleet Reliability and Safe Life	118
44	Exceedance Curve Analysis Notation	124
45	Summation of RMS Levels for Characterizing Exceedance Curve	124

## LIST OF ILLUSTRATIONS (Continued)

<u>Figure</u>		<u>Page</u>
46	Random Force/Time History	128
47	Cumulative Distribution Curve Based on $\omega(Z)$	128
48	Clipped Rice-Bendat-Kowalewski Function	132
49	Normalized Cumulative Distribution Curve for Random Mapping	132
50	Symbolic Representation of Mapping Procedure	133
51	Load Generation Characterization	133
52	Positive and Negative Load Excursions	136
53	RMS Burst Description	136
54	Forced Returns to the Mean	136
55	Strain Gage Locations for 1/5 Scale Specimens	141
56	Setup for Tension and Compression Strain Surveys With Center Support	141
57	Tension Strain Survey: Without Center Support	142
58	Load Versus Strain, Strain Survey Using 1/5 Scale Static Test Specimen K012439	150
59	Load Versus Strain, Strain Survey Using 1/5 Scale Static Test Specimen K012441	150
60	Load Versus Strain, Strain Survey Using 1/5 Scale Static Test Specimen K994588	150
61	Superposition of Stresses for Evaluating Bending Effect	152
62	Group of One-Fifth Scale Static and Constant Amplitude Fatigue Specimens	178



# LIST OF ILLUSTRATIONS (Continued)

<u>Figure</u>		<u>Page</u>
63	One-Fifth Scale Static Specimen K012441	178
64	One-Fifth Scale Constant Amplitude Fatigue Specimen K994566	179
65	Full Size: One-Fifth Scale Static (K012441) and Constant Amplitude Fatigue (K994566) Specimens	179
66	Ten Times Size: One-Fifth Scale Static (K012441) and Constant Amplitude Fatigue (K994566) Specimens	180
67	Twenty Five Times Size: One-Fifth Scale Static (K012441) and Constant Amplitude Fatigue (K994566) Specimens	180
68	Constant Amplitude (Tension-Tension) Fatigue Test: One-Fifth Scale Specimen K012476	181
69	Constant Amplitude (Tension-Tension) Fatigue Test: One-Fifth Scale Specimen K012477	181
70	Constant Amplitude (Tension-Tension) Fatigue Test: One-Fifth Scale Specimen K012478	182
71	Constant Amplitude (Tension-Tension) Fatigue Test: One-Fifth Scale Specimen K012483	182
72	Constant Amplitude (Tension-Tension) Fatigue Test: One-Fifth Scale Specimen K900445	183
73	Constant Amplitude (Tension-Tension) Fatigue Test: One-Fifth Scale Specimen K994587	183
74	Constant Amplitude (Tension-Compression) Fatigue Test: One-Fifth Scale Specimen K012438	184
75	Constant Amplitude (Tension-Compression) Fatigue Test: One-Fifth Scale Specimen K012442	184
76	Constant Amplitude (Tension-Compression) Fatigue Test: One-Fifth Scale Specimen K012462	185

# LIST OF ILLUSTRATIONS (Continued)

<u>Figure</u>		<u>Page</u>
77	Constant Amplitude (Tension-Compression) Fatigue Test: One-Fifth Scale Specimen K012475	185
78	Constant Amplitude (Tension-Compression) Fatigue Test: One-Fifth Scale Specimen K900442	186
79	Constant Amplitude (Tension-Compression) Fatigue Test: One-Fifth Scale Specimen K994568	186
80	Random Loading (1% Lifetime) Test: One- Fifth Scale Specimen K900441	187
81	Random Loading (1% Lifetime) Test: One- Fifth Scale Specimen K900448	187
82	Random Loading (1% Lifetime) Test: One- Fifth Scale Specimen K904955	188
83	Random Loading (1% Lifetime) Test: One- Fifth Scale Specimen K904958	188
84	Random Loading (1% Lifetime) Test: One- Fifth Scale Specimen K905016	189
85	Random Loading (10% Lifetime) Test: One- Fifth Scale Specimen K900447	189
86	Random Loading (10% Lifetime) Test: One- Fifth Scale Specimen K904950	190
87	Random Loading (10% Lifetime) Test: One- Fifth Scale Specimen K904957	190
88	Random Loading (10% Lifetime) Test: One- Fifth Scale Specimen K904959	191
89	Random Loading (10% Lifetime) Test: One- Fifth Scale Specimen K905017	191

# LIST OF ILLUSTRATIONS (Continued)

<u>Figure</u>		<u>Page</u>
90	Random Loading (50% Lifetime) Test: One-Fifth Scale Specimen K900449	192
91	Random Loading (50% Lifetime) Test: One-Fifth Scale Specimen K900450	192
92	Random Loading (50% Lifetime) Test: One-Fifth Scale Specimen K904951	193
93	Random Loading (50% Lifetime) Test: One-Fifth Scale Specimen K904952	193
94	Random Loading (50% Lifetime) Test: One-Fifth Scale Specimen K904953	194
95	Random Loading (50% Lifetime) Test: One-Fifth Scale Specimen K904954	194
96	Random Loading (50% Lifetime) Test: One-Fifth Scale Specimen K904956	195
97	Random Loading (50% Lifetime) Test: One-Fifth Scale Specimen K905015	195
98	Random Loading (50% Lifetime) Test: One-Fifth Scale Specimen K905018	196
99	Random Loading (50% Lifetime) Test: One-Fifth Scale Specimen K905022	196
100	Random Loading (50% Lifetime) Test: One-Fifth Scale Specimen K905023	197
101	Fatigue-to-Failure Tests: One-Fifth Scale Specimen K012443	197
102	Fatigue-to-Failure Tests: One-Fifth Scale Specimen K012464	198
103	Fatigue-to-Failure Tests: One-Fifth Scale Specimen K012479	198

## LIST OF ILLUSTRATIONS (Continued)

<u>Figure</u>		<u>Page</u>
104	Fatigue-to-Failure Tests: One-Fifth Scale Specimen K012480	199
105	Fatigue-to-Failure Tests: One-Fifth Scale Specimen K012481	199
106	Fatigue-to-Failure Tests: One-Fifth Scale Specimen K012484	200
107	Fatigue-to-Failure Tests: One-Fifth Scale Specimen K012485	200
108	Fatigue-to-Failure Tests: One-Fifth Scale Specimen K900443	201
109	Random Loading (10% Lifetime) Test: Group of One-Half Scale Specimens (Front Side)	204
110	Random Loading (10% Lifetime) Test: Group of One-Half Scale Specimens (Back Side)	204
111	Fatigue-to-Failure Test: One-Half Scale Specimen F504619 (Front Side)	205
112	Fatigue-to-Failure Test: One-Half Scale Specimen F504619 (Back Side)	205
113	Fatigue-to-Failure Test: One-Half Scale Specimen F504621 (Front Side)	206
114	Fatigue-to-Failure Test: One-Half Scale Specimen F504621 (Back Side)	206
115	Fatigue-to-Failure Test: One-Half Scale Specimen F504622 (Front Side)	207
116	Fatigue-to-Failure Test: One-Half Scale Specimen F504622 (Back Side)	207
117	Fatigue-to-Failure Test: One-Half Scale Specimen F504623 (Front Side)	208

LIST OF ILLUSTRATIONS (Continued)

<u>Figure</u>		<u>Page</u>
118	Fatigue-to-Failure Test: One-Half Scale Specimen F504623 (Back Side)	208
119	Weibull Density Function - Scale Parameter Fixed Equal to One	210
120	Weibull Density Function - Shape Parameter Fixed Equal to One	211
121	Weibull Failure Rate Function	211

# LIST OF TABLES

<u>Table</u>		<u>Page</u>
I	Experimental Test Program	10
II	Summary of 1/5-Scale Specimens and Test Assignments	11
III	Summary of 1/2-Scale Specimens and Test Assignments	13
IV	Specimen Design Data	21
V	Summary of Acceptance Test Results for Boron Composite Fibers	22
VI	Summary of Statistical Properties Based on Acceptance Test Results for Boron Composite Fibers	24
VII	Physical Properties - Boron-Epoxy	25
VIII	Design Allowables - Boron-Epoxy, Room Temperature, "B" Basis	26
IX	Summary of Dial Gage Surface Measurements for Initial Group of 1/5-Scale Specimen	33
X	Summary of Mission Profile Data	37
XI	Summary of Input Exceedance Data for Random Load History Simulation	46
XII	Data for Actual Composite Exceedance Curve	49
XIII	Summary of Composite Cumulative Exceedances Based on Statistical Analysis of Simulated Random Load Test Tape	51
XIV	Summary of 1/5-Scale Specimen Constant Amplitude Loading Test Results	59
XV	Summary of 1/5-Scale Specimen Static Test Results	64

# LIST OF TABLES (Continued)

<u>Table</u>		<u>Page</u>
XVI	Summary of 1/5-Scale Specimen Residual Strength Tests After Random Loading	66
XVII	Summary of 1/5-Scale Specimen Loading Fatigue-to-Failure Test Results	67
XVIII	Summary of 1/2-Scale Specimen Residual Strength Tests After Random Loading (10% Lifetime)	69
XIX	Summary of 1/2-Scale Specimen Random Loading Fatigue-to-Failure Test Results	70
XX	Fatigue Analysis for 1/5-Scale Fatigue-to-Failure Specimen Based on Miner's Rule	75
XXI	Ranking of Pooled Static and 1% Lifetime Data for 1/5-Scale Specimens	78
XXII	Ranking of 10% Lifetime Data for 1/5-Scale Specimens	80
XXIII	Ranking of 50% Lifetime Data for 1/5-Scale Specimens	81
XXIV	Ranking of Fatigue-to-Failure Data for 1/5-Scale Specimens	82
XXV	Ranking of 10% Lifetime Data for 1/2-Scale Specimens	83
XXVI	Ranking of Fatigue-to-Failure Data for 1/2-Scale Specimens	83
XXVII	Summary of Weibull Parameters Fitted to 1/5- and 1/2-Scale Test Results	85
XXVIII	Wearout Model Parameters	93
XXIX	Estimated Joint Fatigue Performance	96
XXX	Summary of Scaling Factors Based on 1/5- and 1/2-Scale Specimens	99

# LIST OF TABLES (Continued)

<u>Table</u>		<u>Page</u>
XXXI	Summary of Mean Values for Various Sample Sizes (1/5-Scale Specimen Tests)	105
XXXII	Summary of Mean Values for Various Sample Sizes (1/2-Scale Specimen Tests)	107
XXXIII	Summary of 90% Confidence Lower Bound Factors ( $f_{90}$ ) for the Weibull Scale Parameter (Sample Parameter Shown) with Respect to Sample Size	108
XXXIV	Summary of Strain Surveys Conducted	139
XXXV	Tension Strain Survey Using 1/5-Scale Specimen Without Center Support	143
XXXVI	Tension Strain Survey: With Center Support; With Center Support and C-Clamps	144
XXXVII	Compression Strain Survey: With Center Support; With Center Support and C-Clamps	146
XXXVIII	Compression Strain Survey With Center Support (With and Without Jam Bar)	147
XXXIX	Strain Survey Using Static Test Specimens (1/5-Scale)	148
XL	Strain Survey After Constant Amplitude Cycling (5K to 50K)	149
XLI	Stress Increase Factors for Induced Bending Moment Based on Tension Strain Survey	153
XLII	Stress Increase Factors for Induced Bending Moment Based on Static Strain Surveys	154
XLIII	$F_{mij}$ Ranges for Tension and Static Strain Survey Specimen	155
XLIV	Comparison of Strain Survey Specimens Surface Dimensions With Average Specimen Dimensions	156



## L I S T   O F   S Y M B O L S

A/A	= air-to-air segment
a,b	= constants for fitting $\theta(t)$ to strength versus lifetime data
$\hat{a}, \hat{b}$	= maximum-likelihood estimators for the shape and scale parameters respectively
A/E/D	= F-111 models
A/G	= air-to-air cycle
B.M.	= bending moment
$\hat{B}_y$	= maximum likelihood estimate of a scale parameter
C	= flaw size
clip	= clipping ratio
Cp	= factor converting test results to a per-ply basis
C(t)	= crack length as a function of time
dC(t)	= crack length differential
$\frac{dC(t)}{dt}$	= crack length time derivative
D.L.	= design limit
E(t)	= mean for Weibull distribution in terms of a and b
$EXN_{Li}, EXN_{Ri}$	= ordinates to exceedance curve at designated points left and right respectively
FE(t)	= experimental failure load

# LIST OF SYMBOLS (Continued)

$FM_{ij}$	= stress increase factor = $\frac{2 \epsilon_{\max}}{\epsilon_i + \epsilon_j}$
F specimen	= specimen code prefix
$F_R$	= residual strength
$\hat{F}_R(0)$	= characteristic initial residual strength
$F_R(t)$	= residual strength
$F(t)$	= forcing function
$F_{TRU}$	= upper truncation load
$F(s)$	= residual strength cumulative distribution
$F(t)$	= lifetime cumulative distribution, test spectrum
$F(x)$	= cumulative exceedances/mission
$F(X_i), F(X_{iA}),$ $F(X_{i+1}), F(X_{i+1A})$	= ordinates to cumulative exceedance curve used in Press's method
$F(X_T)$	= sum of ordinates to individual RMS level representing lines on the cumulative exceedance versus $(\Delta.B.M.)^2$ plot
$f(s)$	= residual strength density function
$f(x)$	= probability density function
$f_{90}$	= factor for 90% confidence
GAG	= ground-to-air-to-ground cycle
$G(x t)$	= cumulative distribution of environmental loads at time, t

# LIST OF SYMBOLS (Continued)

Hz	= frequency (Hertz)
K specimen	= specimen code prefix
K	= (kips) load
L	= bond overlap length or load
L( )	= combined failure probability
m	= slope of a line representing an RMS level
$N, N_i$	= load cycles
$N_E$	= equivalent number of random load cycles
$N_o$	= number of positive slope crossings of the mean per unit time
$N_o/N_p$	= irregularity factor; number of positive slope crossings of the mean per number of peaks
$N_p$	= number of peaks per unit time
n	= number of specimen ranked
$n_i$	= number of cycles/lifetime
$P_{DL}$	= design limit load
$P_i$	= portion of time spent in a given RMS level
$P_j$	= total load at j cycle
$P_{max}, P_{min}$	= positive and negative load peaks respectively
$P_{mean_j}$	= mean load value

# LIST OF SYMBOLS (Continued)

PSD	= power spectral density
$P_{TRL}$	= lower truncation load
$P_{TRU}$	= upper truncation load
$P(\sigma)$ or $P_s$	= probability of failure and/or survival
$P(Z)$	= cumulative distribution function (reference Appendix I).
R	= stress ratio ( $\sigma_{min}/\sigma_{max}$ per cycle)
RMS	= root mean square (RMS) value
$R(t)$ and $R(x)$	= failure rate and reliability function
r	= crack growth rate parameter
$r_a$	= rank of data
$S_F$	= scaling factor
T	= energy required to drive a flaw
TFR	= terrain following radar
T&G	= touch-and-go landings
TIP	= Transonic Improvement Program
TLL	= truncation load level
$T(t)$	= energy available to drive a flaw at time (t)
t	= bond overlap thickness or lifetime
$\hat{t}$ and $\hat{t}_b$	= characteristic life (general and baseline)
$t_h$	= reference thickness
$t_o$	= initial reference time

# LIST OF SYMBOLS (Continued)

$t_1, t_2 \dots t_R$	= specific times for which the probability of survival (reliability) is to be computed.
$W$	= width of cross section, or work
$W(t)$	= work expended as a function of time
$\bar{W}(t)$	= steady component of work expended as a function of time
$w(Z)$	= Rice-Bendat-Kowalewski probability density function
$X_i$	= random sample $i$ ( $i = 1, 2, \dots, n$ )
$X_{i_r}, X_{i_l}$	= abscissa values at points $r$ and $l$ respectively (reference Appendix I).
$\bar{X}, \mu$	= mean value
$YY_{Bi}, YY_{Bj}$	= ordinates to normalized cumulative distribution curve at points $B_i$ and $B_j$ respectively
$YY_{BN}$	= distribution function coordinate
$Z^+, Z^-$	= positive and negative clip value respectively
$ZZ_{Bi}, ZZ_{Bj}$	= abscissa to normalized cumulative distribution curve at points $B_i$ and $B_j$ respectively.
$ZZ_{BN}$	= distribution function coordinate
$ZZ_{LN}$	= distribution function coordinate
$\alpha, \beta$ or $a, b$	= shape and scale parameters respectively for Weibull distribution
$\alpha_f$	= fatigue shape parameter

# LIST OF SYMBOLS (Continued)

$\alpha_0$	= initial static shape parameter
$\epsilon_i, \epsilon_j$	= measured strains at points i and j respectively
$\epsilon_1, \epsilon_2, \epsilon_3, \epsilon_4$	= measured strains from strain survey
$\epsilon_{\max}$	= maximum strain
$\lambda$	= shape parameter constant for time, t
$\lambda(t), \theta(t)$	= shape and scale parameters respectively dependent on time
$\mu$	= mean
$\nu$	= coefficient of variation
$\phi(\omega)$	= power spectral density (PSD)
$\Gamma$	= standard gamma function
$\sigma$	= RMS, residual strength, or lifetime
$\sigma_a$	= axial stress (psi) = $\frac{\sigma_i + \sigma_j}{2}$
$\sigma_b$	= bending stress (psi) = $\frac{\sigma_i - \sigma_j}{2}$
$\sigma_i, \sigma_j$	= net stress at point i and j respectively (psi)
$\sigma_{\max}, \sigma_{\min}$	= maximum and minimum stress respectively in a fatigue cycle (psi)
$\sigma_x$	= stress in the x direction
$\sigma_y$	= stress in the y direction
$\sigma_0$	= $0^\circ$ flexural stress (psi)

# LIST OF SYMBOLS (Continued)

$\sigma_{90}$	= 90° flexural stress (psi)
$\tau$	= horizontal shear stress (psi)
$\tau_{xy}$	= shear stress
$\omega$	= omega (radians/sec)
$\psi(\tau)$	= autocorrelation function
$\Delta B.M.$	= delta bending moment measured from the mean
$\Delta P_j$	= delta load measured from the mean
$\Delta t$	= time interval between successive loads

# SECTION I

## INTRODUCTION

### 1.1 OBJECTIVE

The objectives of this program were (1) to develop a reliability-based technology for the design of large-scale bonded joints and (2) to develop a data base, using boron-epoxy-to-titanium double-scarf bonded joint specimens to explore the character of the failure process and to determine the joint characteristics which effect structural reliability.

### 1.2 SCOPE AND METHODOLOGY

Experimental programs in composite airframe reliability have followed a metals technology-based characterization strategy. This has included the constant amplitude fatigue (S-N) characterization of laboratory-sized coupons, spot checks of the effects of specific environments, and a limited check of the effect of classical joint design parameters such as  $l/t$  and adhesive type upon joint S-N lifetime. This approach is useful in screening operations, but it is not satisfactory for the design and optimization of fatigue-critical structures. Therefore, this program was conceived to investigate the following critical issues:

1. The load-history sensitivity of large-scale bonded joints to assess the mean time to first failure
2. The implication of residual strength and fatigue lifetime variability on the determination of design safety factors
3. The character of the damage process and determination of the bounds on joint reproducibility that would be achievable in production practice
4. The determination of scale effects in joint design and the impact of scale dependence on the design data reduction scheme
5. The evaluation of the random load history characterization technique as a design data acquisition tool.



A central issue was the investigation of an alternate scheme for the service life design characterization of structural elements. The problem of load-history effects on the lifetime characteristics of a structure was studied.

An experimental program was conducted using 1/5- and 1/2-scale specimens (both 5 inches wide) in five types of tests: (1) strain survey, (2) static, (3) constant amplitude (tension-tension and tension-compression), (4) residual strength, and (5) lifetime (fatigue loaded to failure). The first three types of tests were performed using only 1/5-scale specimens. A strain survey was conducted using 1/5-scale specimens to evaluate the effects of specimen dimensional variations. The extent of these effects and their impact on the test program were evaluated.

Constant amplitude lifetime tests were conducted using 1/5-scale specimens. For these tests, the specimens were subjected to a prescribed constant amplitude cyclic loading until the specimen failed. The purpose of these tests was to provide a basis for evaluating the effectiveness of Miner's linear cumulative damage rule for predicting the fatigue life of bonded joints.

Residual strength tests were performed using 1/5- and 1/2-scale specimens that had been subjected to a prescribed random load history. A cycle-by-cycle random load-history simulation for one lifetime (1334 missions) was generated using exceedance data projected for the transonic wing.

This load-history data was stored on a magnetic tape. A computerized testing system read the magnetic tape and transformed the tape input into a closed loop controlled random load on the specimen. Data were obtained from these tests for characterizing the lifetime strength of composite-to-metal bonded joints, of the type studied, subjected to a random load history.

A computer program was developed for generating a random load-history simulation on a cycle-by-cycle basis; this simulation preserves the cumulative exceedance statistics for a given fatigue spectrum. This program was based on the techniques implemented by Dr. J. C. Halpin of the Air Force Materials Laboratory (Reference 1).

A reliability-based program involves the determination of variability and mean lifetime response of the specimens. Efforts to understand the impact of fatigue variability upon structural design have gained appreciable momentum (References 2, 3, 4, and 5) during recent years. A review of the cited efforts provided the initial impetus to this program. A primary objective in the program

was to provide an engineering understanding of the source of scatter in fatigue lifetime data. Since the generation of fatigue failures appears to be a random process, the method of attack for this program was a generation of statistical data and analysis of the results.

A reliability concepts approach was used. If it can be shown that the reliability approach is feasible for characterizing the strength of this joint type, it may be possible to develop a sound methodology for composite bonded joints in general. The experimental and analytical procedure used to achieve the stated objective are documented in this report.

### 1.3 IMPORTANCE OF JOINTS

The service life of an aircraft is intimately dependent on the reliability of its joints. Experience indicates that structural fatigue failures frequently start at joints. A joint failure in primary aircraft structure must be avoided because of the possible catastrophic results. Joints traditionally store large amounts of energy per volume of material compared to the structure being joined and exhibit brittle fracture characteristics. If the energy stored in a joint is suddenly released, due to failure of the joint, the surrounding structure will also fail unless it is able to dissipate this energy. Therefore, reliable joints are needed to maintain the structural integrity of the aircraft.

### 1.4 FATIGUE-LIFE PREDICTIONS

Fatigue is a random phenomenon that is not fully understood; nevertheless, aircraft designers must address this problem to develop a satisfactory structural design. The designer must perform the necessary analysis, tests, and evaluations to design the structure for stiffness and for static and fatigue strength. In addition, the designer must periodically evaluate the structural integrity of the aircraft for continued usage. This task is of utmost importance for the safe operation of the aircraft; therefore, the fatigue life evaluation must be as realistic as possible.

Safety and economics are both important factors. From a practical standpoint, the fatigue-life assessment should be conservative for safety reasons but not too conservative for economic reasons. If the fatigue-life prediction is too unconservative, the maintenance cost, for a given period of aircraft usage, may be prohibitive.

It is imperative that the fatigue methodology used results in realistic service-life predictions. This requires that the simulated environment characterize actual service histories as closely as possible. Random load fatigue testing using a closed loop test system and a simulated environment characterize actual service histories as closely as possible. Random load fatigue testing using a closed loop test system and a simulated environment should more realistically characterize the fatigue process than constant amplitude loading methods. Thus, the primary emphasis in this test program was to evaluate the lifetime and residual strength characteristics of the bonded joints under simulated service loads and to study the feasibility of using random load testing in the fatigue-life characterization of bonded joints. Material characterization parameters that correlate both mean and variance for static strength and lifetime were determined.

The random load simulation procedure used for this program is described in Appendix I.

### 1.5 RANDOM FATIGUE PARAMETERS

Structural fatigue under realistic random loading is characterized by parameters that vary during the service lifetime. The principal parameters that vary with time include:

1. Material properties
2. Operating loads
3. Operating environments
4. Structural strength.

In addition, initial factors relating to structural reliability exist, such as manufacturing deviations. The realistic characterization of the fatigue process in composites should include at least the random variables above.

## 1.6 LOAD-HISTORY EFFECTS

### 1.6.1 Metals

The load-sequence effects on the fatigue life of metal structures have been investigated by several researchers (References 6 through 12). The load history simulation for a given service load spectrum is important for realistically characterizing the fatigue process. The order and magnitude of the fatigue loading have a significant effect on the fatigue life, the flaw growth, and the residual strength of the structure. The sequence effect of various block loadings (simulating the same load spectrum) on the fatigue life of 2024 and 7075 aluminum is shown in Figure 1 (Page 47 of Reference 13). The low-high sequence produced greater fatigue damage than any of the other loading sequences. The random block sequence was the next most damaging load sequence.

Swanson (Reference 14) observed that cracks are more likely to occur under a randomized loading than a deterministic loading; he also observed that the cracks found in service are more likely to propagate in a random load test than in a block loading test. The literature also suggests that the fatigue damage will be less representative of actual service failures when there is a greater departure from the true randomness in loading.

The rate of crack propagation in 2024-T3 aluminum is dependent upon the loading sequence used (Reference 15). Crack growth is slower for a high-low sequence than for a low-high sequence. This difference in crack growth is attributed to the retardation phenomenon occurring in the crack tip areas. That is, a plastic zone is formed by high tensile stresses in the crack tip region. When the tensile stress is removed or reduced, a residual compressive stress field is left in the plastic zone. This residual stress field preloads the crack and tends to retard the rate of crack growth. Compressive stresses may be produced at the crack tip by gust and landing conditions. Such stresses tend to wipe out or reduce the crack preload which in turn accelerates the rate of crack propagation. The progressive creation and dissipation of the plastic zone continues as the crack propagates.

The retardation phenomenon has been investigated for D6ac steel and this investigation is discussed in References 16 and 17.

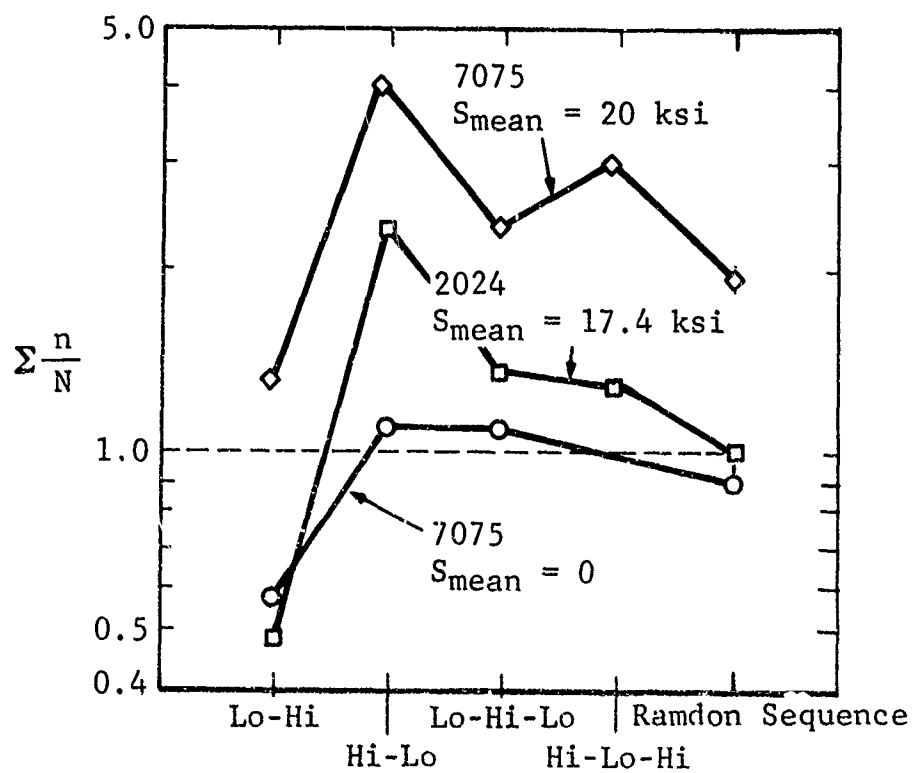
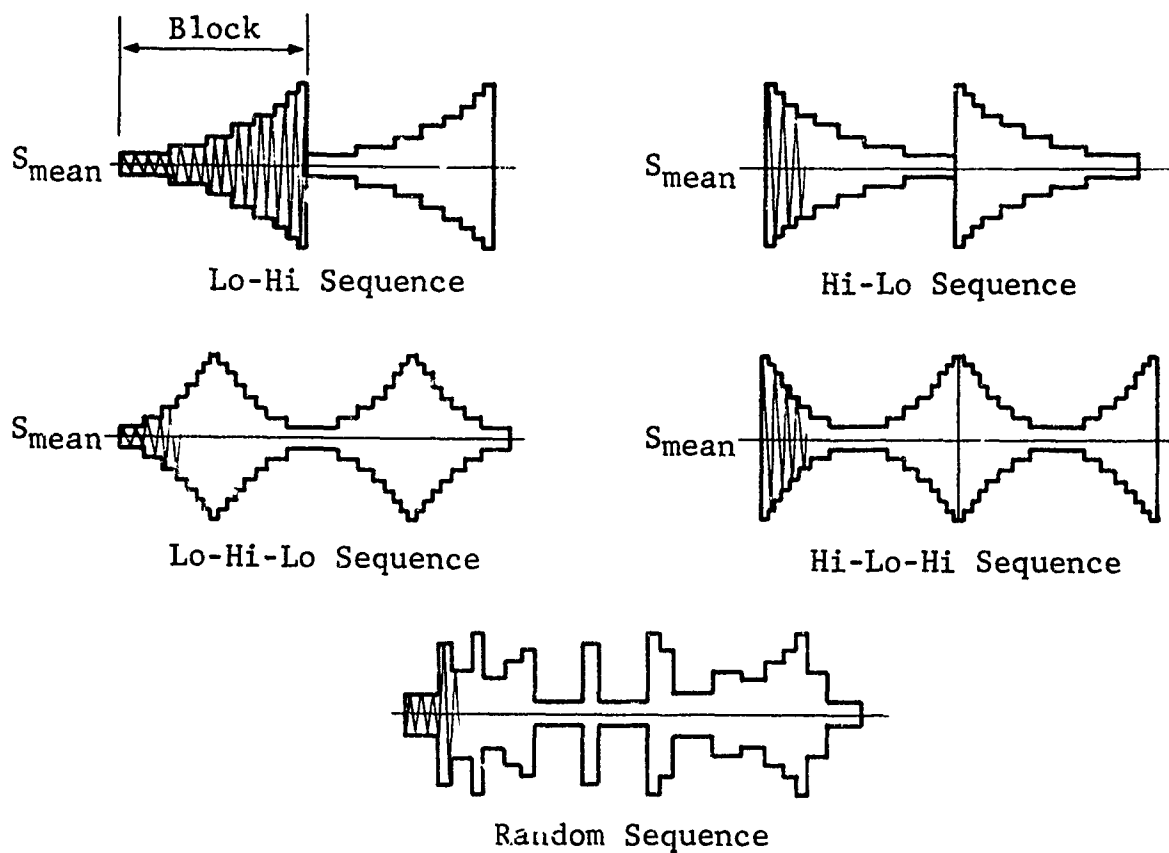


Figure 1 Effect of the Loading Sequence on Fatigue Life

### 1.6.2 Composites

The order and magnitude of the fatigue loading can significantly affect the resulting fatigue life for metals (References 6 through 12). A vigorous development program was required to determine the significance of the load sequence for metals.

The trend in fatigue testing is to use a random loading that simulates the service history. This allows the load sequence effect to be accounted for in the laboratory.

Fatigue data exists for composites (References 18 through 25), but this data is inadequate to evaluate the significance of the load sequence on the fatigue life of composites in the same way as metal. There is no need to investigate the load sequence effect for composites if random load fatigue testing is used because the effect will be reflected in the test results.

### 1.7 FLY-IT-IN-THE-LAB APPROACH

The desire for realism in fatigue testing can be accomplished by the "fly-it-in-the-lab approach." This approach concerns the random simulation of the service load-environment and the application of this simulation to a test specimen, component, or assembly using a computerized closed loop test system.

A random load-history simulation procedure (Reference 26) has been developed to preserve the composite cumulative load exceedances and the waveform defined by  $N_0/N_p$ . The environment simulation has not been developed into an integrated random load test system; however, such a simulation appears technically feasible.

If a random load history and compatible environment can be simulated and adapted to a closed loop test system, this methodology will permit a practical characterization of the fatigue process in the laboratory. The load-environment simulation can be generated by mission or by service life. The degree of realism depends upon the accurate definition of the expected load-environment history and the resulting simulation of this history.

## 1.8 REPORT ORGANIZATION

This report is organized into eight major sections, seven appendices, and a list of references. The test plan and objectives are defined in Section II.

The specimen design, fabrication, and inspection details are discussed in Section III.

Random fatigue testing is discussed in Section IV. This includes the documentation of the random load-history simulation procedure used to generate the test tape employed in the experimental program. The test tape statistics, load calibration, and truncation load levels are also discussed.

The execution of the test program and the test results generated are discussed in Section V. The test results of Section V are evaluated in Section VI. This section concerns the effectiveness of Miner's rule, the statistical evaluation of the test results, scaling factors, sample size, failure modes, effect of residual strength, and fatigue life variability on required design safety factors, etc.

The reliability aspects of bonded joints are discussed in Section VII, and the principles described are used to analyze the test results of Section V. Wearout models, residual strength, Weibull distribution, sample size, etc. are discussed.

The conclusions and recommendations of this investigation are given in Section VIII.

Section VIII is followed by seven appendices and a list of references. The appendices contain the details of the spectrum simulation technique used, the specimen warpage problem, a glossary of technical terms, photographs of failed specimens, statistical properties of the Weibull distribution, and a discussion of a "least-of-two" statistical analysis.

## SECTION II

### TEST PLAN

#### 2.1 TEST OBJECTIVE

The objective of the experimental program was to generate statistical data characterizing the residual strength/lifetime characteristics of boron laminate-to-titanium double-scarf adhesive bonded joints using simulated flight-by-flight loading.

The experimental program is summarized in Table I. Two sizes of bonded specimens were used. These were 1/5- and 1/2- scale boron laminate-to-titanium double-scarf adhesive bonded joints. Specimen identifications and test assignments are summarized in Tables II and III for 1/5- and 1/2-scale specimens, respectively. The F and K prefixes on the specimen numbers in Tables II and III refer to manufacturing period. The K specimens were manufactured before May 1971 and the F specimens were manufactured after October 1971.

#### 2.2 TEST SYSTEMS

A closed loop test system, shown in Figure 2, was used for random load tests. A Baldwin-Tate-Emery Universal test machine was used for static and residual strength tests (Figure 3). Photographs of the system are shown in Figures 3 and 4 and a description of the apparatus used is given in the following paragraphs. The essential elements of this system are:

1. Magnetic tape
2. Varian 620/i computer
3. Servo amplifier
4. Servo valve
5. Hydraulic ram
6. Load cell
7. Test fixture (3 for 1/5-scale specimens and 1 for 1/2-scale specimens)



Table I EXPERIMENTAL TEST PROGRAM

Specimen Size	Type Test	Purpose of Test	Load Max.	Levels (KIPS) Min.	No. Spec.
1/5 Scale	Strain Survey	To evaluate effects of specimen dimensional variations on the test results	--	--	(5)*
	Static	To generate data for statistically characterizing the static strength of composite joints	Failure	--	11
	<u>Constant Amplitude</u> (a) Tension o o o (b) Tension-Compression o o o	To generate a load versus cycles to failure curve which can be used to perform a fatigue analysis using Miner's rule	30 40 50  30 40 50	3 4 5  -6 -8 -10	4 1 7  1 1 5
	<u>Random</u> (a) 1% Lifetime (b) 10% Lifetime (c) 50% Lifetime (d) Fatigue-to-Failure	To provide lifetime data for evaluating the effectiveness of Miner's rule for predicting the fatigue life of composite joints.  To generate a data base for characterizing the strength of composite joints as a function of lifetime.	54.5 ↓	54.5 ↓	5 6 20 20
1/2 Scale	<u>Random</u> (a) 10% Lifetime (b) Fatigue-to-Failure		128.5 ↓	12.85 ↓	5 5

Notes: \*These specimen also used for static and constant amplitude tests.

Total number of specimens for test program - 81 (1/5 scale) 10 (1/2 scale)  
All tests were conducted in a normal laboratory environment.

Table II SUMMARY OF 1/5-SCALE SPECIMENS  
AND TEST ASSIGNMENTS

Specimen I.D.	Test Assignment
F504417	FTF
F504418	FTF
F504419	FTF
F504421	FTF
F504622	FTF
K012437*	S
K012438	CA(T-C)
K012439 <sup>Δ</sup>	S
K012440*	S
K012441 <sup>Δ</sup>	S
K012442	CA(T-C)
K012443	FTF
K012444	CA(T-T)
K012445	CA(T-C)
K012446*	S
K012459*	S
K012461	CA(T-T)
K012462	CA(T-C)
K012463*	S
K012464	FTF
K012465	CA(T-T)
K012474*	S
K012475	CA(T-C)
K012476	CA(T-T)
K012477	CA(T-T)
K012478	CA(T-T)
K012479	FTF
K012480	FTF
K012481	FTF
K012482	CA(T-T)
K012483	CA(T-T)
K012484	FTF
K012485	FTF
K900441	R(1%)
K900442	CA(T-C)
K900443	FTF
K900445	CA(T-T)
K900446	FTF
K900447	R(10%)
K900448	R(1%)

Table II SUMMARY OF 1/5-SCALE SPECIMENS  
AND TEST ASSIGNMENTS (Continued)

Specimen I. D.	Test Assignment
K900449	R(50%)
K900450	R(50%)
K904950	R(10%)
K904951	R(50%)
K904952	R(50%)
K904953	R(50%)
K904954	R(50%)
K904955	R(1%)
K904956	R(50%)
K904957	R(10%)
K904958	R(1%)
K904959	R(10%)
K905015	R(50%)
K905016	R(1%)
K905017	R(10%)
K905018	R(50%)
K905020	R(50%)
K905021	R(10%)
K905022	R(50%)
K905023	R(50%)
K905362	R(50%)
K905363	R(50%)
K905364	FTF
K905365	R(50%)
K905366	R(50%)
K905367	FTF
K905368	FTF
K905369	R(50%)
K905371	R(50%)
K905467	R(50%)
K905468	FTF
K905469	R(50%)
K905470	FTF
K994565	FTF
K994566 <sup>Δ</sup>	CA(T-T)
K994567	CA(T-T)
K994568 <sup>Δ</sup>	CA(T-C)
K994569*	S
K994578	S
K994587	CA(T-T)
K994588 <sup>Δ</sup>	S

Table II (Concluded)

Notes:

S	= Static test to failure
CA(T-T)	= Constant amplitude (Tension-Tension) test to failure
CA(T-C)	= Constant amplitude (Tension-Compression) test to failure
R(X%)	= Random Loading (X% Specified lifetime) and static test
FTF	= Fatigue to failure
*	= Specimen rejected due to excessive dimensional variations
Δ	= Specimen also and for strain survey

Table III SUMMARY OF 1/2-SCALE SPECIMEN AND TEST ASSIGNMENTS

Specimen	Test Assignment
F504619	FTF
F504620	FTF
F504621	FTF
F504622	FTF
F504623	FTF
F504618	R(10%)
F504624	R(10%)
F504625	R(10%)
K012453	R(10%)
K012454	R(10%)

Notes: R(X%) = Random Loading (X% lifetime) and static test  
 FTF = Fatigue to failure

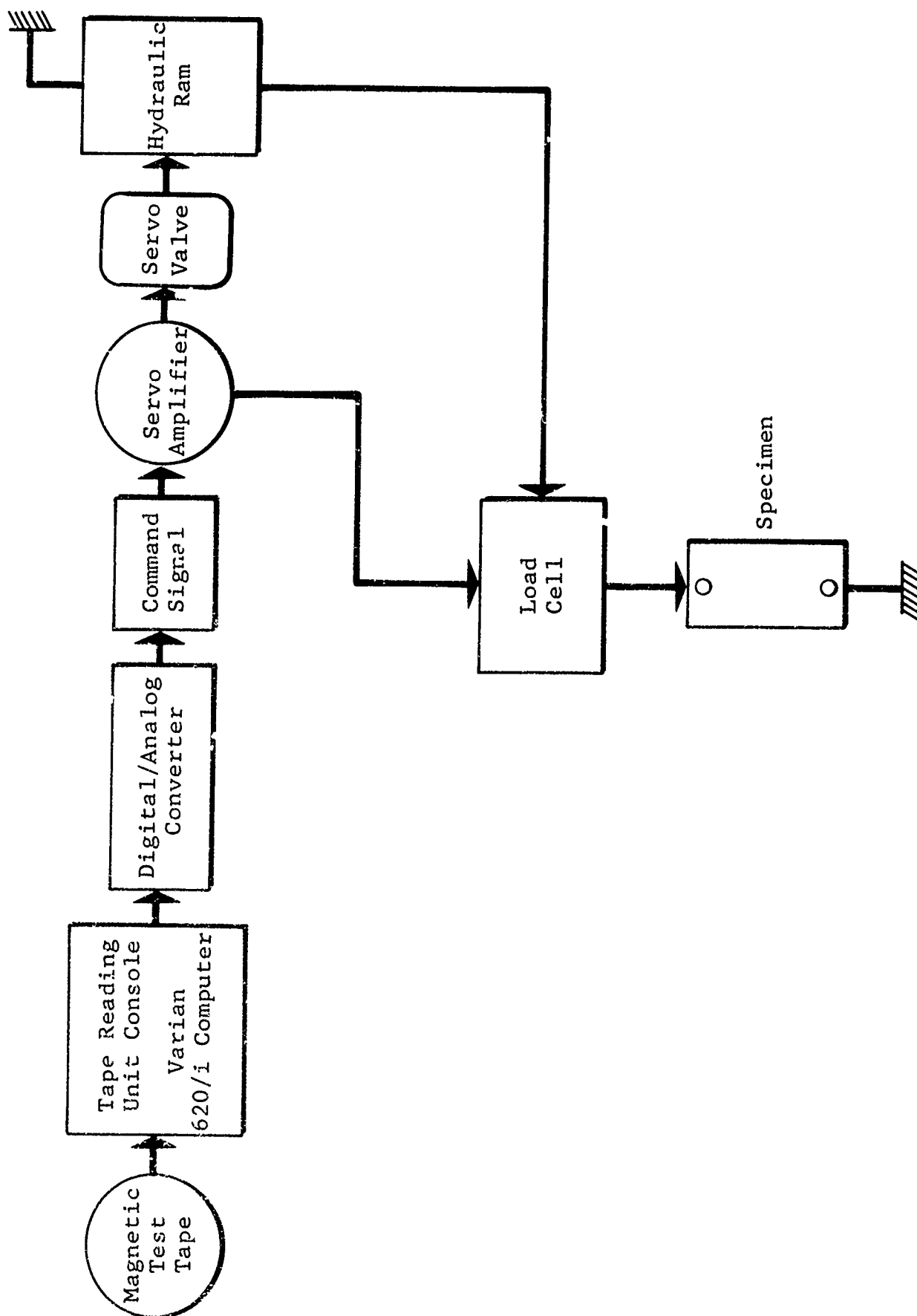


Figure 2 Closed Loop Fatigue Test Schematic

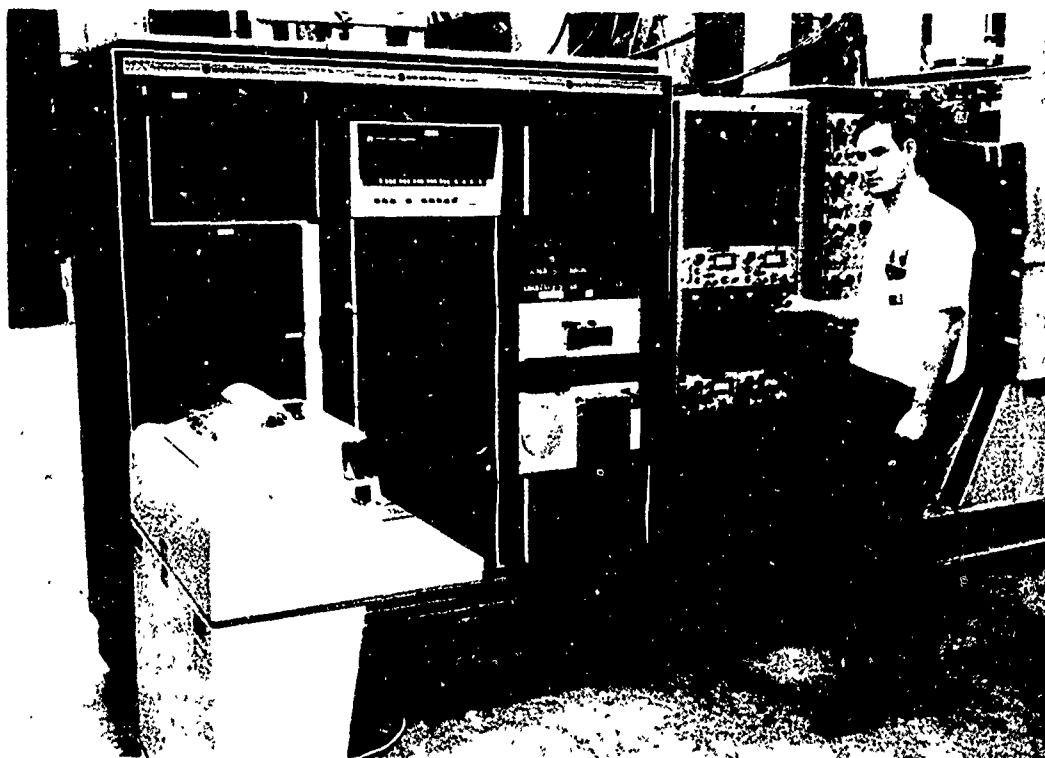


Figure 3 Closed Loop Test System (Test Tape, Varian 620/i Computer, Servo Amplifiers)



Figure 4 Closed Loop Test System (Servo Valve, Hydraulic Ram, Load Cell, Test Fixture and Test Specimen)

8. Test specimen
9. Data recording equipment
10. Strain gauges.

A random load history, simulating a given service spectrum, is generated and stored on magnetic tape. This tape is analyzed by a Varian 620/i digital/analog converter. The digital records on the tape are converted into an analog signal that is sent to the servo amplifier.

A servo valve controls the flow of oil for driving the hydraulic ram. The ram puts out an arbitrary load signal. This signal goes through the load cell back to the servo amplifier. The signal from the load cell is analyzed and adjusted to meet the magnetic tape requirement before the load is applied to the specimen. The servo amplifier compares the signal from the load cell and the random load tape. A compensating load signal is sent directly to the servo valve from the servo amplifier. This signal is compatible with the load requirement from the test tape. The servo valve adjusts the oil flow to the hydraulic ram, which in turns loads the load cell and the specimen. After each load is applied to the specimen, a new signal is sent to the servo amplifier and compared with the signal from the magnetic tape. This process continues until the desired number of loads are applied to the specimen or until the specimen fails. The closed loop test system is used for both the constant amplitude tests and the random tests. The Varian 620/i digital/analog converter is used only for the random fatigue tests.

Four specimens can be tested simultaneously using the closed loop test system. Three 1/5-scale specimen and one 1/2-scale specimen tests can be conducted at the same time. This is possible using a servo valve and servo amplifier for each test fixture used. The loads stored on the magnetic tape are in nondimensional wave form. The desired load on the specimen is obtained by calibrating the load signal output for each servo amplifier. The load history for each specimen is recorded and the load signal is plotted.

When only 1/5-scale specimens are tested, a test rate of about 5 Hz is possible; however, when a 1/2-scale specimen is also tested, the test rate is reduced to 3 or 4 Hz because of system limitations. Since the recording equipment is independent, different lifetime random tests can be run at the same time. Specimens are tested one at a time or in multiples until the test requirements are satisfied.

# SECTION III

## SPECIMEN DESIGN, FABRICATION, AND INSPECTION

### 3.1 SPECIMEN DESIGN DETAILS

The specimen descriptions, design criteria, quality control acceptance tests, and material mechanical properties are discussed in this section.

#### 3.1.1 Description

Boron-laminate-to-titanium adhesive bonded double scarf joint specimens (1/5 and 1/2 scale) were used in the experimental test program. Specimen constituents include

1. Two titanium (6AL-4V) lug ends with a double tapered splice plate
2. Boron-epoxy laminate (Narmco 5505), pre-cut to match template
3. General Dynamics Specification FMS-1013 IA adhesive (Relibond 398, Reliable Manufacturing Company)
4. General Dynamics Specification FMS-1014 IIA adhesive primer.

Drawings of the 1/5- and 1/2-scale specimens are shown in Figure 5 and 6, respectively.

The boron-epoxy laminate was bonded to the titanium lug ends with FMS-1013 IA adhesive to FW6920025 and FW6920044 specification. The fabrication and inspection techniques are discussed in subsection 3.2 and 3.3, respectively.

The FW6920025 (1/5 scale) and the FW6920044 (1/2 scale) specimens had the same  $l/t$  value based on the average taper thickness of the boron-epoxy laminate. The bond areas and the cross-sectional areas through the laminate for the respective specimens (FW6920025 and FW6920094) were proportioned so that the smaller specimen was approximately 1/5-scale size relative to the 1/2-scale specimen.



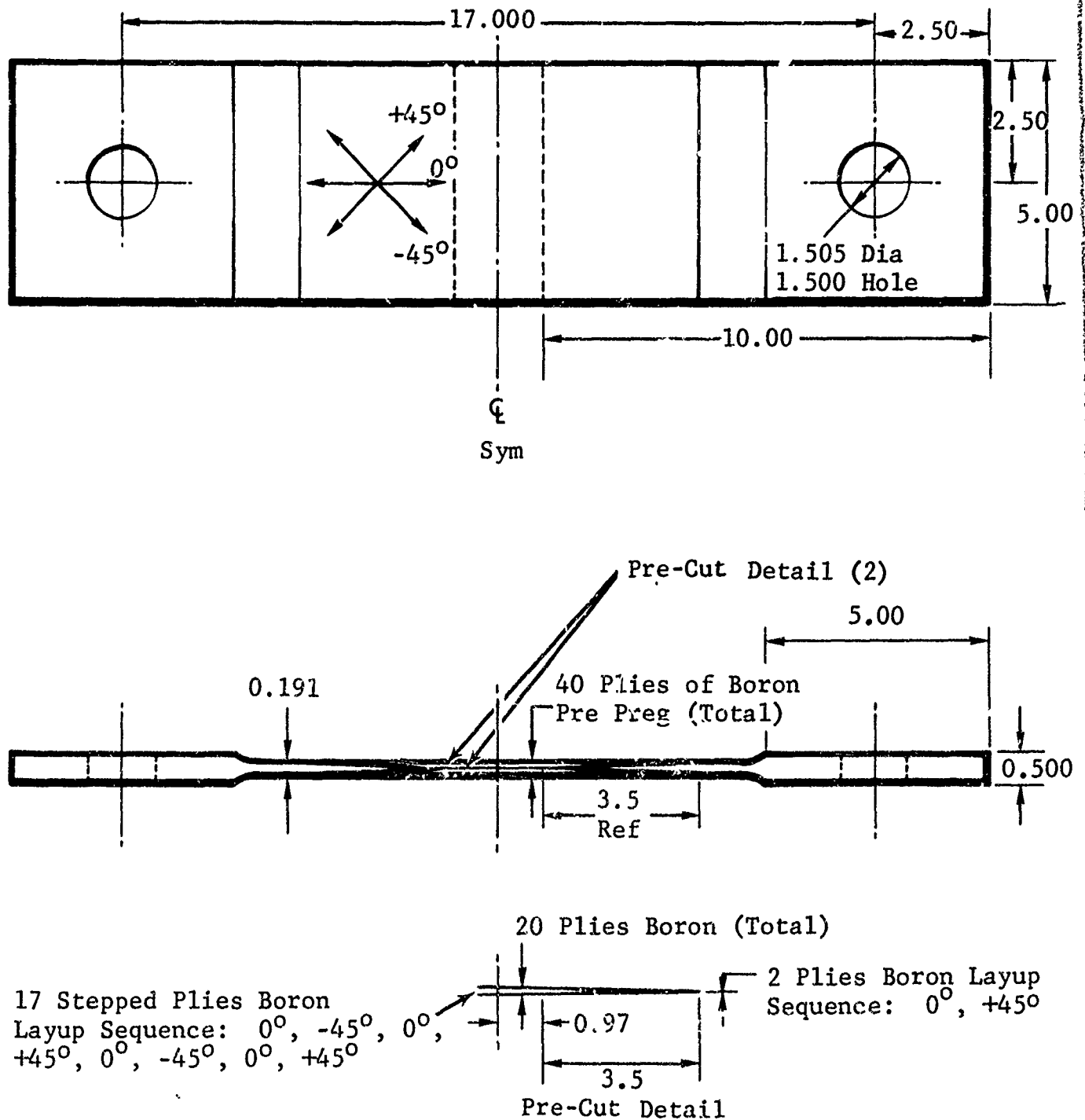


Figure 5 One-Fifth Scale Fatigue Specimen - Boron-to-Titanium Double Scarf Adhesive Bonded Joint

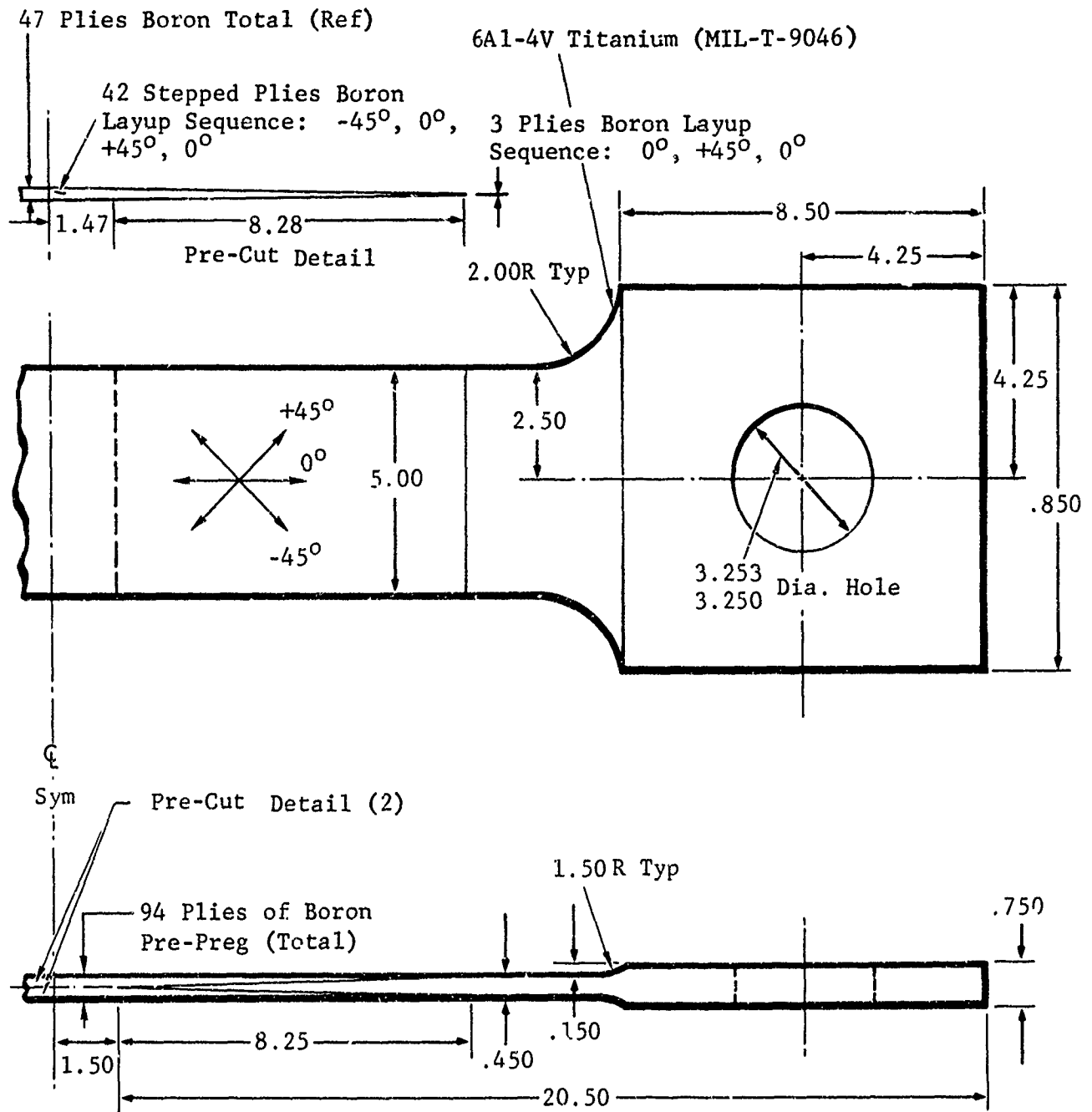


Figure 6 One-Half Scale Fatigue Specimen - Boron-to-Titanium  
Double Scarf Adhesive Bonded Joint

### 3.1.2 Design Criteria

The design development tests leading to the joint configurations used in this program are documented in Reference 27. The original design goal was to develop a full-scale bonded joint with the capacity to transmit 66,000 lbs/in at ultimate load. The reproducibility characteristics of the bonded joints were not known before this program; therefore, joint allowables were established by test. Special factors of safety were used in the Reference 27 program; hence, ultimate load was equal to 1.5 times the limit load. Laminate design allowables based on the "B" criteria of MIL-HDBK 5 were used to determine allowable stress levels.

The full-scale test results of Reference 27 indicated a possible scale effect. These results were used to develop 1/5- and 1/2-scale fatigue specimens for this program compatible with the full-scale specimens of Reference 27.

The dimensions of the scaled specimens are listed in Table IV. The 1/5- and 1/2-scale specimens have the same ratio of laminate thicknesses as the ratio of scarf length. This is reflected in the  $\ell/t$  ratio.

### 3.1.3 Acceptance Tests

The material used for this program was Narmco 5505 boron-epoxy tape per General Dynamics specification FMS-2001A manufactured by Narmco Materials Division of the Whittaker Corporation. The acceptance data obtained at General Dynamics for sample batches of material used in this program are shown in Table V and compared with the requirements of FMS-2001A. Data in Table V are based on the ultimate strength averages of three specimens per point. Statistical properties for the data of Table V are summarized in Table VI.

### 3.1.4 Material Mechanical Properties

Room temperature physical properties for boron-reinforced-epoxy lamina are summarized in Table VII. Material correction factors for temperature of  $-65^{\circ}\text{F}$  to  $420^{\circ}\text{F}$  are also available. Design allowables are summarized in Table VIII for boron-reinforced-epoxy composites at room temperature. A design

Table IV SPECIMEN DESIGN DATA

Scale Size	Geometry (Inches)			L/t	Total Cross Sectional Area (2tw)	Bond Area (2wL)	Design Load/In. (Ultimate)	Design Load (Ultimate)	Laminate Stress (Ult.)	Bond Stress (Ult.)
	2t	L	W							
Full <sup>a</sup>	1.0	14.0	13.8	28.0	13.8 in <sup>2</sup>	386 in <sup>2</sup>	100,000 #/in.	1380 Kips	100 ksi	3580 psi
1/2 <sup>b,d</sup>	0.495	8.25	5.0	33.4	2.475 in <sup>2</sup>	82.5 in <sup>2</sup>	49,500 #/in.	247.5 Kips		3000 psi
1/5 <sup>c,d</sup>	0.212	3.50	5.0	33.1	1.060 in <sup>2</sup>	35.0 in <sup>2</sup>	21,200 #/in.	106 Kips		3038 psi

Notes: a Ref. drawing FW6920028B. detail -21 (Ref. '7 pg. 167, 168)

b Ref. drawing FW6920044 (Figure 6)

c Ref. drawing FW6920025 (Figure 5)

d The scale size is defined with respect to the design load/in. using the full size as a base line. On this basis the 1/2 scale and the 1/5 scale are approximately 1/2.02 scale and 1/4.72 scale respectively.

e All specimen designed to be laminate-stress-critical.

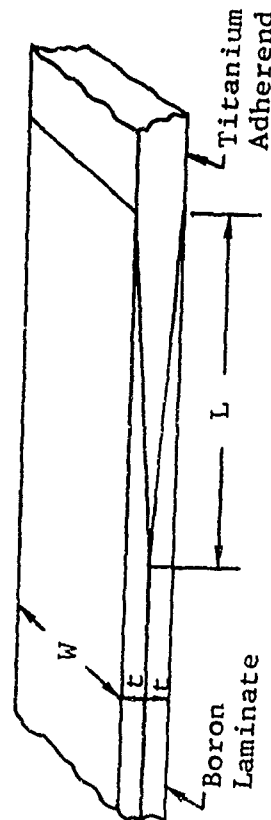


Table V

SUMMARY OF ACCEPTANCE TEST RESULTS FOR  
BORON COMPOSITE FIBERS<sup>a</sup>

T.T. NO.	BATCH NO.	ROLL NO.	DATE TESTED	TEMP.	TRIAL NO.	b $\tau$ (psi)	$\sigma_o^c$ (psi)	$\sigma_{90o}^d$ (psi)
81490	401	5	8-17-70	R.T.	1	15.3	250.4	14.2
					2	16.3	252.8	14.7
					3	16.3	260.6	15.2
					Avg.	16.0	254.6	14.7
				350°F	4	6.8	231.4	12.6
					5	6.8	217.9	12.2
					6	6.5	219.4	11.8
					Avg.	6.7	222.8	12.2
81572	401	14	9-1-70	R.T.	1	13.0	251.4	16.5
					2	15.8	234.2	16.6
					3	16.2	218.6	17.6
					Avg.	15.0	234.7	16.9
				350°F	4	6.5	195.1	11.0
					5	6.8	212.0	12.7
					6	6.7	203.5	12.7
					Avg.	6.7	203.5	12.1
81507	402	Sample	8-17-70	R.T.	1	13.7	238.8	14.8
					2	15.9	225.6	15.4
					3	14.5	215.5	15.9
					Avg.	14.7	226.6	15.4
				350°F	4	8.5	216.2	12.5
					5	8.2	208.3	12.4
					6	7.4	213.8	12.3
					Avg.	8.0	212.7	12.4
81618	402	28	9-1-70	R.T.	1	17.1	276.5	16.9
					2	17.1	274.1	17.2
					3	16.7	281.0	15.9
					Avg.	17.0	277.2	16.7
				350°F	4	7.0	222.2	11.1
					5	7.0	240.2	12.5
					6	6.9	232.4	12.0
					Avg.	7.0	231.6	11.9
81571	402	32	9-1-70	R.T.	1	15.6	267.2	15.7
					2	15.6	270.5	15.7
					3	16.5	265.3	16.8
					Avg.	15.9	267.6	16.1
				350°F	4	6.6	224.6	12.3
					5	6.5	219.7	12.9
					6	6.6	221.4	13.4
					Avg.	6.6	221.9	12.9

Table V SUMMARY OF ACCEPTANCE TEST RESULTS FOR  
BORON COMPOSITE FIBERS<sup>a</sup>  
(Continued)

T.T. NO.	BATCH NO.	ROLL NO.	DATE TESTED	TEMP.	TRIAL NO.	<sup>b</sup> $\tau$ (psi)	<sup>c</sup> $\sigma_0$ (psi)	<sup>d</sup> $\sigma_{90}$ (psi)
749409	402	52	9-18-70	R.T.	1	13.1	258.6	17.3
					2	13.0	268.1	17.0
					3	13.5	217.4	15.7
					Avg.	13.2	248.0	16.7
				350°F	4	5.9	179.0	12.2
					5	6.1	170.9	11.2
					6	5.8	177.5	10.9
					Avg.	5.9	175.8	11.4

Notes: a Acceptance test per FMS-2001

b Horizontal Shear (Required Values: 13 psi at R.T. and 5 psi at 350°F)

c 0° Flexural (Required Values: 225 psi at R.T. and 170 psi @ 350°F)

d 90° Flexural (Required Values: 13 psi at R.T. and 8 psi at 350°F)

Table VI SUMMARY OF STATISTICAL PROPERTIES BASED ON ACCEPTANCE TEST RESULTS FOR BORON COMPOSITE FIBERS

Statistical Property	$\tau$		$\sigma 0^\circ$		$\sigma 90^\circ$	
	R.T.	350°F	R.T.	350°F	R.T.	350°F
Mean (psi) ( $\mu$ )	15.29	6.81	251.48	211.42	16.06	12.15
Variance ( $\sigma^2$ )	1.963	0.442	438.235	357.919	0.908	0.463
Standard Deviation ( $\sigma$ )	1.401	0.665	20.93	18.919	0.953	0.680
Coefficient of Variation ( $\nu$ )	9.164%	9.764%	8.323%	8.949%	5.933%	5.597%

Notes: Same notes apply as given at bottom of Table V.

$$\mu = \frac{\sum_{i=1}^n X_i}{n}$$

$$\sigma = \sqrt{\frac{\sum_{i=1}^n (X_i - \mu)^2}{n}}$$

$$\nu = \left(\frac{\sigma}{\mu}\right) 100$$

$n = 18$  (Reference data Table V).

Table VII PHYSICAL PROPERTIES - BORON-EPOXY

Property	Value
Density, lb/in. <sup>3</sup>	0.073
Ply Thickness, in.	0.0051 to 0.0054
Volume of Reinforcement, %	50 (average)
Thermal Conductivity, $\frac{\text{BTU} - \text{in.}}{\text{hr} - \text{ft}^2 - ^\circ\text{F}}$	2.8 at 200°F <sup>(1)</sup> (0° Lamina)
Linear Coefficient of Thermal Expansion, 10 <sup>-6</sup> in./in./°F	2.5 at 200°F <sup>(2)</sup> , parallel (0° Lamina) 13.0 at 200°F <sup>(2)</sup> , normal (0° Lamina)
Dielectric Constant, 8.2 GHz	27 at R.T. <sup>(3)</sup> (0° Lamina)
Loss Tangent, 8.2 GHz	0.007 at R.T. <sup>(3)</sup> (0° Lamina)
Capacitance, $\mu\mu$ farad, dry	221.5 <sup>(4)</sup> (Unpainted 0° Lamina)
Capacitance, $\mu\mu$ farad, humidity exposure	225.5 <sup>(4)</sup> (Unpainted 0° Lamina)
Specific Heat, BTU/lb/°F	0.327 at 200°F

- NOTES: (1) Data available for temperature range -65°F to 420°F and for specific laminates.
- (2) Data available for temperature range -50°F to 350°F and for specific laminates.
- (3) Data available for temperature range R.T. to 420°F and frequency range 8.2 to 11.0 GHz and for specific laminates.
- (4) Per MIL-R-7705A(ASG). Data also available for specific laminates.
- (5) From Reference 28.



Table VIII DESIGN ALLOWABLES - BORON-EPOXY,  
ROOM TEMPERATURE, "B" BASIS

Property	Direction	
	Parallel to Fiber	Normal to Fiber
<u>Axial</u>		
Modulus of Elasticity, $10^6$ psi	30.0	2.7
Design Limit Tensile Strain, in./in.	0.0040	0.0023
Design Ultimate Tensile Strain, in./in.	0.00600	0.00345
Design Limit Compressive Strain, in./in.	0.0075	0.0075
Design Ultimate Compres- sive Strain, in./in.	0.01125	0.01125
<u>Shear</u>		
Shear Modulus of Rigidity, $10^6$ psi	0.65	
Poisson's Ratio	0.21	
Design Limit Shear Strain, in./in.	0.013	
Design Ultimate Shear Strain, in./in.	0.0195	

ultimate intersection diagram is shown in Figure 7 for ( $O_2/\pm 45$ ) laminate configurations.

### 3.2 FABRICATION TECHNIQUE

Reusable titanium lug ends were used to build the 1/5- and 1/2-scale specimens. Thirty sets of the 1/5-scale lug ends and three sets of the 1/2-scale lug ends were used in the program. Specimens were built, tested, and rebuilt until the required testing was complete.

The fabrication-test recycling procedure is shown in Figure 8. Typical pictures of the specimen elements, tools, and apparatus are shown in Figures 9 and 10.

At the start of the program, tools were available for building five 1/5-scale and one 1/2-scale specimens at the same time. As the testing progressed, it became apparent that a faster rate of 1/5-scale specimen recycling was needed to keep pace with the testing. Five additional tools were made for building the 1/5-scale specimen. With the new tools, ten 1/5-scale specimens could be built at the same time. No additional tools were made for building the 1/2-scale specimens since only ten specimens were required for the test program.

### 3.3 INSPECTION

#### 3.3.1 Fluorescent and Ultrasonic

The titanium lug ends were inspected with fluorescent penetrant per MIL-I-6866 type 1, and the specimens were ultrasonic inspected. Approximately 30 of the first 81 1/5-scale specimens and 3 of the first 10 1/2-scale specimens were inspected as described. It was found that the rate of specimen supply could not stay up with the needs for continuous testing. To avoid testing delays, inspection was waived on the remaining specimens.

#### 3.3.2 Warpage

The first 25 1/5-scale specimens built had a noticeable degree of warpage. The degree of warpage was determined by placing

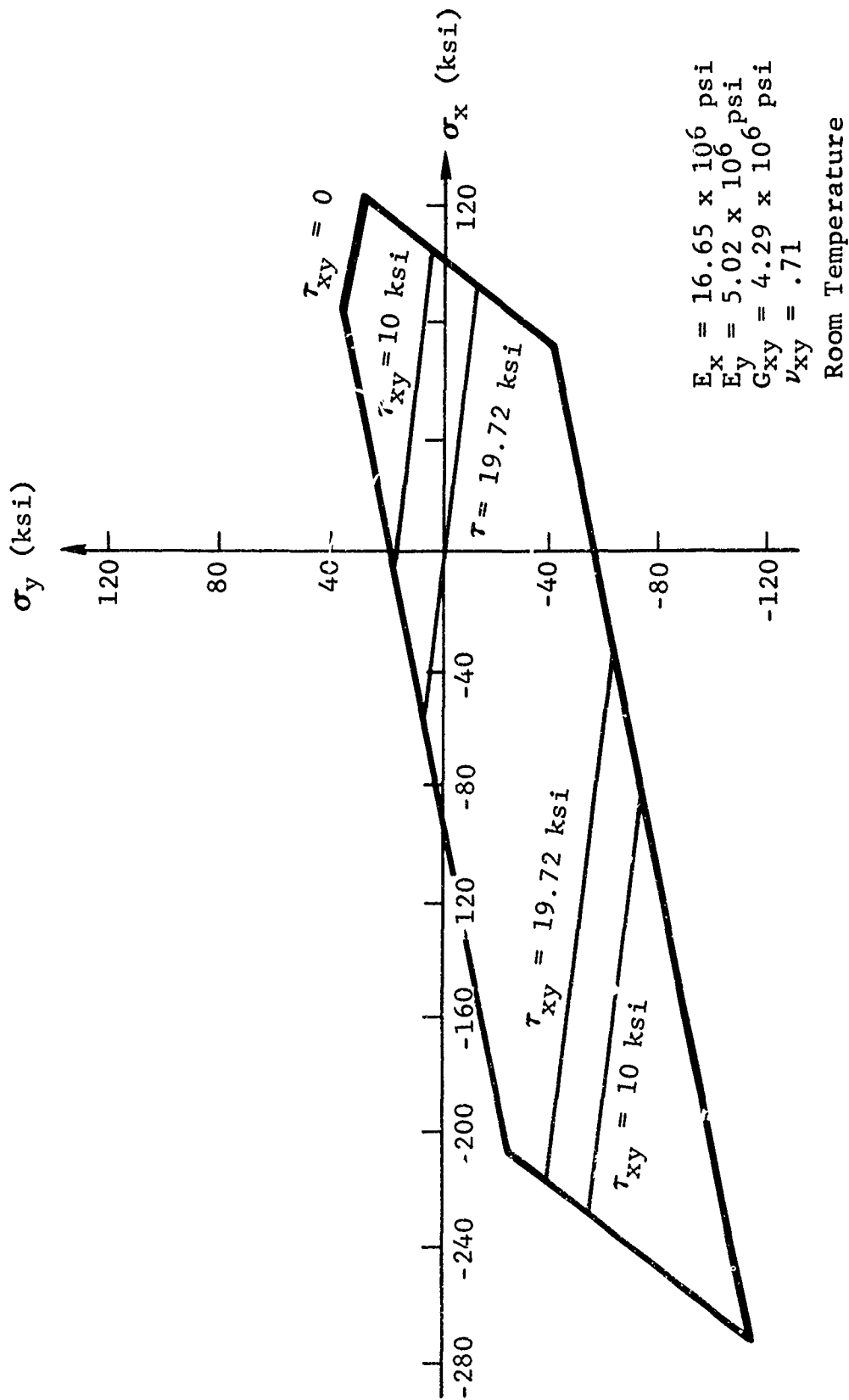


Figure 7 Boron-Epoxy  $[0_2/\pm 45]$  Design Ultimate Interaction Diagram, RT

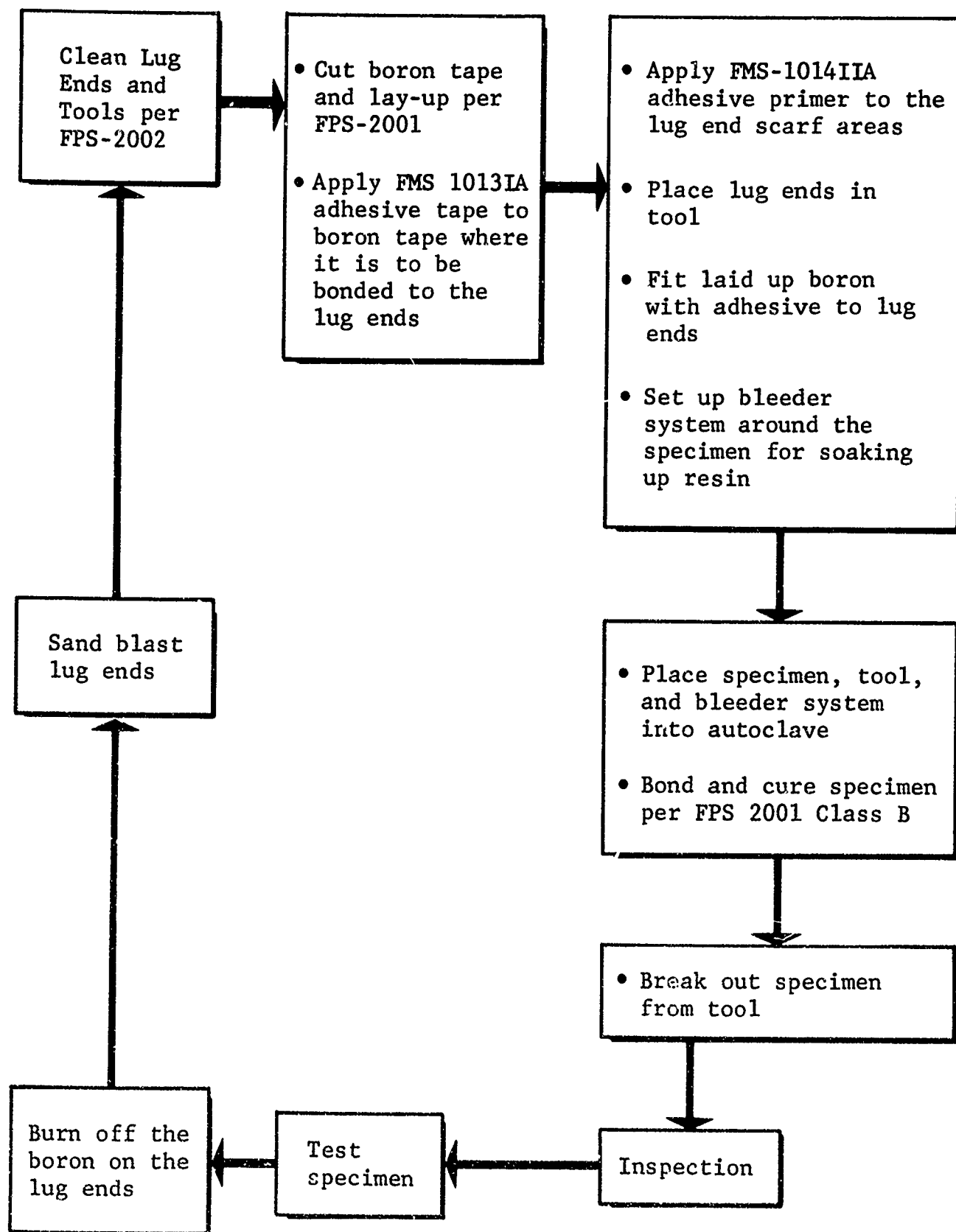


Figure 8 Fabrication-Test-Recycling Procedure

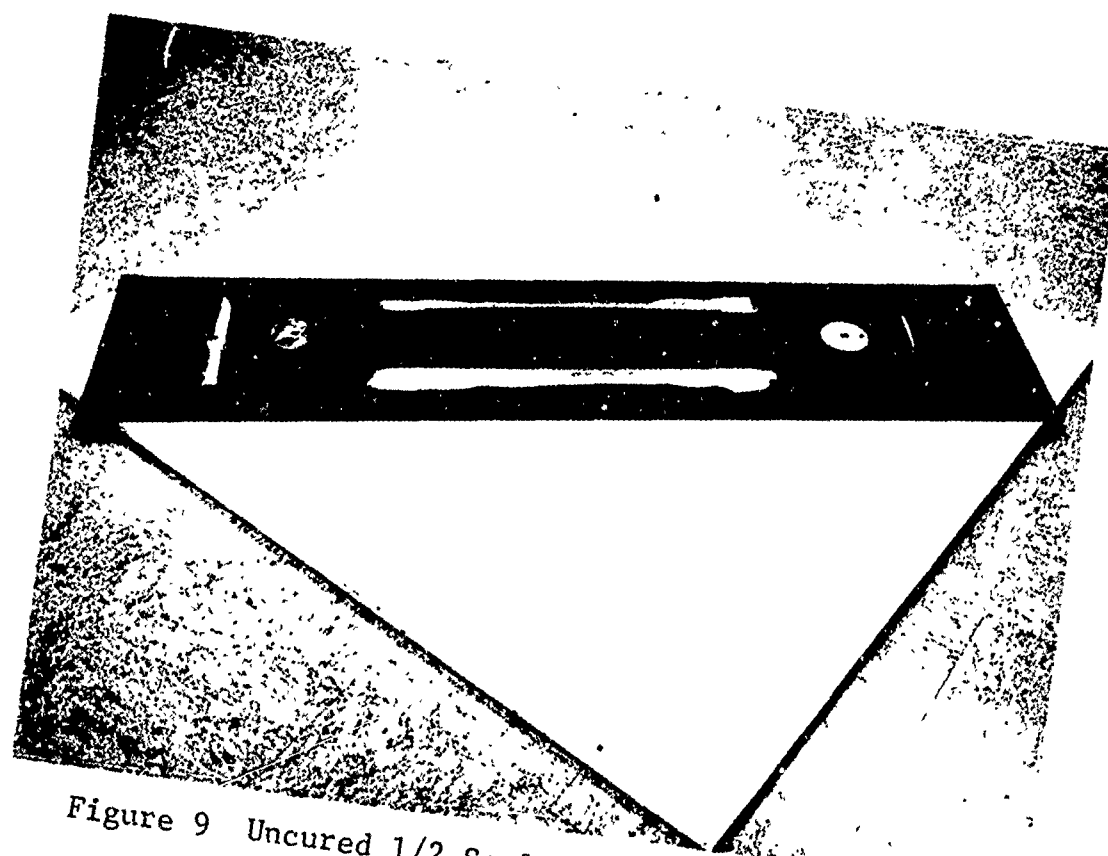


Figure 9 Uncured 1/2 Scale Specimen in Tool with Bleeder Cloth Between Specimen and Tool

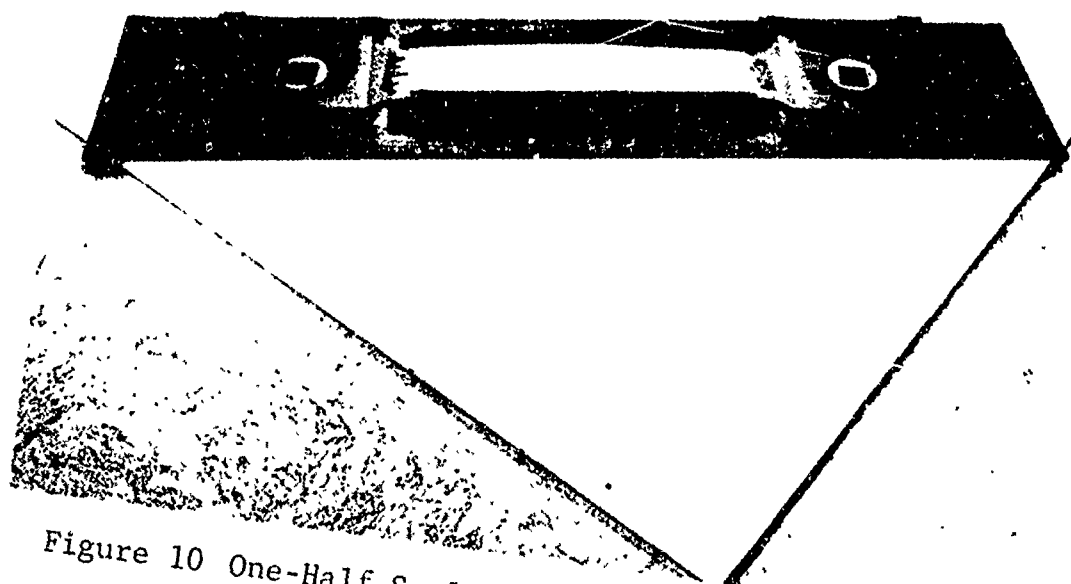


Figure 10 One-Half Scale Specimen Ready for Curing

the specimen on a solid level surface and taking relative dial gauge surface measurements at the locations shown in Figure 11. Relative measurements were taken with respect to surface location 2. Surface measurements are summarized in Table IX for 24 of the 25 specimens measured.

Straightening of specimen K012440 was attempted by heating. Seven of the 24 specimens evaluated were rejected because of excessive warpage. Specimen K012440 was also rejected. The rejected specimens were static tested and the lug ends were recycled. The static test results for these specimens were segregated from the acceptable static test specimens (Table II).

The specimen fabrication procedure was analyzed to correct the warpage problem. It was found that the layers of bleeder cloth between the top surface of the tool and the bottom surface of the specimen prevented the lug ends from resting flat against the surface of the tool. This problem was easily corrected by placing cloth plies between the lug ends and the tool to compensate for the bleeder cloth. All specimens built after this change were visibly checked for flatness by placing specimens on a level surface and observing clearances. None were considered unacceptable. All 1/2-scale specimens were built with allowance for the bleeder cloth thickness; therefore, no warpage problems occurred.

The impact of specimen warpage was investigated to determine if there would be a serious effect on the experimental results. A strain survey was performed to evaluate the effects of specimen warpage. The strain data generated and the analysis performed are given in Appendix VII. It was concluded that the effects of specimen warpage were negligible. This is documented in Appendix II.

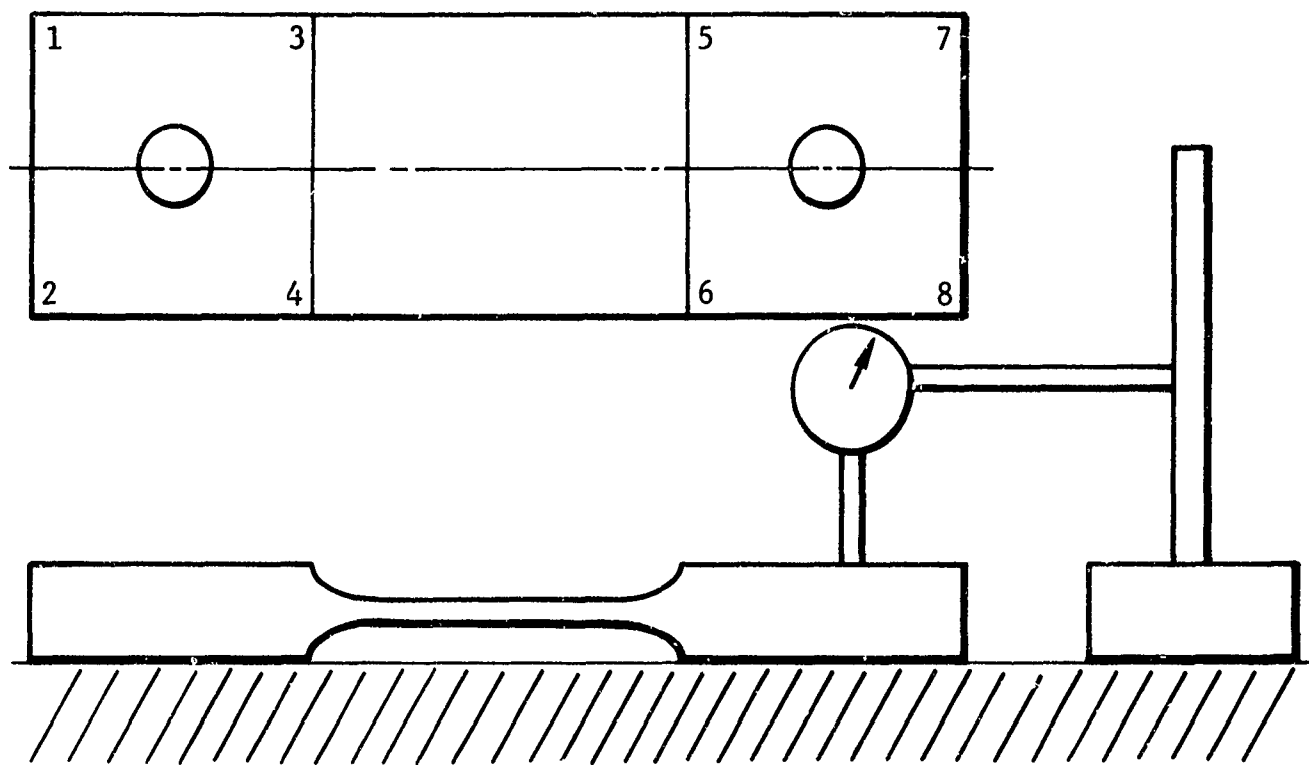


Figure 11 One-Fifth Scale Dial Gauge Surface Measurement Locations

Table IX SUMMARY OF DIAL GAUGE SURFACE MEASUREMENTS  
FOR INITIAL GROUP OF 1/5-SCALE SPECIMEN

Surface Location Specimen	1	2	3	4	5	6	7	8
	(Surface Measurement - Inches) $\Delta$							
K012437*	-0.009	0	-0.008	0.004	0.046	0.094	0.105	0.166
K012438	-0.004	0	0.038	0.041	0.0076	0.042	0.021	0.015
K012439	0.010	0	0.0395	0.034	0.0355	0.064	0.0075	0.033
K012441	-0.009	0	0.014	0.037	0.0245	0.065	-0.010	0.030
K012442	0	0	-0.005	-0.0015	0	0.0495	0.034	0.086
K012443	0	0	0.034	0.028	0.025	0.048	-0.015	0.011
K012444	0	0	-0.021	-0.016	0.050	-0.011	0.043	0.022
K012445	0.001	0	0.025	0.024	0.031	0.0563	0.0038	0.030
K012446*	0.014	0	0.010	0.003	0.050	0.0782	0.1047	0.135
K012459*	0.010	0	-0.011	-0.015	0.042	0.084	0.105	0.162
K012461	0.003	0	-0.003	-0.004	-0.008	0.016	0.014	0.050
K012462	0.006	0	0	0.002	0	0.030	0.035	0.075
K012463*	-0.002	0	-0.003	-0.001	0.025	0.052	0.065	0.103
K012464	-0.009	0	0.032	0.043	0.025	0.039	0	0.021
K012465	-0.001	0	0.025	0.029	-0.001	0.036	-0.019	0.015
K012474*	-0.001	0	-0.006	0.002	0.027	0.086	0.075	0.121
K012475	-0.011	0	-0.015	-0.008	-0.004	-0.024	0.025	0.013
K994566	0.001	0	0.0155	0.014	-0.0135	0.017	0.004	0.033
K994567	0.004	0	-0.011	-0.006	0.002	0.048	0.031	0.071
K994568	0.012	0	0.010	0.001	0.003	0.021	0.0215	0.0465
K994569*	0.078	0	0.083	-0.004	0.089	0.124	0.169	0.204
K994578*	0	0	0	0.006	0.149	0.175	0.175	0.202
K994587	-0.008	0	0.013	0.020	0.011	0.047	-0.007	0.042
K994588	0.003	0	0.006	0.0065	0.001	0.0335	-0.024	0.010

Note: \*Specimen rejected due to excessive dimensional variations.

$\Delta$ Dial gage surface locations are shown in Figure 11.



## SECTION IV

### RANDOM FATIGUE AND LOAD SPECTRUM

The random load history generation procedures used for this program are discussed in this section. These procedures were used to generate the test tape random load simulation discussed in subsection 4.3. A computer program (Reference 26) was developed which simulates the random load history and stores it on a magnetic tape. This tape was used in a computerized closed loop test system. Most of the technical terms used in this section are defined in Appendix III.

#### 4.1 GENERAL DESCRIPTION OF PROCEDURE

The principal steps and essential elements of the random load history simulation procedure are

1. Define Service History
  - a. Mission profiles
  - b. Mission segment types
  - c. Time spent in each segment
  - d. Number of missions
  - e. Exceedances for positive and negative spectra
2. Analyze exceedance curves using method by Press (Reference 29)
  - a. Number of RMS levels for each mission segment type
  - b.  $\sigma$  RMS values
  - c. Clipping ratios
3. Power Spectrum Analysis
  - a. Power Spectral Density (PSD)
  - b.  $N_0$
  - c.  $N_0$
  - d.  $N_0/N_p$

#### 4. Random Number Mapping

- a. Rice-Bendat-Kowalewski probability density function
- b. Cumulative distribution curve
- c. Pseudo random number generator
- d. Acceptable random numbers

#### 5. Load-by-Load Creation

- a. Use mapping procedure repeatedly
- b.  $P_j = P_{\text{mean}j} + (-1)^{j+1} (\text{fitted random no.})_j (\sigma_{\text{RMS}})_i$
- c. Haversine wave form connects successive loads
- d. Bookkeeping

#### 6. Statistical Analysis of Random Load History Simulation

- a. Level crossings
- b. Mean level crossings with positive slope ( $N_0$ )
- c. Total number of loads for simulation

#### 7. Test Tape Generation.

### 4.2 SERVICE HISTORY DESCRIPTION

The random load history simulation used in this program is based on the F-111 TIP "B" wing spectrum, partially documented in Reference 30. This is a maneuver load dominated spectrum (as opposed to a gust critical spectrum). A typical mission profile was developed from this data. The typical mission length was assumed to be 3 hours. For a 4000-hour airplane, this is equivalent to 1334 missions per service lifetime. It was assumed that the typical mission was repeatedly flown 1334 times in one service life. A random load history was generated to simulate the loads occurring in one service life.

A typical fighter aircraft flies 20 to 30 different types of missions. This program was more concerned with studying the effect of a random load history than it was with the fact that a single mission was used to represent one service lifetime. The mission profile and the corresponding exceedance curves for each mission segment type are discussed in paragraphs 4.2.1 and 4.2.2, respectively.

### 4.2.1 Mission Profile

A mission profile describes the type and time of each maneuver by the aircraft in a single mission. Typical maneuvers are climb, cruise, terrain following radar (TFR), air-to-ground cycles (A/G), air-to-air cycles (A/A), ground-to-air-to-ground cycles (GAG), and touch-and-go cycles (T&G). A maneuver or maneuvers are classified by mission segment types. Several mission segment types are required to characterize a single mission. Different missions are described by assembling the mission segment types in various orders.

The mission profile used for the random load-history simulation for this program is shown in Figure 12. This mission profile represents a typical F-111 mission. The mission segment number, the maneuver description, and the time distribution for each maneuver is summarized in Table X.

Table X SUMMARY OF MISSION PROFILE DATA

Mission Segment No.	Maneuver Description	Time Distribution	
		% Mission	Time (Hours)
1	Climb-Cruise	30%	0.90
2	TFR	20%	0.60
3	A/G	15%	0.45
4	TFR	10%	0.30
5	A/A	5%	0.15
6	Cruise, descent, T&G	20%	0.60
Mean wing root B.M. (lg) = $2.1 \times 10^6$ in lb			

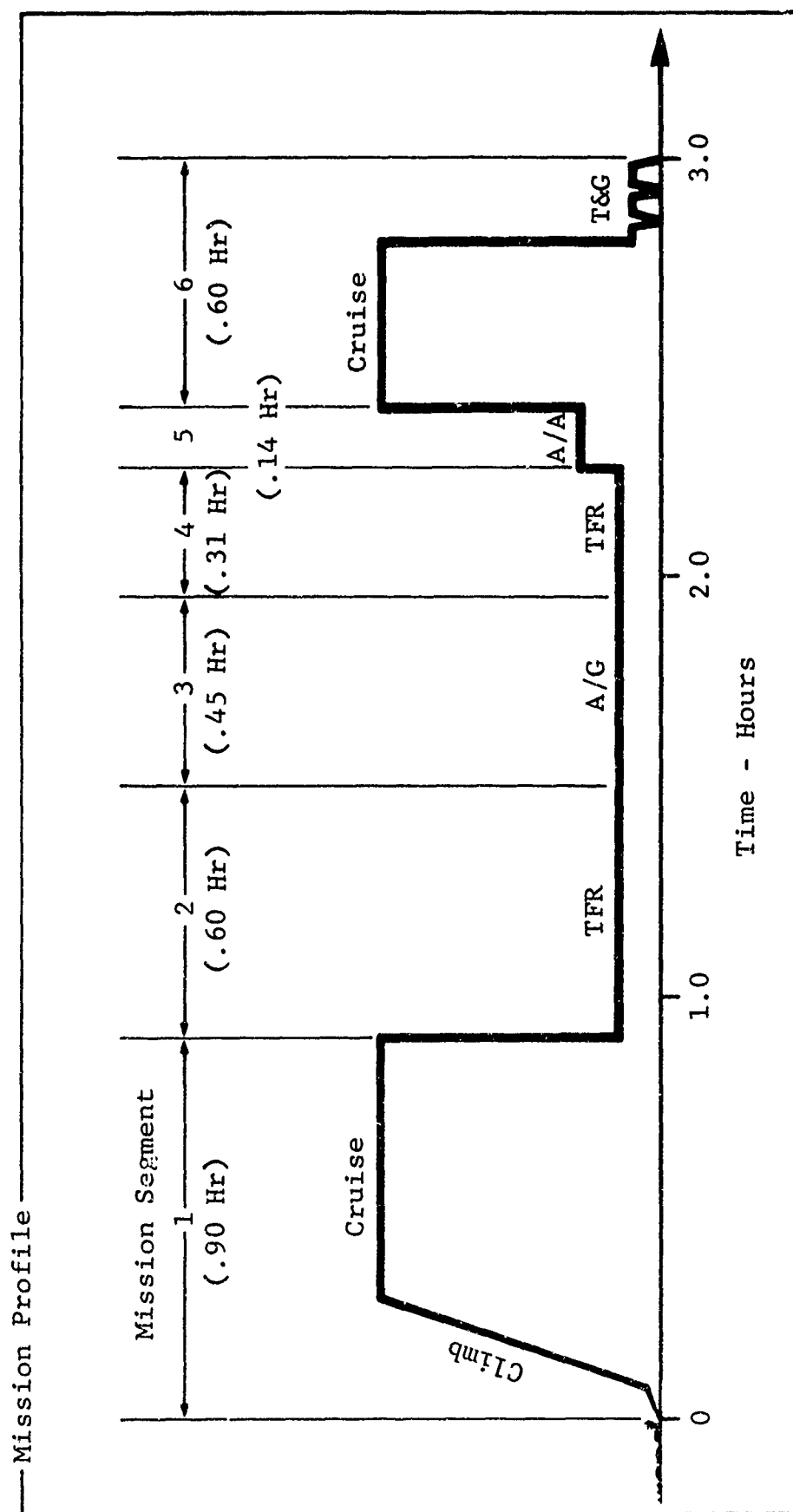


Figure 12 Mission Profile

An exceedance curve defines the number of times per unit time a given delta load level is exceeded for a given mission segment type. The exceedance data for this report is based on the F-111 TIP "B" wing spectrum. Cumulative exceedances per mission were plotted against the wing root ( $\Delta B.M.$ )<sup>2</sup> for analyses purposes. The positive spectrum cumulative exceedance curves used to generate the test tape are given in Figures 13 through 18. For this program, the random load history used in the test was tension; hence, for computational convenience it was assumed that the negative spectra was the same as the positive spectra.

The exceedance curves of Figures 13 through 18 are analyzed using the method of Press (Reference 29). Results are shown on the corresponding figures. Press's method is described in Appendix I. A summary of exceedance curve parameters used for generating the test tape are given in Table XI.

#### 4.3 LOAD HISTORY SIMULATION FOR RANDOM FATIGUE TESTS

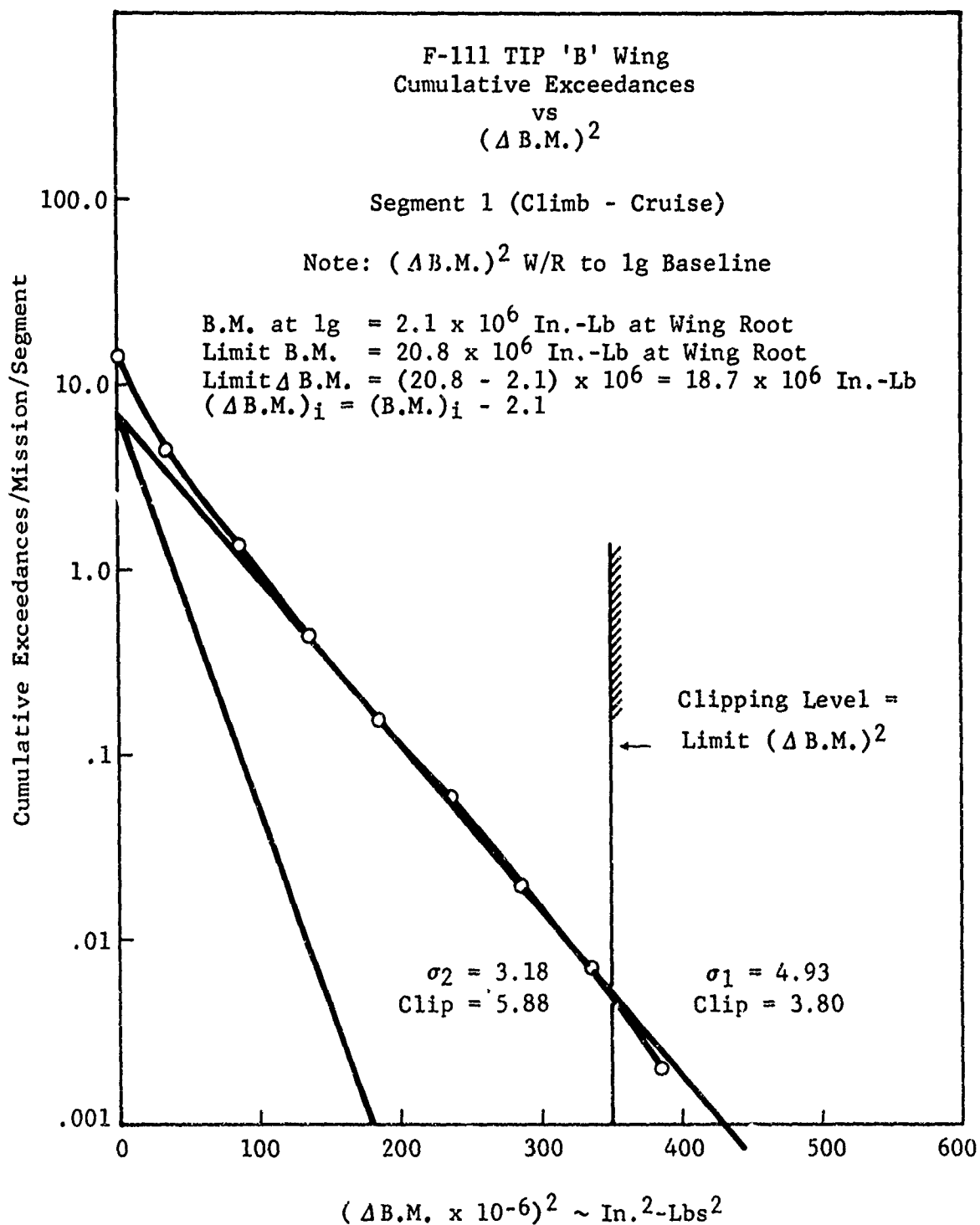
This section describes the input data and its application in the development of the random load history tape employed in the random fatigue tests. The random load simulation is statistically analyzed, and the results are compared to the input composite cumulative exceedances.

The computer program of Reference 26 is used to generate the random load history tape. The procedures described in the previous sections are used.

##### 4.3.1 Description of Input Data

A single mission, defined by the mission profile of Figure 12, was repeatedly flown 1334 times to simulate one lifetime (4000 hours). The input data is described as follows:

1. 6 mission segments
2.  $N_O/N_P = 0.85$  (assumed)
3.  $N_O = 5$  Hz
4. Mean wing root bending moment =  $2.1 \times 10^6$  in. lb (lg, limit)



NOTE: Upper truncation is defined by the clipping level. No central truncation was used other than that implied within the input data. Test machine accuracy provides central truncation at 1/5" of the peak load.

Figure 13 Exceedance Curve Mission Segment 1 (Climb-Cruise)

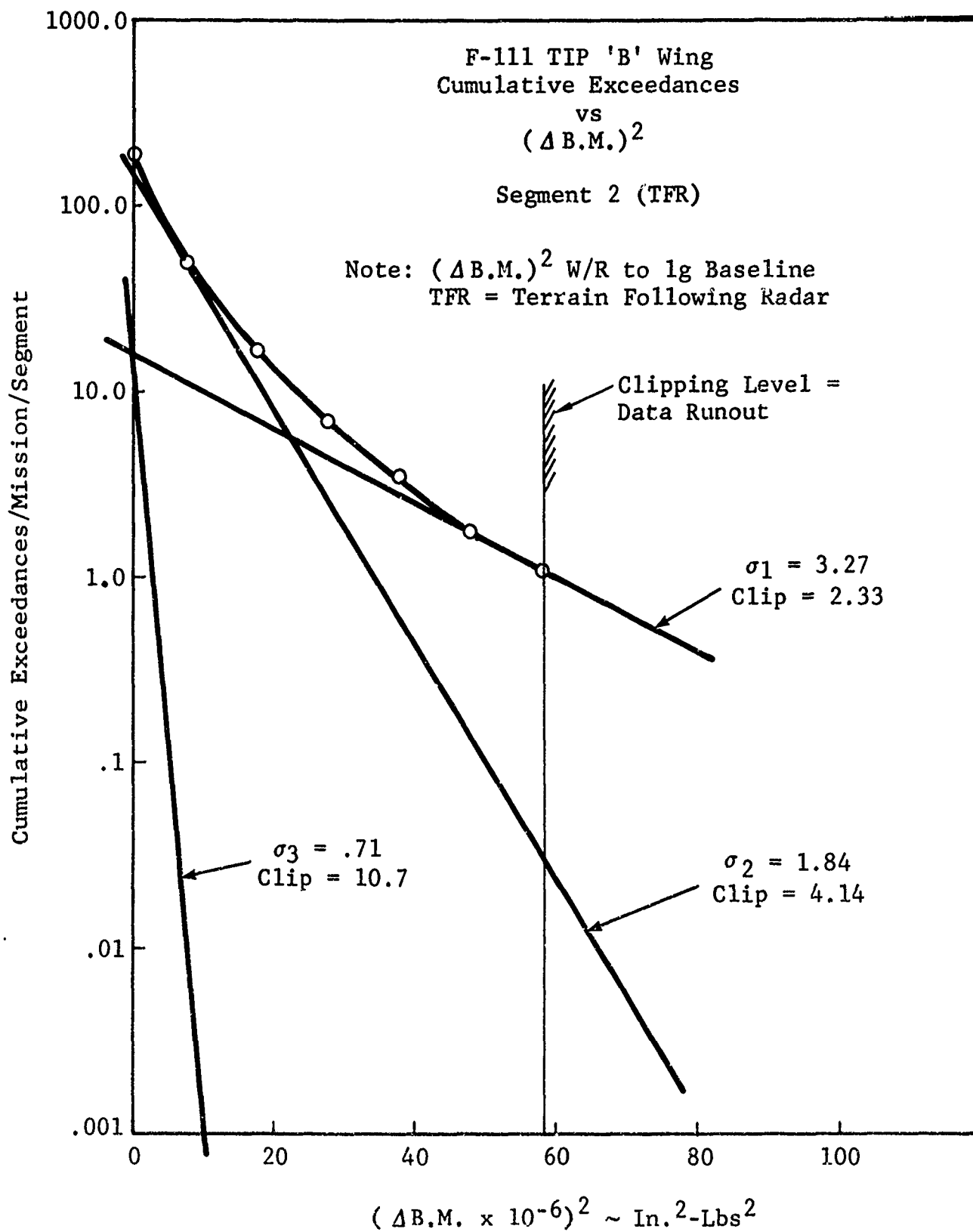


Figure 14 Exceedance Curve Mission Segment 2 (TFR)

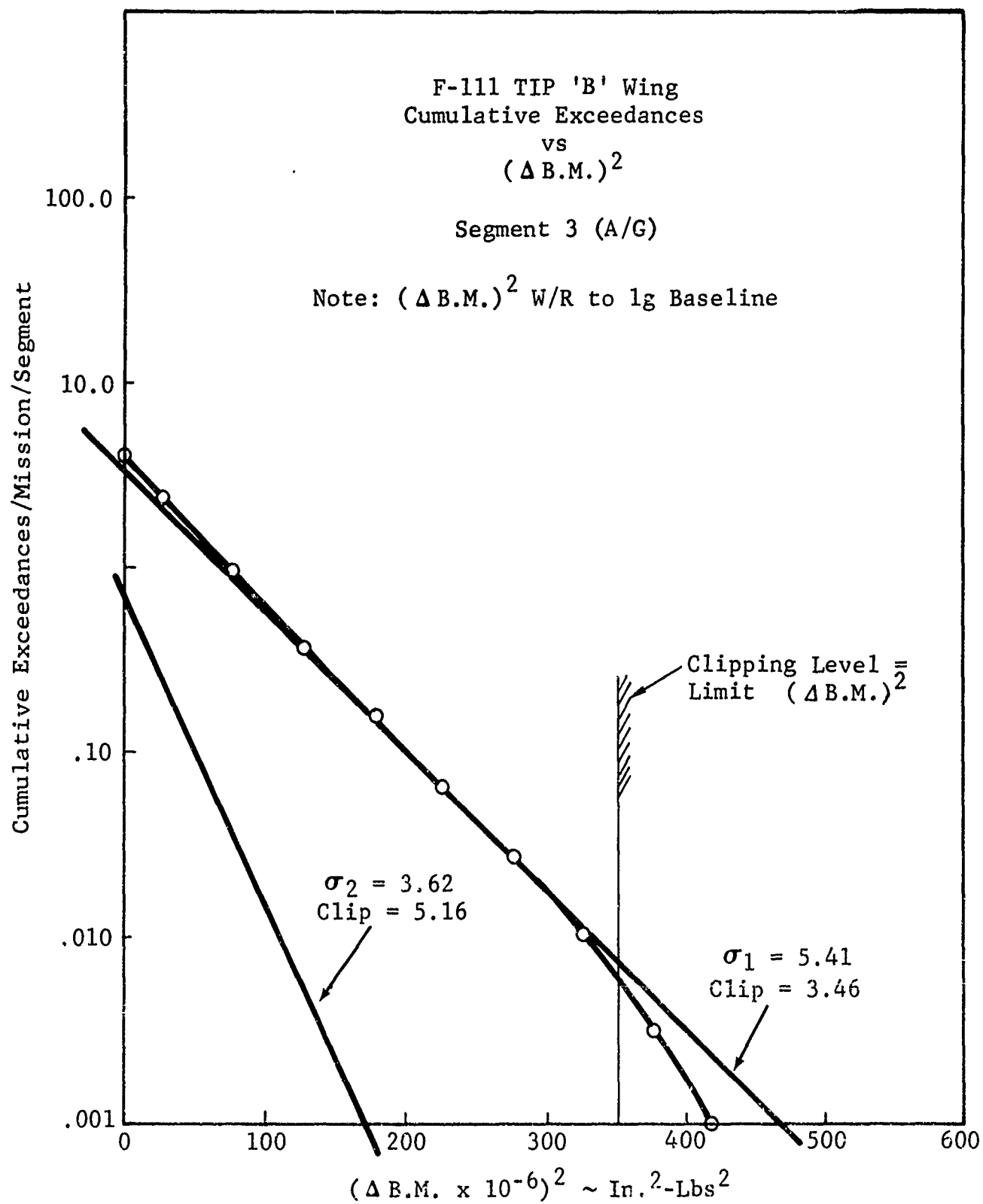


Figure 15 Exceedance Curve Mission Segment 3 (Air-to-Ground)



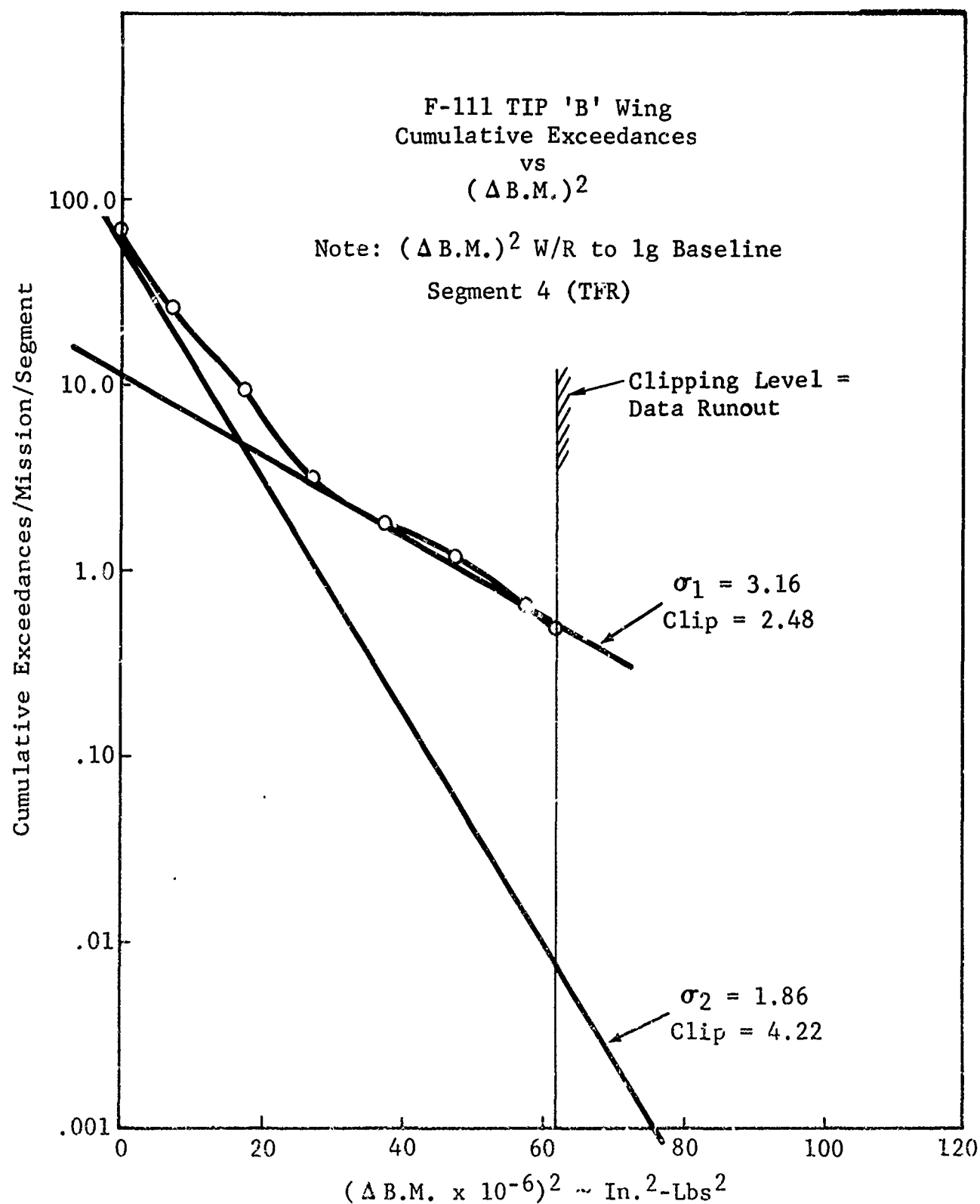


Figure 16 Exceedance Curve Mission Segment 4 (TFR)

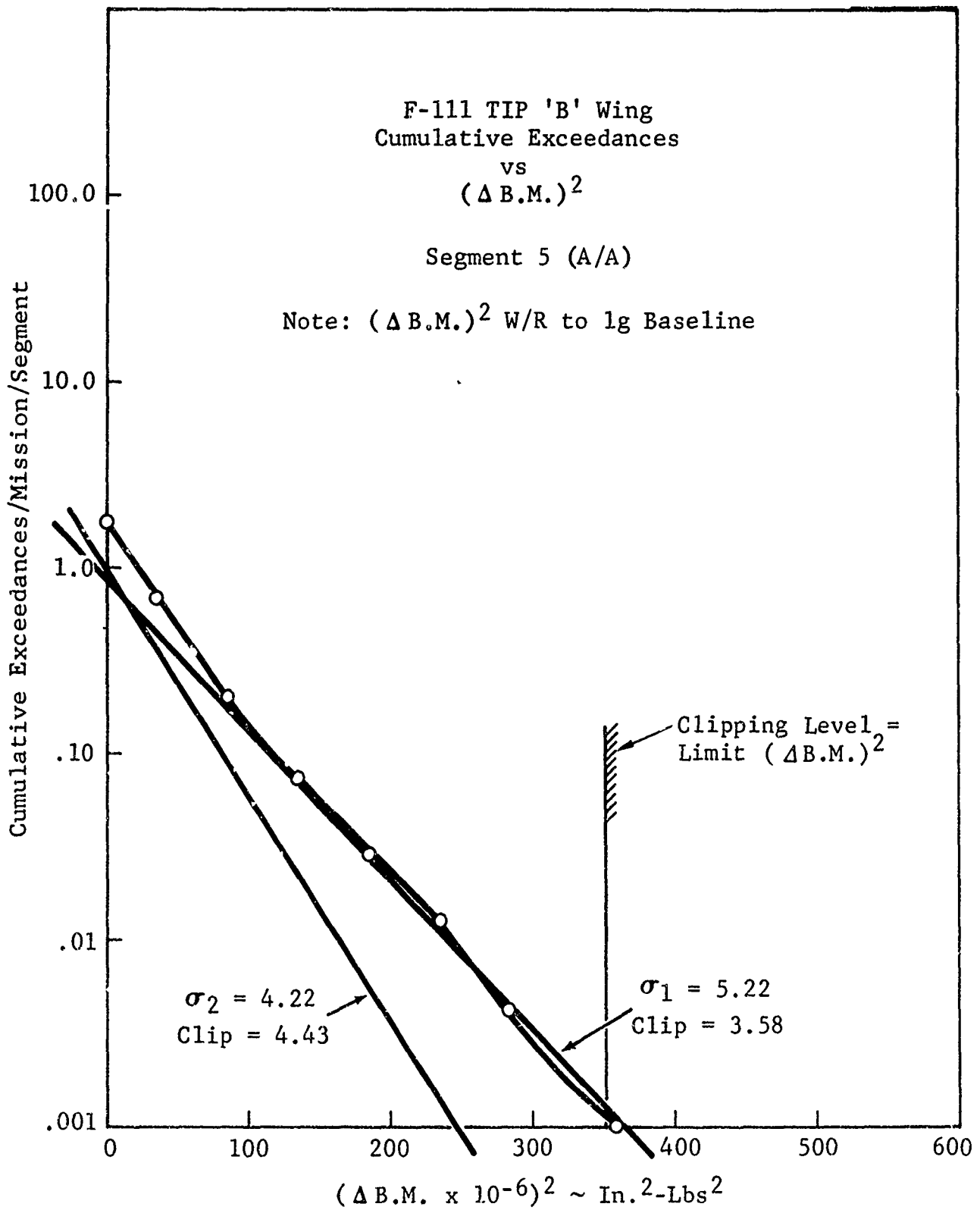


Figure 17 Exceedance Curve Mission Segment 5 (Air-to-Air)

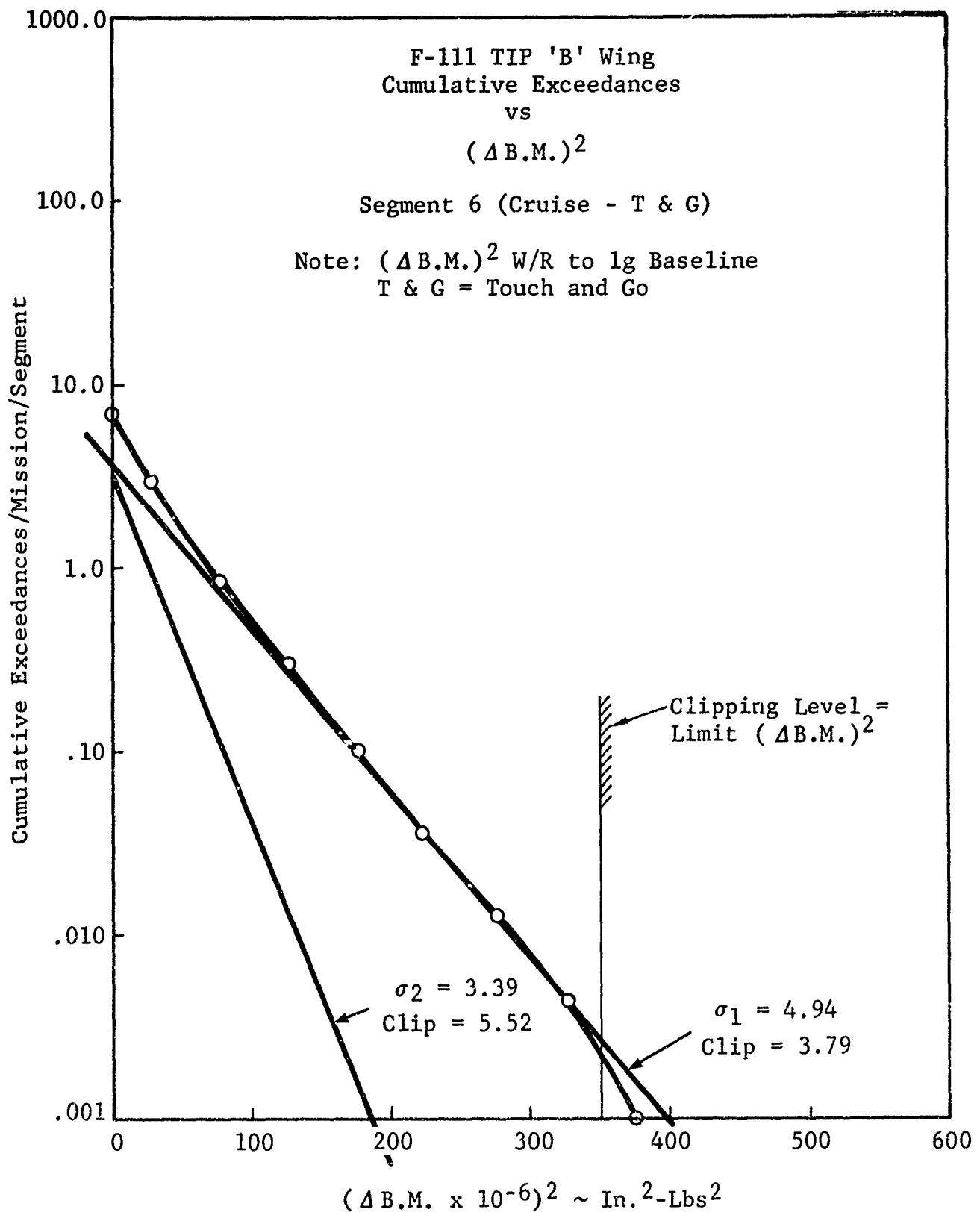


Figure 18 Exceedance Curve Mission Segment 6 (Cruise-T&G)

Table XI SUMMARY OF INPUT EXCEEDANCE DATA FOR RANDOM LOAD HISTORY SIMULATION

Mission Segment No.	RMS Level	$X_{ir}$	$F(X_{ir})$	$X_{il}$	$F(X_{il})$	$\sigma_{RMS}$	Clipping Value	$N P_{oi}$	$P_i$ Distribution Factor
1	1+	318.0	0.01	0.0	7.0	4.93	3.80	7.0	1.0
	1-	318.0				4.93	3.80		
	2+	133.0				3.18	5.88		
	2-	133.0				3.18	5.88		
2	1+	44.5	2.0	10.0	15.0	3.27	2.33	7.97	0.5
	1-	44.5	2.0	10.0	10.0	3.27	2.33	7.97	0.5
	2+	50.0	0.1	14.0	20.0	1.84	4.14	78.49	0.5
	2-	50.0	0.1	14.0	20.0	1.84	4.14	78.49	0.5
	3+	10.0	0.001	3.0	1.0	0.71	10.7	19.31	1.0
	3-	10.0	0.001	3.0	1.0	0.71	10.7	19.31	1.0
	4+	44.5	2.0	10.0	10.0	3.27	2.33	7.97	0.5
	4-	44.5	2.0	10.0	10.0	3.27	2.33	7.97	0.5
	5+	50.0	0.1	14.0	20.0	1.84	4.14	78.49	0.5
	5-	50.0	0.1	14.0	20.0	1.84	4.14	78.49	0.5
3	1+	295.0	0.02	120.0	0.4	5.41	3.46	3.12	1.0
	1-	295.0	0.02	120.0	0.4	5.41	3.56	3.12	1.0
	2+	170.0	0.001	50.0	0.1	3.62	5.16	0.68	1.0
	2-	170.0	0.001	50.0	0.1	3.62	5.16	0.68	1.0
4	1+	60.0	0.56	10.0	6.9	3.16	2.48	3.80	0.333
	1-	60.0	0.56	10.0	6.9	3.16	2.48	3.80	0.333
	2+	66.0	0.004	28.0	1.0	1.86	4.22	29.23	0.5
	2-	66.0	0.004	28.0	1.0	1.86	4.22	29.23	0.5
	3+	60.0	0.56	10.0	6.9	3.16	2.48	3.80	0.333
	3-	60.0	0.56	10.0	6.9	3.16	2.48	3.80	0.333
	4+	66.0	0.004	28.0	1.0	1.86	4.22	29.23	0.5
	4-	66.0	0.004	28.0	1.0	1.86	4.22	29.23	0.5
	5+	60.0	0.56	10.0	6.9	3.16	2.48	3.80	0.333
	5-	60.0	0.56	10.0	6.9	3.16	2.48	3.80	0.333
5	1+	328.0	0.002	40.0	0.4	5.22	3.58	0.83	1.0
	1-	328.0	0.002	40.0	0.4	5.22	3.58	0.83	1.0
	2+	246.0	0.001	100.0	0.06	4.22	4.43	0.99	1.0
	2-	246.0	0.001	100.0	0.06	4.22	4.43	0.99	1.0
6	1+	330.0	0.004	120.0	0.3	4.94	3.79	3.54	1.0
	1-	330.0	0.004	120.0	0.3	4.94	3.79	3.54	1.0
	2+	186.0	0.001	80.0	0.1	3.39	5.52	3.23	1.0
	2-	186.0	0.001	80.0	0.1	3.39	5.52	3.23	1.0

5. Truncation levels,

upper =  $17.0 \times 10^6$  in, lb  
lower =  $1.7 \times 10^6$  in, lb

6. No GAG cycles

7. Maximum clipping value =  $\pm 6.0$

8. RMS correction factor = 1.1347

The exceedance data for characterizing the exceedance curve of Figures 13 through 18 are summarized in Table XI. Shown in this table are:

1. Mission segment numbers
2. Number of positive and negative RMS levels and the order in which they are used in the random load simulation
3. Coordinates for the RMS levels depicted in the exceedance curves for each mission segment type
4. RMS, clipping ratio, and  $N_0 P_i$  values for each RMS level of each mission segment
5. Distribution of time spent in each RMS level.

Applications of the input data and various aspects of the generation procedure are discussed in the following section.

#### 4.3.2 Application of Input Data

The RMS values shown in Table XI were determined using the method of Press (Appendix I). The random load history was generated, load-by-load, using the RMS values in the order listed in Table XI.

In mission segments 1, 3, 5, and 6, all loads were generated for a given RMS value (positive and negative spectra) before going to a different RMS value. The total time spent in these segments, on a  $N_0 P_i$  basis, was small compared to mission segments 2 and 5 (TFR and A/A respectively). For mission segments 2 and 5, the RMS values were not completely decomposed at the same time; instead, the time spent in each RMS value was distributed so that RMS values could be partially decomposed rather than all at once.

The total time spent in a given RMS level is still preserved for each mission segment (Table XI).

An  $N_0/N_p$  value of 0.85 was assumed because of the lack of wave form data. This value is based on F-111 load experience.

No GAG cycles were used in the random load simulation; however, the computer program of Reference 26 has the capability to include such cycles in the load simulation.

A correction factor of 1.1347 was applied to the input RMS values so that the output exceedances and RMS values would match the input data. The correction factor was determined by fitting a fifth degree polynomial through the results, for a simplified case, based on  $N_0/N_p = 0.0, 0.2, 0.4, 0.6, 0.8, \text{ and } 1.0$ .

In generating the test signal, the random numbers were alternately multiplied by positive and negative numbers. For the Gaussian case ( $N_0/N_p = 0.0$ ) there is an equal probability of selecting a positive or negative delta load. The sign alteration is deterministic but the random numbers have an equal probability of being positive or negative. Without some compensation, the procedure generates an actual  $N_0/N_p = 0.5$  for the Gaussian case. Therefore, a load signal adjustment is required to preserve the input exceedances. No adjustment is required when  $N_0/N_p$  equals one (Rayleigh case).

The correction factor, in effect, requires that a greater number of loads be created to simulate the load history. The use of such a factor was justified in this case since the output exceedances agreed with the input exceedances and the essential wave form,  $N_0/N_p$ , was preserved.

#### 4.3.3 Statistical Analysis of Load Simulation

A statistical analysis was performed to justify the random load-history simulation for the actual load history. A composite cumulative exceedance curve (Figure 19) was plotted for the positive spectra using the data of Table XII. The composite cumulative exceedances were determined by summing the ordinates to the cumulative exceedance curves of Figures 13 through 18 for given  $(\Delta B.M.)^2$  values. The resulting cumulative exceedances are summarized in Table XIII.

The BY4 computer program generates random loads one at a time and stores them. Subroutines are employed which count

Table XII DATA FOR ACTUAL COMPOSITE EXCEEDANCE CURVE

(ΔB.M. $\times 10^{-6}$ )	Segment						Cumulative Exceedances (Total)	Remarks
	1	2	3	4	5	6		
0	14.5	190.0	4.0	70.0	1.8	7.0	287.3	(1g Baseline)
20	7.0	13.5	2.7	6.9	1.1	3.8	35.0	
40	4.0	2.9	1.8	1.6	.64	2.2	13.14	
60	2.5	1.0**	1.2	.55**	.38	1.4	7.03	
80	1.5	--	.89	--	.24	.8	3.43	
100	1.0	--	.60	--	.15	.53	2.28	
120	.63	--	.42	--	.097	.35	1.497	
140	.40	--	.29	--	.07	.22	.980	
160	.27	--	.21	--	.048	.15	.678	
180	.17	--	.15	--	.035	.094	.449	
200	.12	--	.11	--	.025	.061	.316	
220	.08	--	.075	--	.016	.040	.211	
240	.054	--	.051	--	.011	.027	.143	
260	.036	--	.037	--	.0067	.017	.0967	
280	.024	--	.026	--	.0044	.013	.0674	
300	.016	--	.018	--	.0028	.008	.0448	
320	.0098	--	.012	--	.0018	.0051	.0287	
340	.0062	--	.0078	--	.0014	.0030	.0184	
360	.0038	--	.0049	--	.0010	.0009*	.0106	
380	.0024	--	.0029	--	--	--	.0053	
400	--	--	.0017	--	--	--	.0017	
420	--	--	.00095*	--	--	--	.00095	

B.M. = Resultant wing bending at SS 70.3

\* = Estimated value beyond truncation level

\*\* = TFR loads are truncated as shown due to an automatic fly-up command that is g level limited.

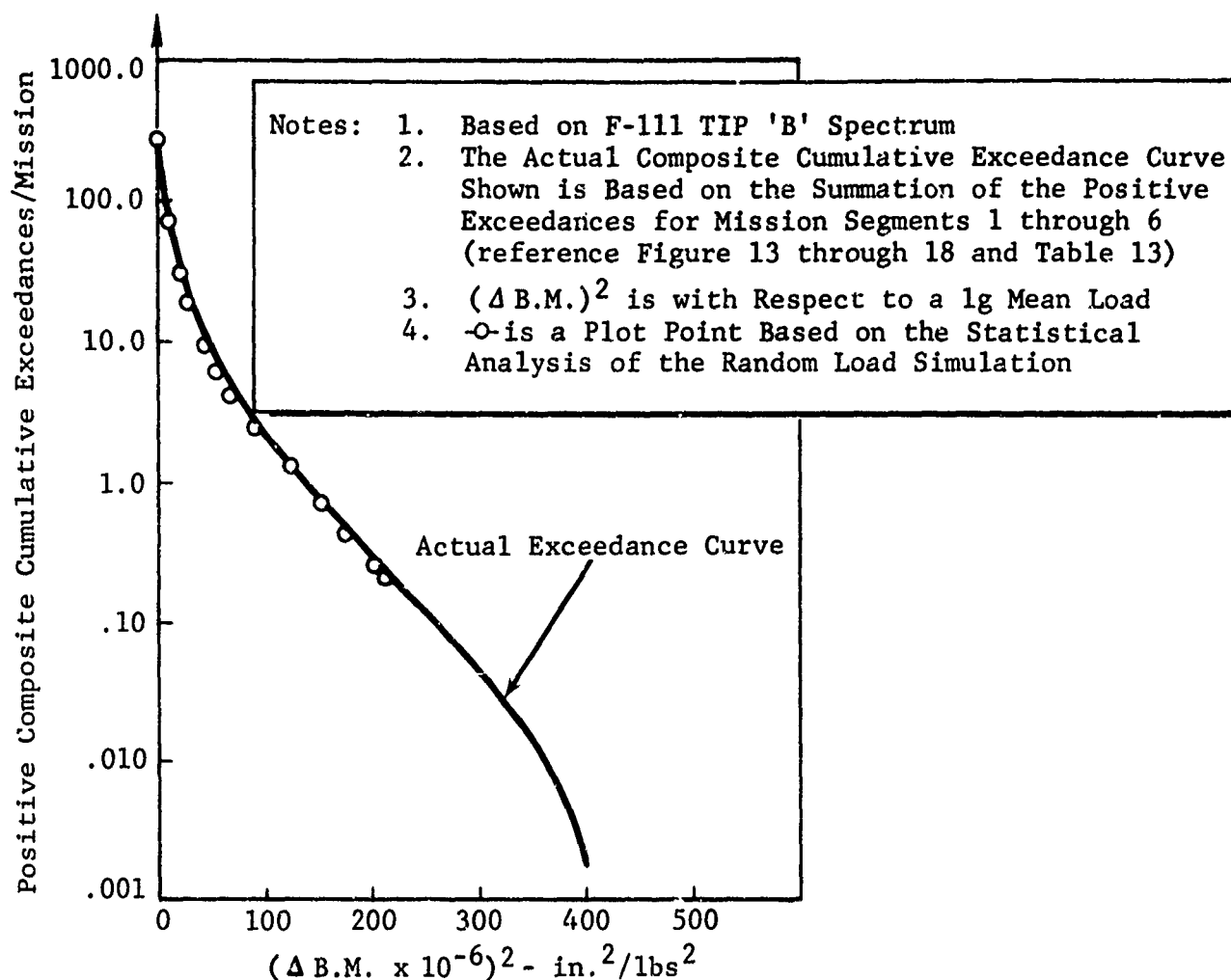


Figure 19 Comparison of Load Simulation Composite Cumulative Exceedances Versus Actual Exceedances

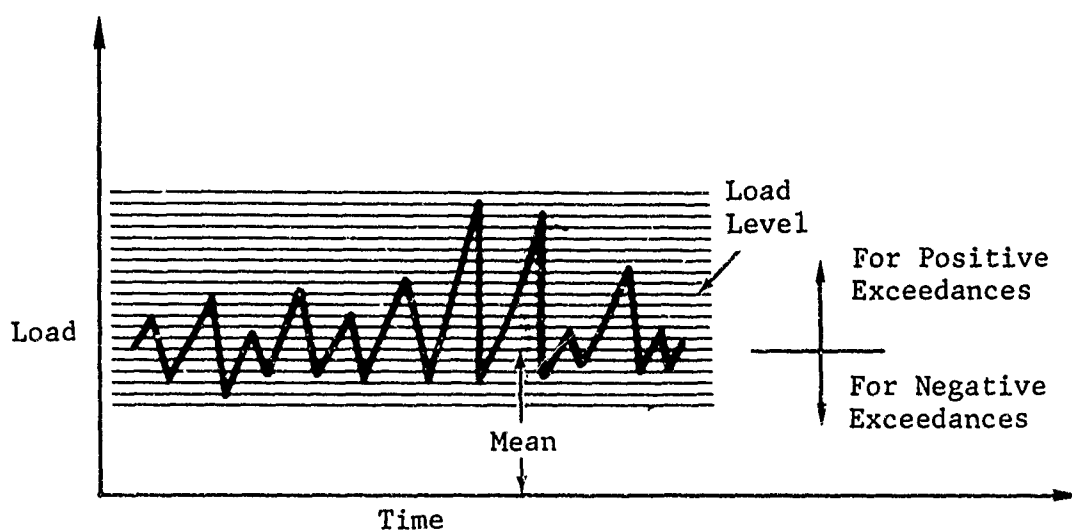


Figure 20 Random Load Statistics



Table XIII SUMMARY OF COMPOSITE CUMULATIVE EXCEEDANCES  
BASED ON STATISTICAL ANALYSES OF SIMULATED  
RANDOM LOAD TEST TAPE

$(\Delta B.M. \times 10^6)^2$	Composite Cumulative Exceedances/Mission <sup>a, b</sup>
0	289.79
0.16	277.78
0.667	252.44
1.520	221.02
2.723	187.09
4.272	154.54
6.165	124.11
8.410	97.08
11.002	74.27
13.943	56.53
17.223	42.39
20.857	31.89
24.840	24.55
29.160	18.76
33.840	14.66
38.860	11.94
44.22	9.59
49.94	7.69
56.01	6.03
62.41	4.92
69.22	4.19
76.21	3.57
83.72	2.98
91.58	2.46
99.60	2.12
108.16	1.79
117.07	1.53
126.11	1.32
135.72	1.01
145.68	0.829
155.75	0.715
166.41	0.579
177.42	0.448
188.51	0.349
200.22	0.268
212.28	0.202
224.40	0

Table XIII Summary of Composite Cumulative Exceedances  
Based on Statistical Analysis of Simulated  
Random Load Test Tape  
(Continued)

Notes: a. Obtained using computer program of Reference 26  
b. Statistics based on analysis of 119,991 load records  
from the test tape.

- Total number of load records on the test tape =  
873,465 (1 lifetime)
- Total number of positive load records on test tape =  
436,732 (1 lifetime)
- Equivalent number of positive load records for  
Rayleigh case ( $N_0/N_p$ ) = 383,258
- $N_0/N_p = \frac{383,258}{436,732} = 0.877$

1. The number of loads in the simulation
2. The positive slope crossings of the mean and at each load level crossed
3. The number of load exceedances at given load levels above and below the mean (Figure 20).

The load statistics are analyzed in batches of 40,000 loads. All loads on the tape can be analyzed by pooling the data for each load batch. A sample output of the load-time history simulation is shown in Figure 21. The exceedances, based on the load simulation for 1 mission and 300 missions, are also compared against the actual exceedances in this figure.

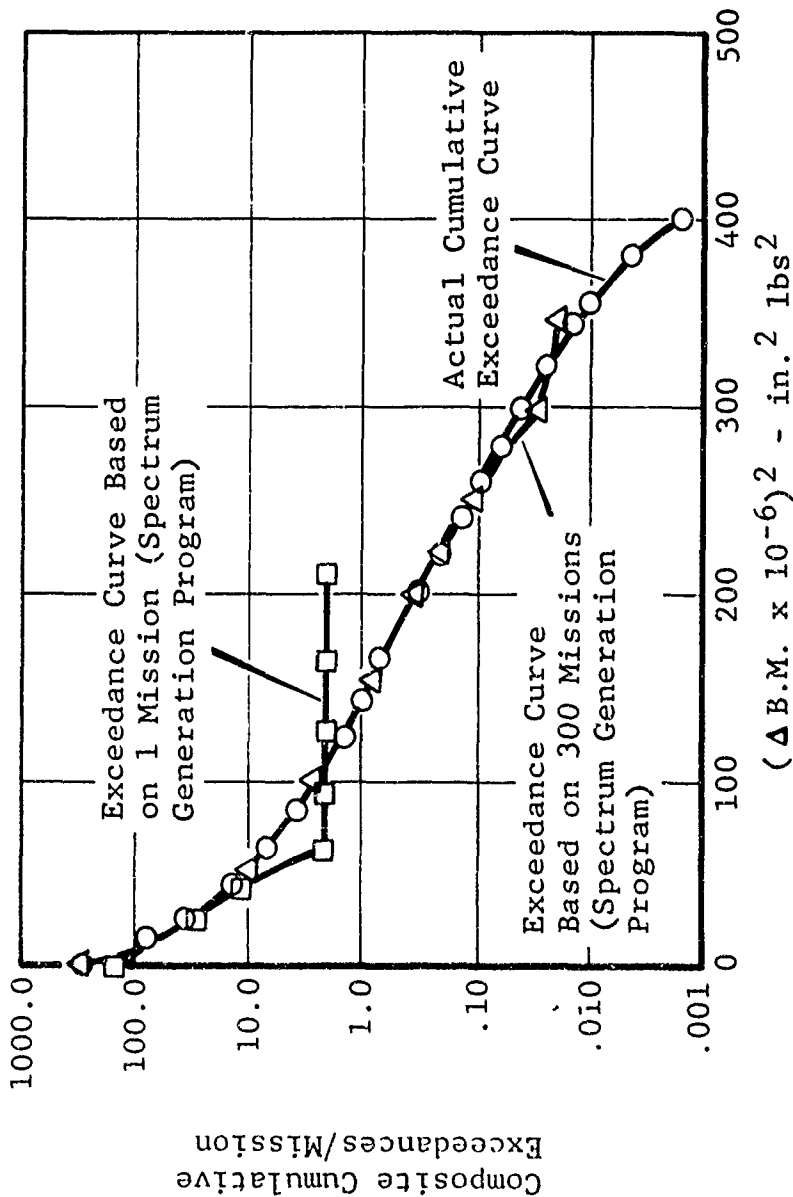
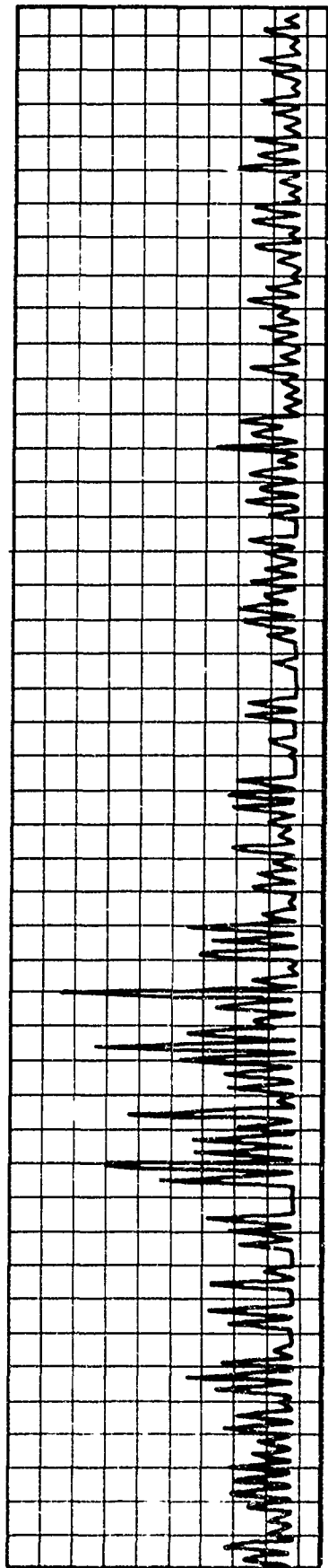
The composite cumulative exceedances, based on the statistical analysis of 119,991 loads on the test tape, are summarized in Table XIII. These results were generated using the BY4 computer program of Reference 26. To compare the simulated load history against the actual load history, the composite cumulative exceedances of Table XII were plotted against the actual cumulative exceedances (Figure 19). The agreement between the simulated load history and the actual load history, as shown in Figure 21, was excellent. A value of  $N_0/N_p$  equal to 0.877 was obtained for the simulated load history. This compares with an input value of 0.85.

It was concluded that the random load history simulation used was a valid representation of the actual load history.

#### 4.3.4 Test Tape

The random load history simulation (digital) is stored on a magnetic test tape. Successive loads on the tape are connected by a haversine wave form. The shape of the load signal is invariant and the amplitude is set by calibrating the maximum specimen load to the maximum signal peak. With this set-up, the same test tape can be used for different size specimens and components. The specimen load calibration procedure is discussed in subsection 4.4.

The test tape simulates one lifetime of random load history with 873,465 load records. The numbers of loads used in a test are counted and the lifetime is computed by dividing the number of loads used by 873,465 loads/lifetime. When all the loads have



Note:

- (1) F-111 TIP 'B' Wing Composite Cumulative Exceedances (Includes 6 Mission Segments) vs.  $(\Delta B.M.)^2$
- (2)  $(\Delta B.M.)^2$  W/R to lg Baseline

Figure 21 Composite Exceedance Correlation and Sample Random Load/Time Signal from Test Tape

been read on the test tape, the tape is rewound and the process is continued until the desired lifetime is reached or the specimen fails.

#### 4.4 SPECIMEN LOAD CALIBRATION

The loading signal must be calibrated with respect to the maximum bending moment on the tape and the desired maximum load on the specimen. Since the signal on the tape is scaled to the maximum peak, the signal can be calibrated for axial load, shear, torsion, etc. (separately).

The design limit (D.L.) load for the 1/5- and 1/2-scale specimens is 66.7K and 157.0K, respectively. The loading signal is calibrated to these loads. These maximum loads are called "100 percent calibration loads."

The 1/5-scale specimen was designed for a 100K ultimate load. The maximum limit load on this specimen is thus 66.7K. The 1/2-scale specimen 100 percent calibration load was determined using the 1/5-scale limit load and ratioing the 1/5- and 1/2-scale specimens cross-sectional areas as shown below.

$$P_{DL} \text{ (1/5 scale)} = 66.7K \text{ limit}$$

1/5-scale cross section: 5" wide by 40 plies thick

1/2-scale cross section: 5" wide by 94 plies thick

Both specimens have the same width; therefore, the calibration load for the 1/2-scale specimen can be computed by ratioing the number of plies for the 1/5- and 1/2-scale specimens.

$$P_{DL} \text{ (1/2 scale)} = \frac{94}{40} \times 66.7 = 157.0K$$

With the above calibration loads, each specimen is subjected to compatible stress histories. This puts the 1/5- and 1/2-scale specimens on the same baseline and allows a direct comparison of the fatigue results. This is important for evaluating the scaling effect.

The closed loop test system can be used to test different specimen sizes simultaneously using the same load type. The load signal is calibrated for each specimen using individual servo amplifiers.

A load truncation level was selected on the following basis:

1. Adequate excursions must be made to ensure a successful time trace for failures in time.
2. The truncation level does not exclude the series of damage producing high loads.

The truncation value would be exceeded once per five missions. This is equivalent to approximately 0.211 exceedances per mission (reference Table XII and Figure 19) or 280 exceedances per lifetime. This level ensures sufficient excursions to the peak load to develop an adequate lifetime distribution.

For this program, upper and lower truncation values of  $17.0 \times 10^6$  in# and  $1.7 \times 10^6$  in#, respectively, were assumed. These levels satisfy the criteria above. The limit wing root bending moment is  $20.8 \times 10^6$  in#. Using these values the maximum and minimum load on the 1/5- and 1/2-scale specimens was computed as shown below.

1/5 scale

$$P_{TRU} = \frac{17.0}{20.8} \times 66.7K = 54.5K$$

$$P_{TRL} = \frac{1.7}{20.8} \times 66.7K = 5.45K$$

1/2 scale

$$P_{TRU} = \frac{17.0}{20.8} \times 157.0K = 128.0K$$

$$P_{TRL} = \frac{1.7}{20.8} \times 157.0K = 12.8K$$

## SECTION V

### TEST PROGRAM EXECUTION

#### 5.1 INTRODUCTION

A description of the tests conducted and the results obtained are given in this section. The types of tests conducted are summarized in subsection 2.4.

#### 5.2 CONSTANT AMPLITUDE TESTS

In this subsection, the constant amplitude tests conducted are described and the results of these tests are summarized.

##### 5.2.1 Tension-Tension

The purpose of the tension-tension tests was to generate constant amplitude load versus cycles to failure data needed to predict the specimen fatigue life for a given loading spectrum based on Miner's rule. Twelve tests were performed using 1/5-scale specimen ( $R = 0.10$ ). Three sets of constant amplitude loading were used: (1) 3 to 30K, (2) 4 to 40K, and (3) 5 to 50K. Only one specimen (K012432) was tested using the 4 to 40K loading because of the failure of one of the titanium lugs under this loading. The lug cracked at one end of specimen K994567 under a 3 to 30K cyclic loading. The cracked lug problem is discussed in paragraph 5.2.3.

Each tension-tension specimen was mounted in fixture 5 as shown in Figure 22. Only specimens K012465 and K994567 had strain gauges, and these were read only for the strain surveys. The applicable cyclic loading was continuously applied to the specimen at 3 Hz until failure occurred. The specimens tested, the cyclic loading used, the cycles to failure, and the test completion dates are summarized in Table XIV. Photographs of typical failed specimens are included in Appendix IV.

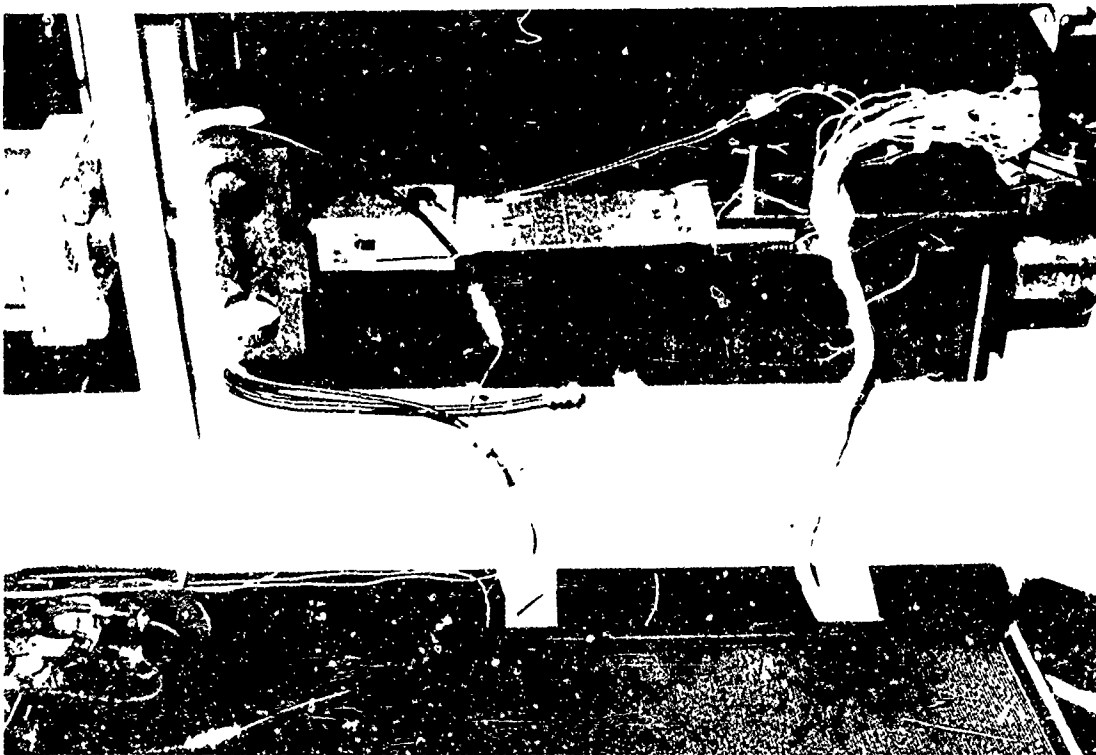


Figure 22 Setup for Constant Amplitude  
Tension-Tension Strain Survey

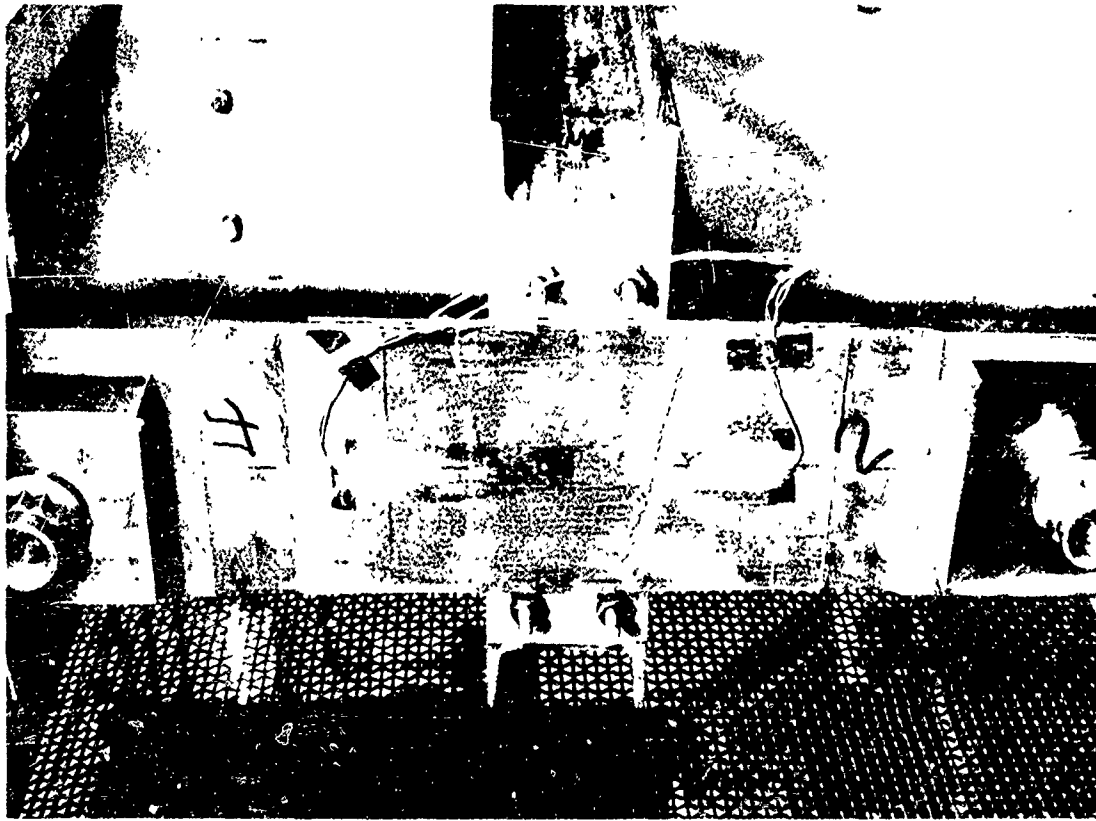


Figure 23 Tension-Compression Constant  
Amplitude Setup with Center  
Support Shown Removed



Table XIV SUMMARY OF 1/5-SCALE SPECIMEN  
CONSTANT AMPLITUDE LOADING TEST RESULTS

Specimen I.D.	Type Test	Cyclic Loading (KIPS)	Cycles To Failure	Test Complete Date
K994587fg	Tension-Tension ↑	3 to 30	202,667	3-22-71
K012444f		↓	113,938	3-24-71
K012461f		↓	1,296,000 <sup>a</sup>	4-15-71
K994567f		3 to 30	598,310 <sup>b</sup>	5-3-71
K012482		4 to 40	101,750 <sup>c</sup>	5-4-71
K012465f	↓	5 to 50	7,545	3-17-71
K994566d,f		↑	5,458	3-17-71
K012476g		↑	5,210	5-3-71
K012477g		↑	31,800	5-12-71
K012478g		↑	11,071	5-12-71
K012483g		↓	2,205	5-12-71
K900445fg		5 to 50	25,643	5-14-71
K012445	Tension-Compression <sup>e</sup>	-6 to 30	494,580 <sup>b</sup>	4-22-71
K012442fg	↑	-8 to 40	26,674	5-7-71
K994568fg	↓	-10 to 50	2,665	3-15-71
K012475fg		↑	1,790	5-6-71
K012438fg		↑	1,839	5-6-71
K012462fg		↓	3,193	5-10-71
K900442 g		-10 to 50	2,959	5-11-71

- Notes: a No specimen failure  
b Lug cracked out at one end  
c Complete lug failure at one end  
d Also used for strain survey  
e Specimen supported at the center by two channels with teflon rub strips next to specimen  
f Built prior to manufacturing procedure change for leveling the titanium lug ends in the tool (reference paragraph 3.3.2).  
g Photographs of failed specimens given in Appendix IV.

### 5.2.2 Tension-Compression

Tension-compression constant amplitude tests were performed to (1) characterize the fatigue life of the 1/5-scale specimens under load reversals and (2) compare the fatigue damaging effects of tension-tension versus tension-compression cyclic loading.

Press-fit bushings were used in the lug ends to minimize the "play" between the lugs and pins. This precaution was taken to protect the lugs against the dead space induced impact caused by load reversals.

Specimens were mounted in fixture 6 using the center support option. The center support was needed to stabilize the specimen under compressive load. The test set-up is the same as that shown in Figure 23 except specimen K994568 was the only one with strain gauges and these gauges were read only for the strain survey.

The tests were conducted using three sets of constant amplitude loading: (1) -6 to 30K, (2) -8 to 40K, and (3) -10 to 50K. The lug cracked at one end of specimen K012445. This problem is discussed in paragraph 5.2.3.

The test results are shown in Table XIV. Typical specimen failures are shown in Appendix II.

### 5.2.3 Lug Problem

Lug cracks developed in specimens K012445, K994567, and K012482. Two of the specimens are shown in Figures 24 and 25.

A fatigue analysis was performed with and without the effects of the press fit bushings ( $R = -0.20$ ) using Miner's rule. No lug failure could be justified by this analysis.

Similar lug failures have been observed at low stress levels in D6ac specimens (Reference 31). In this case, lug failures occurred at low stress levels even though the lug net section was more than ten times larger than the minimum cross section. This phenomenon was unexplainable, but it could be eliminated by increasing the lug net section stress.

To protect the titanium lugs, the cyclic load levels were increased from 3 to 30K to 5 to 50K and from -6 to 30K to -10 to 50K. Changing the cyclic loading did not affect the purpose of



Figure 24 Broken Lug for Specimen K994567

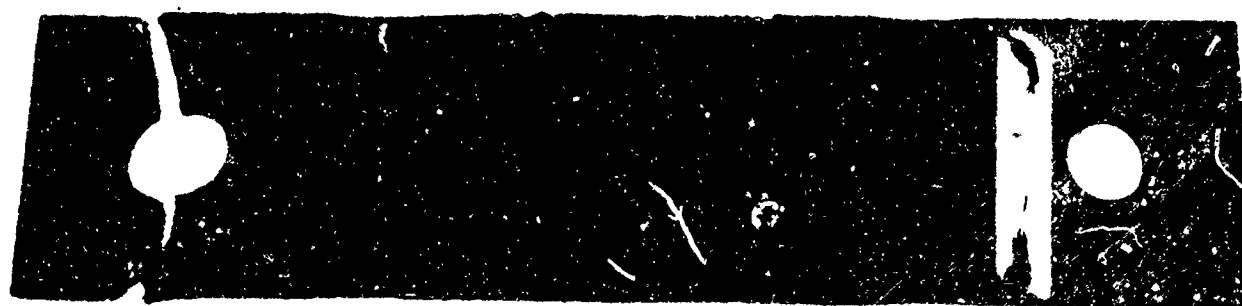


Figure 25 Broken Lug for Specimen K012482

the constant amplitude tests. No lug failures were experienced after these load changes. Cracked or failed lug ends were not repaired and reused in future specimens.

### 5.3 STATIC TESTS

Eleven 1/5-scale specimens were static tested using the Baldwin-Tate-Emery Universal test machine. Seven of the eleven specimens tested were previously rejected due to excessive warpage. Specimen K012440 was partially straightened by heating under load before the static test. The test set-up is shown in Figure 26 except only three specimens were instrumented.

The static test results are shown in Table XV for all specimens tested. The average failing load is given with and without the results for the rejected specimens. Pictures of typical failed specimens are shown in Figure 27.

### 5.4 RANDOM LOAD TESTS

Random load tests were performed to characterize the fatigue life of 1/5- and 1/2-scale specimens. The random load-history simulation (stored on magnetic tape) for the spectrum described in Section IV was used with the closed loop test system shown in Figures 3 and 4.

Residual strength tests and fatigue-to-failure tests were performed. The residual strength tests were conducted by first subjecting the specimen to a prescribed random load history simulating a fractional service lifetime and then determining the static strength of the specimen.

The desired random load history was put on the specimens using three test fixtures for the 1/5-scale specimens and one test fixture for the 1/2-scale specimens. The test system used permitted the simultaneous testing of three 1/5-scale specimens and one 1/2-scale specimen. When all fixtures were used simultaneously, a test rate between 3 and 4 Hz was possible. A 5 Hz test rate could be achieved with only one or two specimens. The number of fixtures used at the same time depended upon the specimen supply. Due to the specimen recycling time, only two or three specimens were usually tested at the same time. However, all fixtures were used during some periods.

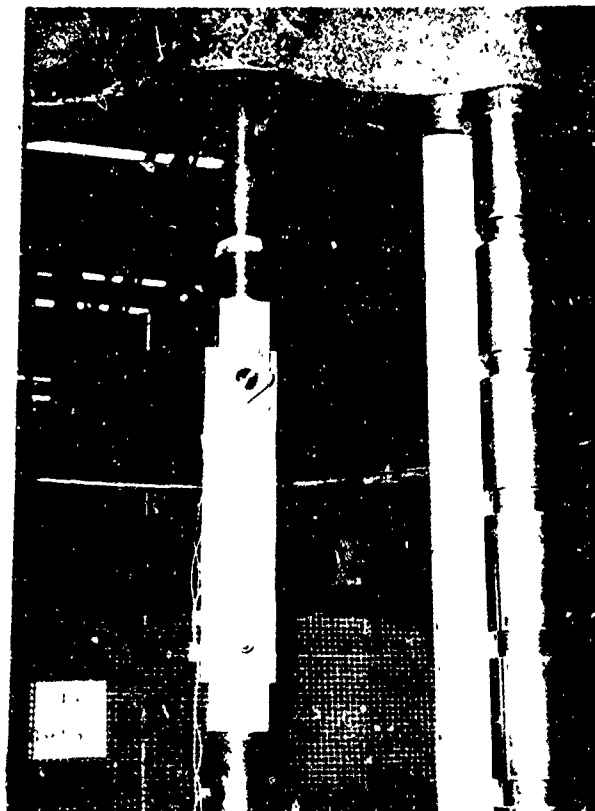


Figure 26 Set Up for Static Strain Survey

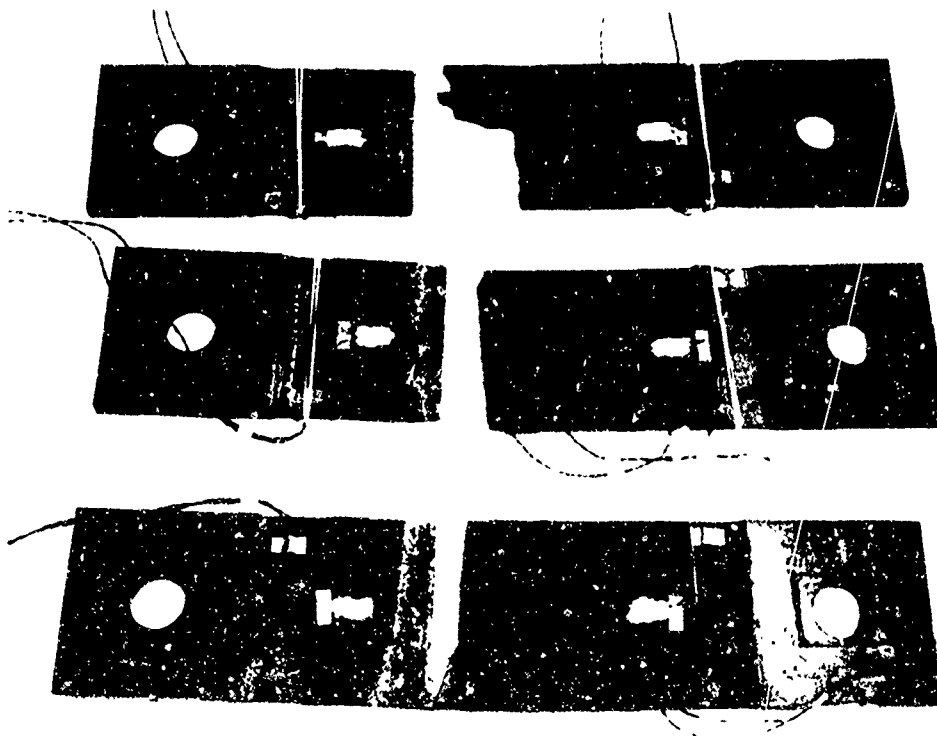


Figure 27 Typical 1/5-Scale Specimen Static Test Failures

Table XV SUMMARY OF 1/5 SCALE SPECIMEN  
STATIC TEST RESULTS

SPECIMEN <sup>c</sup> I.D.	Date Tested	Failing Load (KIPS)	Average Failing Load(KIPS)
K994588 d,e,f	3-17-71	86.6	↓ 100.9
K012439 d,e,f	3-17-71	109.8	
K012441 d,e,f	3-17-71	106.4	
K012440 <sup>a</sup>	3-30-71	119.0	↓ 105.5
K994578 <sup>b</sup>	4-14-71	89.2	↓ 102.7
K012459 <sup>b</sup>	↑	110.4	
K012446 <sup>b</sup>		111.2	
K012463 <sup>b</sup>		98.0	
K012437 <sup>b</sup>		108.5	
K012474 <sup>b</sup>		99.0	
K994569 <sup>b</sup>	4-14-71	92.0	

- Notes: a Specimen was straightened to reduce dimensional variations prior to testing
- b Rejected specimen with excessive dimensional variations
- c Specimen are listed in the order tested
- d Specimen also used for static strain survey
- e Built prior to manufacturing procedure change for leveling the titanium lug ends in the tool (ref. paragraph 3.3.2).
- f Photographs of failed specimens given in Appendix IV.

Details of the 1/5-scale and 1/2-scale specimen tests and the results are discussed in paragraphs 5.4.1 and 5.4.2 , respectively.

#### 5.4.1 One-Fifth Scale Specimens

##### 5.4.1.1 Residual Strength Tests

Residual strength tests were performed using specimens that were first subjected to a 1, a 10, and a 50 percent lifetime of random loading. The percentage lifetime load history is based on the use of a fractional amount of the total load records stored on the magnetic tape.

Thirty-one residual strength tests were performed. The specimen breakdown is as follows:

1. 5 at 1 percent lifetime
2. 6 at 10 percent lifetime
3. 20 at 50 percent lifetime.

The test set-up for the random loading is shown in Figure 22 (no strain gauges). A Baldwin-Tate-Emery Universal test machine was used to evaluate static strength. Table XVI summarizes the specimens used, the types of testing, the residual strengths, and the test completion dates. Photographs of typical specimen failures are included in Appendix IV.

##### 5.4.1.2 Fatigue-to-Failure Tests

Twenty fatigue-to-failure tests were conducted using the random load-history simulation described in Section IV. These tests were performed to determine the lifetimes of 1/5-scale boron-to-titanium double scarf adhesive bonded joints under random loading. This information was needed for a statistical data base.

For these tests, a specimen was placed in a fixture, as shown in Figure 22, and subjected to a continuous random loading until failure. The specimens used, the lifetimes to failure, and the test completion dates are shown in Table XVII. Photographs of typical specimen failure are presented in Appendix IV.

TABLE XVI SUMMARY OF 1/5 -SCALE SPECIMEN  
RESIDUAL STRENGTH TESTS AFTER RANDOM LOADING

Specimen <sup>f</sup> I.D.	Type Test	Residual Strength (KIPS)	Test Complete Date
K900448g	1% lifetime <sup>a</sup> ↑	104.4	5-20-71
K900441g		114.0	5-20-71
K904958g	↓	108.4	5-26-71
K905016g		109.1	5-26-71
K904955g	1% lifetime <sup>a</sup>	90.2	5-26-71
K900447g	10% lifetime <sup>b</sup> ↑	79.4	5-21-71
K904950g		105.0	5-21-71
K905017g	↓	110.6	5-26-71
K904957g		104.6	5-26-71
K904959g	10% lifetime <sup>b</sup> ↓	106.0	5-26-71
K905021		108.6	11-9-71
K900449g	50% lifetime <sup>c</sup> ↑	---- <sup>d</sup>	5-24-71
K900450g		115.6	5-24-71
K904951g	↓	73.5	5-26-71
K904952g		79.6	5-26-71
K904953g	↓	----	5-26-71
K904954g		86.0	6-1-71
K904956g	↓	106.0	↑
K905015g		96.0	
K905022g	↓	102.0	↓
K905023g		95.0	
K905018g	↓	110.0	6-1-71
K905020		111.9	11-9-71
K905362	↓	116.7	↑
K905363		110.4	
K905365	↓	111.0	↓
K905366		105.0	
K905369	↓	99.3	11-9-71
K905371		113.0	11-17-71
K905467	50% lifetime <sup>c</sup> ↓	103.5	11-17-71
K905469		92.5	11-17-71

- Notes: a Equal to 8735 records from random load tape  
b Equal to 87347 records from random load tape  
c Equal to 436,733 records from random load tape  
d Specimen failed at 308,230 records (35.3% lifetime)  
e Specimen failed at 347,577 records (39.8% lifetime)  
f Specimen are listed in the order tested for each type test.  
g Photographs of failed specimens given in Appendix IV.



Table XVII SUMMARY OF 1/5-SCALE SPECIMEN RANDOM  
LOADING FATIGUE-TO-FAILURE TEST RESULTS

Specimen I.D.	Records to Failure	Lifetime <sup>a</sup>	Test Complete Data
K012464 c,d	1,067,867	1.22	4-23-71
K012443 c,d	883,438	1.01	4-27-71
K994565	1,947,900	2.23	4-28-71
K012480d	296,434	0.34	5-7-71
K012479d	634,950	0.73	5-10-71
K012484d	401,362	0.46	5-12-71
K900443d	718,310	0.82	5-12-71
K012481d	633,168	0.73	5-14-71
K012485d	565,738	0.65	5-20-71
K900446	768,087	0.88	5-21-71
K905368	3,549,533	4.06	11-19-71
K905367	3,280,383	3.76	11-22-71
K905470	708,000	0.81	11-24-71
K905364	4,446,134 <sup>b</sup>	5.07	12-1-71
F504622	1,227,120	1.40	12-7-71
F504418	2,112,026	2.41	12-16-71
K905468	3,203,241	3.66	12-19-71
F504421	2,885,579	3.30	12-21-71
F504419	1,256,040	1.43	1-4-72
F504417	1,108,994	1.27	1-6-72

Notes: a One lifetime = 873,465 records (one time through the random load tape)

b Random load test was stopped and specimen was static tested to 109.5K

c Built prior to manufacturing procedure change for leveling the titanium lug ends in tool (ref. paragraph 3.3.2).

d Photographs of failed specimens given in Appendix IV.

#### 5.4.2 One-Half Scale Specimens

Five 10-percent lifetime residual strength tests and five fatigue-to-failure tests were performed. The tests employed the same random load history (with a different load calibration than the 1/5-scale specimens to maintain the same stress level in both specimens) and procedure used for the 1/5-scale specimens. The test set-up for putting the random loading on the specimens and performing the fatigue-to-failure tests is shown in Figure 28. These tests were conducted to make a preliminary evaluation of the scaling effect between the 1/5- and 1/2-scale specimens.

The residual strength and the fatigue-to-failure test results are given in Tables XVIII and XIX, respectively. Typical specimen failures are shown in Appendix V.

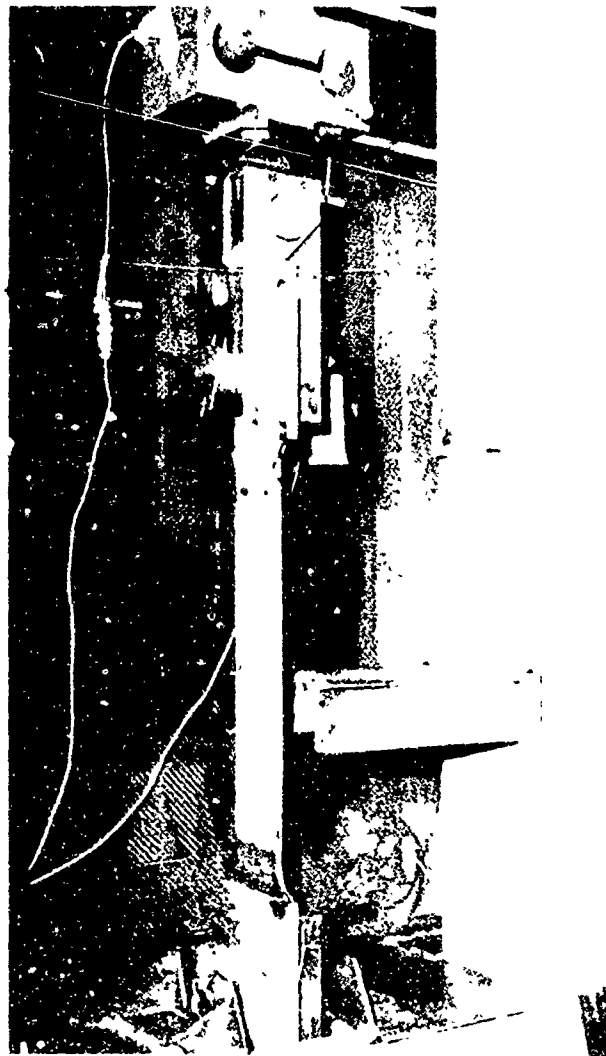


Figure 28 Setup for 1/2 Scale Specimen Tests

Table XVIII SUMMARY OF 1/2-SCALE SPECIMEN  
RESIDUAL STRENGTH TESTS AFTER RANDOM LOADING (10% LIFETIME)<sup>a</sup>

Specimen I.D.	Residual Strength (KIPS)	Test Complete Date
K012453	236.5	12-3-71
K012454	240.0	12-3-71
F504624b	168.5	2-8-72
F504625b	206.0	2-8-72
F504618b	219.0	2-8-72

- Notes:
- a Equal to 87347 records from random load tape. Test fixture number 12 used for random loading.
  - b Photographs of failed specimens given in Appendix V.

Table XIX SUMMARY OF 1/2-SCALE SPECIMEN RANDOM  
LOADING FATIGUE-TO-FAILURE TEST RESULTS

SPECIMEN I.D.	RECORDS TO FAILURE	LIFETIME <sup>a</sup>	TEST COMPLETE DATE
F504620	450,258	0.57	12-10-71
F504622 b	685,366	0.78	12-23-71
F504619 b	387,884	0.44	12-30-71
F504621 b	198,220	0.23	1-4-72
F504623 b	730,151	0.84	1-13-72

Notes: a One lifetime = 873,465 records (one time through the random load tape). Test fixture number 12 used for random loading.

b Photographs of failed specimens given in Appendix V.

## SECTION VI

### EVALUATION OF TEST RESULTS

The test results compiled from the tests described in Section V are analyzed in this section.

An assessment of Miner's rule for computation of life under random loadings was made. The major portion of the test program was devoted to evaluation of the lifetime/residual strength characteristics of the 1/5- and 1/2-scale bonded joints. These evaluations included residual strength and lifetime distribution functions and an evaluation of scale effects.

#### 6.1 FATIGUE ANALYSIS FOR ONE-FIFTH SCALE SPECIMEN

A fatigue analysis, based on Miner's linear damage rule, is presented in this section for the 1/5-scale specimen. This analysis employs a load versus cycles to failure curve based on static and constant amplitude fatigue tests and the same loading spectrum used for the random load test tape. The predicted fatigue life is compared against the mean lifetime obtained for the 1/5-scale fatigue-to-failure tests (Reference Table XVII). This comparison is used to evaluate the effectiveness of Miner's rule for predicting the fatigue life of composite bonded joints.

##### 6.1.1 Procedure Used

The fatigue analysis is based on the following procedure:

1. Divide up the cumulative exceedance curve versus  $\Delta$  B.M. into six segments as shown in Figure 29. Determine the total bending moment for each segment using,

$$(B.M.)_i = (\Delta B.M.)_i + 2.1$$

where  $(B.M.)_i$  = total bending moment ( $\times 10^{-6}$  in.#)  
at the wing root for segment i.

$(\Delta B.M.)_i$  = delta bending moment measured from  
the vertical axis of Figure 10 to the  
center of segment i.

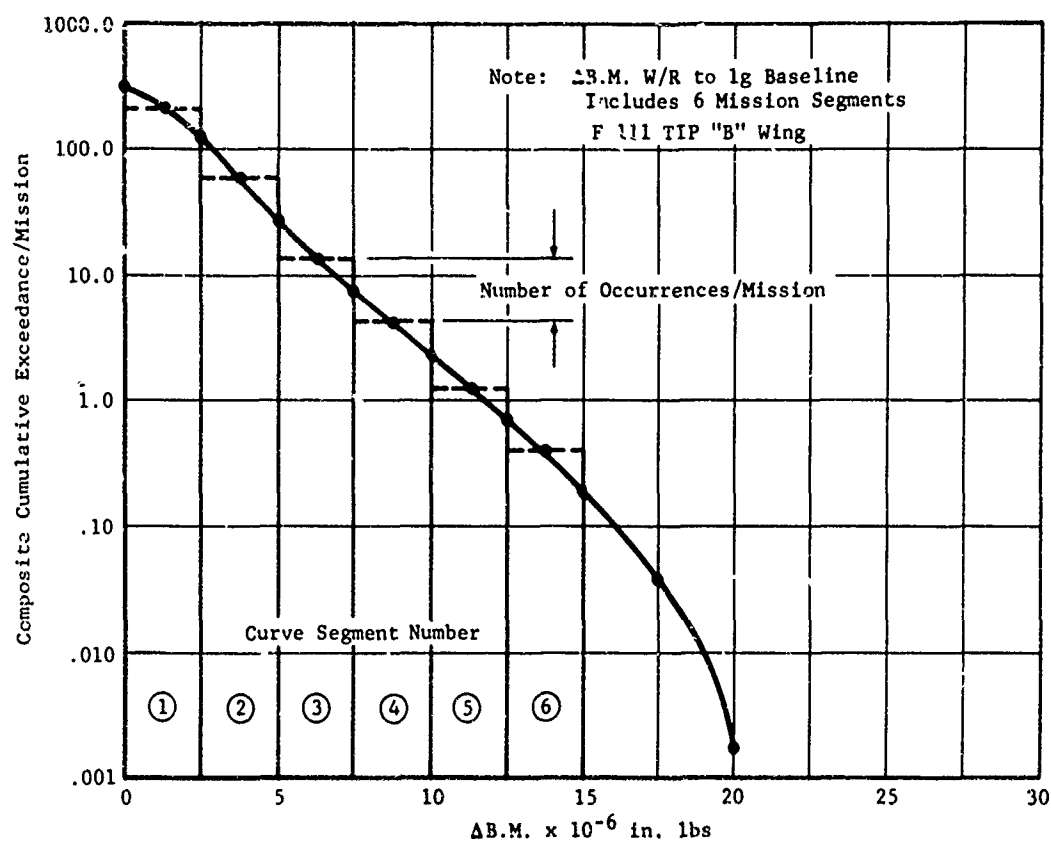


Figure 29 Composite Cumulative Exceedances Vs.  $\Delta B.M.$

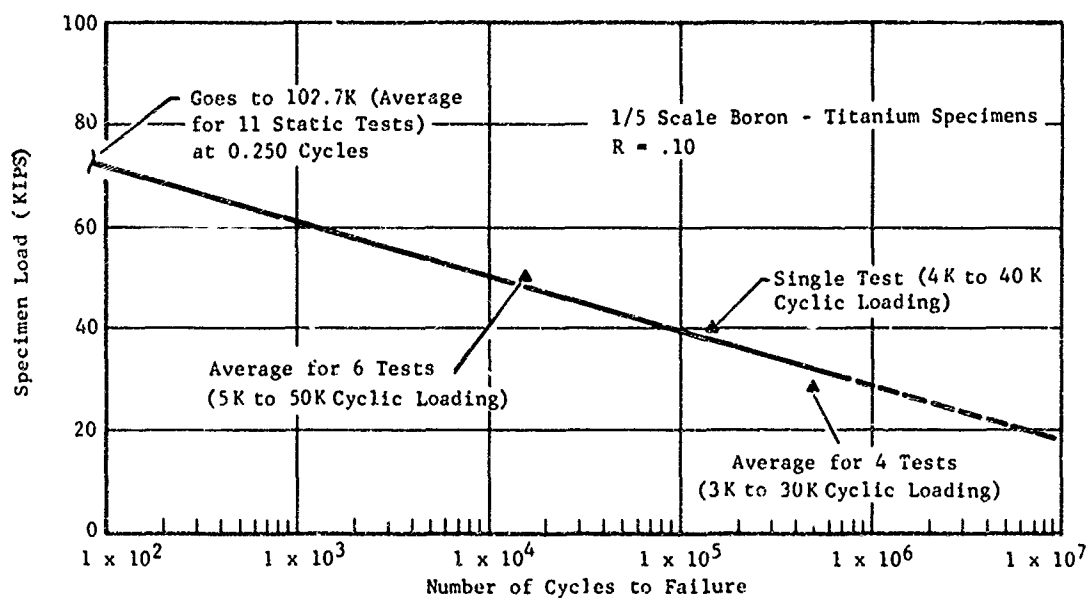


Figure 30 Load Vs. Cycles to Failure

2.1 = bending moment ( $\times 10^{-6}$  in.#) at the wing root of lg.

The total maximum limit bending moment at the wing root is  $20.8 \times 10^6$  in. lbs. An upper truncation bending moment of  $17.0 \times 10^6$  in. lbs was used for the test tape; therefore, the last segment in Figure 29 is at  $14.9 \times 10^6$  in. lbs ( $14.9 + 2.1 = 17.0$ ). The lower truncation bending moment for the test tape was  $1.7 \times 10^6$  in. lbs.

2. Using Figure 29, determine the total number of times per mission that the bending moment for each segment occurs. The total number of occurrences is equal to the difference between the ordinates of the curve shown in Figure 29 at the beginning and end of each segment. The total number of cycles ( $n_i$ ) for a given bending moment is equal to the total number of occurrences for each segment. There are 1334 missions in a lifetime. The total number of occurrences in a lifetime, for a given bending moment, is equal to 1334 times the number of occurrences per mission.

3. Determine the load on the specimen for each segment shown in Figure 29 using

$$P_{load} = \frac{(B.M.)_i \times 66.7K}{20.8}$$

where 66.7K is the limit load for the 1/5-scale specimen. A  $P_{load}$  value is computed for each segment shown in Figure 29.

4. Develop a load versus cycles to failure curve using the test results summarized in Table XIV. This curve is shown in Figure 30.
5. Determine the number of cycles ( $N_i$ ) to failure using Figure 30, corresponding to the  $P_{load}$  value for each segment shown in Figure 29.
6. The fatigue damage for each segment of Figure 30,  $(\frac{n_i}{N_i})$ , is determined separately and then summed to get the total fatigue damage  $\sum \frac{n_i}{N_i}$ . The predicted fatigue

life of the 1/5-scale fatigue-to-failure specimen is computed as follows:

$$\text{Fatigue Life} = \frac{1}{\sum \frac{n_i}{N_i}}$$

### 6.1.2 Fatigue Life Computations Using Miner's Rule

The fatigue analysis performed is shown in Table XX. The results are evaluated in paragraph 6.2.3 to determine the effectiveness of Miner's rule for predicting the fatigue life of bonded composite joints under random load.

### 6.1.3 Effectiveness of Miner's Rule

A fatigue life of 5.12 lives was predicted for the 1/5-scale fatigue-to-failure specimen based on Miner's rule. This compares with a mean lifetime of 1.812 (Reference Table XVII) based on twenty 1/5-scale fatigue-to-failure specimens subject to a random fatigue loading (Test Tape). Miner's rule in this case overpredicts the fatigue by a factor of 2.82.

The predicted fatigue life, based on the analysis presented, should be a conservative prediction (shorter life) in view of the following:

1. The analysis conservatively assumes that one random load occurrence is equivalent to one load cycle. The definition of a load cycle is not clear for a random loading. If one assumes three random loads constitutes one load cycle, then an equivalent number of load cycles can be computed using

$$N_E = \frac{n_i - 1}{2}$$

where  $N_E$  = equivalent number of load cycles (Reference Figure 31).

$n_i$  = total number of loads in random history

$n_i - 1$  = number of 1/2 load cycles.



Table XX FATIGUE ANALYSIS FOR 1/5-SCALE FATIGUE-TO-FAILURE SPECIMEN  
BASED ON MINER'S RULE

Segment No.	EXN <sub>Li</sub>	EXN <sub>Ri</sub>	(EXN <sub>Li</sub> - EXN <sub>Ri</sub> )	n <sub>i</sub>	(B.M.) <sub>i</sub>	( $\frac{B.M.}{20.8}$ ) <sub>i</sub>	P <sub>load</sub> (KIPS)	N <sub>i</sub>	$\frac{n_i}{N_i}$
1	290	120	170	226,780	3.35	0.160	10.7	>10 <sup>7</sup>	0.023
2	120	26	94	125,396	5.85	0.281	18.8	7 x 10 <sup>6</sup>	0.018
3	26	7.8	18.2	24,279	8.35	0.402	26.8	1.3 x 10 <sup>6</sup>	0.019
4	7.8	2.2	5.6	7,470	10.85	0.521	34.8	2.6 x 10 <sup>5</sup>	0.029
5	2.2	0.73	1.47	1,961	13.35	0.641	42.8	5.2 x 10 <sup>4</sup>	0.038
6	0.73	0.22	0.51	680	15.8	0.760	50.5	1.0 x 10 <sup>4</sup>	0.068

Predicted life for 1/5run-out specimen =  $\frac{1}{0.195} = 5.12$  lives

$$\sum \frac{n_i}{N_i} = 0.195$$

- Notes: 1. EXN<sub>Li</sub> - EXN<sub>Ri</sub> = occurrences per mission
2. n<sub>i</sub> = (EXN<sub>Li</sub> - EXN<sub>Ri</sub>) x 1334 = No. of cycles per lifetime
3. (B.M.)<sub>i</sub> = ΔB.M. + 2.1
4. N<sub>i</sub> obtained from Figure 30 for given P<sub>load</sub> value.
5. Reference discussion in paragraph 6.2.3.

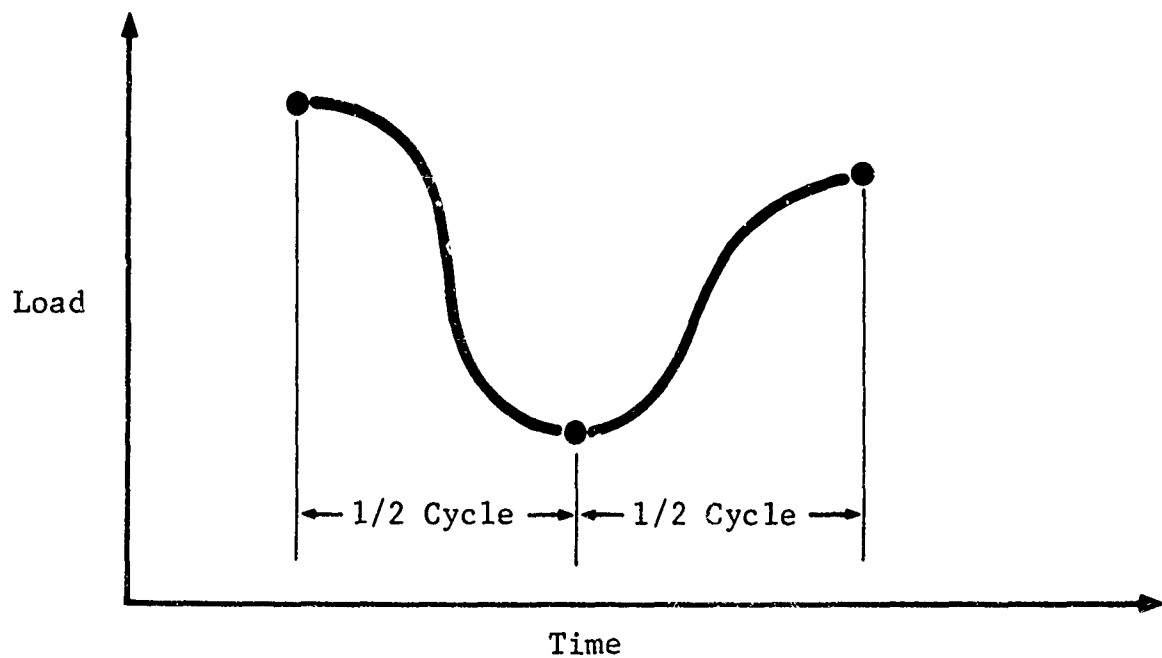


Figure 31 Equivalent Random Load Cycle

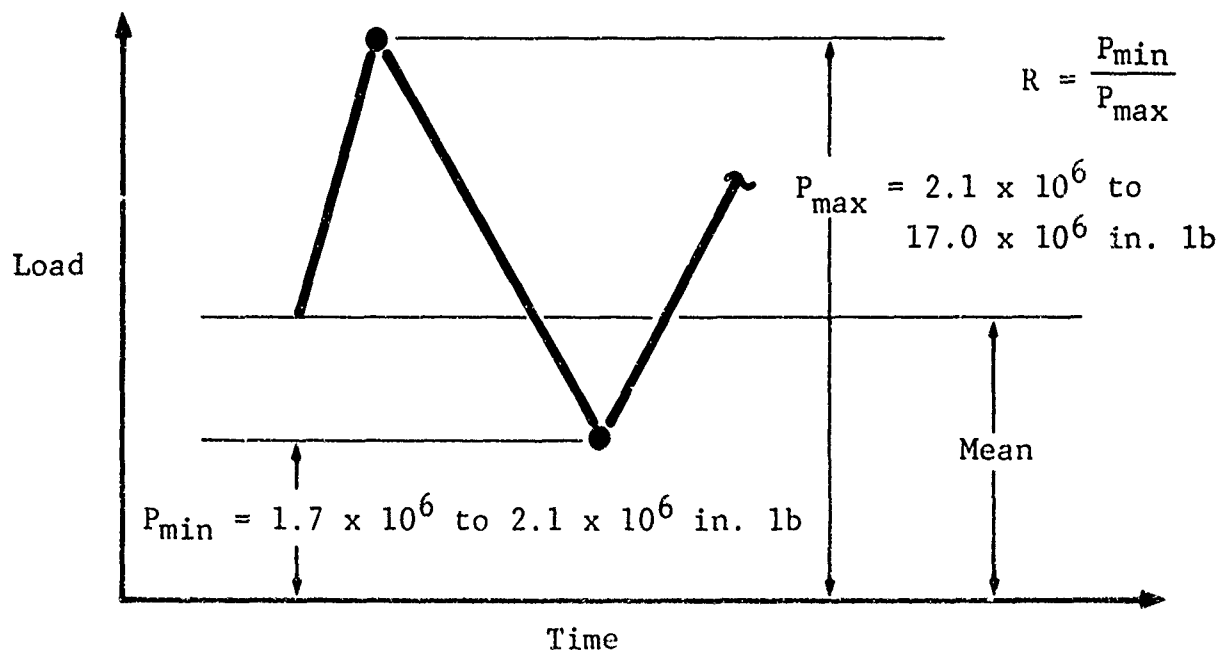


Figure 32 Stress Ratio (R) Variation for Random Load Test Tape

If the equivalent load cycle concept is used in the fatigue analysis, less fatigue damage would result; consequently, a longer fatigue life would be predicted.

2. The stress ratio,  $R$  (minimum stress/maximum stress in a fatigue cycle), for the equivalent random load cycle is larger over the load history (more positive) than  $R$  for the constant amplitude cycles. The test tape random load history had a mean of  $2.1 \times 10^6$  in. lbs with an upper and lower truncation of  $17.0 \times 10^6$  in. lbs respectively. The range of possible values for  $P_{\max}$  and  $P_{\min}$  is  $2.1 \times 10^6$  in. lbs to  $17.0 \times 10^6$  in. lbs and  $1.7 \times 10^6$ , respectively. This means that  $R$  is equal to 0.10 only when  $P_{\max}$  and  $P_{\min}$  are equal to the truncation value in the load cycle. The other possible ratios of  $P_{\max}$  to  $P_{\min}$  will be greater than 0.10 over the service history (Figure 32).

Fatigue damage decreases as  $R$  increases (becomes more positive). Since the fatigue-to-failure specimens for the random fatigue loading experienced  $R$  values greater than 0.10 during testing, they should exhibit a longer fatigue life than the case where  $R$  is a constant 0.10 during testing. The 2.82 factor between the predicted fatigue life, based on Miner's rule, and the actual mean life obtained by random testing is considered to be low in view of the discussion above.

The results presented in this section indicate that Miner's rule is inadequate for predicting the fatigue life of bonded composite joints under random loading.

## 6.2 EVALUATION OF THE RANDOM FATIGUE DATA

Two steps were executed in the reduction of the random fatigue data. First, the load and lifetime traces were plotted on Weibull coordinates to observe correlation of the observations with a Weibull distribution. Second, a first-order analysis of the observed phenomena was made on the basis of a damage growth hypothesis. Positive correlation has been achieved with the damage growth model.

The ranked raw data is given in the following tables:

1. Pooled static and 1 percent lifetime data  
1/5 scale - Table XXI

Table XXI RANKING OF POOLED STATIC AND 1% LIFETIME DATA  
FOR 1/5-SCALE SPECIMENS

Specimen	Test	P (KIPS)	Rank ( $r_a$ )	Probability of Failure $\frac{r_a}{n+1}$
K012440	S	119.0	16	0.941
K900441	1%	114.0	15	0.883
K012446	S	111.2	14	0.824
K012459	S	110.4	13	0.765
K012439	S	109.8	12	0.706
K905016	1%	109.1	11	0.647
K012437	S	108.5	10	0.588
K904958	1%	108.4	9	0.529
K012441	S	106.4	8	0.471
K900448	1%	104.4	7	0.412
K012474	S	99.0	6	0.353
K012463	S	98.0	5	0.294
K994569	S	92.0	4	0.236
K904955	1%	90.2	3	0.177
K994578	S	89.2	2	0.118
K994588	S	86.6	1	0.059

Notes: S = Static test, 1% = 1% lifetime  
Mean Failing Load = 103.51K  
Reference Tables XV and XVI.

2. Ten percent lifetime residual strength data, 1/5 scale - Table XXII
3. Fifty percent lifetime residual strength data, 1/5 scale - Table XXIII
4. Lifetime data, 1/5 scale - Table XXIV
5. Ten percent lifetime data, 1/2 scale - Table XXV
6. Lifetime data, 1/2 scale - Table XXVI

Residual strength and/or lifetime was plotted against the probability of failure on Weibull paper for the applicable cases. Straight lines were drawn through each batch of data points (reference Figures 33, 34, and 35). It should be noted that the pooled static and one percent lifetime data randomly oscillate about the best fit lines. The high load tail of the 10 and 50 percent lifetime data is approximately linear; however, the low outliers do not fit the same line. This factor is significant in the second pass data reduction. A summary of the least squares fit Weibull data is tabulated in Table XXVII.

### 6.3 RESIDUAL STRENGTH CHARACTERIZATIONS

Numerous cumulative damage theories have been developed for metallic materials. The design problem encountered by using these various theories, which include Miner's rule, is that a design based on only theory can consistently expect more than a decade of disagreement between the theoretical life and the empirically observed life. In addition, application of a theory such as Miner's rule requires a very large data base for the material under consideration. Such a data base is available for certain types of metallic materials, but only limited data has been developed for advanced composite materials. Classically, development of a large data base requires establishing static and fatigue S/N data for several stress concentrations and stress ratios. A data base development approach such as this would not be economically feasible for advanced composite materials because the "tailoring" capability of the basic lamina allows for too many possible laminate configurations to characterize in the classical manner. Thus, either lack of funds to generate a large data base or lack of confidence in current cumulative damage theories to predict life could be reasons to justify investigation of a new method for characterizing cumulative damage.

Table XXII RANKING OF 10% LIFETIME DATA FOR  
1/5-SCALE SPECIMENS

Specimen	Residual Strength (KIPS)	Rank ( $r_a$ )	Probability of Failure $\frac{r_a}{n+1}$
K905017	110.6	6	0.857
K905021	108.6	5	0.715
K904959	106.0	4	0.571
K904950	105.0	3	0.428
K904957	104.6	2	0.286
K900447	79.4	1	0.143

Notes:  $n$  = Number of specimen ranked

Mean Residual Strength = 102.37K

Reference Table XVI.

Table XXIII RANKING OF 50% LIFETIME DATA FOR  
1/5-SCALE SPECIMENS

Specimen	Residual Strength (KIPS)	Rank ( $r_a$ )	Probability of Failure $\frac{r_a}{n+1}$
K905362	116.7	20	0.954
K900450	115.6	19	0.905
K905371	113.0	18	0.857
K905020	111.9	17	0.810
K905365	111.0	16	0.762
K905363	110.4	15	0.715
K905018	110.0	14	0.667
K904956	106.0	13	0.619
K905366	105.0	12	0.571
K905467	103.5	11	0.524
K905022	102.0	10	0.476
K905369	99.3	9	0.428
K905015	96.0	8	0.381
K905023	95.0	7	0.333
K905469	92.5	6	0.286
K904954	86.0	5	0.238
K904952	79.6	4	0.191
K904951	73.5	3	0.143
K900449	<sup>a</sup> 54.5	2	---- <sup>b</sup>
K904953	<sup>a</sup> 54.5	1	---- <sup>b</sup>

Notes: <sup>a</sup>Maximum load in spectrum

<sup>b</sup>Specimen failed before reaching a 50% lifetime

n = Number of specimen ranked

Mean Residual Strength = 101.5K (Excluding K900449 & K904953)

Reference Table XVI.

Table XXIV RANKING OF FATIGUE-TO-FAILURE DATA  
FOR 1/5-SCALE SPECIMENS

Specimen	Lifetime	Rank ( $r_a$ )	Probability of Failure $\frac{r_a}{n+1}$
K905364	5.07	20	0.954
K905368	4.06	19	0.905
K905367	3.76	18	0.857
K905468	3.66	17	0.810
F504421	3.30	16	0.762
F504418	2.41	15	0.715
K994565	2.23	14	0.667
F504419	1.43	13	0.619
F504622	1.40	12	0.571
F504417	1.27	11	0.524
K012464	1.22	10	0.476
K012443	1.01	9	0.428
K900446	0.88	8	0.381
K900443	0.82	7	0.333
K905470	0.81	6	0.286
K012479	0.73	5	0.238
K012481	0.73	4	0.191
K012485	0.65	3	0.143
K012484	0.46	2	0.095
K012480	0.34	1	0.048

Notes: n = Number of specimen ranked  
Mean lifetime = 1.812  
Reference Table XVII.



Table XXV RANKING OF 10% LIFETIME DATA FOR  
1/2-SCALE SPECIMENS

Specimen	Residual Strength (KIPS)	Rank ( $r_a$ )	Probability of Failure $\frac{r_a}{n+1}$
K012454	240.0	5	0.834
K012453	236.5	4	0.666
F504618	219.0	3	0.500
F504625	206.0	2	0.333
F504624	168.5	1	0.167

Notes:  $n$  = number of specimen ranked

Mean residual strength = 214.0K

Reference Table XVIII

Table XXVI RANKING OF FATIGUE-TO-FAILURE DATA  
FOR 1/2-SCALE SPECIMENS

Specimen	Lifetime	Rank	Probability of Failure $\frac{r_a}{n+1}$
F504623	0.84	5	0.834
F504622	0.78	4	0.666
F504620	0.57	3	0.500
F504619	0.44	2	0.333
F504621	0.23	1	0.167

Notes:  $n$  = Number of specimen ranked

Mean lifetime = 0.572

Reference Table XIX

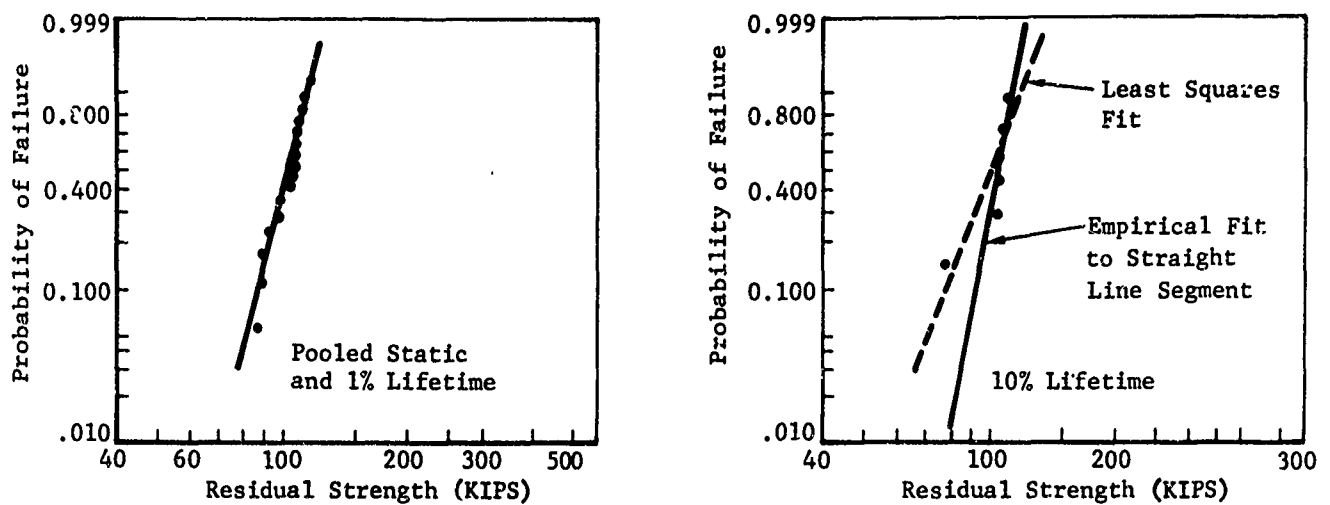


Figure 33 Probability of Failure Versus Residual Strength Plot on Weibull Paper for 1/5 Scale Static and 10% Lifetime

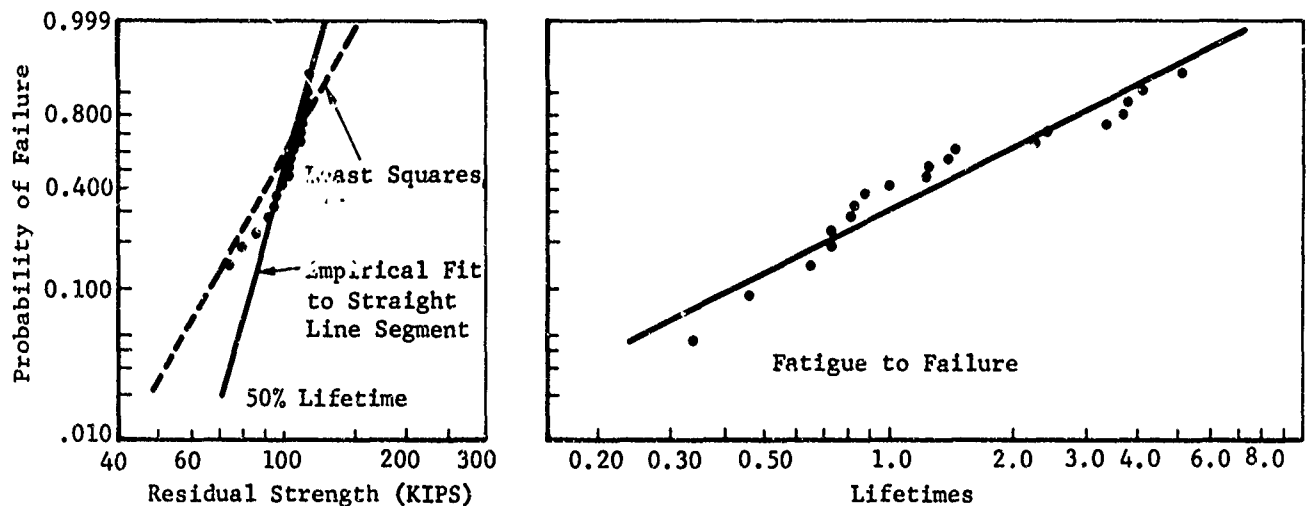


Figure 34 Probability of Failure Versus Residual Strength and/or Lifetime Plot on Weibull Paper for 1/5 Scale 50% Lifetime and Fatigue to Failure

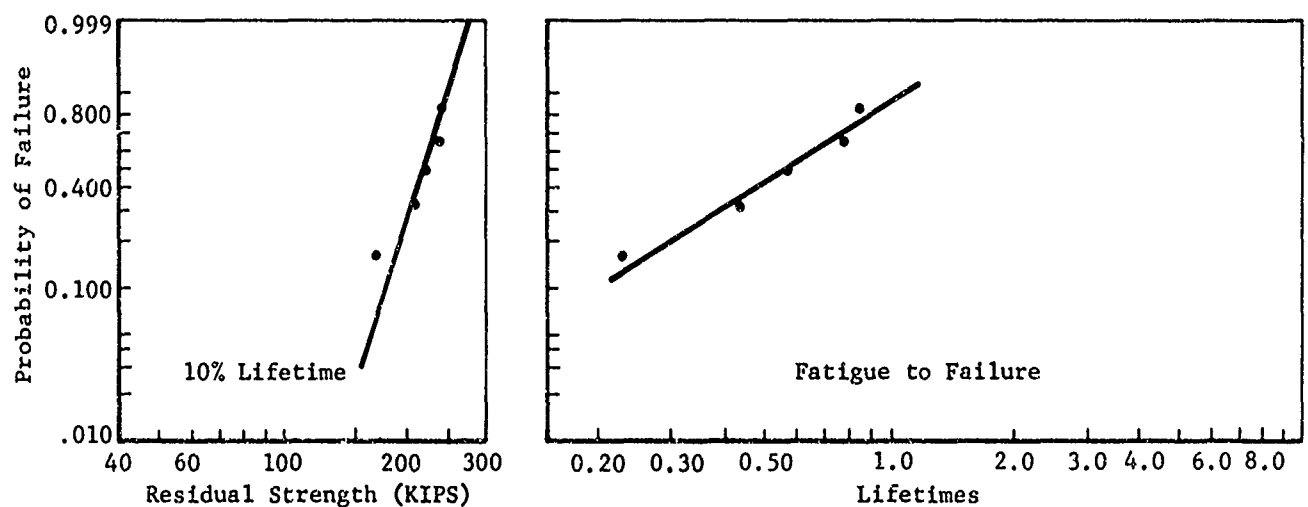


Figure 35 Probability of Failure Versus Residual Strength and/or Lifetime Plot on Weibull Paper for 1/2 Scale 10% Lifetime and Fatigue to Failure

Table XXVII SUMMARY OF WEIBULL PARAMETERS FITTED TO  
1/5-AND 1/2-SCALE TEST RESULTS

Test	Scale	Number of Specimens	Weibull Parameters <sup>b</sup>			Reference Table
			$\alpha$	$\beta^c$	$\gamma_s$	
Static	1/5	16 <sup>a</sup>	11.58	108.0	11%	XXI
10% Lifetime	1/5	6	7.38	108.9	16%	XXII
50% Lifetime	1/5	20	4.94	105.8	23%	XXIII
Fatigue-to-Failure	1/5	20	1.44	1.99	68%	XXIV
10% lifetime	1/2	5	7.05	227.6	17%	XXV
Fatigue-to-Failure	1/2	5	1.95	0.67	53%	XXVI

Notes: a Data pooled for eleven static and five 1% lifetimes.

b Based on procedure described in Section VII.

c See Appendix VII to account for the least-of-two scale effects

The Weibull distribution seems to fit the high probability of failures rather well; however, the lower probabilities of failure tend to deviate from the straight line on the Weibull plots (Figures 33, 34, and 35). The straight line through the data points on the Weibull paper must be extended beyond the data to the probability of failure level desired. Extrapolated results on this basis have a degree of uncertainty. If the data points, at the lower probability of failure levels, tend to curve away from the vertical axis on the Weibull plot, then the straight line extrapolation at the lower end should be conservative. The curvature of the first failure and of the residual strength distributions correlates with the proposed wearout model.

The slope of the straight line through the data plotted on the Weibull paper decreased with lifetime. Since  $\alpha$  decreases as the slope decreases, the coefficient of variation (or scatter) increases. The slopes of the straight lines through the 10 percent lifetime data on the Weibull plot for the 1/5- and 1/2-scale specimens were approximately equal (Figures 33 and 35). The same tendency was observed for the 1/5- and 1/2-scale fatigue-to-failure cases. For the 10 percent lifetime case,  $\alpha$  was 7.38 and 7.05 for the 1/5- and 1/2-scale specimens, respectively (Table XXVII). In the fatigue-to-failure case,  $\alpha$  was 1.44 and 1.95 for the 1/5- and 1/2-scale specimens, respectively. Although a limited number of specimens were used, the results imply that  $\alpha$  is independent of specimen size. The shape parameter can be defined using a given number of small scale tests and the same value can be applied to different specimen sizes. The mean residual strength or mean lifetime can be defined for the larger specimens with a limited number of tests. The scaling factor between the different specimen sizes can be determined by applying the  $\alpha$  for the small specimen to the larger specimen and using the respective mean values.

The fatigue-to-failure data for the 1/5-scale specimens were pooled and assumed to represent a homogeneous population. Analysis of the data showed that the specimens fabricated and tested before 5-21-71 and those fabricated and tested after 11-19-71 (after a six-month program delay) indicated that the population was not homogeneous. The sign test (a nonparametric test, Reference 32) indicates only a 0.0107 chance of the fatigue-to-failure data being from a single population. Analysis of each data set, assuming a Weibull distribution, yielded the following results:

1. Specimens fabricated and tested before 5-21-71,  $\alpha_f = 2.07$  and  $\hat{t} = 1.03$

2. Specimens fabricated and tested after 11-19-71,  $\alpha_f = 1.75$  and  $\hat{t} = 3.14$ .

The trend was for average fatigue lifetime to increase in time, which is suggestive of a learning curve.

Even though the empirical data seemed to segregate into two groups, the data were pooled for final analysis. Two reasons are used to justify the decision:

1. In the analysis of laminate data, Reference 33, it was determined that an unconservative analysis of the specimen variation would be obtained if batch-to-batch variation was not included.
2. The test program was designed to provide reliability data relevant to the production design of large-scale bonded joints and the batch-to-batch variation is a significant portion of the expected production variability.

Although the effect of the fatigue shape parameter is significant, the pooled value of  $\alpha_f = 1.44$  is conservative.

All of the remaining analyses were executed with the assumption of a homogeneous fatigue-to-failure population.

#### 6.4 RESIDUAL STRENGTH - LIFETIME DISTRIBUTION BASED UPON PROPAGATION OF INITIAL FLAWS

It has been postulated (Reference 34) that flaw growth can be characterized in terms of residual strength capacity; hence, life and residual strength distributions are related by a flaw-growth equation to the initial static distribution. In this format, the specification of the reliability of structural component requires the definition of a residual strength-lifetime and lifetime-maximum load relationship. The empirical determination of these relationships was obtained through simulated service testing using the closed loop, digitally controlled random fatigue facility.

A detailed fracture mechanics analysis of the test specimen has not been exercised. All experimental observations have been made with respect to the residual strength capacity of the joints,  $F_R(t)$ . A summary of the 1/5-scale random fatigue data is shown in Table XXVII. A significant broadening of the residual strength can be seen.

The bonded joint is heterogeneous enough to defy precise definition of the microscopic stress field and geometry of the flaw field. It is assumed that the dispersion of filaments in the polymer matrix combined with voids and other micro-defects may be represented by a flaw field  $C$  (where  $C$  is a symbolic representation of a dispersion of flaws). Rivlin and Thomas (Reference 35) proposed that during the quasi-static growth of a flaw at which the external work change is zero that the change in the free energy of deformation is given by

$$-\frac{1}{t_h} \left[ \frac{\partial W}{\partial C} \right] = T \quad (1)$$

where

$W$  = strain energy  
 $T$  = characteristic tearing energy  
 $t_h$  = reference thickness.

The criterion is similar in form to Griffith's (Reference 36), but  $T$  is not a surface-free energy. The structure will remain stable until the following inequality is violated

$$-\frac{1}{t_h} \left[ \frac{\partial W}{\partial C} \right] = T < T_c \quad (2)$$

where  $T_c$  is the critical energy associated with fracture and is a material property. If the structure is elastic, a first-order approximation to the energy available to drive the flaw becomes

$$T \propto CW \propto C \frac{F^2}{K} \quad (3)$$

where

$K$  = specimen stiffness  
 $F$  = applied load.

The instability condition becomes equivalent to the Griffith condition:

$$F_R \sqrt{C} \propto \sqrt{KT_c}. \quad (4)$$

An engineering approximation to the fatigue crack growth problem may be gained by extending the quasi-static analysis to the time-

dependent fatigue problem. Assume that the rate of flaw size growth  $dC(t)/dt$  is proportional to a power function of the work available to create new surface  $T(t)$  where both quantities are  $(t)$  time dependent. This assumption yields

$$\frac{dC(t)}{dt} \propto T(t)^r \quad (5)$$

where  $r$  is an arbitrary constant. If  $C(t)$  is slowly changing compared to the random fluctuations of  $W(t)$ , the steady work increase  $\bar{W}(t)$  may be considered. This yields the expression

$$T(t) \propto C(t)\bar{W}(t) \quad (6)$$

and substituting Equation (6) into Equation 5 yields

$$C(t)^{-r} dC(t) = A_1 \bar{W}(t)^r dt \quad (7)$$

where  $A_1$  is a constant of proportionality. Equation 7 may be formally integrated to yield

$$\int_{C_0}^{C_t} C(t)^{-r} dC(t) = A_1 \int_{t_0}^t \bar{W}(t)^r dt \quad (8)$$

where the subscript  $(o)$  defines the initial conditions. The integral on the right side of Equation 8 cannot be evaluated analytically. The test spectrum  $F(t)$  was developed as a random process that preserved the expected cumulative statistics for the aircraft studied. Each mission segment was simulated with bursts of random loads so that each half cycle was statistically independent but asymptotically integrated in time yielding the desired cumulative exceedances. The resulting history  $F(t)$  is a stationary random process; hence,

$$\int_{t_0}^t \bar{W}(t)^r dt \quad (9)$$

can be replaced by the expression

$$A_2 [t-t_0] \quad (10)$$

where the constant  $A_2$  is to be experimentally determined. The left side of Equation 7 may be integrated to yield

$$C_o^{[-r+1]} - C_t^{[-r+1]} = A_1 A_2 [r-1] [t-t_o] \quad (11)$$

and since  $A_1$  and  $A_2$  are arbitrary constants, they may be combined to yield

$$C_o^{[-r+1]} - C_t^{[-r+1]} = A_3 [r-1] [t-t_o]. \quad (12)$$

Equation 12 may be converted to a residual strength form by using Equation 4. Since

$$F_R \sqrt{C} \propto \sqrt{KT_c} = B_1 \quad (13)$$

Equation 12 may be rearranged to yield

$$F_{R(o)}^{2[r-1]} - F_{R(t)}^{2[r-1]} = A_3 B_1^{2[r-1]} [r-1] [t-t_o] \quad (14)$$

and the constants  $A_3$  and  $B_1^{2[r-1]}$  may be combined to yield

$$F_{R(o)}^{2[r-1]} - F_{R(t)}^{2[r-1]} = A_4 [r-1] [t-t_o]. \quad (15)$$

The initial ( $t = 0.0$ ) residual strength distribution is assumed to be Weibull (Reference 37)

$$P(F_{R(o)} > F_R) = \exp - \left\{ \frac{F_R}{\hat{F}_{R(o)}} \right\}^{\alpha_o} \quad (16)$$

where  $\alpha_o$  is the shape parameter,  $\hat{F}_{R(o)}$  is the scale parameter at time  $t_o$ , and  $F_R$  is the random variable. To produce a time-dependent residual strength function, it is noted that the set of values  $F_R(t) > F_R$  is the same as the set of values (Equation 15) where

$$F_{R(o)} > \left\{ F_R^{2[r-1]} + A_4 [r-1] [t-t_o] \right\}^{\frac{1}{2[r-1]}}. \quad (17)$$



Hence, the probability that  $F_R(t) > F_R$  is just the probability that Equation 17 holds. Equation 16 gives this probability as

$$P(F_R(t) > F_R) = P\left[F_R(o) > \left\{F_R^{2[r-1]} + A_4[r-1] [t-t_o]\right\}^{\frac{1}{2[r-1]}}\right]$$

$$= \exp - \left\{ \left[ \frac{F_R}{\hat{F}_R(o)} \right]^{2[r-1]} + \left[ \frac{A_4[r-1] [t-t_o]}{\hat{F}_R(o)^{2[r-1]}} \right] \right\}^{\alpha_f} \quad (18)$$

where

$$\alpha_f = \frac{\alpha_o}{2[r-1]} \quad (19)$$

It can be established that Equation 18 will be very close to a Weibull distribution for fatigue lifetime (t) if fatigue failures are obtained at a load level  $F_{TRU}$  (the truncation load in the fatigue spectrum) that is of the order  $\hat{F}_R(o)/2$  or less. By assigning a specific value  $F_{TRU}$  for  $F_R$  in Equation 18 and rearranging the expression

$$P(F_R(t) > F_{TRU}) = \exp - \left\{ \frac{t}{\left[ \frac{\hat{F}_R(o)^{2[r-1]}}{A_4[r-1]} \right]} \right. \quad (20)$$

$$\left. + \left[ \frac{F_{TRU}}{\hat{F}_R(o)} \right]^{2[r-1]} - \frac{A_4[r-1] t_o}{\hat{F}_R(o)^{2[r-1]}} \right\}^{\alpha_f}$$

the desired result may be obtained. Let Equation 20 be written in the form

$$P(F_R(t) > F_{TRU}) = \exp - \left\{ \frac{t}{\hat{t}_b} + \text{ERROR} \right\}^{\alpha_f} \quad (21)$$

where

$$\hat{t}_b = \left[ \frac{\hat{F}_R(o)^{2[r-1]}}{A_4[r-1]} \right] \quad (22)$$

and is the approximate characteristic failure lifetime for the baseline load spectrum  $F(t)$ .

Under the conditions that

$$(1) \quad t_o \equiv 0 \quad \therefore \quad \left[ \frac{A_4[r-1] [o]}{\hat{F}_R(o)^{2[r-1]}} \equiv 0 \right]$$

$$(2) \quad \frac{F_{TRU}}{\hat{F}_R(o)} < \frac{1}{2} \quad \text{and } r > 4$$

the error term in Equation 21 would be less than 0.0156, which would yield a mode location error of less than two percent. Thus, for bonded joints which exhibit substantial wearout, the lifetime distribution using Equation 20 would be essentially Weibull with parameters  $\alpha_f$  and  $t_b$ .

Correlation of the wearout model with the experimental data follows in the next section.

## 6.5 RANDOM FATIGUE DATA EVALUATION

A reduction and evaluation of the 1/5-scale specimen wearout data and the 1/2-scale specimen scaling experiment are presented in the following paragraphs.

### 6.5.1 One-Fifth Scale Wearout Data

A qualitative evaluation of the character of the wearout data can be made by observing Table XXVII. The important observations are that the initial static distribution broadened significantly at the 50 percent lifetime trace while only a small change in characteristic strength was noted. This behavior is in agreement with the assumptions made in development of the wearout model.

A wearout model was evaluated by global fitting the pooled static and 1 percent lifetime data, the 10 percent lifetime data, and 50 percent lifetime data and the lifetime distribution data. The fit was accomplished by forming an error function of the form

$$ERR = \sum_{i=1}^n ({}_iF_E(t) - {}_iF_R(t))^2 \quad (23)$$

where

$n$  = total number of data points

$FE(t)$  = experimental value

and where the summation was over the number of points in the experimentally established data set. The error function was minimized using the technique in Reference 38.

A summary of the best fit results are shown on Table XXVIII.

Table XXVIII WEAROUT MODEL PARAMETERS

$\hat{F}_R(o) \times 10^{-2}$ (KIPS $\times 10^{-2}$ )	$\alpha_o$ (dimensionless)	$r$ (dimensionless)	$A_4$ (*)	$t_o$ (lifetimes)
1.091	11.62	6.065	.2351	0.0

$$(*) \quad \frac{(\text{KIPS} \times 10^{-2})}{(\text{lifetimes})}^{2(r-1)}$$

Use of the data presented in Table XXVIII requires that the loads (KIPS) be scaled by the factor  $10^{-2}$ . The form of the wearout model with the scaled values becomes

$$P(F_R(t) > F_R) = \exp - \left\{ \left[ \frac{F_R \times 10^{-2}}{1.091 \times 10^{-2}} \right]^{10.13} + .4928[t] \right\}^{1.147} \quad (24)$$

The computed versus observed residual strength and lifetime distributions, as determined using Equation 24, are summarized in Figure 36. The correlation of the observed distributions yields material-related parameters ( $F_R(o)$ ,  $\alpha_o$ ,  $r$ ,  $A_4$ ) that allow screening in terms of physical properties. The observed growth rate  $r$  is typical of polymer materials and indicates that the adhesive or adherand polymer constituents are dominating the joint reliability characteristics. If a tighter lifetime distribution is desired, the available control parameter is  $\alpha_o$ .

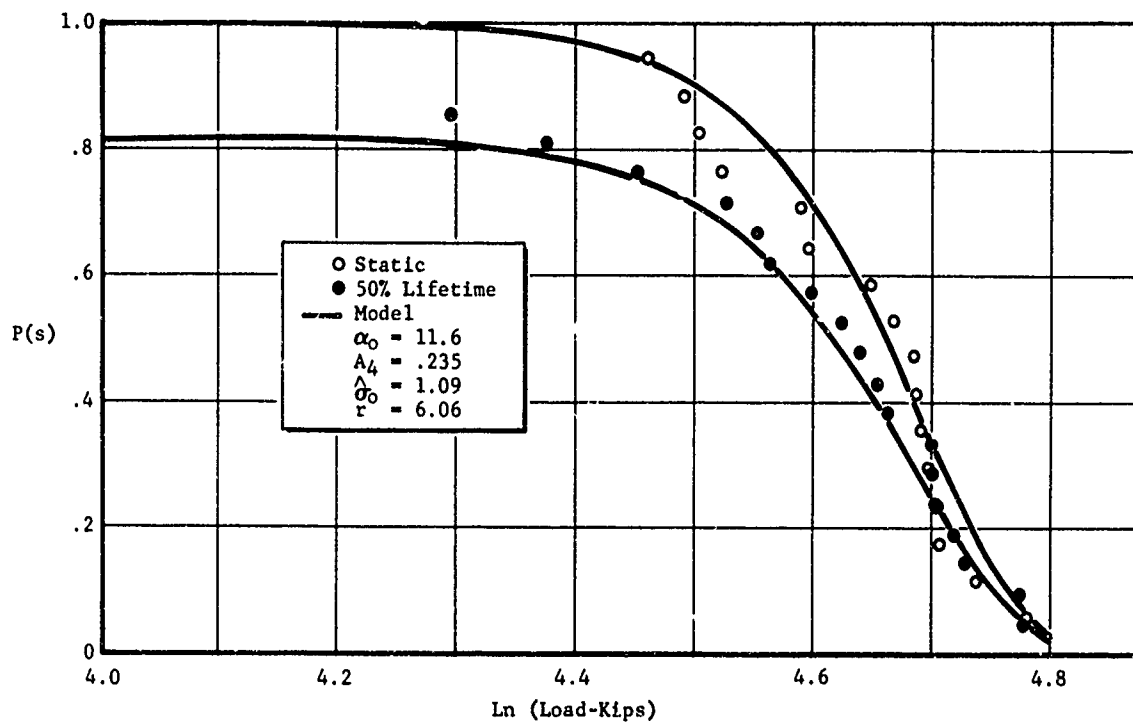


Figure 36 Residual Strength Distributions

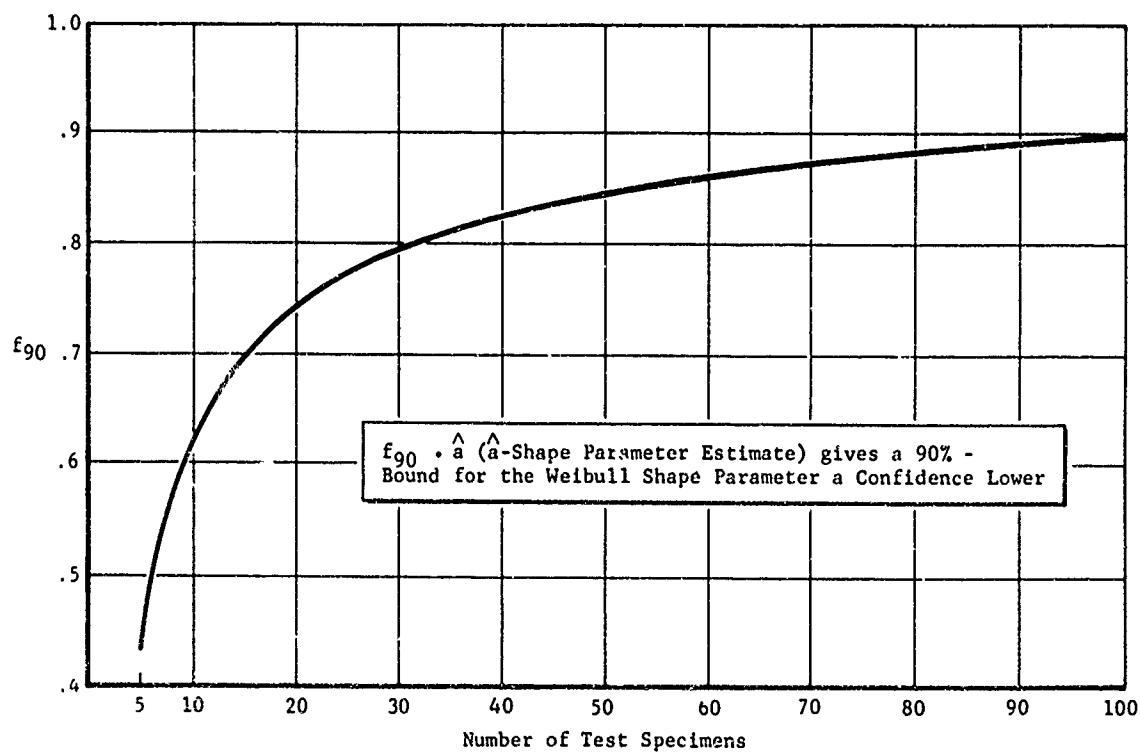


Figure 37 Factors  $f_{90}$  for a 90%-Confidence Lower Bound for the Weibull Shape Parameter

In order to further explore the meaning of the data presented, it is of interest to determine operational load levels associated with various reliabilities for the same scale bonded joint. The baseline spectrum was defined in terms of a random history  $F(t)$  truncated at a load level  $F_{TRU}$ . The information to be derived is the lifetime capability of the joint under reduced load. No experimental data is available; therefore, the form of the evaluation used was based on metal fatigue behavior. In the range of cycles to failure from  $10^2$  to  $10^6$ , the mean life behavior (or correspondingly  $\hat{t}$ ) is linear in  $\ln(\text{life})$  vs  $\ln(\text{amplitude})$  coordinates for various metals (Reference 3). For aluminum, the ratio of the  $\ln(\text{life})$  vs  $\ln(\text{amplitude})$  function is  $-2r$ .

Consider the transformation (Reference 39) of the reference spectrum (the spectrum used under this program)  $F(t)$  by the function,

$$G(t) = B_2 F(t) \quad (25)$$

and since the spectrum is truncated at  $F_{TRU}$ . The truncation load for the transformed spectrum is

$$G_{TRU} = B_2 F_{TRU} \quad (26)$$

The truncation load and characteristic life are related as follows. The  $\ln \hat{t}$  vs  $\ln G_{TRU}$  is assumed linear with a slope of  $(-2r)$ . The  $\ln(\text{life})$  vs  $\ln(\text{amplitude})$  function will be

$$\ln \hat{t} = 2r \ln B_2 + \text{constant} \quad (27)$$

where the assumed relation is fixed at the known data derived point  $B_2 = 1$  and  $\hat{t} = \hat{t}_b$ .

From equations 22, 26, and 27

$$\hat{t} = \frac{\hat{F}_R(0)^{2[r-1]}}{A_4[r-1]} \left[ \frac{F_{TRU}}{G_{TRU}} \right]^{2r} \quad (28)$$

Utilizing the approximate lifetime relation given in Equation 21 (assuming that  $\text{ERROR} = 0.0$  and generalizing  $\hat{t}_b$  to  $\hat{t}$ ) together with Equation 28 the safe load capacity of the specimen can be computed. Two cases were computed: the load level which yields a characteristic life of 4.0 lifetimes and the load level which yields a 0.99 probability of achieving 4.0 lifetimes. The results are summarized in Table XXIX, where the probability of surviving one lifetime is  $P_s$  for  $t=1$  and the required static safety factor (F.S.) are shown.

The difference in the estimate of  $\hat{t} = 2.03$  for the baseline data in Table XXIX and the experimental value of  $\hat{t} = 1.99$  in Table XXVII is due to the influence of the residual strength data in the global fit. The value given in Table XXVII is the result of a one-dimensional fit only.

Table XXIX ESTIMATED JOINT FATIGUE PERFORMANCE

Case	G <sub>TRU</sub> KIPS	$\hat{t}$ Lifetimes	P <sub>s</sub> for t = 1.0 Dimensionless	F.S. (1)
Baseline Data (.368 surviving t = 2.03)	54.5	2.03	0.637	1.54
0.368 surviving t = 4.0	51.5**	4.00	0.816	1.72
0.99 surviving t = 4.0	37.0**	220.4***	0.999	2.27

$$(1) \text{ F.S.} = \frac{102.7}{(1.22)G_{\text{TRU}}} = \frac{\mu(\text{static})}{\text{Limit Load}}$$

\*\*Equation 28

\*\*\*Equation 21, generalized for  $\hat{t}$ .

### 6.5.2 Scale Effects

Size effects have been observed in metals and glass (References 40 through 43). Small-scale specimens generally exhibit greater strength per volume of material and longer fatigue lives than their full-size counterparts. The small-scale specimens tend to have longer fatigue lives than full-size specimens although both are subjected to the same stress history.

Composite bonded joint specimens also exhibit size effects. The random load fatigue test results for the 1/5- and 1/2-scale specimens were used to evaluate the scaling effect.

Economically, it is desirable to characterize the allowable static and fatigue strength of full-size joints using small-scale specimens. To achieve a realistic characterization, the size

relationship (or scaling effect) between the small- and full-size specimen should be established using a realistic random load history and compatible environment. If small-scale specimens can be used to develop realistic design allowables, then a practical design methodology can be developed.

The scaling effect was evaluated using the 1/5- and 1/2-scale specimen test results for the 10 percent lifetime and the fatigue-to-failure cases. Scaling factors ( $S_F$ ) were computed for these cases four different ways, i.e.,

$$1. \quad S_F = (\mu_{1/5} / \mu_{1/2}) \times C_p \quad (29)$$

$$2. \quad S_F = (\beta_{1/5} / \beta_{1/2}) \times C_p \quad (30)$$

$$3. \quad S_F = (\beta_{1/5} / \bar{\beta}_{1/2}) \times C_p \quad (31)$$

$$4. \quad S_F = (\beta_{1/5} / \hat{\beta}_{1/2}) \times C_p \quad (32)$$

where

$\mu_{1/5}, \mu_{1/2}$  = Mean values for the 1/5- and 1/2-scale specimens, respectively

$\beta_{1/5}, \beta_{1/2}$  = Characteristic values for 1/5- and 1/2-scale specimen respectively based on least squares fit

$\bar{\beta}_{1/2}$  = Computed characteristic value

$$= (\mu_{1/2} / \mu_{1/5}) \times \beta_{1/5}$$

based on  $\alpha_{1/5} = \alpha_{1/2}$ .

$\hat{\beta}_{1/2}$  = Computed characteristic value based on the maximum likelihood estimator,  $\hat{\beta}_{MLE}$

$$\hat{\beta}_{MLE} = \left( \frac{1}{n} \sum_{i=1}^n x_i^{\alpha} \right)^{\frac{1}{\alpha}}$$

based on  $\alpha_{1/5} = \alpha_{1/2}$  with  $x_i \equiv$  residual strength or lifetime.

The 1/5- and 1/2-scale specimens were both 5 inches wide with a thickness of 40 and 94 plies, respectively (Figures 5 and 6). Since the specimen widths were the same, the mean or characteristic residual strengths were computed on a per-ply basis to put the results on the same baseline. The ratio of the ply thickness for the 1/2- and 1/5-scale specimens, i.e. 94/40, is equal to 2.35. This multiplying factor converts to the residual strength data for the 1/5- and 1/2-scale specimens to the same baseline and is defined as  $C_p$ . Mean and characteristic lifetimes for the 1/5- and 1/2-scale specimens are directly comparable; therefore,  $C_p$  is unity for fatigue-to-failure comparisons.

The parameters  $\mu_i$  and  $\beta_i$  ( $i = 1/5$  and  $1/2$ ), for computing  $S_F$ , were taken from Tables XXI, XXIV, XXVI, and XXVII. Details are given in the following sections for defining  $\beta_{1/2}$  and  $\bar{\beta}_{1/2}$ . The scaling factors were computed using Equations 29 through 32. The results are summarized in Table XXX.

#### 6.5.2.1 Definition of $\bar{\beta}_{1/2}$

$\bar{\beta}_{1/2}$  was computed using  $\mu_{1/5}$ ,  $\mu_{1/2}$ , and  $\bar{\beta}_{1/2}$ . This approach was considered to determine if  $\beta_{1/2}$  could be reasonably estimated using only a few 1/2-scale specimens to define  $\mu_{1/2}$  and a larger number of 1/5-scale specimens to define  $\mu_{1/5}$  and  $\beta_{1/5}$ . If feasible, this could reduce the number of 1/2-scale specimens required to evaluate  $S_F$  using characteristic values.

The mean value ( $\mu$ ) may be expressed in terms of  $\beta$  and the gamma function ( $\Gamma$ ) as follows:

$$\mu_i = \beta_i \Gamma \left( \frac{1}{\alpha_i} + 1 \right) \quad (i = \text{scale size}).$$

If  $\alpha_{1/5}$  and  $\alpha_{1/2}$  are equal, then  $\frac{\mu_{1/5}}{\mu_{1/2}} = \frac{\beta_{1/5}}{\beta_{1/2}}$ .

Solving for  $\beta_{1/2}$  and using the notation  $\bar{\beta}_{1/2}$  to distinguish the  $\beta$  from the least squares type,

$$\bar{\beta}_{1/2} = \frac{\mu_{1/2}}{\mu_{1/5}} \times \beta_{1/5}.$$

$\bar{\beta}_{1/2}$  was used in Equation 31 to compute  $S_F$ . The results are summarized in Table XXX.



Table XXX SUMMARY OF SCALING FACTORS BASED ON  
1/5- and 1/2-SCALE SPECIMENS

Lifetime	$\mu_{1/5}$	$\mu_{1/2}$	$\beta_{1/5}$ (e)	$\beta_{1/2}$ (e)	$\bar{\beta}_{1/2}$	$\hat{\beta}_{1/2}$	Scaling Factor ( $S_F$ )			
							Eq. 29	Eq. 30	Eq. 31	Eq. 32
10% ( $C_p=2.35$ )	102.37K(a)	214.0K(c)	108.9	227.6K	227.6K	217.0K(f)	1.12	1.12	1.12	1.18
Fatigue-to Failure ( $C_p=1.0$ )	1.812(b) Lifetimes	0.572(d) Lifetime	1.99 Lifetime	0.67 Lifetime	0.63 Lifetime	0.592(g) Lifetime	3.18	2.97	3.16	3.36

Notes:

- (a) Reference Table XXII  
(b) Reference Table XXIV  
(c) Reference Table XXV  
(d) Reference Table XXVI  
(e) Reference Table XXVII  
(f) Based on  $\alpha_{1/2} = 7.38$  (Table XXVII)  
(g) Based on  $\alpha_{1/2} = 1.44$  (Table XXVII)

#### 6.5.2.2 Definition of $\hat{\beta}_{1/2}$

If the  $\alpha$  value is known for a small-scale specimen, then the  $\beta$  value can be computed for larger specimens using the maximum likelihood estimator, i.e.,

$$\hat{\beta}_{1/2} = \left( \frac{1}{n} \sum_{i=1}^n \frac{\alpha_{1/2}}{x_i \alpha_i} \right)^{\frac{1}{\alpha_{1/2}}}$$

where :  $\alpha_{1/2} = \alpha_{1/5}$  (assumed)

$n$  = number of specimen

$x_i$  = residual strength and/or lifetime for given specimen.

$\hat{\beta}_{1/2}$  values were computed for the 10 percent lifetime and the fatigue-to-failure cases using  $\alpha_{1/5}$  equal 7.38 and 1.44, respectively (Table XXVII). Scaling factors were computed using  $\hat{\beta}_{1/2}$  in Equation 32. The results are summarized in Table XXX.

#### 6.5.2.3 Discussion

The results shown in Table XXX indicate that there is a scaling effect between different size bonded composite joint specimens. This effect is significant and must be given careful consideration in developing design allowables.

The results show that the scaling factors increase with lifetime. In fact, the scaling factor for the fatigue-to-failure case was about three times larger than that for the 10 percent lifetime case. This implies that the governing scaling factor depends on the fatigue life requirement rather than the static strength requirement.

The scaling factors were based on 1/5- and 1/2-scale specimens. The lifetime scaling factor for a full-size specimen was not estimated since a linear extrapolation would have been required. Without a sufficient number of full-size specimens tests, at least three different specimen sizes should be used to credibly extrapolate the scaling factor to a full-size specimen.

The computed scaling factors were the same order of magnitude for the respective cases irrespective of the method used. The two largest scaling factors, 3.18 and 3.36 (Table XXX), were based on the ratio of the mean lifetimes and the ratio  $\hat{\beta}_{1/5}/\hat{\beta}_{1/2}$ .

respectively. Both methods should be used to compute  $S_f$ . The results should be compared and the larger scaling factor should be used for design.

The results of this investigation indicate a reasonable potential for using small-scale specimens to characterize the life-time properties of full-size specimens. The scaling factor is a definable quantity and it should be evaluated using a realistic random load history and compatible environment.

## 6.6 JOINT FAILURE MODES

Joint failures were analyzed by

1. Visual inspection of the broken specimen
2. Microscopic inspection of the failure surfaces
3. Visual inspection (by naked eye and by magnifying glass) of photographs of broken specimens (Appendix IV and V).

The test types studied were

1. Static
2. Constant Amplitude
3. Random Fatigue
  - a. Residual Strength (1, 10, 50% lifetime)
  - b. Fatigue-to-Failure.

The three failure modes observed were (1) laminate failure, (2) bond failure, and (3) complex failure (laminate and bond). Specimen K904950 (Figure 86) characterizes the laminate failure mode, specimen K905023 (Figure 101) characterizes the bond failure mode, and specimen K012476 characterizes the complex mode. Different failure modes were observed for the same test cases (both 1/5 and 1/2 scale). For this reason, it is difficult to confidently relate the failure modes to a particular type of loading. Generally, however, it appears that the laminate failure mode is predominate for the static cases and that the progressive bond failure mode prevails for the fatigue specimen.

## 6.7 EFFECT OF SAMPLE SIZE

The question treated in this section is: what size sample should be taken to adequately characterize various distribution parameters associated with a particular element or component?

Extremely large sample sizes are usually limited in number due to fabrication and testing costs. Without doing a complete trade-off study between the cost of various sample sizes and the value of the statistical information gained from such samples, the problem is looked at in a qualitative manner. This allows for selection of a sample size that is relatively efficient in maximizing statistical information gain for each test dollar spent.

In general, the value of statistical information gained does not increase linearly with the sample size. Therefore, dollar wise, a point of diminishing returns is reached by increasing the sample size. A qualitative measure of the amount of statistical information contained in a sample for estimating a distribution parameter is the number that the point estimate (estimate based only on observed values) must be multiplied by in order to obtain a new estimate with an associated high degree of confidence.

### 6.7.1 Sample Size Effects on Establishing Shape and Scale Parameters Based Upon the Particular Results of This Program

The number of specimens required to achieve an equivalent confidence in the estimate of the Weibull shape and scale parameters is a key issue in the design of a cascaded test program. As shown in Figure 37, the penalty paid to obtain a 90-percent confidence lower bound on the shape parameter is only a function of sample size. The improvement in the estimate is steep through 17 specimens where the slope of the curve  $df_{90}/dn$  is greater than 1.0. The return diminishes rapidly above 17 specimens.

The number of specimens required to achieve equivalent confidence in the Weibull scale parameter for the case of a 90-percent confidence lower bound for an estimated shape parameter is shown in Figure 38 and known shape parameter is shown in Figure 39. The number of specimens required to estimate the scale parameter is a function of the shape parameter.

Examples of the data requirements can be developed from the specific data obtained under this program.

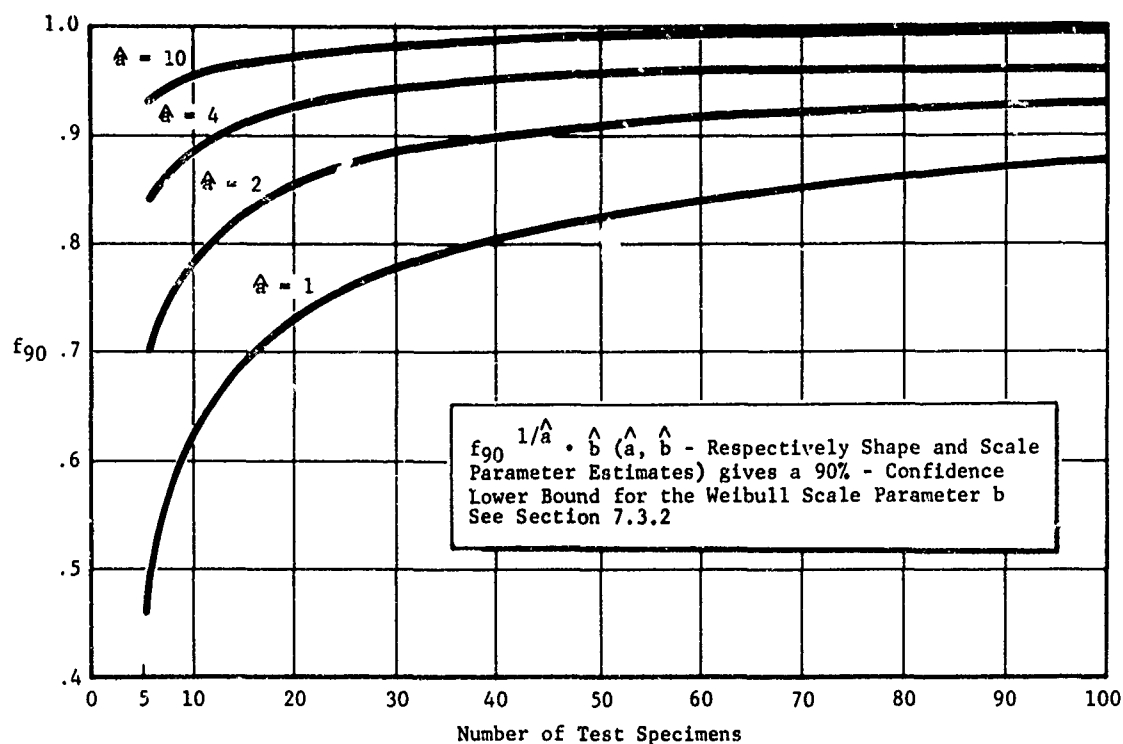


Figure 38 Factors  $f_{90}$  for a 90%-Confidence Lower Bound for the Weibull Scale Parameter

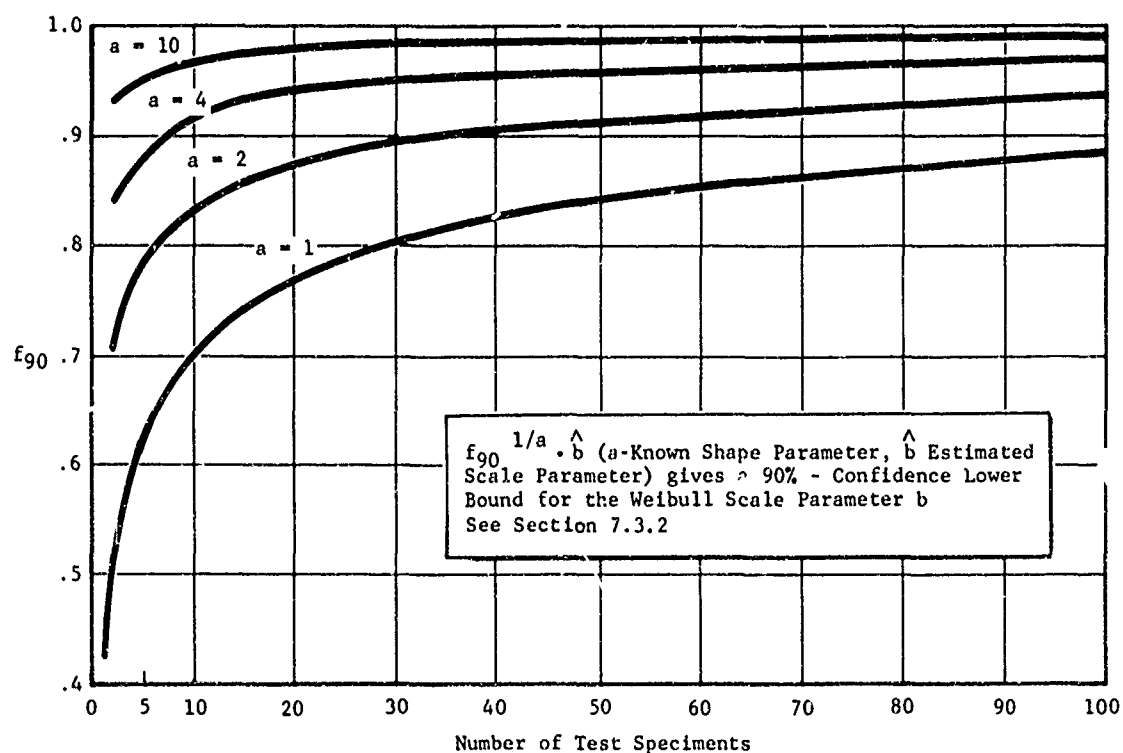


Figure 39 Factors  $f_{90}$  for a 90% - Confidence Lower Bound for the Weibull Scale Parameter - Shape Parameter Known

The apparent shape parameter for the static data shown in Column 1 of Table XXXI was  $\alpha_0 = 10.6$ . From Figure 37 the appropriate penalty in  $f_{90}$  to achieve a 90-percent confidence estimate of  $\alpha_0$  is  $f_{90} = 0.66$ . For this sample size the corresponding confidence level is obtained for the scale parameter with a penalty of  $f_{90} = 0.92$ . Note that the penalty required in scale parameter would be only 0.87 if only five specimens were used. For high shape parameters, the expected convergence to a mean is rapid and can be heuristically observed in the data presented in Column 1 of Table XXXI. The data set converges to the mean within the first 5 specimens and then simply oscillates randomly about the mean value. The 50-percent lifetime data was the slowest to converge, and as noted in Table XXVII, it had a shape parameter of 4.94. At a shape parameter of 4.94, 20 specimens would be required to achieve the same design penalty ( $f_{90} = .94$ ), and two specimens would be required at a shape parameter of 10, Figure 40.

In subsection 6.4, it was noted that the homogeneity of the fatigue-to-failure population could not be established. The shape parameter of the data subsets were 2.07 and 1.75 indicating that a shape parameter for the type of joint probably is not much larger than 2.0. Over 100 specimens would be required to achieve a penalty of  $f_{90} = 0.94$  at a shape parameter of 2.0, Figure 39. This problem is reflected in the slow convergence (or lack of convergence) in the fatigue-to-failure data.

A summary of the observations made from the test data follows.

1. A larger sample size is required to establish the mean lifetime than it is to establish the mean static and residual strength.
2. At least 5 specimens should be used to define the mean static strength.
3. At least 100 specimens should be used to achieve an estimate of mean fatigue life that would be consistent with the static strength observations.
4. Fifteen specimens appears to be a reasonable number to define the mean residual strength for the 50 percent lifetime case (1/5 scale).
5. The number of specimens used to define the mean,  $\alpha$ , coefficient of variation, and factor of safety must be consistent with the confidence limit factor desired. The confidence level factor increases as the number of specimen increases but so does the cost. The number of

Table XXXI SUMMARY OF MEAN VALUES FOR VARIOUS SAMPLE SIZES  
(1/5-Scale Specimen Tests)

Number of Specimen <sup>a</sup>	Static Tests (n=11) (KIPS)	1% Lifetime (n=5) (KIPS)	10% Lifetime (n=6) (KIPS)	50% Lifetime (n=20) (KIPS)	Fatigue-to-Failure (n=20) Lifetimes
1	86.6	104.4	79.4	---	1.22
2	98.2	109.2	92.2	<sup>b</sup> 115.6	1.12
3	100.9	108.9	98.3	94.5	1.49
4	105.5	108.9	99.9	89.5	1.20
5	102.2	105.2	101.1	---	1.11
6	103.6		102.3	88.7	0.99
7	104.7			92.1	0.97
8	103.8			92.8	0.94
9	104.3			94.1	0.91
10	103.8			94.2	0.91
11	102.7			95.9	1.19
12				97.6	1.41
13				99.3	1.36
14				100.2	1.63
15				101.1	1.61
16				101.3	1.66
17				101.2	1.78
18				101.9	1.86
19				102.0	1.84
20				101.5	1.81
Sample Mean	102.7	105.2	102.3	101.5	1.81
Reference Table	XV	XVI	XVI	XVI	XVII

Notes:

- <sup>a</sup> In same order tests were conducted. <sup>b</sup> Specimen failed before reaching 50% lifetime.  
Mean values based on only those specimen reading a 50% lifetime.  
(n=k) denotes the total number of k specimens in the sample.

specimens required to do a credible job involves a trade-off between the confidence level and the cost.

6. The results of Table XXXII indicate that the confidence level factor is less for the fatigue-to-failure case than for the static or other residual strength cases. The factor of safety required is governed by the fatigue-to-failure requirement; yet, the results show that the confidence level was less for this case (for a given sample size) than the other cases. Therefore, careful attention must be given to the sample sizes and corresponding degree of confidence in the statistical parameters.

A summary of  $f_{90}$  confidence lower bound factors for the Weibull scale parameter (assuming  $\alpha$ 's are known) with respect to sample size are given in Table XXXIII for 1/5- and 1/2-scale specimens. The  $f_{90}$  factors in this table were estimated from Figure 39 assuming the computed  $\alpha$  values in the table were confidently known.

In the 1/5-scale fatigue-to-failure case, a maximum likelihood value of 1.44 was computed for the Weibull shape parameter ( $\alpha$ ) based on 20 tests (reference Table XXXIII). The 90-percent confidence lower bound for  $\alpha$ , based on 20 tests, is approximately 0.74. This means that there is a 90-percent confidence that  $\alpha$  will be no smaller than  $0.74 \times 1.44$  or 1.06. The coefficient of variation corresponding to  $\alpha$  of 1.44 and 1.06 is approximately 0.68 and 0.93, respectively (see Figure 40 and Appendix VI). From Figure 40, it is seen that the coefficient of variation increases as  $\alpha$  decreases. The larger the coefficient of variation, the larger the factor of safety must be to meet the reliability goal.

#### 6.8 EFFECT OF RESIDUAL STRENGTH AND FATIGUE LIFE VARIABILITY ON REQUIRED DESIGN SAFETY FACTORS

The effect of residual strength and fatigue life variability on the safety factors required for design are dealt with in the following paragraphs.

Safety factors are commonly used to account for the variation in residual strengths and fatigue lives. The results of this program indicate that the distribution of residual strength broadens with lifetime. This implies that static design safety factors for bonded joints should be projected to the one lifetime



Table XXXII SUMMARY OF MEAN VALUES FOR VARIOUS  
SAMPLE SIZES (1/2-Scale Specimen Tests)

Number of Specimens <sup>a</sup>	10% Lifetime (n=5) (KIPS)	Fatigue-to- Failure (n=5) Lifetime
1	236.5	0.57
2	238.3	0.68
3	215.0	0.59
4	212.7	0.51
5	214.0	0.57
Sample Mean	214.0	0.57
Reference Table	XVIII	XIX

Notes:

a In same order tests were conducted

(n=k) denotes the total number of k specimen  
in the sample

Table XXXIII SUMMARY OF 90% CONFIDENCE LOWER BOUND FACTORS ( $f_{90}$ ) FOR THE WEIBULL SCALE PARAMETER (SHAPE PARAMETER KNOWN) WITH RESPECT TO SAMPLE SIZE (1/5- and 1/2-Scale Specimens)

Scale	Test	$\alpha$	Number of Test Specimen						
			5	10	15	20	30	50	100
1/5	Static <sup>a</sup>	11.58(16)	0.950	0.966	0.975	0.978	0.085	0.987	0.991
	10% Lifetime	7.38(6)	0.930	0.950	0.962	0.970	0.977	0.981	0.988
	50% Lifetime	4.94(20)	0.890	0.924	0.940	0.948	0.958	0.963	0.977
	Fatigue-to-Failure	1.44(20)	0.710	0.765	0.800	0.824	0.850	0.877	0.913
1/2	10% Lifetime <sup>b</sup>	7.05(5)	0.930	0.950	0.962	0.970	0.977	0.981	0.988
1/2	Fatigue-to-Failure <sup>c</sup>	1.95(5)	0.785	0.835	0.860	0.075	0.806	0.911	0.938

Notes: (x) denotes number of specimen used to define  $\alpha$  (reference Table XXVIII).  
 $f_{90}$  values for 90% confidence in  $\beta$  when  $\alpha$  is known, estimated using Figure 39.

a  $f_{90}$  estimated for  $\alpha = 10.0$ .

b same estimated  $f_{90}$  values as for the 10% lifetime (1/5 scale) case assumed

c  $f_{90}$  estimated for  $\alpha = 2.0$ .

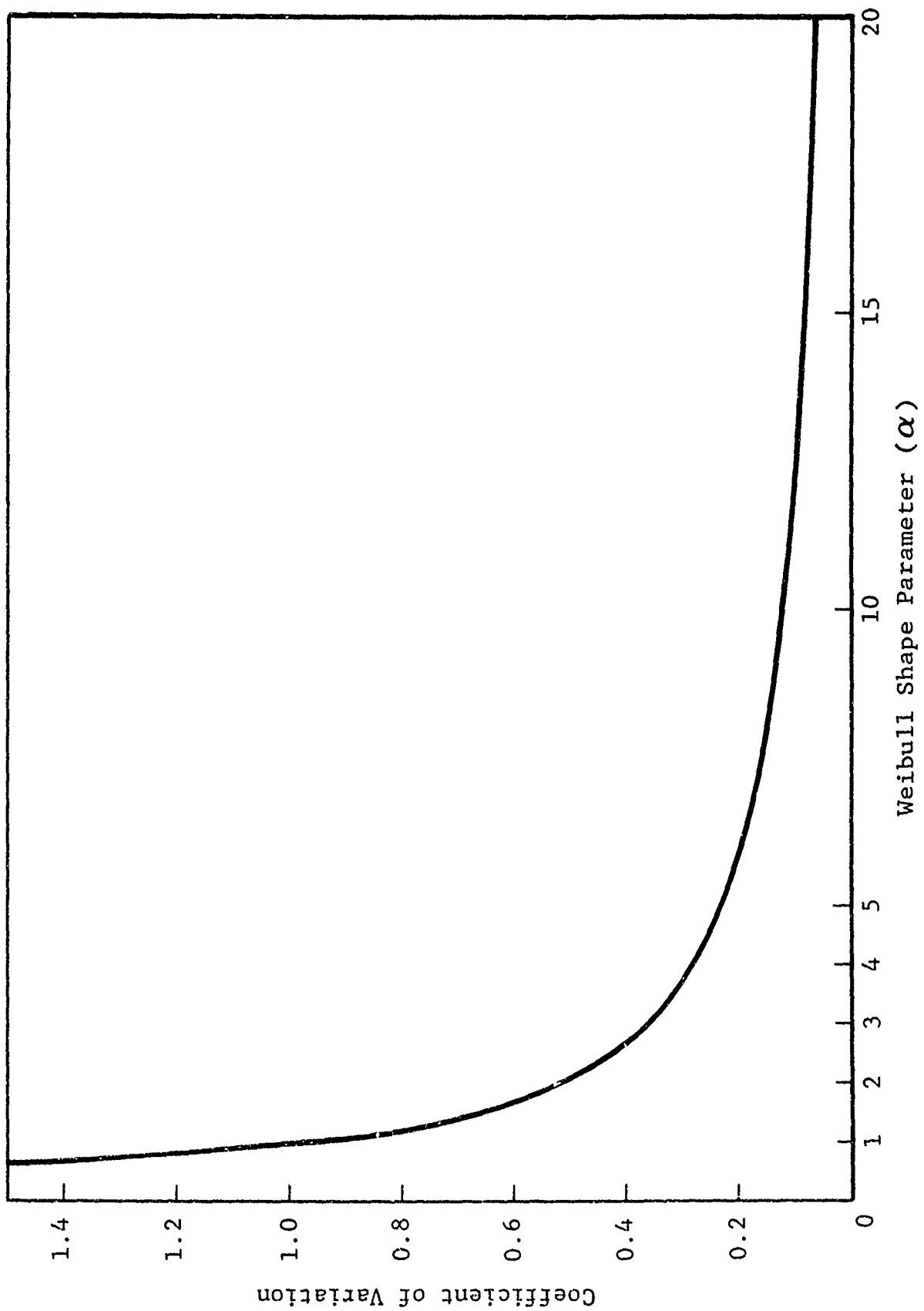


Figure 40 Coefficient of Variation for Weibull Distribution

residual strength distribution since it will require the greatest safety factor.

The flaw growth rate exponent and the static shape parameter affect the fatigue lifetime distribution for bonded joints. When the primary load transfer mechanism is through the adhesive bond, the flaw growth rate exponent is essentially constant. The static shape parameter can be controlled. If the shape parameter is doubled, the resulting joint scatter is equivalent to notched aluminum (Reference 3).

The mean life of a specimen was strongly influenced by the specimen scale. The scale effect has not been analytically treated; however, it appears to invalidate the concept of a stress analysis based design that projects large-scale designs on the basis of experimental data gained for small coupons. Full-scale testing of major bonded joints will be mandatory.

Although the fatigue scatter factor requirement will drive the design in these instances, the designer must have this parameter transformed into a static strength requirement in order to actually design the part. In transforming the fatigue scatter factor into a static safety factor that accounts for fatigue, it can be seen that this safety factor will depend on several statistical considerations including the materials fatigue coefficient of variation, anticipated random environment, the reliability goal established for a specific lifetime, and the statistical relationship of time and residual static strength.

# SECTION VII

## RELIABILITY ASPECTS OF BONDED JOINTS

### 7.1 INTRODUCTION

The reliability aspects of boron-to-titanium bonded scarf joints are discussed in this section. The concept of a reliability-based joint design and the data requirements are also considered.

### 7.2 STRENGTH-TIME RELATIONSHIPS

The primary objective of this program was to develop an understanding of the material-related parameters affecting the reliability characteristics of a large-scale bonded joint. For this study, the expected service history was assumed to be constant within the fleet and described by a set of mission-related exceedance curves. The reliability model evaluation reduces to the determination of  $G(x|t)$ , the cumulative distribution of loads, and  $F_R(t)$  the static residual strength function.

The service life reliability of a component is derived here based on an arbitrary operational load distribution.

Let  $G(x|t)$  denote the cumulative distribution of environmental loads at time  $t$ , i.e.,  $G(x|t)$  is the probability that a single load occurrence will have magnitude less than or equal to  $x$  at time  $t$ . Let  $F_R(t)$  denote the cumulative residual static strength determination of the component after a service life of length  $t$ . Let  $t_1, t_2, \dots, t_k, \dots$  be the specific times for which probability of survival (reliability) is to be computed. Also, let  $f(F_R(t_k))$  denote the residual strength probability density function characterized by a set of time-dependent parameters and assume (for computational convenience) that this function is fixed over each small time interval  $(t_{k-1}, t_k)$ .

$$g(x = F_R(t_k)) = \{ G(x = F_R(t_k)) \}^N \quad (29)$$

which is the probability that all loads in the block of time  $(t_{k-1}, t_k)$  are less than the value  $F_R$ , where  $N$  is the expected number of load cycles in the time interval  $(t_{k-1}, t_k)$ . Then  $L(t_k)$  defined by

$$L(t_k) = \int_0^{\infty} g(x = F_R(t_k)) f(F_R(t_k)) dF_R \quad (30)$$

is the probability that during the time interval  $(t_{k-1}, t_k)$  a load will not exceed the residual strength of the component and cause failure. Finally, let  $R(t_k)$  be the probability that the structural component survives each time interval up to and including the  $k^{\text{th}}$  interval  $(t_{k-1}, t_k)$ ; then,  $R(t_k)$  can be written in terms of  $L(t_k)$  as follows:

$$\begin{aligned} R(t_1) &= L(t_1) \\ R(t_2) &= L(t_1) L(t_2) \\ &\cdot \\ &\cdot \\ &\cdot \\ R(t_k) &= \prod_{i=1}^k L(t_i). \end{aligned} \quad (31)$$

Equation 31 represents the service-life reliability as a function of time.

### 7.3 RESIDUAL STRENGTH FUNCTION

A positive correlation with a residual strength model has been obtained. The model development is presented in subsection 6.5. The model defines the residual strength function  $F_R(t)$ . The experimentally observed residual strength function has a monotonically decreasing residual strength and increasing coefficient of variation on residual strength in time. The parameter estimation techniques used to fit the experimental data at strength or time traces follows.

### 7.3.1 Maximum-Likelihood Estimators

The density function of the two-parameter Weibull distribution with shape parameter  $a$  and scale parameter  $b$  is given by

$$f(x | a, b) = \frac{a}{b} \left(\frac{x}{b}\right)^{a-1} \exp\left(-\frac{x}{b}\right)^a \quad (32)$$

The likelihood function for a sample of  $n$  observation is

$$\bar{L} = \prod_{i=1}^n f(x_i | a, b) = \left(\frac{a}{b}\right)^n \prod_{i=1}^n \left(\frac{x_i}{b}\right)^{a-1} \exp\left(-\sum_{i=1}^n \left(\frac{x_i}{b}\right)^a\right) \quad (33)$$

Taking the logarithm of (33) and then differentiating with respect to  $b$  and  $a$  in turn and equating to zero, the following equations are obtained:

$$\frac{\partial \ln(L)}{\partial b} = -\frac{na}{b} + \frac{a}{b^{a+1}} \sum_{i=1}^n x_i^a = 0 \quad (34)$$

$$\frac{\partial \ln(L)}{\partial a} = \frac{n}{a} - n \ln b + \sum_{i=1}^n \ln x_i - \sum_{i=1}^n \left(\frac{x_i}{b}\right) = 0 \quad (35)$$

The maximum-likelihood estimators,  $\hat{a}$  and  $\hat{b}$ , for the shape and scale parameters  $a$  and  $b$  are obtained by solving Equations (34) and (35) for  $a$  and  $b$  yielding

$$\hat{b} = \left( \frac{\sum_{i=1}^n x_i^{\hat{a}}}{n} \right)^{1/\hat{a}} \quad (36)$$

and

$$\hat{a} = \frac{n \sum_{i=1}^n x_i^{\hat{a}}}{\sum_{i=1}^n x_i^{\hat{a}} \ln x_i - \sum_{i=1}^n x_i^{\hat{a}} \sum_{i=1}^n \ln(x_i)} \quad (37)$$

where  $x_i, i=1, 2, \dots, n$ , represent a random sample of size  $n$ . Equation (37) is solved by an iterative procedure using a "guess" as the initial value of  $\hat{a}$ . Equation (36) is then solved using the  $\hat{a}$  obtained from the solution of Equation (37). An IBM System 370 Computer has been programmed to solve Equations (36) and (37). The computer program is designated as TW9.

The results of Reference 44 can be used to estimate the shape and scale parameters  $a$  and  $b$  at various confidence levels (see Reference 3). The random variables  $\frac{\hat{a}}{a}$  and  $\hat{a} \ln(\hat{b}/b)$  are distributed independently of the parameters  $a$  and  $b$ ; thus, the distribution of these random variables is the same regardless of the "true" underlying values of  $a$  and  $b$ .

Thoman et al., Reference 44, have empirically evaluated by Monte Carlo techniques the distributions of  $\hat{a}/a$  and  $\hat{a} \ln(\hat{b}/b)$  for various sample sizes. Using these distributions, confidence intervals for the parameters  $a$  and  $b$  are easily obtainable. Confidence factors,  $f_{90}$ , for a 90-percent confidence lower bound on the shape parameter  $a$  as a function of sample size are given in Figure 37. Confidence factors,  $f_{90}$ , for a 90-percent confidence lower bound on the scale parameter  $b$  as a function of sample size are given in Figure 38.

Using Figure 37, a 90-percent confidence lower limit for the shape parameter  $a$  is obtained by multiplying  $\hat{a}$  by the abscissa value of Figure 37 corresponding to the proper number of specimens. A 90-percent confidence lower limit for the scale parameter  $b$  is obtained by multiplying  $\hat{b}$  by the abscissa value, corresponding to the proper number of specimens in Figure 38, to the  $1/\hat{a}$  power.

### 7.3.2 Estimation of Scale Parameter When the Shape Parameter is Known

In this section, a two-parameter Weibull distribution with known shape parameter  $a$  and unknown scale parameter  $b$  is assumed to be the underlying distribution. In this case, the cumulative distribution is given by  $F(x|a,b) = 1 - \exp - (\frac{x}{b})^a$ . The maximum-likelihood estimator  $\hat{b}$ , of the scale parameter  $b$ , obtained from Equation (30) is given by

$$\hat{b} = \left( \frac{\sum_{i=1}^n x_i^a}{n} \right)^{\frac{1}{a}} \quad (38)$$



where  $x_i$ ,  $i=1,2,\dots,n$ , represent a random sample from the above Weibull distribution.

It is shown in Reference 3 that the quantity  $2n(\frac{\hat{b}}{b})^a$  has a Chi-squared distribution with  $2n$  degrees of freedom. If an interval estimate,  $\hat{b}_\gamma$ , of  $b$  is required which satisfies the equation

$$\Pr (\hat{b}_\gamma \leq b) = \gamma, \quad (39)$$

the  $\hat{b}_\gamma$  is defined using the Chi-squared distribution by

$$\hat{b}_\gamma = \left[ \hat{b} \left( \frac{1}{2n} X_\gamma^2(2n) \right)^{-1/a} = \hat{b} \left( \frac{2n}{X_\gamma^2(2n)} \right)^{\frac{1}{a}} \right] \quad (40)$$

where  $X_\gamma^2(2n)$  is the  $\gamma$ -fractile of the Chi-squared variate with  $2n$  degrees of freedom.

Confidence factors,  $f_{90} = (2n/X_\gamma^2(2n))$ , for a 90-percent confidence lower bound on the scale parameter  $b$  as a function of sample size are given in Figure 39. The 90-percent confidence lower limit for the scale parameter  $b$  is obtained by multiplying  $\hat{b}$  by the abscissa value (corresponding to the proper number of specimens) in Figure 39 to the  $1/a$  power.

## 7.4 SAFE-LIFE ESTIMATES

In this section, a procedure is stated for obtaining safe-life estimates as a function of desired reliability and fleet size. The strategy proposed in Reference 3 for safe-life predictions is the basis for this approach, which will allow for the estimation of the wing tension splice joints safe operational life.

### 7.4.1 Individual Components

The reliability for an individual fleet member is developed for various levels of safe-life. This reliability is defined as the probability that service failure will occur after some specified safe-life for that individual member. These estimates are based on the estimated service-life distribution. Once a service-life distribution for a component is decided upon, then for fixed levels of reliability the safe-life of the component can be

determined. In Figure 41, the safe-life is the abscissa value of life that corresponds to one minus the desired reliability on the ordinate probability-of-failure coordinate.

#### 7.4.2 Safe-Life Estimation for a Fleet

In this step, estimates are obtained for the reliability of a fleet of structural components. The results allow for the specification of the first and/or second and/or third, etc., failure safe-life probabilities.

If the reliability of an individual component is  $R$ , then the probability of less than  $n$  failures,  $\bar{R}_{n,N}$ , in a fleet consisting of  $N$  components is given by

$$\bar{R}_{n,N} = \sum_{i=0}^{n-1} \binom{N}{i} (1-R)^i R^{N-i}, \quad (41)$$

where  $\binom{N}{i} = \frac{N!}{i! (N-i)!}$  and  $\bar{R}_{n,N}$  is the reliability of the  $n$ -th weakest in a fleet of  $N$ . Using Equation (41), safe-life estimates for a fleet are obtained in the same manner as for individual components. The relationship between  $R$  and  $\bar{R}_{n,N}$  for various values of  $N$  and  $n$  is illustrated in Figure 42. Safe-life as a function of desired fleet reliability is illustrated in Figure 43.

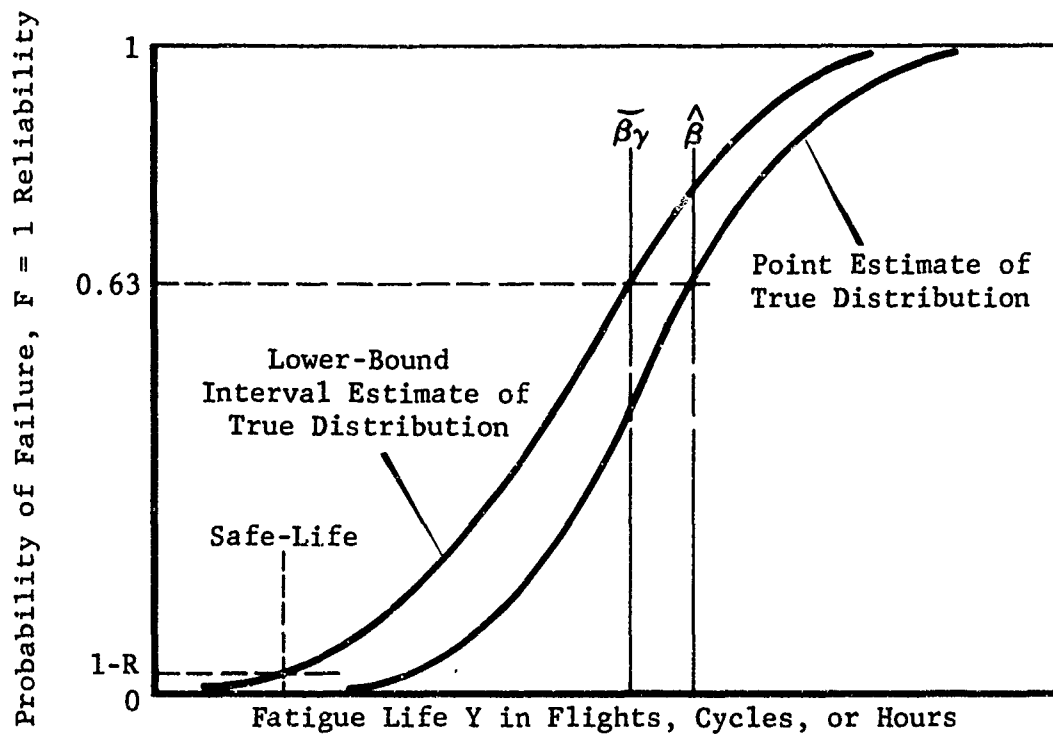


Figure 41 Service Fatigue Life Distribution

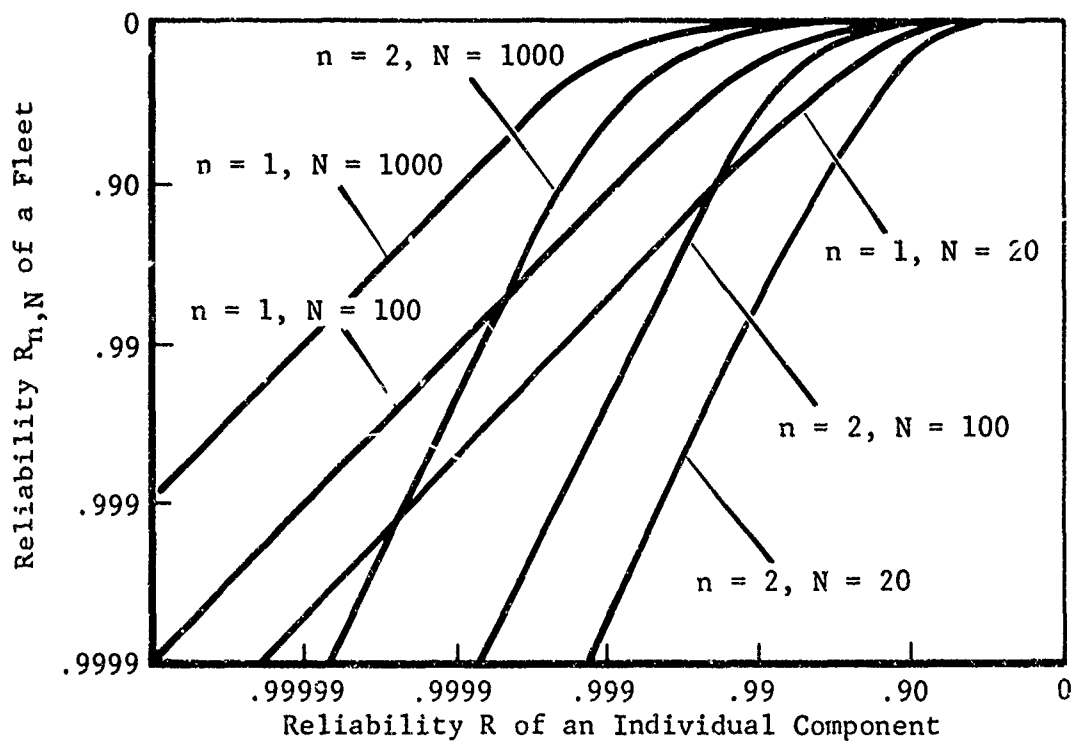


Figure 42 Fleet Reliability as a Function of Individual Component Reliability

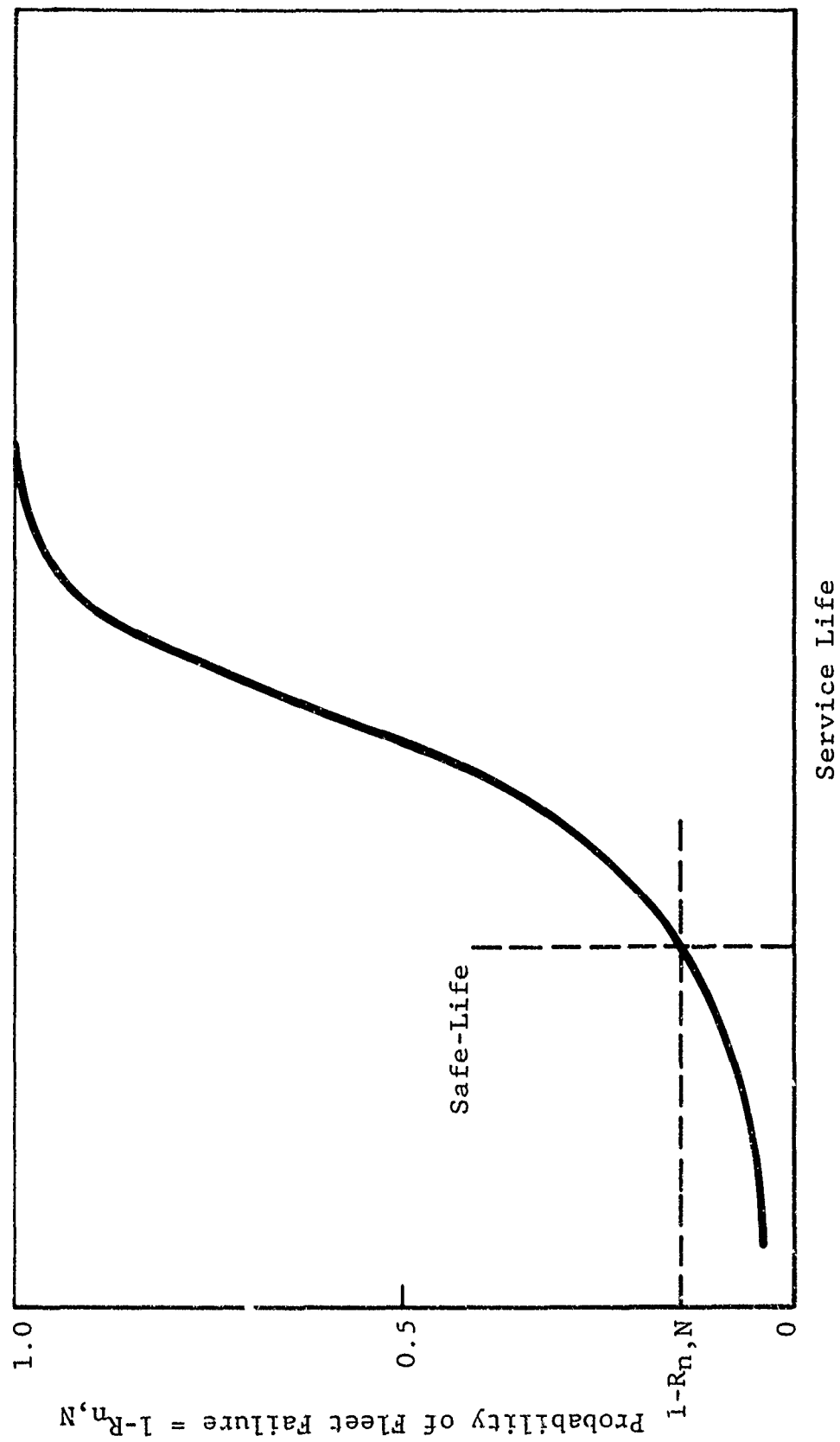


Figure 43 Fleet Reliability and Safe-Life

## SECTION VIII

### CONCLUSIONS AND RECOMMENDATIONS

#### 8.1 INTRODUCTION

The objectives stated in Section I were accomplished during this investigation. While some additional questions were answered, others were also raised. The conclusions and the recommendations for further work are summarized in this section.

#### 8.2 CONCLUSIONS

The conclusions of this investigation are summarized below:

1. Miner's rule is inadequate for predicting the fatigue life of bonded composite joints under random loading. The predicted fatigue life, based on Miner's rule, was about three times longer than that obtained by test.
2. The fatigue life characterization of bonded composite joints should be based on a random load history and a compatible environment. The load history effects are not fully understood for composites, but there is no justification for constant amplitude fatigue testing if the random fatigue-environment test philosophy is adopted.
3. A scaling effect does exist between different specimen sizes subjected to the same random stress history. The scaling factor increases with lifetime. The value needed for design is governed by the fatigue life requirements rather than the static strength requirements. The scaling factor is significant for composite bonded joints and must be carefully evaluated to obtain realistic design allowables. The results of this investigation indicate that the scaling factor is a definable quantity and confirms the feasibility of using small-scale specimens to characterize the static and fatigue life of full-size specimens. The specimen scale sizes must be carefully defined to achieve a scale compatibility between different specimens. More statistical data is needed to

determine the number of specimens required to define the scaling factors and to perform a credible reliability analysis.

4. Three modes of failure were observed, i.e. bond, laminate, and complex (bond and laminate). The laminate mode of failure was observed for several static and short life-time residual strength tests. A bond failure mode was observed for some of the fatigue tests. Due to the mixture of failure modes, no definite conclusions were reached on the failure process or the type of failure mode expected for a particular fatigue test.
5. The boron-to-titanium adhesive bonded double scarf joint type used for this study exhibited a relatively short fatigue life and considerable scatter in the test results. In an actual design situation, a much larger factor of safety (or reduced stress level) would be required than that used for the design of the 1/5- and 1/2-scale specimens to achieve a satisfactory service life.
6. Statistical inferences for a single boron-to-titanium adhesive bonded double scarf joint can be made using the test results of the double scarf joint specimen for this program. The relationship between the statistical distribution of a single joint and the distribution of the least-of-two joints (such as the double scarf joint specimen used for this study) are discussed in Appendix VII. If the underlying statistical distribution of failure is Weibull, then the distribution of both the single joint and least-of-two joints have the same shape parameter  $\alpha$ , but the scale parameter for the single joint is given by  $2^{1/\alpha} \beta$  where  $\beta$  is the scale parameter of the least-of-two joints.
7. The residual strength-versus-lifetime wearout curve for the 1/5-scale specimens did not exhibit the same shape as the constant amplitude S-N type curve. The wearout curve (residual strength versus lifetime) was concave downward with slight initial residual strength loss followed by rapidly degrading residual strength. The S-N curve was convex downward, yielding increasing life with decreasing stress amplitude. Positive correlation was achieved with the initial flaw field - kinetic crack growth based wearout mode.

8. The number of specimens required to define the factor of safety must be consistent with the expected confidence level in the statistical parameters. Since the coefficient of variation increases for the Weibull distribution as  $\alpha$  decreases, careful consideration must be given to the sample size and its impact on cost and the required factor of safety.
9. The random load history simulation used in this program preserves the composite cumulative exceedance statistics and the assumed waveform. Different random load simulations are possible for the same load history; all of these satisfy the cumulative exceedance statistics. The question arises as to which random load simulation procedure should be used for conducting random fatigue tests. Even though all random load simulations satisfy the composite exceedance statistics for the same load history will the same fatigue lines be obtained? The effect of different random load simulations on the fatigue life should be studied, and if there are significant differences, a standard simulation procedure should be developed for the aerospace community.

### 8.3 RECOMMENDATIONS

Recommendations for further research are summarized below. The RMS endurance curves are described in Reference 45.

1. Determine the character of an RMS-stress endurance curve for at least two joint design concepts to define an alternate joint design process. The RMS-stress endurance function should be correlated with a residual strength model.
2. Investigate design concepts that either negate the scale effect or reduce the static variability of bonded joints. Determine if the concepts result in improved fatigue reliability.
3. Develop an integrated random load and environment test capability and assess the effects of realistic service environment on joint performance.
4. Alter the joint design criteria and test strategy and establish design stress versus scale factors that will yield satisfactory fatigue performance.

5. Begin a rational investigation of the wearout and life-time characteristics of bolted joints.



# APPENDIX I

## DETAILS OF THE SPECTRUM SIMULATION TECHNIQUE

Four of the pertinent elements in the preparation of the random load history simulation procedure are discussed in detail in this section. Included are Press' method for decomposing exceedance curves into a series with a Gaussian distribution basis, power spectral analysis, random number mapping, and load sequence generation.

### PRESS' METHOD FOR ANALYZING EXCEEDANCE CURVES

The exceedance curves of paragraph 4.2.2 can be characterized by RMS levels, by time spent at each RMS level ( $P_i$ ), and by clipping ratios. This information can be used to develop a simulated random load history and a load-by-load basis. Press and his co-workers (Reference 29) developed a method for decomposing exceedance curves into a series with a Gaussian basis. This method is described below using Figures 44 and 45.

1. Construct a straight line that is tangent to the tail of the exceedance curve depicted in Figure 44. This line characterizes the first RMS level to be used for approximating the observed distribution. Additional straight lines, or RMS levels, may be required to realistically approximate the observed distribution. The value can be determined from the slope of the straight line constructed. The number of straight lines required depends upon the shape of the exceedance curve and the accuracy desired.
2. Construct a second straight line characterizing the second RMS level, which intersects the first straight line at a point where  $F(X_i)$  is one-half the actual  $F(X_{iA})$  for the same  $X_i$  value and is tangent, at the upper end of the line, to the exceedance curve. The intersection point between the two lines can be determined by comparing the ordinate to the first straight line, for a given  $X_i$ , to the corresponding ordinate to the exceedance curve.

Note:  $F(X_i) = 1/2 F(X_{iA})$

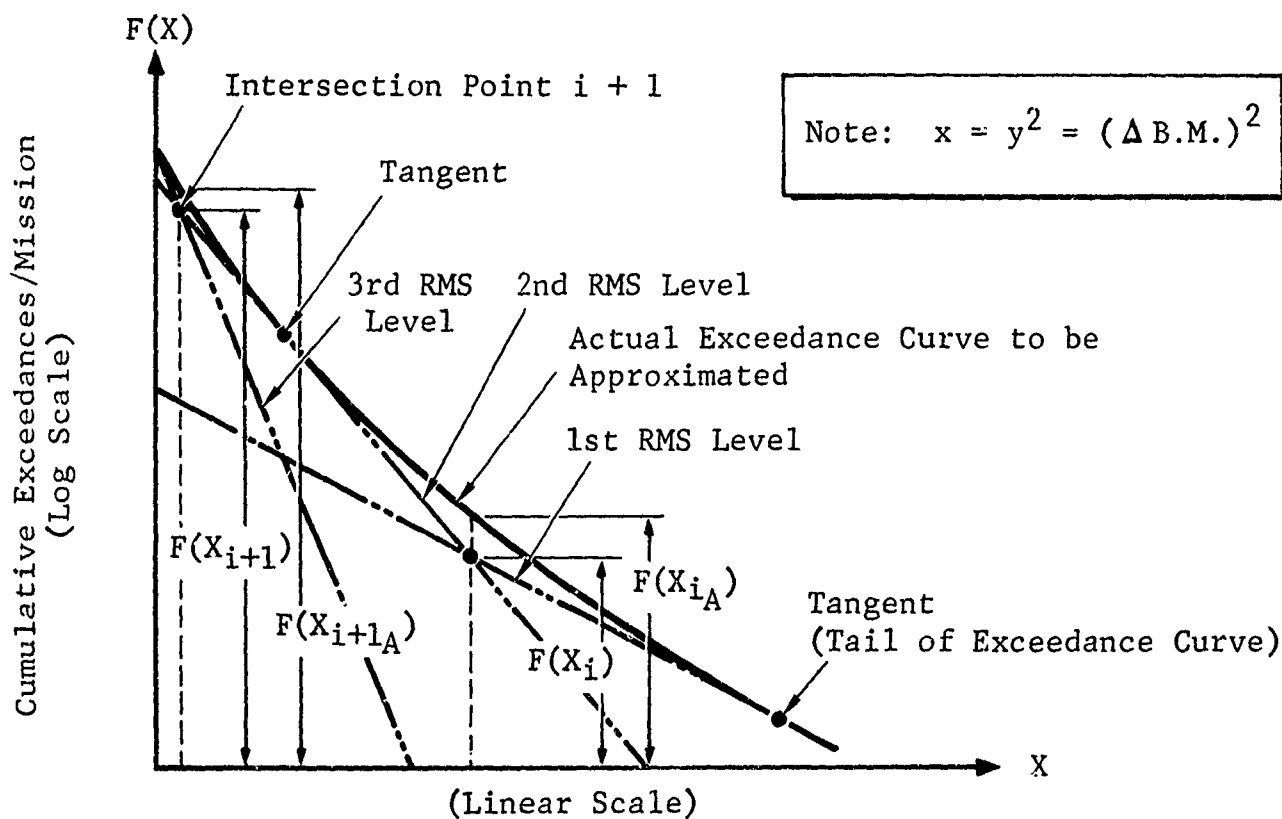


Figure 44 Exceedance Curve Analysis Notation

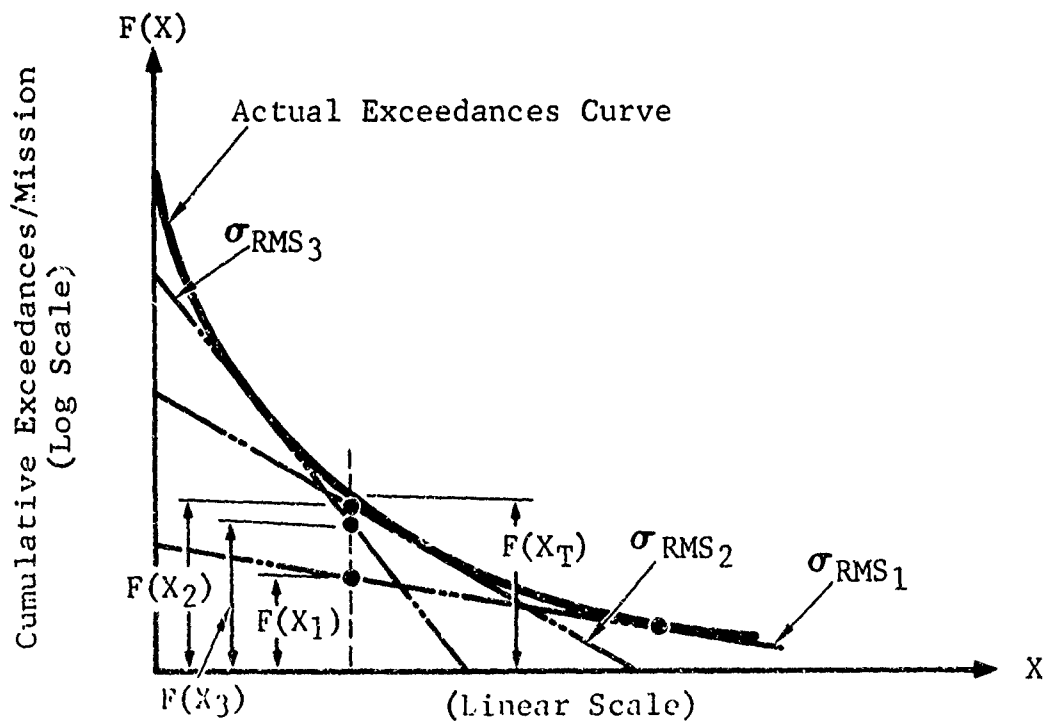


Figure 45 Summation of RMS Levels for Characterizing Exceedance Curve

Additional straight lines, if required, can be constructed in a similar manner using the last line constructed and the exceedance curve segment above the point where the last line was tangent to the curve. The third line intersects the second line at point  $i + 1$  as shown in Figure 44.

$$\text{Note: } F(X_{i+1}) = 1/2 F(X_{i+1A})$$

Only two or three RMS levels are usually required to approximate the actual exceedance curve. The RMS level, characterized by each line, is maximum for the first line developed and the RMS value decreases for successive lines. The sum of the ordinates to each RMS level (characterizing line) for a given  $X_i$  value is equal to the ordinate of the exceedance curve at the same  $X_i$  (abscissa) value (reference Figure 45), i.e.,

$$F(X_T) = F(X_1) + F(X_2) + F(X_3).$$

3. Compute  $\sigma_{\text{RMS}}$  values from the slopes of the straight lines representing each RMS level. Using the notation of Figure 44, the slope,  $m$ , of line  $i$  can be determined using two arbitrarily selected coordinate points on the line, i.e.,

$$m = \text{Slope} = \frac{1}{2\sigma^2 \text{RMS}_i} \quad \text{or} \quad \sigma_{\text{RMS}_i} = \frac{\sqrt{1}}{2m}$$

$$m = \frac{\ln F(X_{i\ell}) - \ln F(X_{ir})}{X_{ir} - X_{i\ell}} = \frac{\ln F(X_{i\ell})/F(X_{ir})}{X_{ir} - X_{i\ell}}.$$

The equation for  $\sigma_{\text{RMS}_i}$  follows:

$$\sigma_{\text{RMS}_i} = \sqrt{\frac{X_{ir} - X_{i\ell}}{2 \ln \{F(X_{i\ell})/F(X_{ir})\}}}.$$

4. Compute the time spent at each RMS level ( $P_i$ ).  $NoP_i$  is the zero intercept value for each RMS level and can be determined using similar triangles as depicted in Figure 44. The following expressions are obtained.

$$\frac{\ln \left\{ F(x_{ie}) / F(x_{ir}) \right\}}{x_{ir} - x_{il}} = \frac{\ln (N_o P_i) - \ln F(x_{ie})}{x_{il}}$$

$$\ln (N_o P_i) = \left\{ \frac{x_{il}}{x_{ir} - x_{il}} \right\} \ln \left\{ F(x_{il}) / F(x_{ir}) \right\} + \ln F(x_{il})$$

If  $x_{il}$  is equal to zero, then

$$\ln (N_o P_i) - \ln F(x_{il})$$

or

$$P_i = \frac{F(x_{il})}{N_o} \quad x_{il} = 0.$$

In general,

$$P_i = \frac{e^X}{N_o}$$

where

$$X = \left\{ \frac{x_{il}}{x_{ir} + x_{il}} \right\} \ln \left\{ F(x_{il}) / F(x_{ir}) \right\} + \ln F(x_{il}).$$

The term  $N_o P_i$  describes the total number of load exceedances from the mean for each RMS level. The portion of time spent in a given RMS level is computed by dividing the total number of exceedances from the mean (for a given mission segment type exceedance curve) into the total number of exceedances for a given RMS level.

## POWER SPECTRAL ANALYSIS

The power spectral analysis is an exact method for determining the random load history waveform for a stationary random process in which the power spectral density (PSD) is constant over

the frequency band of interest. For other random force/time histories, as shown in Figure 46, it is possible to approximate the autocorrelation function  $\psi(\tau)$  and the power spectral density function  $\phi(\omega)$ , i.e.,

$$\psi(\tau) = \lim_{T \rightarrow \infty} \frac{1}{2T} \int_{-T}^T y(t)y(t+\tau)dt \quad (42)$$

and

$$\phi(\omega) = \frac{2}{\pi} \int_0^{\infty} \psi(\tau) \cos \omega \tau d\tau \quad (43)$$

where  $y(t)$  = applicable load amplitude or load factor. Rice (Reference 46) developed the following expressions for the number of positive slope crossings of the mean load level per unit time ( $N_o$ ) and the number of peaks per unit time ( $N_p$ )

$$N_o = \frac{1}{2\pi} \left[ \frac{\int_0^{\infty} \omega^2 \phi(\omega) d\omega}{\int_0^{\infty} \phi(\omega) d\omega} \right]^{1/2}$$

$$N_p = \frac{1}{2} \left[ \frac{\int_0^{\infty} \omega^4 \phi(\omega) d\omega}{\int_0^{\infty} \omega^2 \phi(\omega) d\omega} \right]^{1/2}$$

The terms  $N_o$ ,  $N_p$  and  $N_o/N_p$  define the waveform content of the random load signal.

To develop the waveform information desired, the PSD content must be matched to an actual service history. Available flight recorder data for fighter-type aircraft were surveyed, but no suitable waveform data was found.

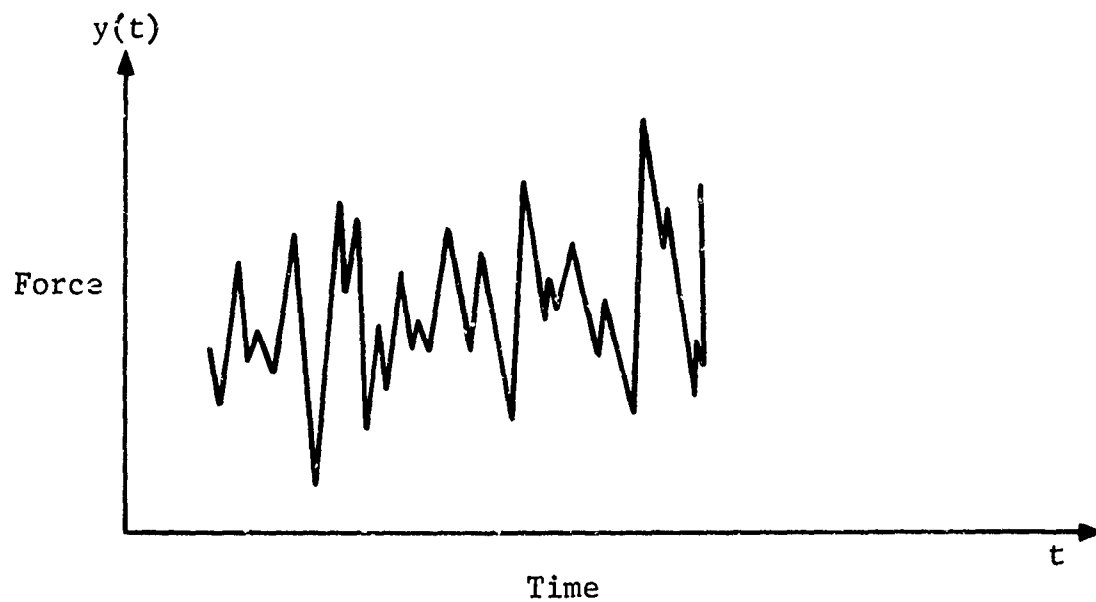
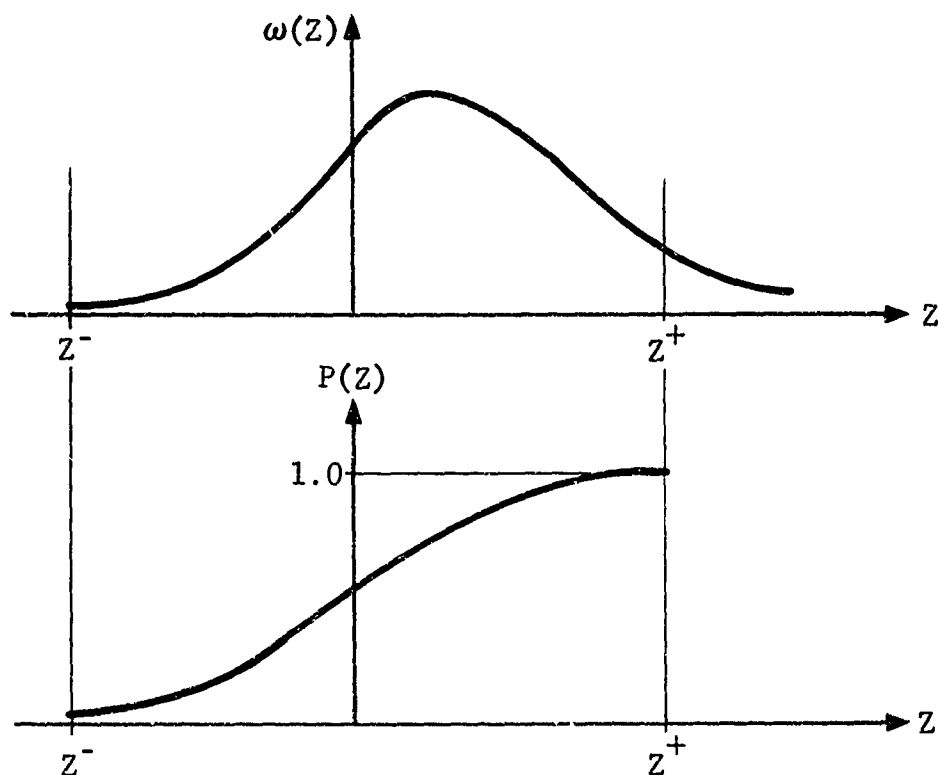


Figure 46 Random Force/Time History



Note: 
$$P(Z) = \int_{Z^-}^Z \omega(z) dz$$

Figure 47 Cumulative Distribution Curve Based on  $\omega(Z)$

The load spectrum used for the test tape is based on an F-111 A/E/D mission analysis (Reference 47). The data reduction for this analysis was based on the following assumptions:

1. The peak loads  $y(t)$  must be at least  $lg$  above or below the  $lg$  flight level value.
2. The load/time trace must have a rise and fall of at least  $lg$  and 50 percent of the incremental peak value (the incremental peak value is equal to the peak value minus  $lg$ ).

All waveform data is filtered out using these assumptions.

Due to the lack of waveform data, a value was assumed for the irregularity factor ( $N_o/N_p$ ); consequently, a power spectral analysis was not required. Nevertheless, a power spectral analysis is theoretically feasible for computing  $N_o$ ,  $N_p$  and  $N_o/N_p$  values when the PSD content is known for the service history. For this reason the framework for a power spectral analysis is retained for the computer program of Reference 26.

#### RANDOM NUMBER MAPPING

The Rice-Bendat-Kowalewski functions, the corresponding cumulative distribution function, and the random number mapping procedure are discussed in this section. Random number mapping is required to generate random delta loads that satisfy a prescribed statistical distribution for the population.

#### Rice-Bendat-Kowalewski Function

The random loads generated must fit a frequency distribution compatible with the possible load occurrences for the population. An aircraft experiences both positive and negative load exceedances during operation. There are generally many more positive load exceedances than negative ones. A frequency distribution function is needed which describes a population of positive and negative loads in a prescribed proportion. The Rice-Bendat-Kowalewski function (References 46, 48, and 49 respectively) satisfies this requirement. This function combines the Gaussian and the Rayleigh distributions. When  $N_o/N_p$  is equal to 0.0,  $W(Z)$  reduces to the Gaussian distribution and when  $N_o/N_p$  is equal to 1.0,  $W(Z)$  reduces to the Rayleigh distribution. For intermediate  $N_o/N_p$  values,  $W(Z)$  is a mixed mode distribution. Since the Rice-Bendat-Kowalewski

function preserves the irregularity factor,  $N_o/N_p$ , for incremental load changes, this function was used in the random load history simulation.

Rice-Bendat-Kowalewski Function (Page 171 of Reference 50) is given below

$$W(Z) = \frac{K_1}{\sqrt{2\pi}} e^{-Z^2/2K_1^2} + \left(\frac{N_o}{N_p}\right) Z e^{-Z^2/2} [1-P(Z/K_2)]$$

where:

$$K_1 = \left\{ 1 - (N_o/N_p)^2 \right\}^{1/2}$$

$$K_2 = K_1 / (N_o/N_p)$$

$$P(Z/K_2) = \frac{1}{\sqrt{2\pi}} \int_{Z/K_2}^{\infty} e^{-y^2/2} dy \quad (\text{Error function, } y \text{ being a dummy variable})$$

$W(Z)$  = Probability density function

$Z$  = Normalized variable for the density function

$N_o$  = Number of positive slope crossings of the mean per unit time

$N_p$  = Number of positive peaks per second.

$N_o/N_p$  = Irregularity factor

#### Cumulative Distribution

A cumulative distribution curve  $\{P(Z) \text{ versus } Z\}$  is generated by summing incremental areas under the normalized  $W(Z)$  curve. Normalization involves adjusting the ordinates to the  $W(z)$  curve so that the area under the  $W(Z)$  curve, between the positive and negative clip limits, ( $Z^+$  and  $Z^-$  respectively) is equal to 1.0.  $P(Z)$  is described in Figure 47 in terms of  $W(Z)$ .



The cumulative distribution curve,  $P(Z)$ , is needed to determine random values of  $Z$  compatible with the distribution for the population. Acceptable values for  $Z$ , which fit the  $P(Z)$  distribution, are determined using the mapping procedure described in the following paragraph.

### Mapping Procedure

Each random load in the service-history simulation is based on a random number. A mapping procedure is used to "fit" the random numbers drawn to a given statistical distribution; i.e., the Rice-Bendat-Kowalewski function. Random numbers are used to characterize the RMS values for each RMS level of each mission segment type and each mission.

The random number mapping procedure used in the BY4 computer program (Reference 26) is described below. This procedure is used to generate loads on a load-by-load basis.

1. Compute 400 values of the Rice-Bendat-Kowalewski function,  $(Z)$ , for a given  $N_0/N_p$  value. Assume a clipping ratio of  $\pm 6.0$ . The resulting curve is depicted in Figure 48.
2. Generate a normalized cumulative distribution curve using the results above. Since the area under  $W(Z)$  between  $Z$  equal  $\pm 6.0$  is less than 1.0 the incremental areas are normalized to make the total area under  $W(Z)$  equal to 1.0. Such a curve is shown in Figure 49.
3. Define the clipping ratios for each RMS level for both the positive and negative spectra and for all segments. Assume symmetrical clipping about  $ZZ$  equal to zero. Determine for each clipping ratio the corresponding segment of the cumulative distribution curve for which the ratio applies. The cumulative distribution curve between points  $i$  and  $j$  depicts an applicable curve segment. Points  $i$  and  $j$  on the curve are defined by  $(ZZ_{Bi}, YY_{Bi})$  and  $(ZZ_{Bj}, YY_{Bj})$ , respectively.
4. Each mission segment has a positive and negative (spectra) clipping value for each RMS level. Clipping is assumed symmetric for both the positive and negative spectra. Two vertical lines are drawn in Figure 50 to represent the largest clipping ratio for a given RMS level. A box is formed between the lines  $k - j$ ,  $j - ZZ_{Bj}$ ,  $ZZ_{Bj} - ZZ_{Bi}$ , and  $ZZ_{Bi} - k$ , and since this box characterizes the largest

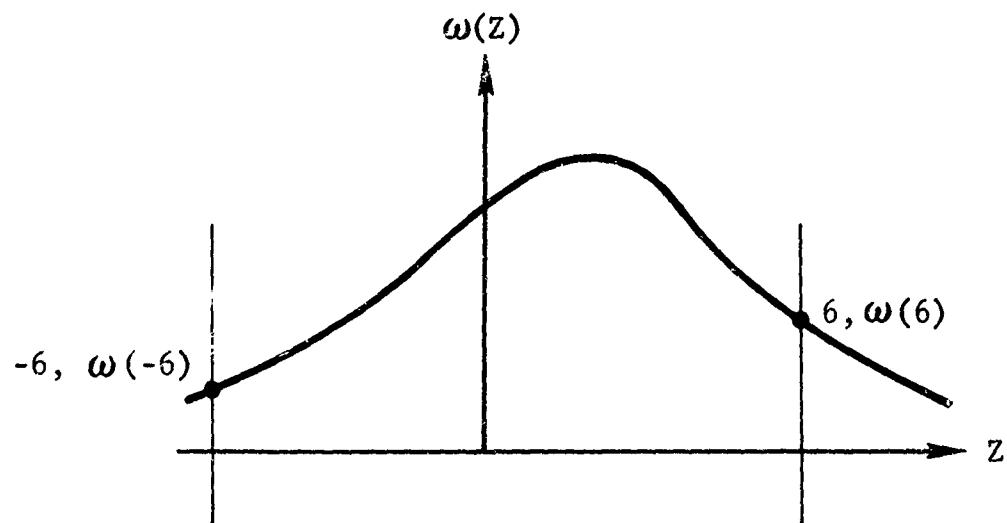


Figure 48 Clipped Rice-Bendat-Kowalewski Function

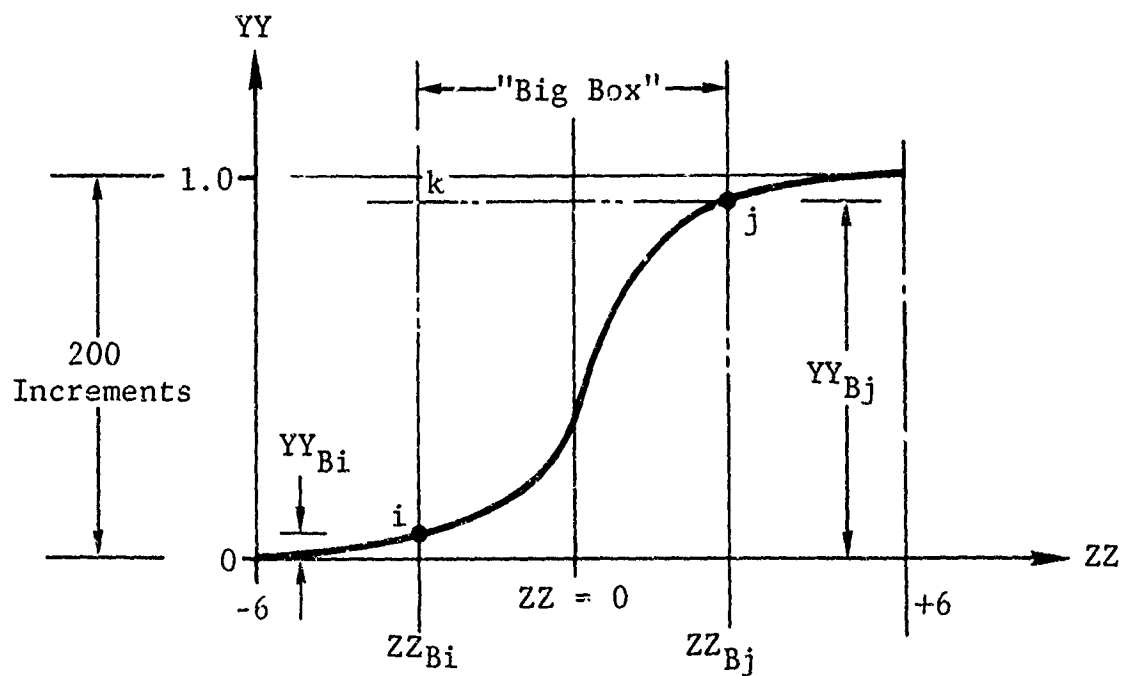


Figure 49 Normalized Cumulative Distribution Curve for Random Mapping

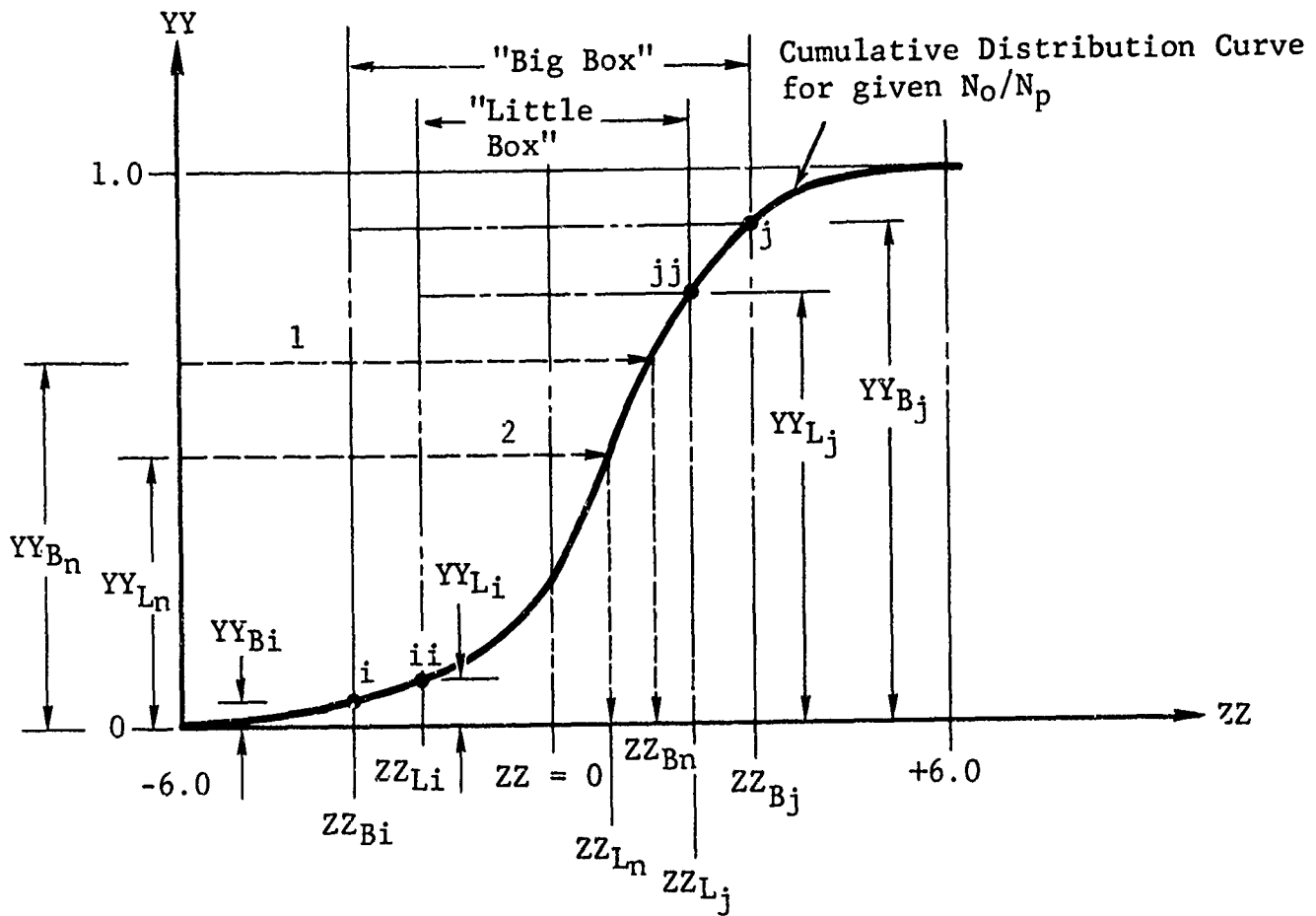


Figure 50 Symbolic Representation of Mapping Procedure

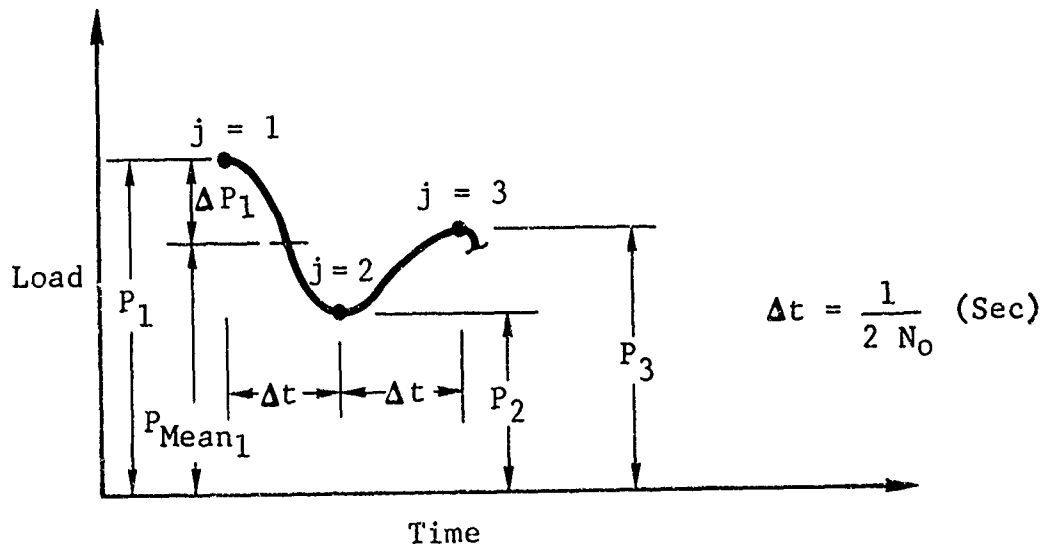


Figure 51 Load Generation Characterization

clipping ratio, it is called the "Big Box." In a similar manner, a smaller box can be formed within the "Big Box" to characterize the smaller clipping ratio. This box is called the "Little Box." Random numbers that fit both boxes must be selected.

5. A sequence of pseudo-random numbers between 0.0 and 10,000 are generated using the programmed procedure of Reference 51 and each number is divided by 10,000 to scale it to the YY axis. Two modified random numbers ( $ZZ_{Bn}$  and  $ZZ_{Ln}$ ) are generated for each pseudo-random number in the sequence. The first scaled random number in the sequence is resealed to fit the "Big Box" and the first acceptable random number for this box,  $ZZ_{Bn}$ , is obtained from the library data generated by the program.  $ZZ_{Bn}$  corresponds to the point  $YY_{Bn}$  on the cumulative distribution curve between segment i - j.  $YY_{Bn}$  is defined by the following equation.

$$YY_{Bn} = YY_{Bi} + (YY_{Bj} - YY_{Bi}) * RN_n$$

where

$YY_{Bn}$  = Scaled random number applicable to curve segment i - j ("Big Box")

$YY_{Bi}$ ,  $YY_{Bj}$  = Ordinate of the cumulative distribution curve at  $ZZ_{Bi}$  and  $ZZ_{Bj}$  respectively (largest clipping ratio for given RMS level)

$RN_n$  = Scaled random number, n, from the sequence.  
(n = 1 for first random number).

An acceptable random number for the "Little Box" ( $ZZ_{Ln}$ ) is determined using  $YY_{Bn}$  and the following equation,

$$YY_{Ln} = YY_{Lj} + (YY_{Lj} - YY_{Li}) * YY_{Bn}$$

where

$YY_{Ln}$  = Scaled random number applicable to "Little Box."

$YY_{Li}$ ,  $YY_{Lj}$  = Ordinate of the cumulative distribution curve at  $ZZ_{Li}$  and  $ZZ_{Lj}$  respectively (smallest clipping ratio for given RMS level).

The technique described is symbolized in Figure 50.

## Load-by-Load Generation

The load-by-load generation procedure of Reference 26 is described in this section. This procedure is based on the idea implemented by Dr. J. C. Halpin of the Air Force Materials Laboratory (Reference 1).

The essential steps in the procedure are

1. Draw a random number and fit to cumulative distribution curve (fitted R.N.)<sub>j</sub>
2. Compute the delta load measured from the mean using,

$$\Delta P_j = (-1)^{j+1} (\text{fitted R.N.})_j * (\sigma \text{ RMS})_i$$

Note:  $j = 1$  for first load,  $j = 2$  for second load, etc.

$i = \text{RMS level}$

3. Compute the load peak value using

$$P_j = P_{\text{mean } j} + \Delta P_j$$

Note: The sign of  $\Delta P_j$  can be positive or negative

4. Increment the time by  $1/2 N_0$  (sec) and generate the next load. A haversine waveform is used to connect successive loads. This process continues until the required number of loads have been generated for the service history simulation. This procedure is characterized in Figure 51.

The loading signal starts with a positive excursion from the mean. A negative excursion follows each positive one until the time spent in the positive or negative RMS level has been consumed (Figure 52). Usually more positive load excursions occur than negative ones; therefore, more positive loads must be generated than negative ones to preserve the exceedance statistics.

The time to be spent in each RMS level (positive and negative) for each mission segment type is computed from the corresponding exceedance curve. After each load is generated, the time is incremented and the next load is generated. The BY4 computer program (Reference 26) keeps track of the time spent in the positive and negative RMS levels and preserves the distribution of positive and negative load excursions in a RMS burst. A RMS burst is the

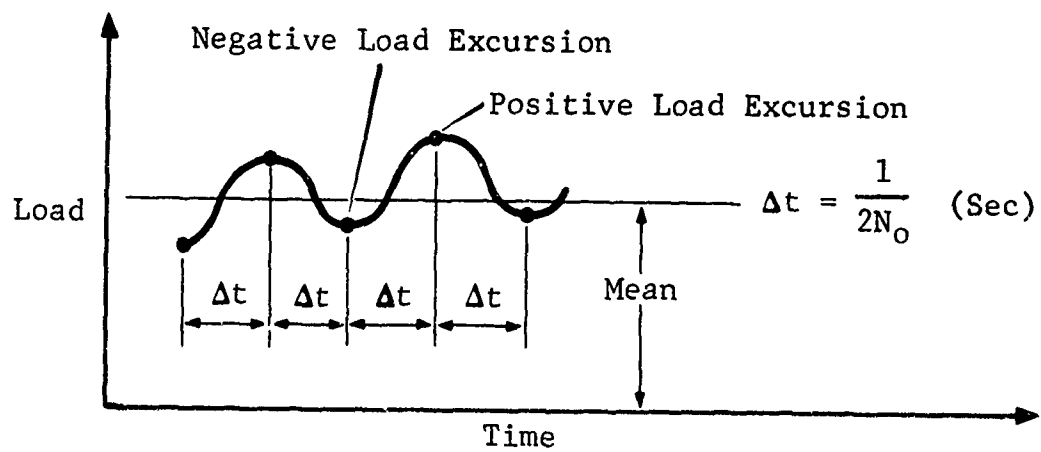


Figure 52 Positive and Negative Load Excursions

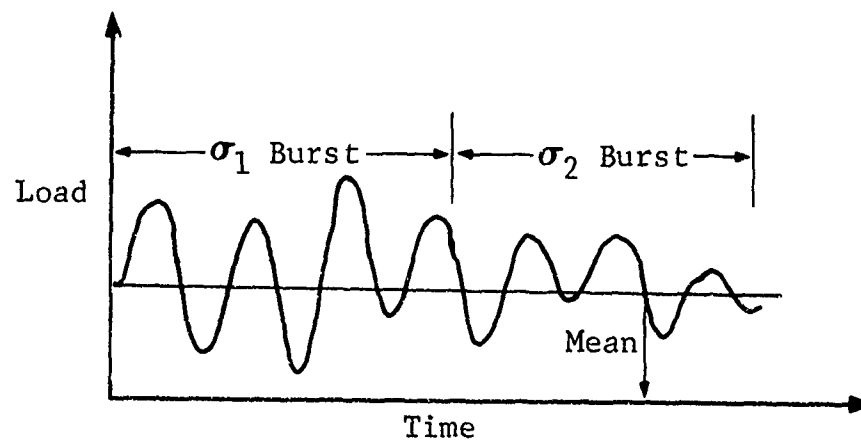


Figure 53 RMS Burst Description

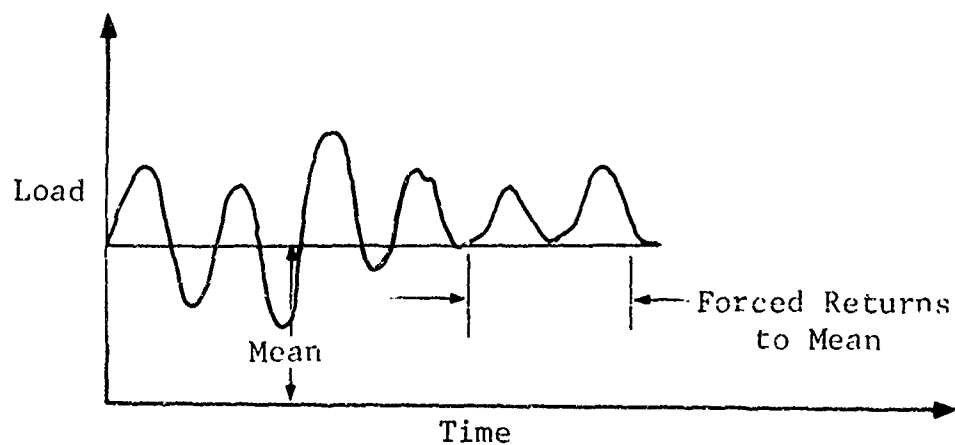


Figure 54 Forced Returns to the Mean

load time history simulation for a given positive and negative RMS level (reference Figure 53).

The BY4 program is written so that the load signal will return to the mean after each positive load excursion when all negative load excursions for a given RMS level have been generated or vice versa. The time is incremented for a forced return to the mean; however, this time is not counted toward the total time required to generate the positive or negative loads for a given RMS level (reference Figure 54). A forced return to the mean is not included in the total load count for the simulation.

The procedure developed to support this contract activity is a pilot procedure only. The difficulties encountered will require further exploration.

The method of creating the delta load increment leads to an error in input to output  $N_o/N_p$ . A polynomial correction function was used to remove this error.

A capability for generation of an asymmetric history for only the case of  $N_o/N_p = 1.0$  was developed and checked.

## A P P E N D I X   I I

### W A R P A G E   P R O B L E M

#### STRAIN SURVEYS

Strain surveys were conducted using 1/5-scale specimens. These surveys were performed to (1) determine the feasibility and/or need for removing or reducing the warpage effect in the initial 25 1/5-scale specimen and (2) evaluate the significance of the warpage effect on the test results. The strain surveys conducted are summarized in Table XXXIV.

The tension and compression strain surveys were performed to determine the feasibility and/or need for reducing the warpage effects. The static strain surveys were conducted to evaluate the effect and significance of induced bending stresses due to specimen warpage. A strain survey was also performed on a specimen that had been subjected to a prior constant amplitude load history. The purpose of this survey was to evaluate the significance of specimen warpage after cyclic loading.

Five typical 1/5-scale specimens were selected from the initial 25 built. The dimensional variations are shown in Table IX. Specimen K994568 was used for the tension and compression strain surveys and specimen K994566 was used for the constant amplitude strain surveys. Specimens K012439, K012441, and K994588 were used for the static strain surveys. Four strain gauges were mounted back-to-back on each specimen as shown in Figure 55. The strain survey descriptions and results are given in the following sections.

#### Tension Strain Survey

The tension strain surveys were performed using a 1/5-scale specimen mounted in fixture 6 (Figure 56). Strain surveys were conducted with and without a center support or jam bar. Figure 57 shows the test set-up for the center support case without jam bar. The center support is made up of two long channels (welded to the fixture), two short channels, two teflon rub strips, two support angles, nuts, and bolts. A Teflon rub strip is attached to each short channel with countersunk bolts. The specimen is mounted between the two short channels with the Teflon rub strips next to the specimen. Four bolts tie the two short channels together as shown in Figure 56. Washers were used with these bolts



Table XXXIV SUMMARY OF STRAIN SURVEYS CONDUCTED

Survey I.D.	Description
Tension Checkout	(a) 0 to 60K to 0 without center support
	(b) 0 to 20" to 0 with center support
	(c) 0 to 20K; jam bar installed for equalizing strains; 20K to 60K to 0.
Compression Checkout	(a) 0 to 20K without C-clamps; clamps installed & load reduced to -10K; clamps readjusted to equalize strains; -10K to 60K to -10K to 0.
	(b) 0 to -10K without jam bar; added jam bar to equalize strains, -10K to 0.
Static	Static tested three specimen; read strains for 10K increments; loaded to failure.
Constant Amplitude	(a) Cycled specimen for 260 cycles using 5K to 50K and then conducted strain survey.
	(b) Same as (a) except 3300 cycles were put on before strain survey.

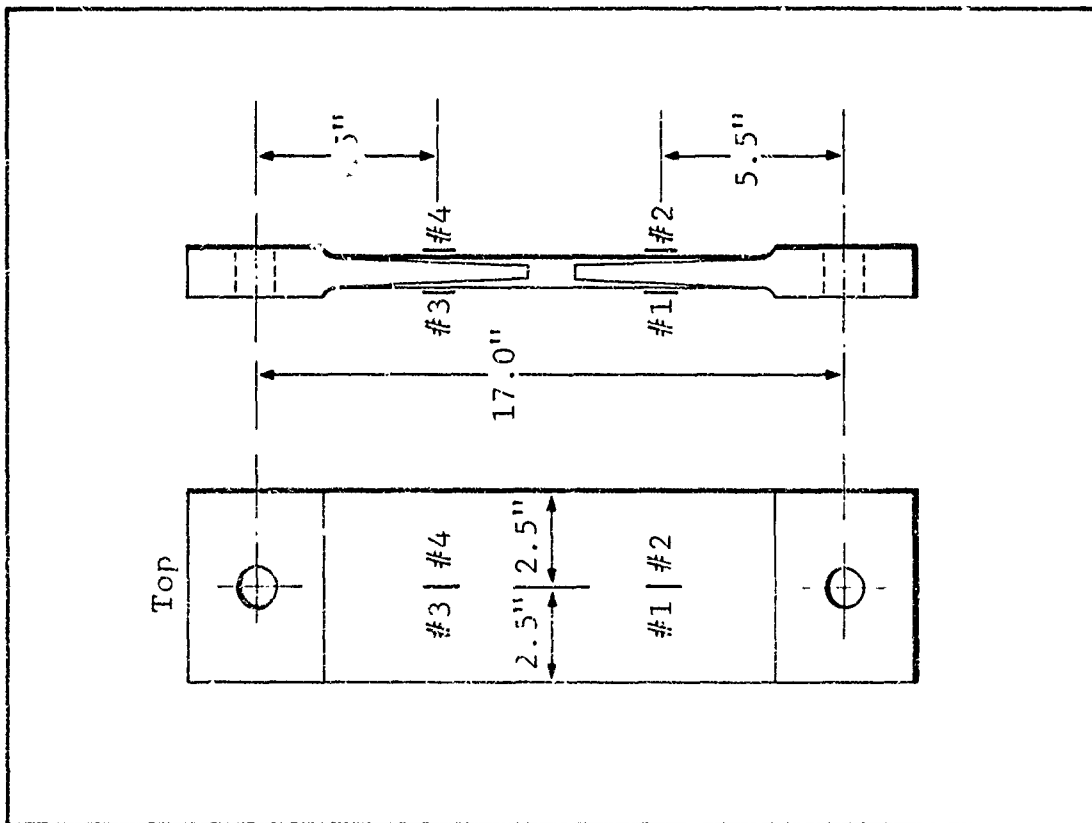


Figure 55 Strain Gage Locations for  
1/5-Scale Specimens

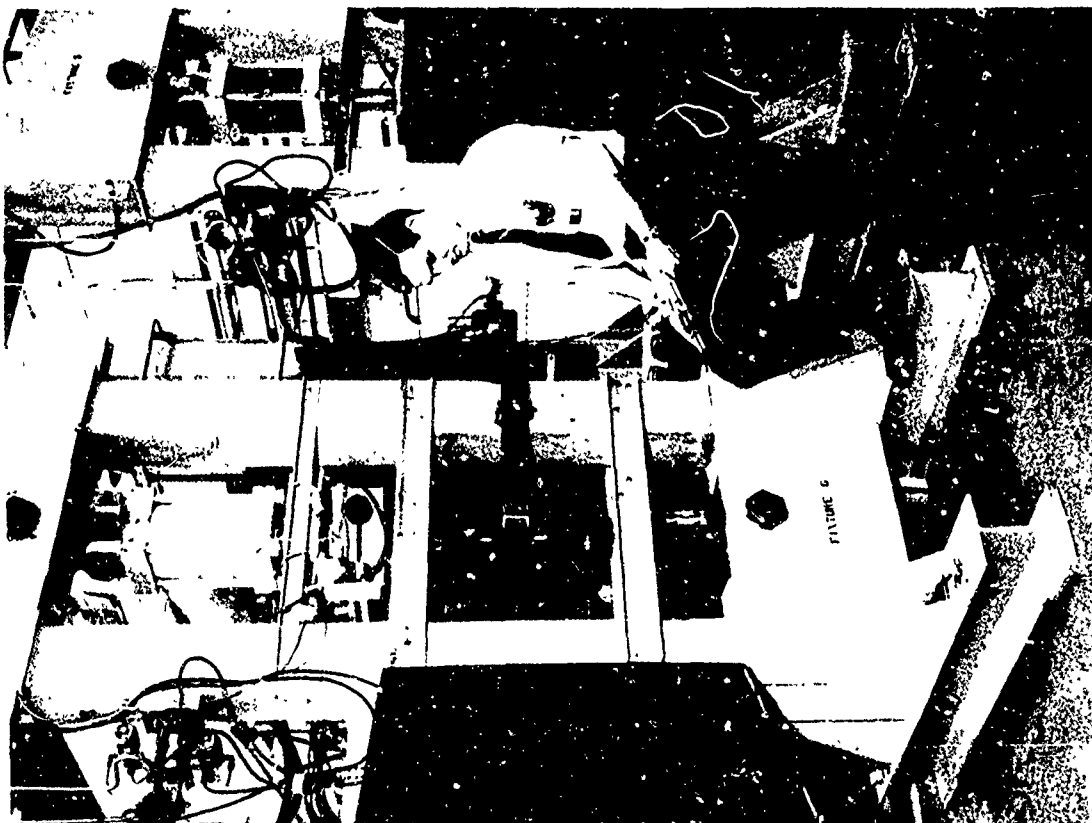


Figure 56 Set Up for Tension and Compression  
Strain Surveys with Center Support

to separate the channels. With this arrangement there is no mechanical attachment between the specimen and the center support. The center support is removed by taking out the two short channels. The jam bar is composed of a 1" diameter steel rod with threaded ends and mating nuts. When the jam bar is used some of the washers are removed between the two short channels so that the teflon can be forced against the specimen by the jam bar. The jam bar is placed between the left hand vertical support of fixture 6 and the face of the corresponding short channel. Pressure is put on the specimen by torquing the jam bar nuts. The strain gauges were read for a given loading and the jam bar was adjusted to equalize the back-to-back strain gauge readings.

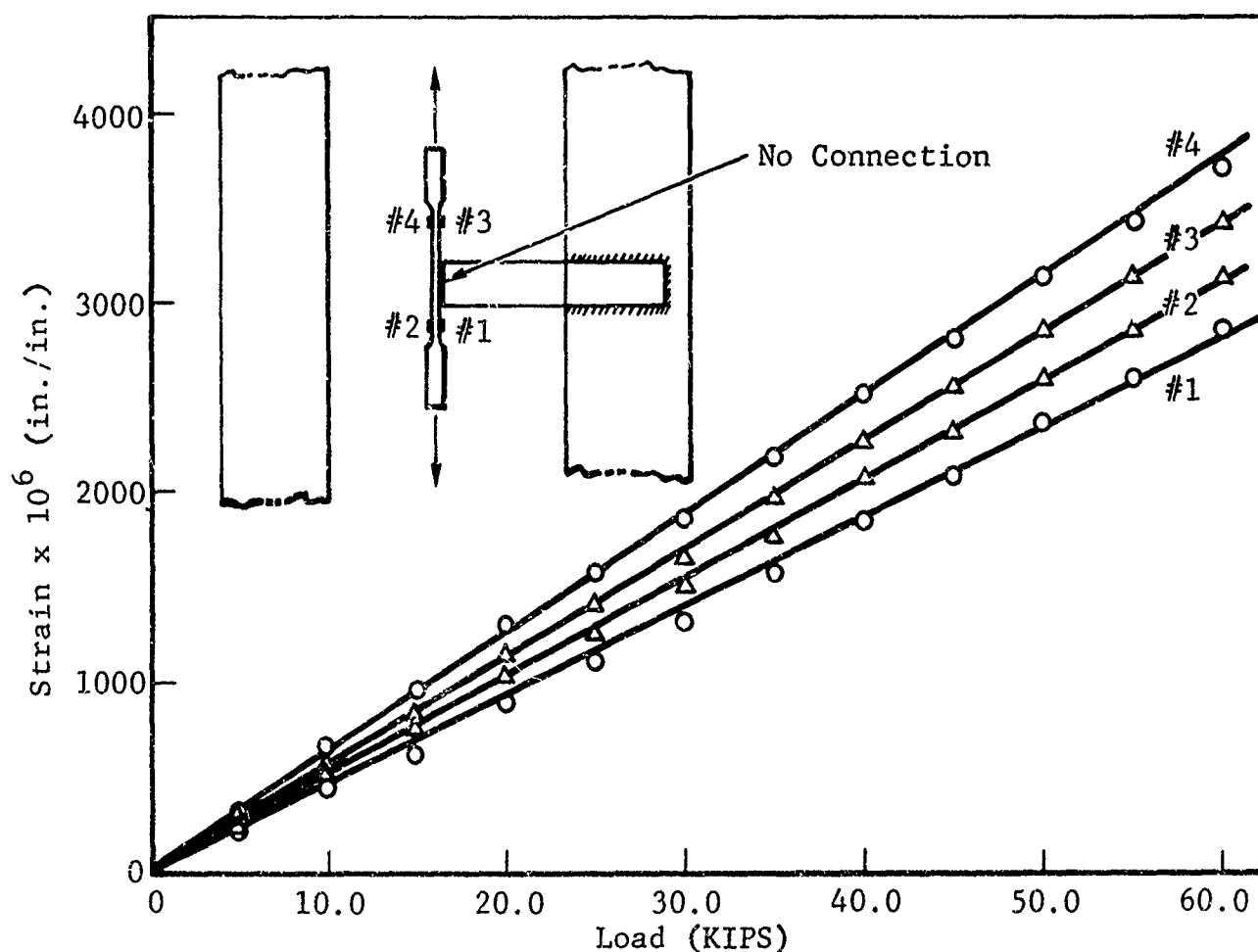


Figure 57 Tension Strain Survey; without Center Support

Using the various support options the specimen was loaded in increments and the strains were read. To preclude lamina yielding a maximum load of 60K was used. The strain gauge readings for the cases studied are summarized in Table XXXV and XXXVI. The strains are plotted in Figure 57 for the case without the center support.

Table XXXV TENSION STRAIN SURVEY USING 1/5-SCALE  
SPECIMEN WITHOUT CENTER SUPPORT

Load (KIPS)	Strains x 10 <sup>0</sup> (in/in)			
	$\epsilon_1$	$\epsilon_3$	$\epsilon_2$	$\epsilon_4$
0	16	12	11	12
5	212	324	245	283
10	451	672	522	587
15	662	974	765	850
20	908	1313	1042	1159
25	1118	1597	1278	1414
30	1332	1874	1513	1667
35	1600	2207	1796	1979
40	1866	2539	2082	2290
45	2105	2824	2331	2558
50	2371	3144	2613	2865
55	2614	3435	2866	3141
60	2877	3737	3133	3434
40	1814	2489	2025	2238
20	847	1253	981	1093
0	-6	18	23	-9

Note: Specimen K994568 used for survey

Table XXXVI TENSION STRAIN SURVEY: WITH CENTER SUPPORT;  
WITH CENTER SUPPORT AND JAM BAR

Load (KIPS)	Strains $\times 10^6$ (in/in)				Remarks
	$\epsilon_1$	$\epsilon_3$	$\epsilon_2$	$\epsilon_4$	
0	15	11	9	13	With center support & no jam bar
20	906	1286	1010	1156	With center support & no jam bar
20	1008	1174	1182	961	With center support & jam bar adjustment 1
20	1008	1169	1109	1041	With center support & jam bar adjustment 2
20	1005	1176	1108	1048	With center support & jam bar adjustment 3
20	1005	1182	1106	1049	With center support & jam bar adjustment 4
25	1215	1478	1347	1324	With center support & jam bar adjustment 4
30	1464	1805	1613	1630	
35	1695	2108	1869	1912	
40	1948	2430	2137	2219	
45	2193	2734	2396	2512	
50	2458	3057	2671	2815	
55	2678	3326	2908	3074	
60	2950	3651	3188	3391	
50	3928	3025	2677	2685	With center support & jam bar adjustment 5
40	3352	2403	2158	2090	
30	1418	1776	1646	1500	
20	947	1128	1131	907	
10	512	476	637	325	
0	141	-100	221	-171	

### Compression Strain Survey

A compression strain survey was performed using specimen K994568 and test fixture 6 (Figure 57). The same basic apparatus used for the tension strain survey was used for this strain survey. In addition, two C-clamps were used to clamp the two short channels against the specimen. The specimen was mounted in fixture 6 using a given support option. C-clamps and a jam bar were used to adjust the strain gauge readings. Loads were applied to the specimen in increments and the strain gauges were read. The maximum tension and compression load used was 60K and -10K, respectively. The strain gauge data generated is shown in Table XXXVII and XXXVIII.

### Static Test Strain Survey

Static strain surveys were conducted using specimen K012439, K012441, and K994588 and a Baldwin-Tate-Emery Universal test machine. The specimens were mounted as shown in Figure 26. Load was applied to the specimen in 10K increments until failure occurred. The strain gauge readings at each load level and the failing loads are summarized in Table XXXIX. The load versus strain is plotted for applicable specimens in Figures 58, 59, and 60.

### Constant Amplitude Strain Survey

This strain survey was performed to evaluate the effect of specimen warpage on a specimen with a prior constant amplitude load history. Specimen K994566 was mounted in fixture 5 as shown in Figure 22, and the strains were read under zero load. Two strain surveys were performed. Two-hundred and sixty cycles of 5K to 50K constant amplitude loading were first applied to the specimen. Static loads were applied in increments and the strains were read. After reaching a maximum load of 50K the load was reduced in increments to zero and the strains were read at each load level. An additional 3040 cycles of the 5K to 50K constant amplitude loading was applied to the specimen and a new strain survey was performed as before. The strain gauge data generated is summarized in Table XL.

Table XXXVII COMPRESSION STRAIN SURVEY: WITH CENTER SUPPORT;  
WITH CENTER SUPPORT AND C-CLAMPS

Load (KIPS)	Strains x 10 <sup>6</sup> (in/in)				Remarks
	$\epsilon_1$	$\epsilon_3$	$\epsilon_2$	$\epsilon_4$	
0	14	10	11	11	With center support (no jam bar or C-clamp)
20	977	1287	1118	1125	With center support (no jam bar or C-clamp)
20	1018	1247	1195	1047	With center support (C-clamps installed)
15	757	895	908	726	
10	524	567	642	431	
5	309	252	397	148	
0	86	-53	179	-147	
-2	-23	-235	38	-294	
-4	-87	-355	-55	-389	
-6	-159	-491	-153	-494	
-8	-240	-653	-274	-615	
-10	-311	-813	-389	-729	
-10	-463	-640	-596	-545	
0	-69	121	-25	58	With center support (C-clamps Adjustment 1)
20	942	1306	1087	1154	
25	1320	1441	1443	1301	
30	1569	1763	1715	1596	
35	1810	2066	1974	1878	
40	2065	2383	2252	2177	
45	2311	2681	2510	2455	
50	2581	3006	2794	2762	
55	2833	3299	3053	3044	
60	3098	3612	3327	3339	
40	2029	2346	2212	2135	
20	1065	1118	1170	1000	
0	165	-147	172	-146	
-10	-236	-905	-415	-704	
0	161	-155	173	-151	

Table XXXVIII COMPRESSION STRAIN SURVEY WITH CENTER SUPPORT  
(WITH AND WITHOUT JAM BAR)

Load (KIPS)	Strain $\times 10^6$ (in/in)				Remarks
	$\epsilon_1$	$\epsilon_3$	$\epsilon_2$	$\epsilon_4$	
0	13	12	9	9	With center support and no jam bar
-2	-83	-188	-145	-125	
-4	-155	-335	-258	-228	
-6	-222	-466	-364	-324	
-8	-298	-631	-490	-435	
-10	-374	-788	-612	-543	
-10	-572	-576	-652	-496	With center support and jam bar
-8	-461	-369	-489	-344	
-6	-383	-245	-384	-249	
-4	-321	-143	-302	-159	
-2	-203	21	-161	-21	
0	-105	122	-75	80	



Table XXXIX STRAIN SURVEY USING STATIC TEST SPECIMENS (1/5-SCALE)

Specimen I.D.	K012439				K012441				K994588			
	#1	#2	#3	#4	#1	#2	#3	#4	#1	#2	#3	#4
0	6.6	5.6	-6.6	-3.6	-3.6	5.6	-0.6	5.6	1.6	5.6	-7.6	5.6
20	--	--	--	--	--	--	--	--	--	--	--	--
0	-983.6	-983.6	-995.6	-990.6	-991.6	-982.6	-989.6	-983.6	-989.6	-986.6	-997.6	-984.6
10	694.6	695.6	391.6	389.6	662.6	692.6	387.6	389.6	497.6	405.6	560.6	721.6
20	1271.6	1301.6	899.6	863.6	1248.6	1286.6	840.6	853.6	1010.6	918.6	1103.6	1325.6
30	1851.6	1911.6	1434.6	1364.6	1838.6	1882.6	1322.6	1350.6	1538.6	1464.6	1665.6	1934.6
40	2418.6	2499.6	1964.6	1867.6	2412.6	2468.6	1810.6	1848.6	2065.6	2012.6	2223.6	2529.6
50	2998.6	3100.6	2523.6	2398.6	2996.6	3874.6	2328.6	2372.6	2615.6	2595.6	2806.6	3156.6
60	3575.6	3697.6	3083.6	2932.6	3574.6	3879.6	2860.6	2897.6	3144.6	3156.6	3363.6	3750.6
70	4185.6	4295.6	3649.6	3473.6	4160.6	4872.6	3377.6	3441.6	3686.6	3752.6	3934.6	4366.6
80	4769.6	4880.6	4189.6	4014.6	4739.6	4859.6	3905.6	3959.6	4221.6	4325.6	4491.6	4970.6
90	5360.6	5473.6	4790.6	4561.6	5321.6	5466.6	4464.6	4525.6	--	--	--	--
100	5959.6	6085.6	5346.6	5125.6	5930.6	6057.6	5008.6	5086.6	--	--	--	--
110	--	--	--	--	--	--	--	--	--	--	--	--
Remarks:	Failing Load = 109.8K				Failing Load = 106.4K				Failing Load = 86.6K			

Note: Strain gage readings above are multiplied by 10<sup>-6</sup> in/in.

Table XL STRAIN SURVEY AFTER CONSTANT AMPLITUDE CYCLING (5K TO 50K)

Load (KIPS)	Strain x 10 <sup>6</sup> (in/in) $\epsilon$				Remarks
	$\epsilon_1$	$\epsilon_2$	$\epsilon_3$	$\epsilon_4$	
0	5	5	6	4	260 cycles of 5K to 50K applied to K994566 before strain survey
5	280	226	269	241	
10	600	511	547	589	
15	867	748	774	867	
20	1186	1043	1060	1211	
25	1465	1305	1313	1500	
30	1774	1598	1601	1828	
35	2049	1861	1858	2116	
40	2370	2163	2155	2448	
45	2651	2433	2426	2745	
50	2962	2735	2724	3065	
40	2304	2102	2093	2381	
30	1721	1550	1546	1772	
20	1121	984	997	1140	
10	525	437	474	499	
0	-13	7	-16	15	
0	-5	-1	-31	13	3300 cycles of 5K to 50K applied to K994566 before strain survey
10	602	480	506	578	
20	1207	1046	1047	1225	
30	1804	1614	1597	1852	
40	2378	2174	2144	2456	
50	2983	2751	2723	3083	
0	7	-11	-22	4	

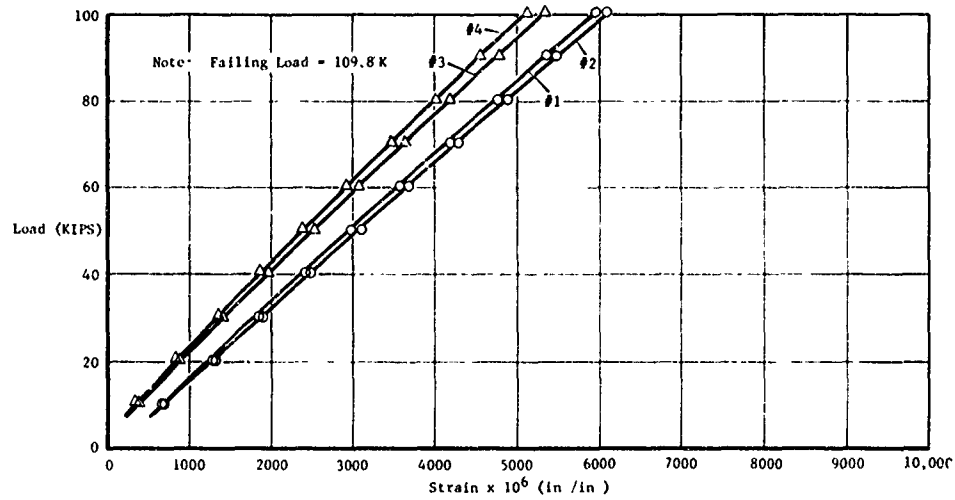


Figure 58 Load Vs. Strain, Strain Survey Using 1/5 Scale Static Test Specimen K012439

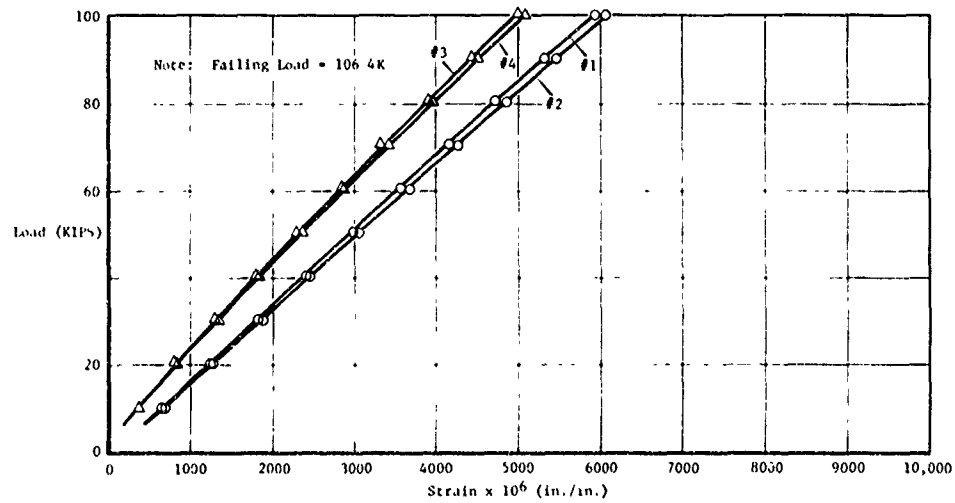


Figure 59 Load Vs. Strain, Strain Survey, Using 1/5 Scale Static Test Specimen K012441

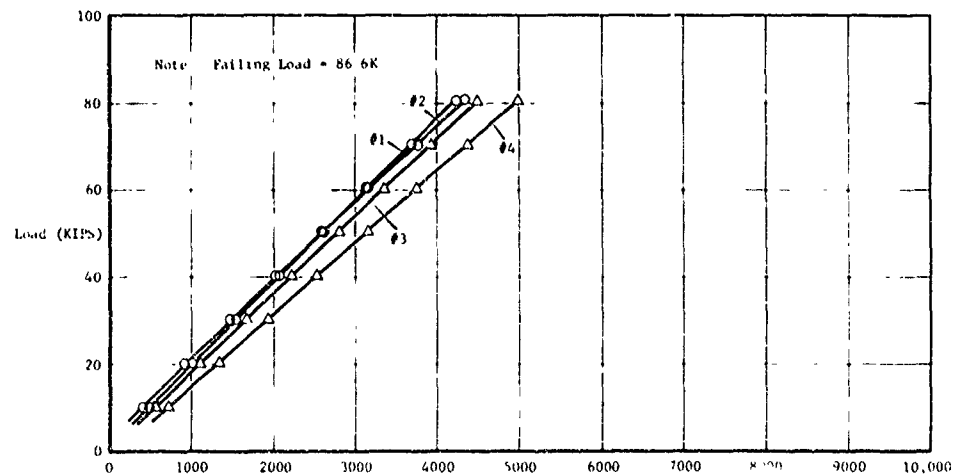


Figure 60 Load Vs. Strain, Strain Survey Using 1/5 Scale Static Test Specimen K994588

## DATA EVALUATION

The initial set of 1/5-scale specimens built were warped in varying degrees. The warpage problem was eliminated in future specimens by modifying the manufacturing procedure. An evaluation was made in this section to determine the significance of specimen warpage on the test results.

### Use of Warped One-Fifth Scale Specimen

The effects of specimen warpage and their impact on the tension and compression test results are evaluated in this section. A discussion is given for justifying the use of selected warped specimens.

#### Evaluation of Strain Surveys

##### Feasibility of Negating Warpage in Specimen Constraint -

Tension and compression strain surveys were performed using various constraints for negating the effects of specimen warpage. It was found that constraints could be imposed on the specimen for equalizing the strains rather well for a fixed loading condition but the effect could not be retained for different load levels (ref. Tables XXXV through XXXVIII). It was concluded that the effect of specimen warpage could not be satisfactorily negated by imposing specimen constraints.

Significance of Induced Bending - The significance of induced bending, due to specimen warpage, is evaluated in this section using the tension and static strain survey results. The effect of the induced bending stress is evaluated by determining the contribution of the bending stress to the total stress in the specimen. This contribution is evaluated in terms of a stress increase factor,  $F_{mi-j}$ , defined below.

$$F_{mi-j} = \frac{2 \epsilon_{\max}}{\epsilon_i + \epsilon_j}$$

where

$F_{mij}$  = stress increase factor for bending moment

$\epsilon_i, \epsilon_j$  = back-to-back strain gauge readings for gauge i and j.

$\epsilon_{\max} = \epsilon_i$  when  $\epsilon_i > \epsilon_j$

$\epsilon_j$  when  $\epsilon_j > \epsilon_i$

$F_{mij}$  is based on the assumption that the extreme fiber stresses on the specimen cross section ( $\sigma_i, \sigma_j$ ) are composed of a uniform stress,  $\sigma_a$ , and a bending stress,  $\sigma_b$ , and the two can be determined by superposition as shown in Figure 61.

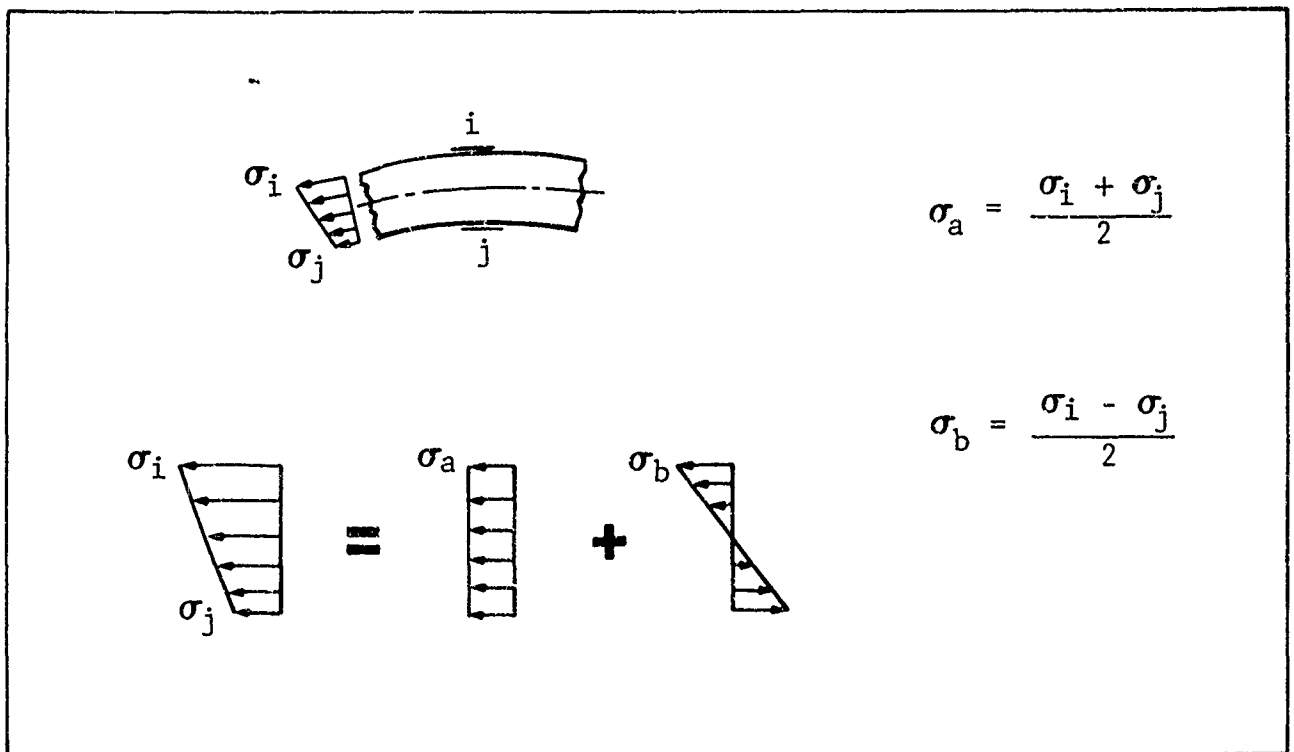


Figure 61 Superposition of Stresses for Evaluating Bending Effect

The stress increase factor for induced bending is computed by dividing the average stress,  $\sigma_a$ , into the maximum extreme fiber stress ( $\sigma_i$  or  $\sigma_j$ ). Since the increase factor,  $F_{mij}$ , is non-dimensional strains are used in place of stresses.

Table XLI STRESS INCREASE FACTORS FOR INDUCED BENDING  
MOMENT BASED ON TENSION STRAIN SURVEY

Load (KIPS)	$\epsilon_{\max}$ (#1 or #2) $\times 10^{-6}$ in/in	$\epsilon_{AVE1-2} = \frac{\epsilon_1 + \epsilon_2}{2}$ $\times 10^{-6}$ in/in	$F_{m1-2} = \frac{\epsilon_{\max}}{\epsilon_{AVE1-2}}$	$\epsilon_{\max}$ (#3 or #4) $\times 10^{-6}$ in/in	$\epsilon_{AVE3-4} = \frac{\epsilon_3 + \epsilon_4}{2}$ $\times 10^{-6}$ in/in	$F_{m3-4} = \frac{\epsilon_{\max}}{\epsilon_{AVE3-4}}$
0	16	13.5	1.185	12	12.0	1.000
5	245	228.5	1.072	324	303.5	1.068
10	522	486.5	1.073	672	629.5	1.068
15	765	713.5	1.072	974	912.0	1.068
20	1042	975.0	1.069	1313	1236.0	1.062
25	1278	1198.0	1.067	1597	1505.5	1.061
30	1513	1422.5	1.064	1874	1770.5	1.058
35	1796	1698.0	1.058	2207	2093.0	1.054
40	2082	1974.0	1.055	2539	2414.5	1.052
45	2331	2218.0	1.051	2824	2691.0	1.049
50	2613	2492.0	1.049	3144	3004.5	1.046
55	2866	2740.0	1.046	3435	3288.0	1.045
60	3133	3005.0	1.043	3737	2585.5	1.042
40	2025	1919.5	1.055	2489	2363.5	1.053
20	981	914.0	1.073	1253	1173.0	1.068
0	23	8.5	2.706	18	4.5	4.000

Note: Loads and strains taken from Table XXXVI.

Table XLJI STRESS INCREASE FACTORS FOR INDUCED BENDING MOMENT BALANCE ON STATIC STRAIN SURVEYS

Load (KIPS)	$\epsilon_{\max}$ (#1 or #2) $\times 10^{-6}$ in/in	$\epsilon_{\text{AVE}1-2} = \frac{\epsilon_1 + \epsilon_2}{2}$ $\times 10^{-6}$ in/in	$F_{m1-2} = \frac{\epsilon_{\max}}{\epsilon_{\text{AVE}}}$	$\epsilon_{\max}$ (#3 or #4) $\times 10^{-6}$ in/in	$\epsilon_{\text{AVE}3-4} = \frac{\epsilon_3 + \epsilon_4}{2}$ $\times 10^{-6}$ in/in	$F_{m3-4} = \frac{\epsilon_{\max}}{\epsilon_{\text{AVE}}}$
K012439	10	695	1.0007	391	390.0	1.0026
	20	1301	1.0117	899	381.0	1.0204
	30	1911	1.0159	1734	1399.0	1.0250
	40	2499	1.0165	1964	1915.5	1.0253
	50	3100	1.0167	2523	2460.5	1.0254
	60	3697	1.0168	3083	3007.5	1.0251
	70	4295	1.0129	3649	3561.0	1.0247
	80	4880	1.0115	4189	4101.5	1.0213
	90	5473	1.0104	4790	4675.5	1.0245
	100	6085	1.0105	5346	5225.5	1.0211
K012441	10	692	1.0222	389	388.0	1.0026
	20	1286	1.0149	853	846.5	1.0077
	30	1882	1.0118	1350	1336.0	1.0105
	40	2468	1.0115	1848	1829.0	1.0104
	50	3074	1.0129	2372	2350.0	1.0094
	60	3679	1.0145	2897	2878.5	1.0064
	70	4272	1.0133	3441	3409.0	1.0094
	80	4859	1.0125	3959	3932.0	1.0069
	90	5466	1.0134	4525	4494.5	1.0068
	100	6057	1.0106	5086	5047.0	1.0077
K994588	10	497	1.1019	721	640.5	1.1257
	20	1010	1.0477	1325	1214.0	1.0914
	30	1538	1.0247	1934	1799.5	1.0747
	40	2065	1.0129	2529	2376.0	1.0644
	50	2615	1.0038	3156	2981.0	1.0587
	60	3156	1.0019	3750	3556.5	1.0544
	70	3752	1.0089	4366	4150.0	1.0520
	80	4325	1.0122	4970	4730.5	1.0506

NOTE: Load and strains taken from Table XL.

Stress increase factors,  $F_{mij}$ , are summarized in Tables XLI and XLII for the tension and static strain surveys, respectively. The results in both cases show that  $F_{mij}$  generally decreases as the load increases. This indicates that specimens tend to self align with increasing load.  $F_{mij}$  ranges are shown in Table XLIII for the tension and static strain survey specimens.

Table XLIII  $F_{mij}$  Ranges for Tension and Static Strain Survey Specimen

Specimen	Strain Survey	$F_{mij}$ Range (KIPS)
K994568	Tension	1.074(5) to 1.043(60)
K012439	Static	1.0026(10) to 1.0211(100)
K012441	Static	1.0222(10) to 1.0106(100)
K994588	Static	1.1257(10) to 1.0506(80)

Effect of Cyclic Loading - A strain survey was performed using a specimen subjected to a prior loading history. The results shown in Table XL indicate that the strain readings taken after 260 cycles and 3300 cycles, respectively, were essentially unchanged. At the 50K load level, the  $F_{mij}$  factor was approximately 1.04 after 260 and 3300 cycles, respectively.

#### Rejection Criteria

The dimensional variations for the twenty-four specimens in Table IX were surveyed and all specimens with a surface measurement equal to or greater than 0.100 inch at any of the eight locations shown in Figure 11 were rejected. Using this criteria seven specimens were rejected and seventeen were accepted (Table IX). The dial gauge surface measurements at points 1 through 8 were averaged for the seventeen specimens accepted. The surface dimensions for the five specimens used for the strain surveys are compared against the mean surface dimensions in Table XLIV.



Table XLIV COMPARISON OF STRAIN SURVEY SPECIMENS SURFACE DIMENSIONS  
WITH AVERAGE SPECIMEN DIMENSIONS

Surface Location <sup>a</sup> Specimen <sup>b</sup>	1	3			4		5		6		7		8	
		(Surface Measurement			Inches)									
K012439c	0.010	0.0395	0.0340	0.0355	0.064	0.0075	0.033							
K012441c	-0.009	0.014	0.037	0.0245	0.065	-0.010	0.030							
K994566d	0.001	0.0155	0.014	-0.0135	0.017	0.004	0.033							
K994568e	0.012	0.010	0.001	0.003	0.021	0.0215	0.0465							
K994588c	0.003	0.006	0.0065	0.001	0.0335	-0.024	0.010							
Average Specimen <sup>b</sup>	-0.00012	0.01159	0.0144	0.0111	0.0339	0.0097	0.0355							

NOTES: a Reference Figure 11  
b Mean dimensions based on 17 acceptable specimens in Table IX  
c Used for static strain survey  
d Used for the tension and compression strain survey

The surface dimensions for the specimens used for the strain surveys represents reasonably well the average specimen depicted in Table IX.

#### Justification for Specimen Usage

Specimen tend to straighten out as the load is increased; therefore, the effects of warpage at failure are negligible. The static test results of Table XV indicate that the warpage is a second order effect because the rejected specimens exhibited static failing loads of the same order of magnitude as the accepted specimen. Also, there was no distinction in the failure modes.

Twelve warped specimens were used to conduct the constant amplitude fatigue-to-failure tests. Seven specimens were used for the tension-tension tests, and five were used for the tension-compression tests. The tension-tension constant amplitude test results for the warped and unwarped specimens (built after the warpage problem was corrected) all fell in a reasonable scatter band (Table XIV).

The tension-compression constant amplitude test results for the warped specimen did not differ very much with the unwarped specimen results. For example, specimen K900442 failed at 2959 cycles of a -10K to 50K loading and the unwarped specimens failed between 1790 and 3193 cycles. The scatter in the data does not appear to be unreasonable. The tension-compression tests were performed to (1) characterize the fatigue life of the specimens under this type of loading and (2) permit a comparison of the relative damaging effects of a tension-tension constant amplitude loading versus a tension-compression loading. The test results based on the warped and unwarped specimens satisfy these objectives.

Two fatigue-to-failure tests were performed using warped specimens (K012443 and K012464). The lifetimes for these specimens fall well in the range of values for all specimen tested (Table XVII).

# APPENDIX III

## GLOSSARY OF TECHNICAL TERMS

The principal technical terms used in this report are defined in this section.

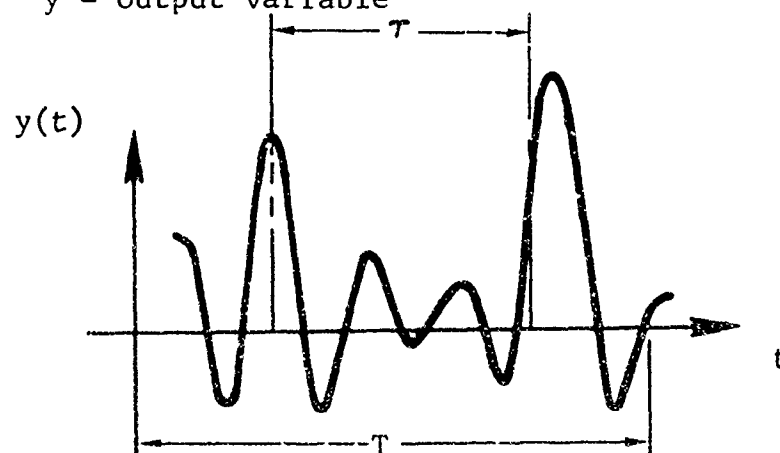
1. A/A: Air-to-air cycle
2. A/G: Air-to-ground cycle
3. Angular frequency (omega): The angle  $\theta$  through which the body rotates divided by the time required to perform this rotation, or

$$\omega = \theta / t$$

4. Asymmetric spectrum: An asymmetric spectrum, as used in this report, is one which has different positive and negative exceedances for given mission segment types.
5. Autocorrelation function: A function describing the dependence of data at one time  $t$  to that of another time  $t + \tau$

$$\psi(\tau) = \lim_{T \rightarrow \infty} \frac{1}{2T} \int_{-T}^T y(t)y'(t + \tau)dt$$

where:  $\psi(\tau)$  = autocorrelation function  
 $\tau$  = variable time delay (sec)  
 $T$  = period (sec)  
 $y$  = output variable



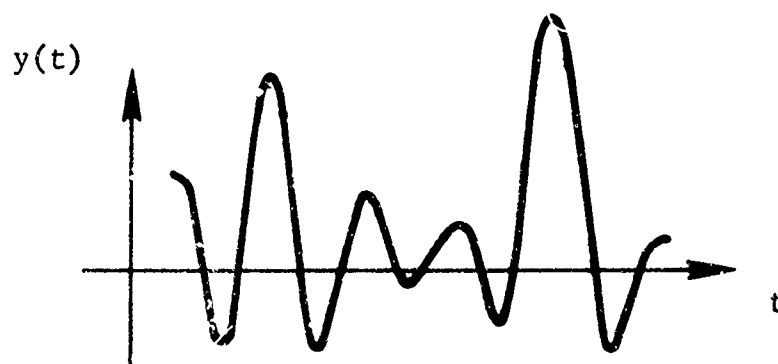
$\psi(\tau)$  is needed to compute  $N_0$  and  $N_p$ .  
 (Reference 52, page 19).

6. Average: The sum of the results divided by the number of trials, i.e.,

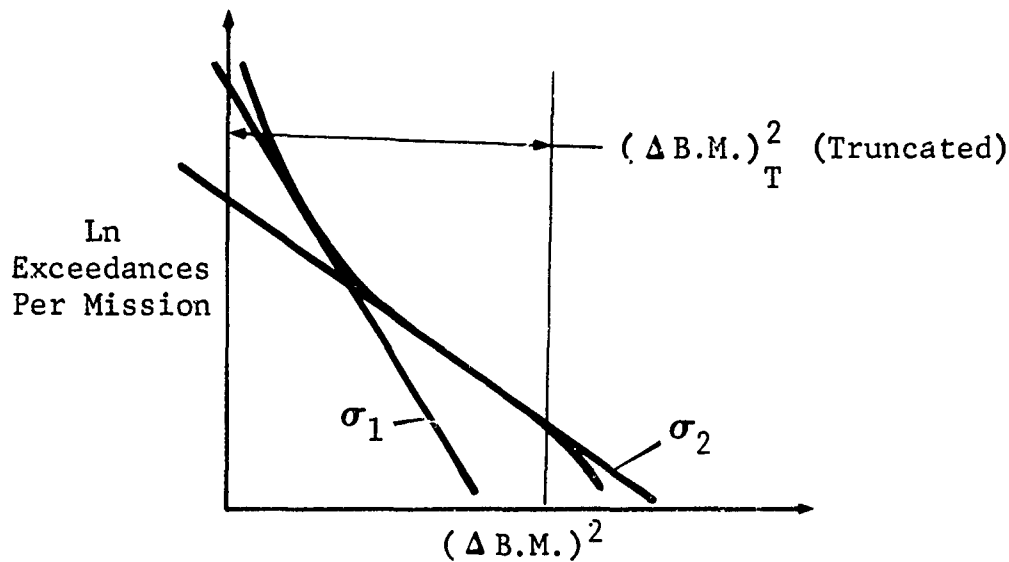
$$\text{Average} = \frac{\sum_{i=1}^n x_i}{n} \quad \begin{array}{l} \text{where } X_i = \text{result for trial } i \\ n = \text{number of trials} \end{array}$$

7. Brittle material: A material for which strength is uniquely determined by the distribution of flaws and toughness. Rupture is caused by raising the stress intensity at the greatest flaw to the critical value.
8. Broad band process: A broad band process is a stationary process whose mean square spectral density has significant value over a band or range of frequencies which is roughly the same order of magnitude as the center frequency of the band. A wide range of frequencies appears in representative sample functions of such a process. (Reference 52 pp. 17-18.)

In a typical aircraft broad band random load versus time signal  $N_0/N_p$  is less than one (see below).



9. Clipping ratio: The maximum value of the load signal amplitude (actually achieved or a truncated value) divided by the RMS value. Clipping values are determined for each RMS level required to characterize the exceedance curves for each mission segment type. The tail of the exceedance curve is truncated as shown below. The truncation level can usually be determined intuitively because the tail of the exceedance curve tends to wander at the higher load level because the frequency of occurrence is much less and there is a general lack of statistics.



$$\text{Clip} = \frac{\sqrt{(\Delta B.M.)^2}}{\sigma_i} \quad i = 1, 2, \dots, n$$

10. Closed loop test system: A testing system which uses servo/hydraulic test equipment to trace a set of desired load time excursions with fidelity.
11. Coefficient of variation (CV): Defined as the RMS ( $\sigma$ ) value divided by the mean or

$$CV = \frac{100 \sigma}{\bar{x}} \quad (\%)$$

where  $\sigma$  = RMS value

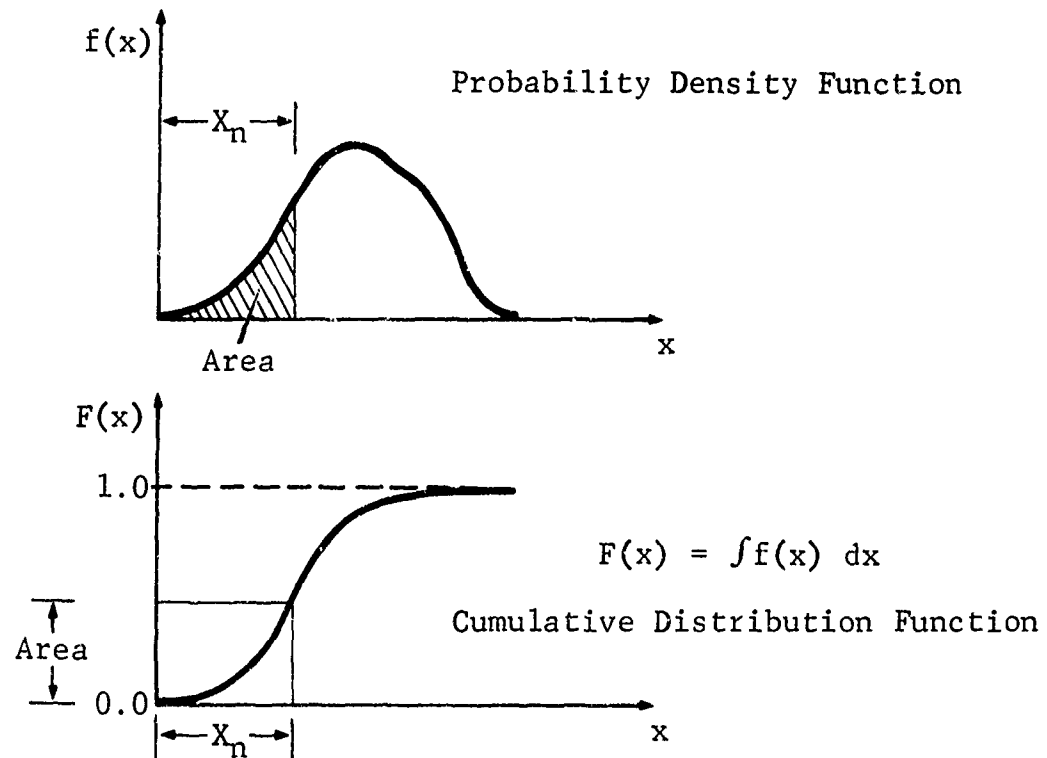
$\bar{x}$  = mean value of  $x$  for sample

The coefficient of variation can be used to estimate the tail of the distribution curve from a limited sample.

12. Confidence level: A measure of the confidence in the results with respect to sample size.
13. Cumulative distribution function: The cumulative probability distribution function,  $F(x)$ , defines the probability that a random variable will be equal to or less than  $x$ . Symbolically,

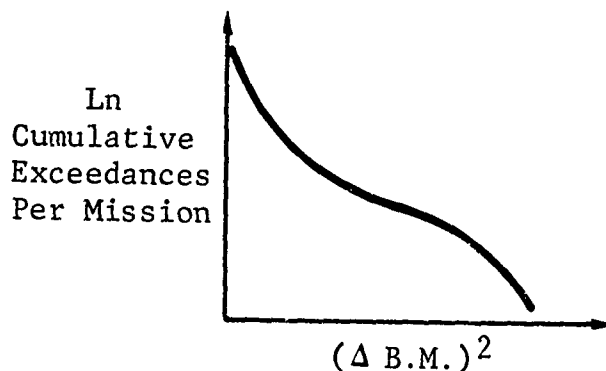
$$F(x) = \text{probability} \{x_n \leq x\}.$$

$F(x)$  defines the area under the probability density curve between selected limits. The range of  $F(x)$  is from 0 to 1.0. Refer to the sketches below for further description.



14. Ensemble: The entire load history in time and amplitude of a random load signal which has an infinite number of load samples and given time range.
15. Ergodic process: An ergodic process is one in which the timewise behavior of  $y(t)$  over a long period of time will exhibit the same average properties as corresponding ensemble averages at various fixed times.
16. Exceedance curve: A curve which characterizes statistically the load history for a given mission segment type. An exceedance curve defines the number of times per mission a given load exceeds the mean value for a given mission segment type. The exceedance curve for this report is plotted as the  $(\Delta B.M.)^2$  (abscissa, linear) versus the cumulative number of exceedances per mission (ordinate, log plot). Exceedance curves are generated for positive and negative spectra using measured flight data. The complete fluctuating load history for each mission segment type of the mission profile may be characterized by an appropriate

exceedance curve. A typical exceedance curve is shown below.



A composite cumulative exceedance curve characterizes statistically the load history for all mission segment types comprising a mission. The composite cumulative exceedance curve is obtained by summing the exceedances for the positive and negative spectra (separately). A composite cumulative exceedance curve can also be generated for all missions in a service life in a similar manner.

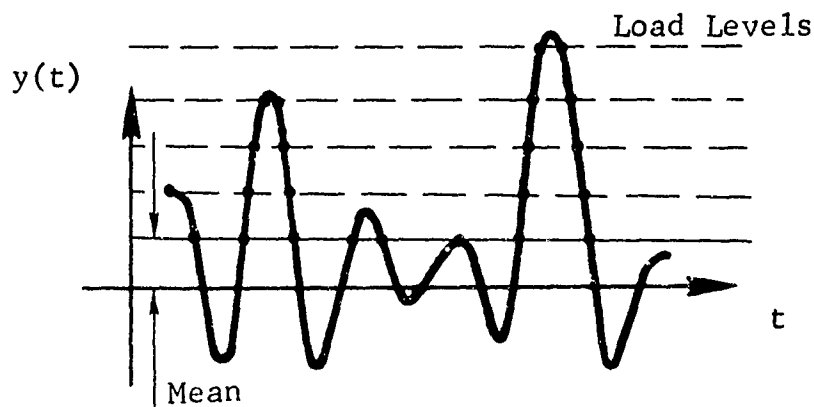
17. Fatigue failure: A structural failure (either rupture or a dangerous length subinternal flaw) which necessitates repair or replacement of the vehicle or part. The failure is caused by the combined mechanical/chemical normal service environments.
18. Flaw distribution: The statistical distributions of flaw sizes in a structure.
19. Frequences of occurrence: The number of times a given event occurs in the population.
20. GAG: Ground-air-ground cycle
21. Gaussian Random Process: "A random process  $\{y_k(t)\}$  is said to be a Gaussian random process if, for every set of fixed times  $\{t_n\}$ , the random variables  $y_k(t_n)$  follow a multi-dimensional normal distribution." (Reference 52, Page 91.)
22. Gust loads: Fluctuating loads imposed on the aircraft by air turbulence.
23. Irregularity factor ( $N_0/N_p$ ): Defines the number of positive slope crossings of the mean per positive peaks per unit time.  $N_0$  and  $N_p$  can theoretically be calculated from the power spectral density. Due to lack of aircraft wave form data an assumed value of 0.85 was used for this report.  $N_0/N_p$  must

be defined to evaluate the Rice-Bendat-Kowalewski function.

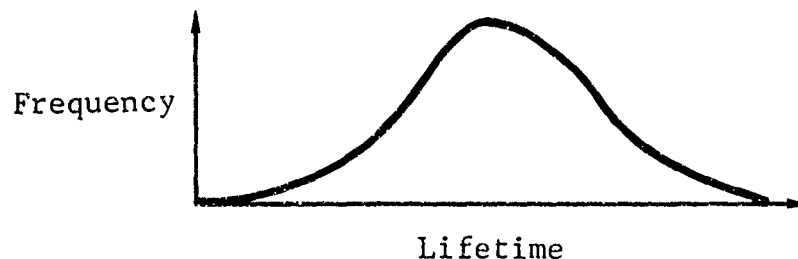
NOTE:  $N_0/N_p = 1.0$  (Rayleigh)

$N_0/N_p = 0.0$  (Gaussian)

24. Level crossings: Refers to the number of load peaks above (positive spectra) or below (negative spectra) a given load level in a given time span. The number of load peaks above or below selected load levels are counted for the simulated random load history and the results are used to check agreement with the actual load history exceedances.

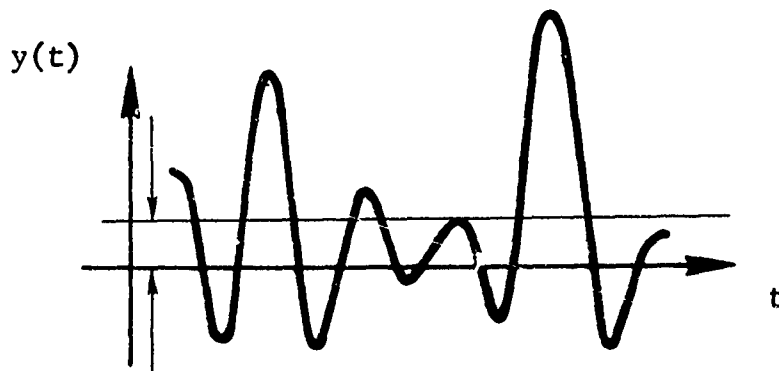


25. Lifetime distribution: A probability frequency distribution which characterizes the time to specimen failure. Fatigue lifetimes are determined experimentally by continuously testing specimen under a simulated random load history until failure occurs. A Weibull distribution fitted to the test results provides a physical description of the fatigue process. A typical lifetime distribution curve is depicted below.



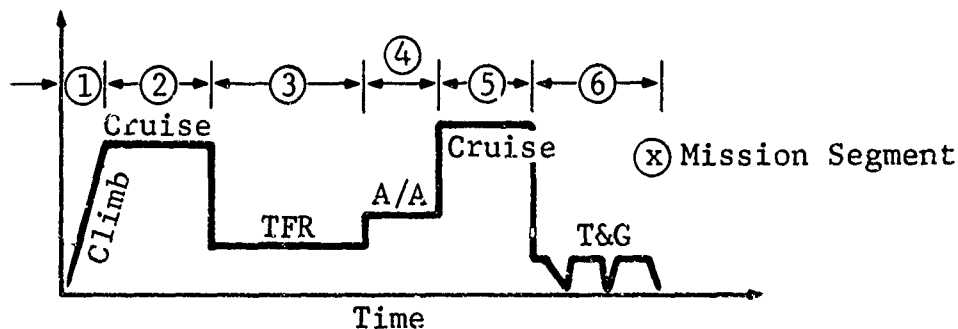
26. Mean load: The reference load level from which the load amplitude is measured. In most aircraft applications a lg load is considered to be the reference load level. The mean load level at lg may vary for each condition. For a symmetric history the reference is the algebraic mean.





Mean Load

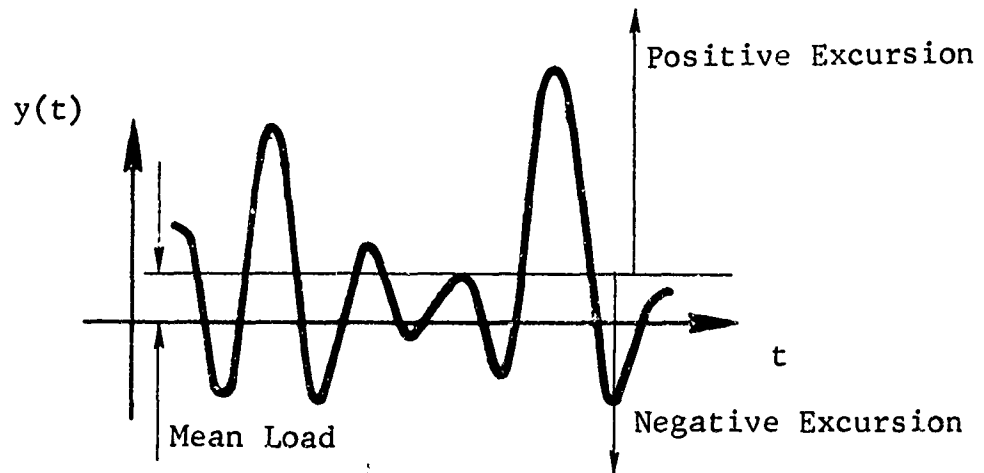
27. Mission profile: Characterizes the activities or maneuvers the airplane is expected to encounter during a mission and the time spent in each activity. The activities are characterized by mission segment types. A typical mission profile is depicted below:



28. Mission Segment: A mission segment defines the type of activity the aircraft encounters during a mission. A mission is composed of different mission segment types. The order of the segments and the time spent in each segment type distinguishes the missions flown. Typical mission segment types are climb, cruise, TFR, A/G, A/A, GAG, and T&G. The load history for each mission segment type is characterized by exceedance curves.
29. Narrow band process: "A narrow band process is a stationary random process whose mean square spectral density has significant values only in a band or range of frequencies whose width is small compared with the magnitude of the center frequency of the band. Only a narrow range of frequencies appear in representative samples of such a process." (Reference 13, page 153). A typical narrow band signal is shown on page 17 of Reference 52.

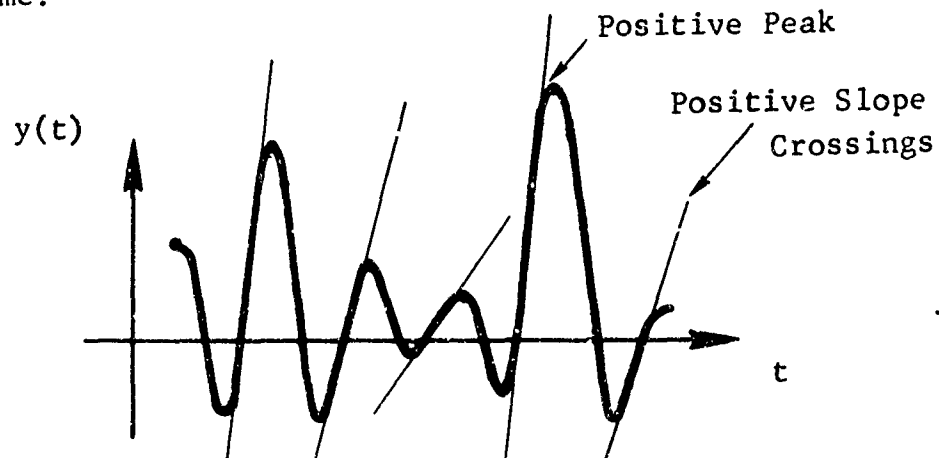
30. Negative spectra: Characterizes the load exceedances below the mean.

31. Negative load excursion: A load fluctuation below the mean value.



32.  $N_0$ : The number of positive slope crossings of the mean per unit time.

33.  $N_p$ : The number of positive peaks (mathematical maximum) per unit time.



34.  $P_i$ : Define the portion of time spent at each RMS level.

35. Population: A collection of all possible observations for an event. For example, all airplanes in the fleet compromise a population. A portion of the airplanes in the fleet is a sample.

36. Positive spectra: Characterizes the load exceedances above the mean.

37. Positive load excursion: A load fluctuation above the mean. (Reference sketch under negative load excursion.)

38. Power spectral analysis: This is an analysis in which  $N_o$  and  $N_p$  are computed from the power spectral density function (PSD). The expressions below were developed by Rice (Reference 42).

$$N_o = \frac{1}{2\pi} \left[ \frac{\int_0^\infty \omega^2 \phi(\omega) d\omega}{\int_0^\infty \phi(\omega) d\omega} \right]^{1/2} \quad (\text{Reference 29, page 26})$$

$$N_p = \frac{1}{2\pi} \left[ \frac{\int_0^\infty \omega^4 \phi(\omega) d\omega}{\int_0^\infty \omega^2 \phi(\omega) d\omega} \right]^{1/2}$$

where  $\phi(\omega)$  = power spectral density function

$$\phi(\omega) = \frac{2}{\pi} \int_0^\infty \psi(\tau) \cos \omega \tau d\tau$$

$$\psi(\tau) = \lim_{T \rightarrow \infty} \frac{1}{2T} \int_{-T}^T y(t)y(t+\tau)dt =$$

autocorrelation function

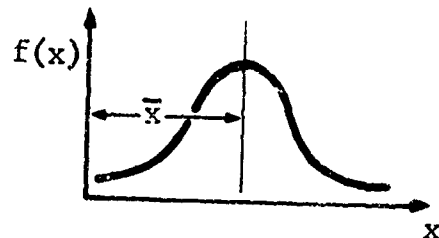
$\omega$  = angular frequency (radian/sec)

$f$  = cyclic frequency (Hz)

39. Power spectral density function (PSD): A frequency analysis of the mean square of the random variable. The PSD characterizes the amount of energy in a frequency band. The total energy is obtained by adding the spectral density for each frequency increment along the spectrum. Using the PSD the distribution of level crossings, peaks, and ranges may be computed for simulating a loading history (Reference 13, page 157 and Reference 52, page 22).
40. Probability: The ratio of the expected number of occurrences of an event divided by the total number of possible occurrences.
41. Probability density function: A function which characterizes the frequency of occurrence of possible events in a population. The probability density functions used in this report are summarized below:

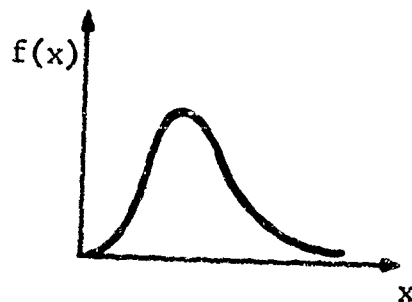
o Gaussian (Normal)

$$f(x) = \frac{1}{\sigma \sqrt{2\pi}} \exp \left[ -\frac{(x - \bar{x})^2}{2\sigma^2} \right]$$



o Rayleigh

$$f(x) = \frac{x}{C^2} \exp \left[ -\frac{x}{2C^2} \right]$$



o Weibull

$$f(x) = \frac{\alpha}{\beta} \left( \frac{x}{\beta} \right)^{\alpha-1} \exp \left[ -\left( \frac{x}{\beta} \right)^{\alpha} \right]$$

$\alpha$  = shape parameter

$\beta$  = scale parameter (characteristic value)

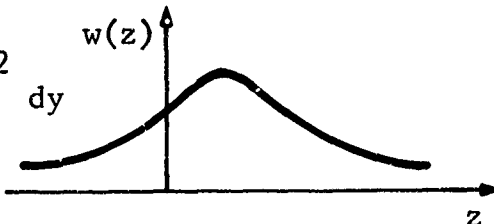
for  $\alpha = 2$  the Weibull becomes Rayleigh with scale parameter  $\sqrt{2}C$

o Rice

$$W(Z) = \frac{K_1}{\sqrt{2\pi}} e^{-Z^2/2K_1^2} + \frac{N_0}{N_p} Z e^{Z^2/2} [1 - P(Z/K_2)]$$

$$\text{where: } K_1 = \left\{ 1 - \frac{N_0}{N_p} \right\}^{1/2}$$

$$K_2 = \frac{K_1}{(N_o/N_p)}$$

$$P(Z/K_2) = \frac{1}{\sqrt{2\pi}} \int_{Z/K_2}^{\infty} e^{-y^2/2} dy$$


(References 46, 49 and 53).

42. Random load: A load from the total load population which fits a prescribed statistical distribution.
43. Random load history: An ensemble of random loads which characterizes the load history for a single mission, for several missions, or for a complete service life.
44. Random number mapping: This is a procedure for generating random loads by fitting random numbers drawn from a rectangular distribution to a given cumulative distribution. For this report the Rice-Bendat-Kowalewski Cumulative distribution function is used. A detailed description of the procedure is given in Appendix I.
45. Ranking data: The probability of survival,  $P(x)$  for a given set of test results can be expressed using the equation below:

$$P(x) = \frac{r_{\alpha}}{n+1}$$

where:  $r_{\alpha}$  = rank of the data

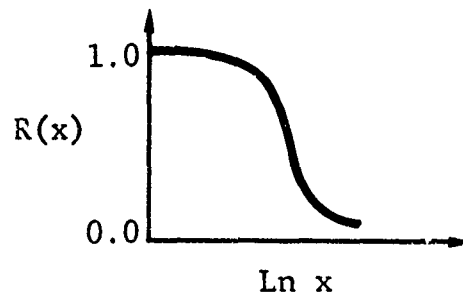
$n$  = number of tests in the data set

The data is ranked in descending order of magnitude. The largest value has a rank of 1.0, the next largest has a rank of 2.0, and so forth with the smallest value having a rank of  $n$ . For this report the probability of survival, based on the ranking procedure, is compared with the theoretical values obtained from a Weibull distribution fitted to the test results. This comparison shows how well the Weibull distribution fits the observed probabilities of survival based on the ranking procedure. (Reference 42, page 38 and Reference 37)

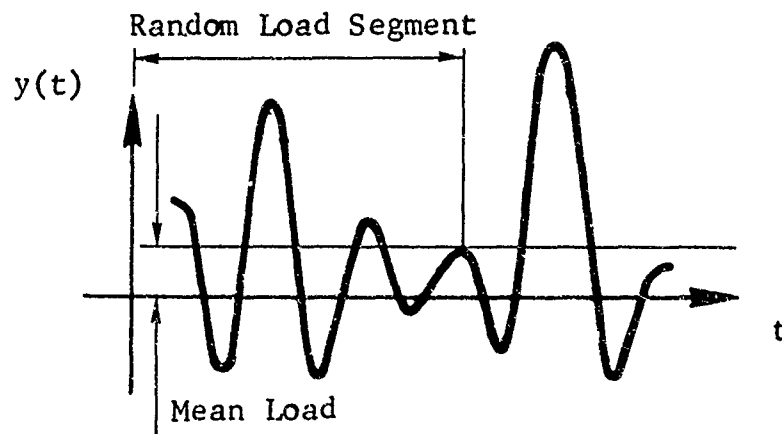
46. Reliability function: The reliability function,  $R(x)$ , defines the probability that a value of the random variable is greater than  $x$ . Symbolically,

$$R(x) = \text{probability } \{x_n > x\} = 1 - F(x)$$

where:  $F(x)$  - cumulative distribution function



47. Reliability goal: A reliability standard to which an element, a component, or assembly is to meet.
48. Residual strength: The static strength remaining in a member after the member has been subjected to a given load history, environment, or other damage.
49. RMS burst: A segment of the random load signal which characterizes all the loads for a single RMS level (positive and negative spectra) for a given mission segment and mission segment type. Two or three RMS levels are usually required to characterize the exceedance curve for a given mission segment type.



50. RMS level: The exceedance curves for various mission segment types are characterized by different RMS values according to the method of Press (Reference 29). Each RMS value required

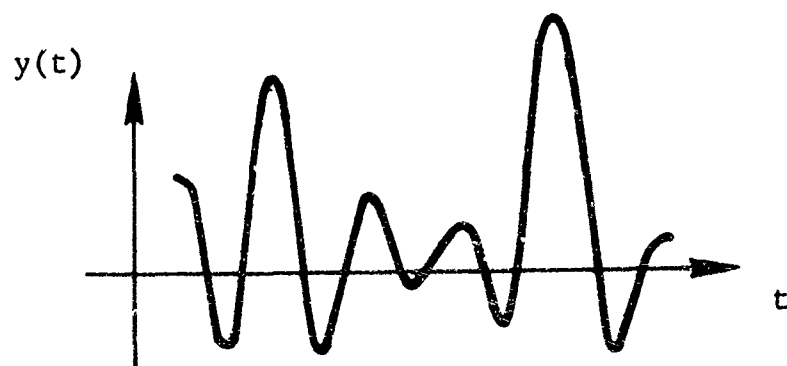
to characterize the exceedance curve is called an RMS value. Two or more RMS levels are usually required to characterize the exceedance curve for a given mission segment type.

51. Root-mean-square (RMS): The RMS value is a statistical term which characterizes the load deviations from the mean. For this report the mean is at the 1g load level. The mean square value is given by:

$$\sigma_{\text{RMS}}^2 = \lim_{T \rightarrow \infty} \frac{1}{T} \int_0^T y^2(t) dt$$

where:  $T$  = observation time

$y(t)$  = ordinate to the load signal



The RMS value is equal to the positive square root of the mean square value, i.e.,

$$\sigma_{\text{RMS}} = \sqrt{\sigma_{\text{RMS}}^2}$$

RMS values are determined from exceedance curves for given RMS levels by the Method of Press (29). The RMS value can also be estimated in terms of discrete loads measured from the mean ( $\bar{x}$ ) using the equation below.

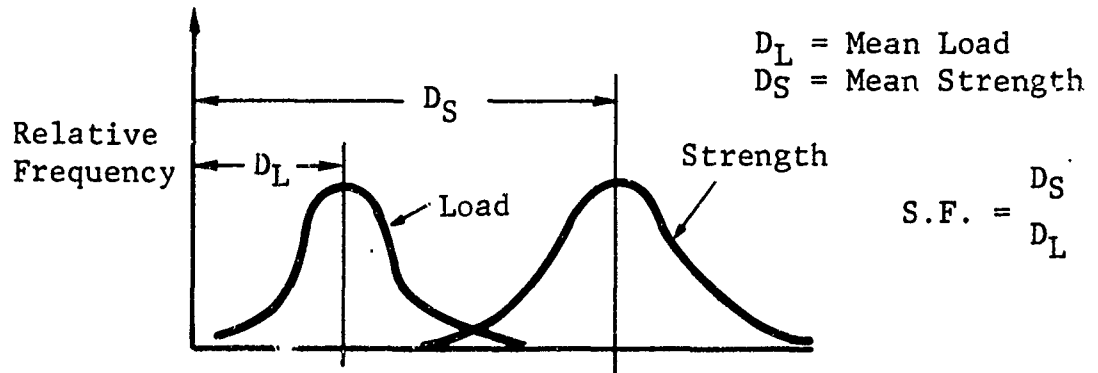
$$\sigma_{\text{RMS}} = \sqrt{\frac{\sum_{i=1}^n (x_i - \bar{x})^2}{n-1}}$$

where:  $n$  = total number of loads

$x_i$  = value of load  $i$

$\bar{x}$  = mean value for all measurements

52. Safety factor: In structural reliability analysis the safety factor is the ratio of the mean strength divided by the mean load. Due to the variation in load and strength, the safety factor must be selected with respect to an acceptable probability of failure. The load and strength distributions are depicted below. Failures can be represented by the shaded area at the tails of the distributions.



53. Sample: A sample is a particular set of observations out of the set of all possible observations in the population. One airplane out of all airplanes in the fleet constitutes a sample from the population.
54. Scaling factor: A factor which allows one to characterize the fatigue life of full-size components under a random load history using small-scale specimens. Small specimens generally have longer fatigue lives than their full-size counterparts subjected to the same stress history. The scale factor is used to scale small specimen fatigue results to full-size structures.
55. Scale parameter ( $\beta$ ): A characteristic value of the Weibull distribution below which 63.2% of the values for the random variable are expected to fall. It can be determined by fitting the Weibull distribution to the test data. For residual strength distributions  $\beta$  is expressed in pounds and for lifetime distributions,  $\beta$  is expressed in lifetime. An equation for the probability of survival (Weibull) is given below:

$$P(\sigma) = e^{-\left(\frac{\sigma}{\beta}\right)^\alpha}$$

where  $P(\sigma)$  = probability of surviving residual strength,

$\sigma$  = residual strength



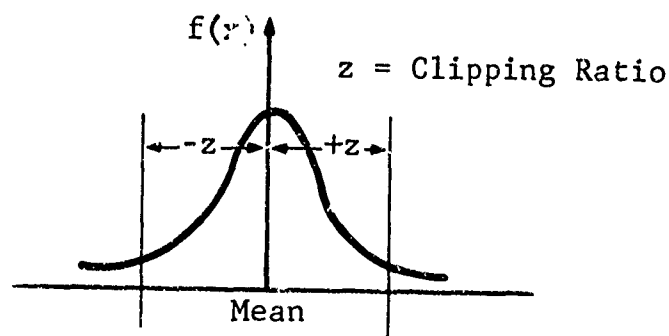
$\beta$  = scale parameter (characteristic value)

$\alpha$  = shape parameter

56. Scatter: A group of specimen built to the same specifications and tested with the same fatigue loading will have different fatigue lives. If all things were truly equal all the specimen should have the same fatigue life. Scatter is a term used to describe the variation in fatigue lives. The amount of scatter is often described by the lifetime RMS value; e.g., design life equals (scatter factor  $\times$  test life).
57. Service life: The service life of an airplane is a specified time which the airplane is expected to perform its intended purpose. Service life projections are continually made on airplanes in the fleet to evaluate the safety for continuous usage. Fighter aircraft are designed for 4000 hours of usage. A typical F-111 aircraft is expected to fly about 1334 missions during its service life. For test purposes in this program the random load history is simulated for one service life and is stored on digital magnetic tape.
- This load history represents one lifetime of usage. Four or more lifetimes are usually required to satisfy the fatigue life requirements; i.e. a scatter factor of 4.
58. Servo amplifier: A device for adjusting the servo valve output to make it consistent with the input load requirement from the magnetic tape.
59. Servo valve: A valve which controls the flow of oil for driving the hydraulic loading ram. It receives a feed back signal from the servo amplifier.
60. Shape parameter ( $\alpha$ ): A nondimensional parameter of the Weibull distribution. The shape of the resulting Weibull distribution curve is governed by this parameter. Also refer to scale parameter ( $\beta$ ).
61. Stationary random process: A process in which the statistical parameters are constant with respect to time.
62. Statistics: The scientific collection and analysis of data, and the projection of estimates therefrom. Statistics is not an end in itself; rather it is an aid to judgement in arriving at valid conclusions, testing theories, measuring phenomena, discovering relationships, or projecting estimates under different conditions. Statistics is only a tool and it

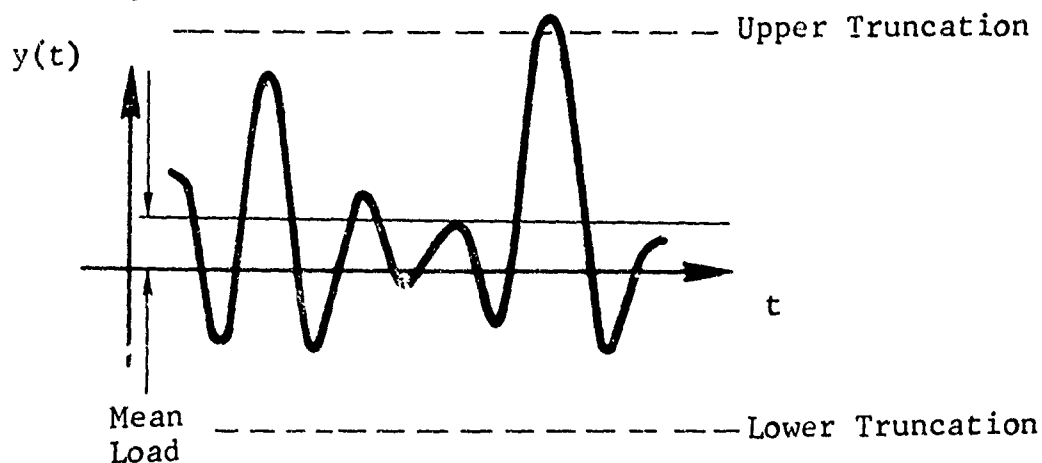
must be remembered that it is not a substitute for professional knowledge and experienced judgment. Sound judgment, however, cannot be made with confidence without the use of this tool.

- 63. Stress intensity factor (K): The stress intensity factor is a parameter used in fracture mechanics for characterizing the elastic stresses in the area of a crack tip. K depends upon the loading mode and the geometry of the crack.
- 64. Structural reliability philosophy: In the structural reliability approach the probability of structural failure is predicted considering the variations in strength and applied loading. Conventional structural design methods, on the other hand, evaluate the integrity of the structure on a margin of safety basis. Since the structural reliability approach statically characterizes the variation in strength and loading it permits a more realistic assessment of the structural integrity. (Reference safety factor discussion).
- 65. Symmetric clipping: A clipping ratio is computed for each RMS level for both the positive and negative spectra exceedance curves for each mission segment type. This clipping value defines the limits for the tail to the probability density curve on the positive side of the mean or characteristic value. When the density curve on the negative side of the mean is clipped the same way as the opposite side symmetric clipping is said to be used (refer to sketch below).



- 66. Symmetric spectrum: A symmetric spectrum, as used in this report, is one in which the positive and negative exceedances are the same for given mission segment types.
- 67. TFR: Terrain following radar
- 68. T&G: Touch and go landings

69. TIP: Transonic Improvement Program; predecessor to USAF "TACT" program being directed by the AFFDL.
70. Truncation level: The number of large load occurrences in the load history population are infrequent compared to the number of smaller load occurrences. Unless a very large sample of the load history is taken there is generally a lack of statistics to adequately characterize the large load occurrences. In such cases the loads are cut off or truncated at some reasonable maximum load level. In this report the  $(\Delta B.M.)^2$  loads from the exceedance curves and the maximum positive and negative load excursion from the mean random load signal are truncated. Truncation of the exceedance curves is discussed under clipping ratios. Truncation of the random load signal is depicted below. The only centered truncation used resulted from input data or test machine accuracy.



71. Variance ( $\sigma^2$ ): A statistical term defined as follows:

$$\sigma^2 = \frac{\sum_{i=1}^n (x_i - \bar{x})^2}{n-1}$$

where:  $n$  = number of measurements

$x_i$  = value of measurement  $i$

$\bar{x}$  = mean value for all measurements

72. Waveform: In a random process the waveform content characterizes the load peaks, the frequency of load occurrence.

and load reversals. The wave form is characterized by the irregularity factor ( $N_o/N_p$ ).

- 73. Wearout curve: A curve in which the residual static strength is plotted against lifetime. This curve graphically characterizes the residual strength of the specimen with respect to service life.
- 74. White noise: A term used to indicate that the power spectral density (PSD) is constant over the frequency range of interest.

The term "White noise" was coined due to the fact that all frequencies contribute to the random process in a manner similar to the contribution of all colors to white light. (Reference 13, page 157.)

APPENDIX IV  
PHOTOGRAPHS OF 1 / 5 - SCALE  
SPECIMEN FAILURES

Specimen photographs in this section are grouped according to test types with the specimens for each group given in numerical order. Joint failure modes are discussed in subsection 6.7.

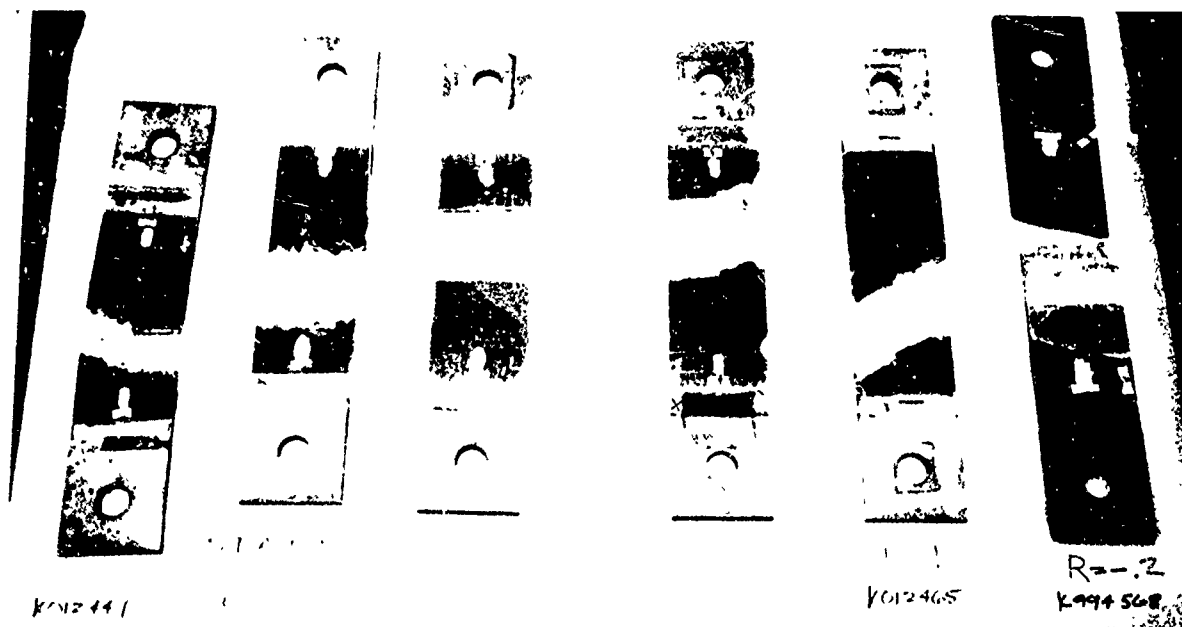


Figure 62 Group of One-Fifth Scale Static and Constant Amplitude Fatigue Specimens

### STATIC TEST

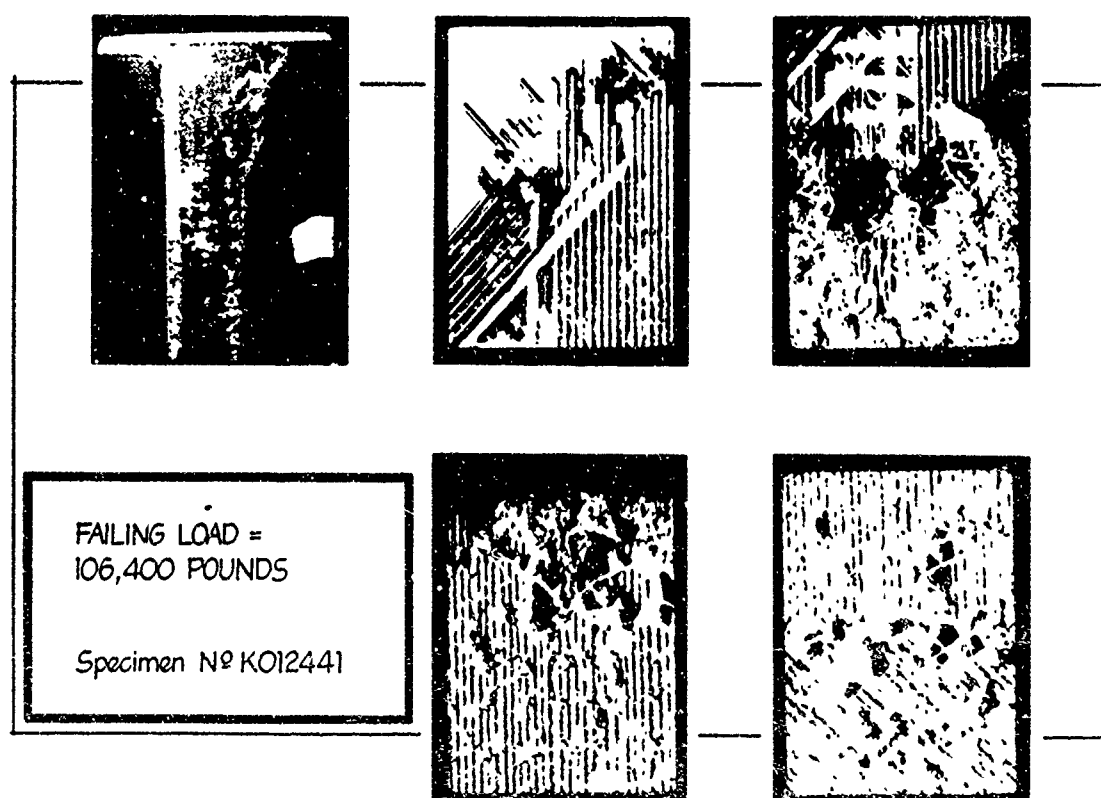


Figure 63 One-Fifth Scale Static Specimen K012441

*FATIGUE TEST*

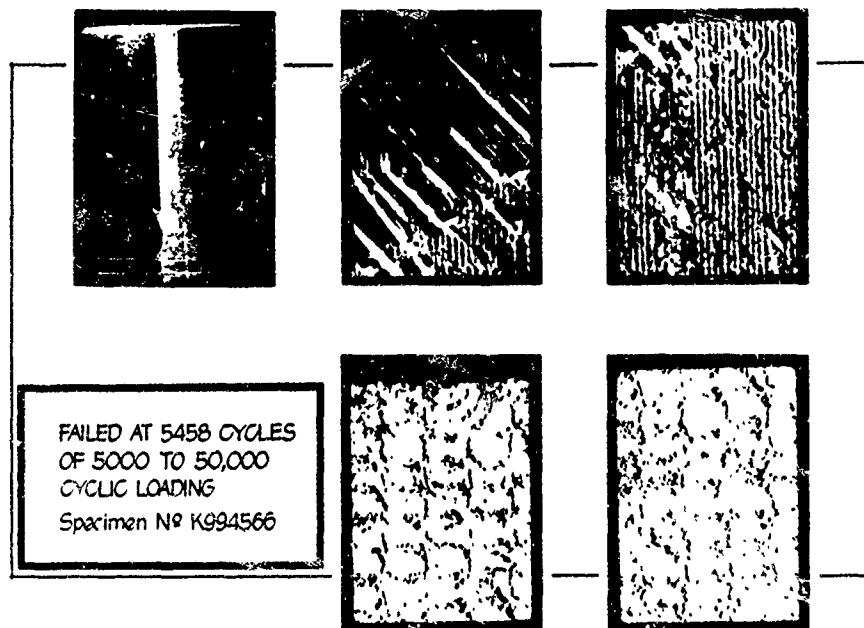


Figure 64 One-Fifth Scale Constant Amplitude Fatigue Specimen K994566

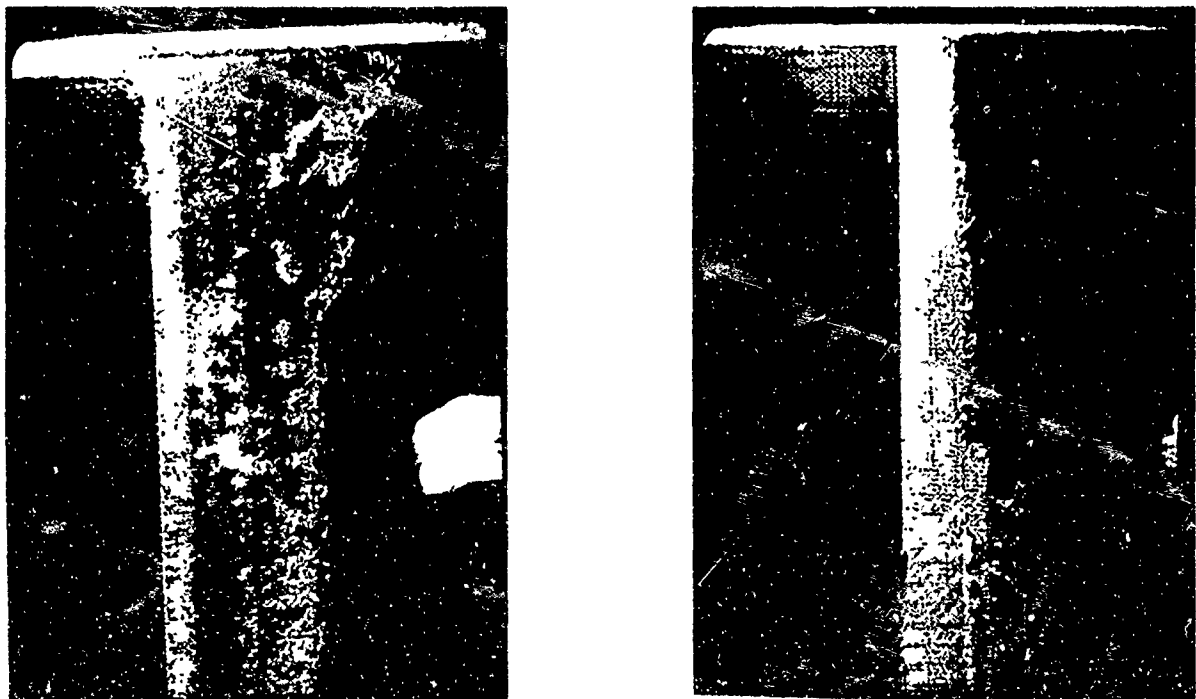


Figure 65 Full Size: One-Fifth Scale Static (K012441) and Constant Amplitude Fatigue (K994566) Specimens

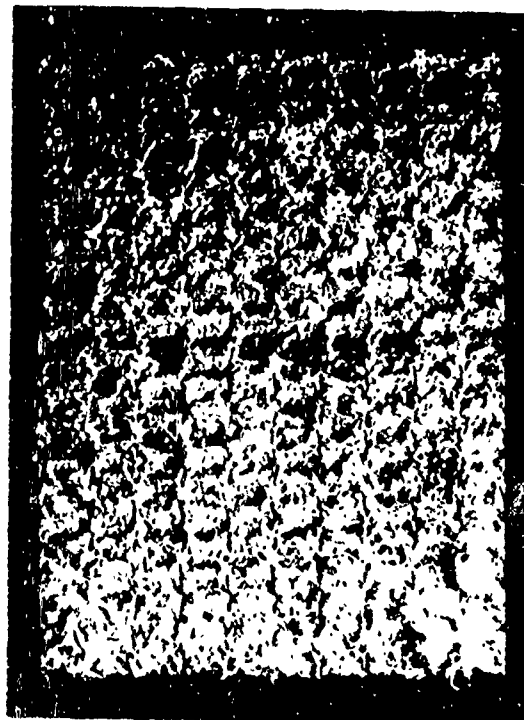
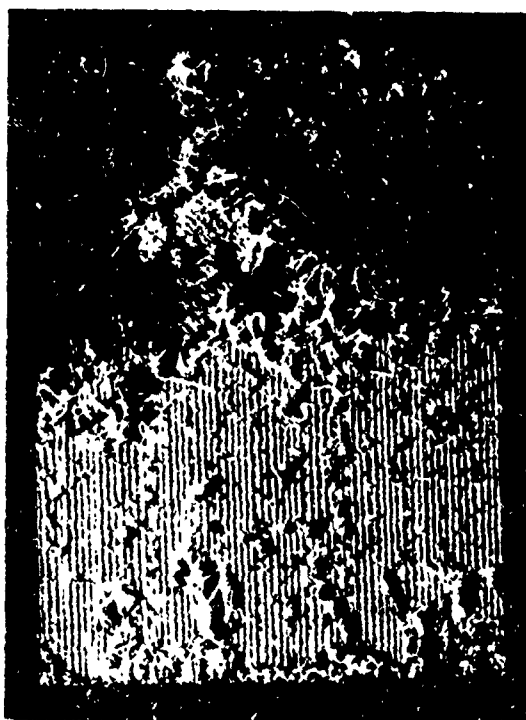


Figure 66 Ten Times Size: One-Fifth Scale Static (K012441) and Constant Amplitude Fatigue (K994566) Specimens



Figure 67 Twenty Five Times Size: One-Fifth Scale Static (K012441) and Constant Amplitude Fatigue (K994566) Specimens



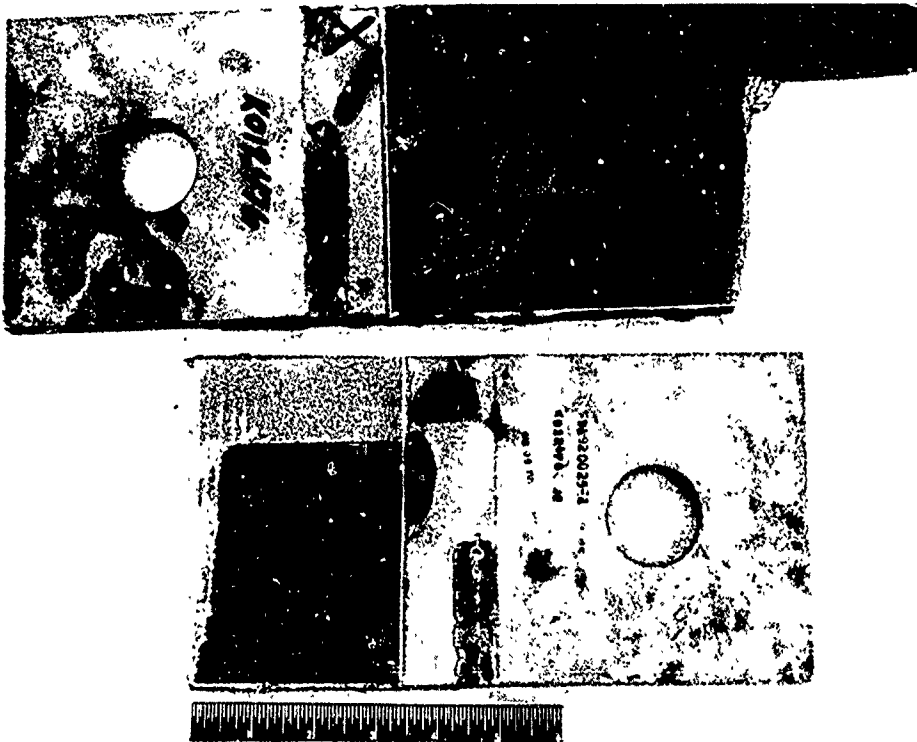


Figure 68 Constant Amplitude (Tension-Tension) Fatigue Test:  
One-Fifth Scale Specimen K012476



Figure 69 Constant Amplitude (Tension-Tension) Fatigue Test:  
One-Fifth Scale Specimen K012477

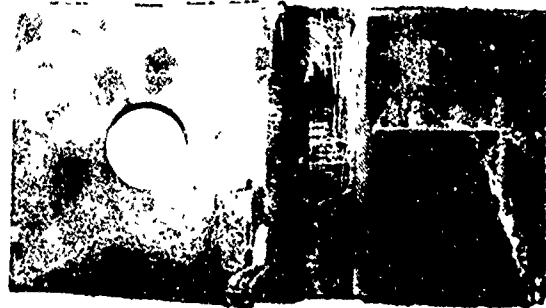
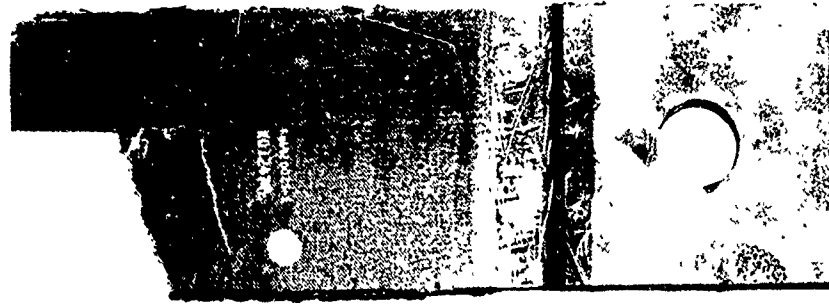


Figure 70 Constant Amplitude (Tension-Tension) Fatigue Test:  
One-Fifth Scale Specimen K012478



Figure 71 Constant Amplitude (Tension-Tension) Fatigue Test:  
One-Fifth Scale Specimen K012483



Figure 70 Constant Amplitude (Tension-Tension) Fatigue Test:  
One-Fifth Scale Specimen K012478

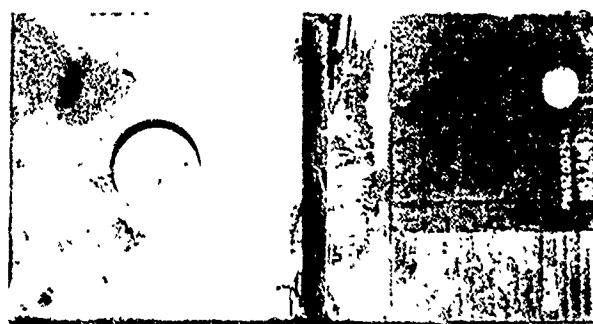


Figure 71 Constant Amplitude (Tension-Tension) Fatigue Test:  
One-Fifth Scale Specimen K012483



Figure 72 Constant Amplitude (Tension-Tension) Fatigue Test:  
One-Fifth Scale Specimen K900445

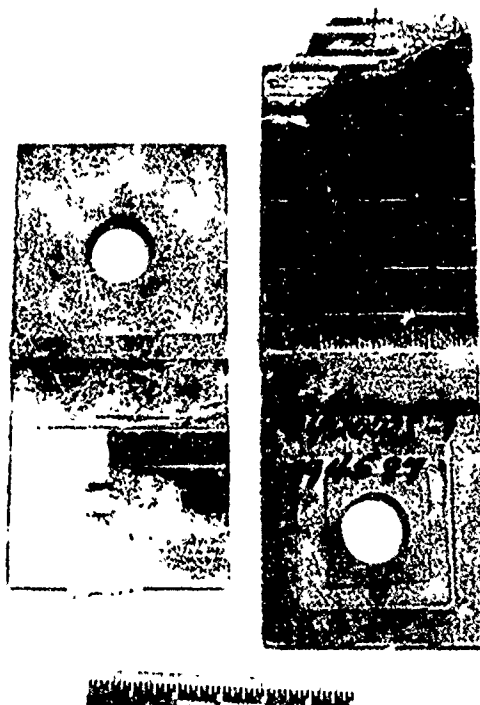


Figure 73 Constant Amplitude (Tension-Tension) Fatigue Test:  
One-Fifth Scale Specimen K994587

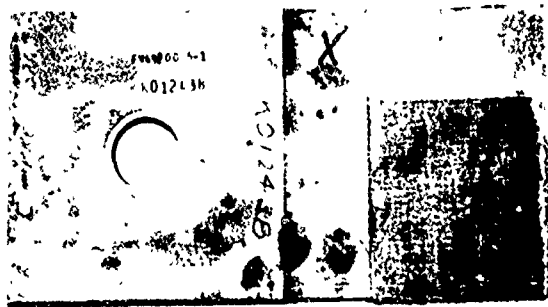


Figure 74 Constant Amplitude (Tension-Compression) Fatigue Test:  
One-Fifth Scale Specimen K012438

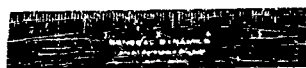


Figure 75 Constant Amplitude (Tension-Compression) Fatigue Test:  
One-Fifth Scale Specimen K012442

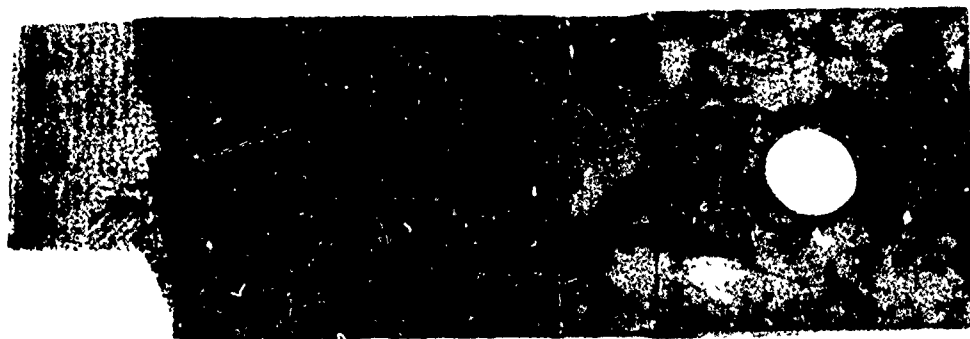


Figure 76 Constant Amplitude (Tension-Compression) Fatigue Test:  
One-Fifth Scale Specimen K012462

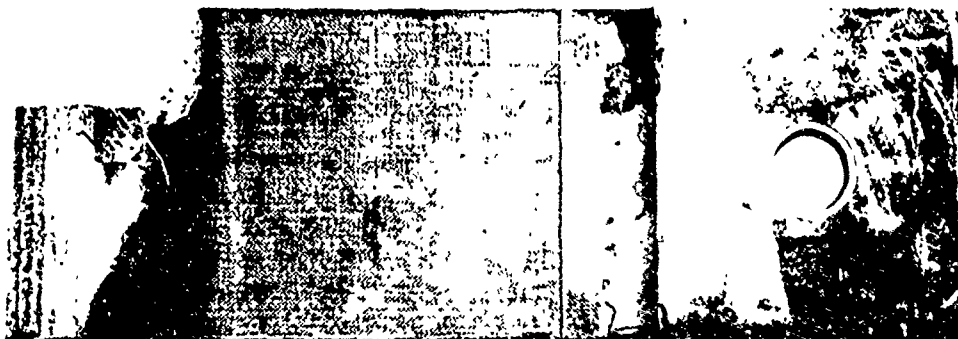
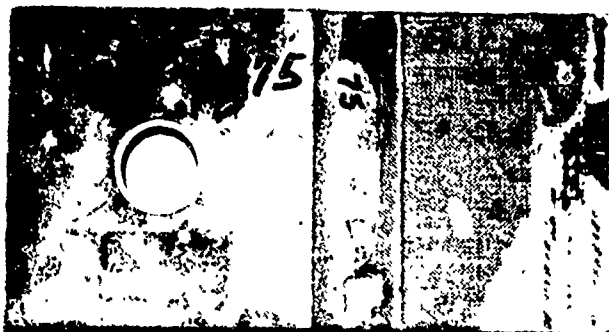


Figure 77 Constant Amplitude (Tension-Compression) Fatigue Test:  
One-Fifth Scale Specimen K012475

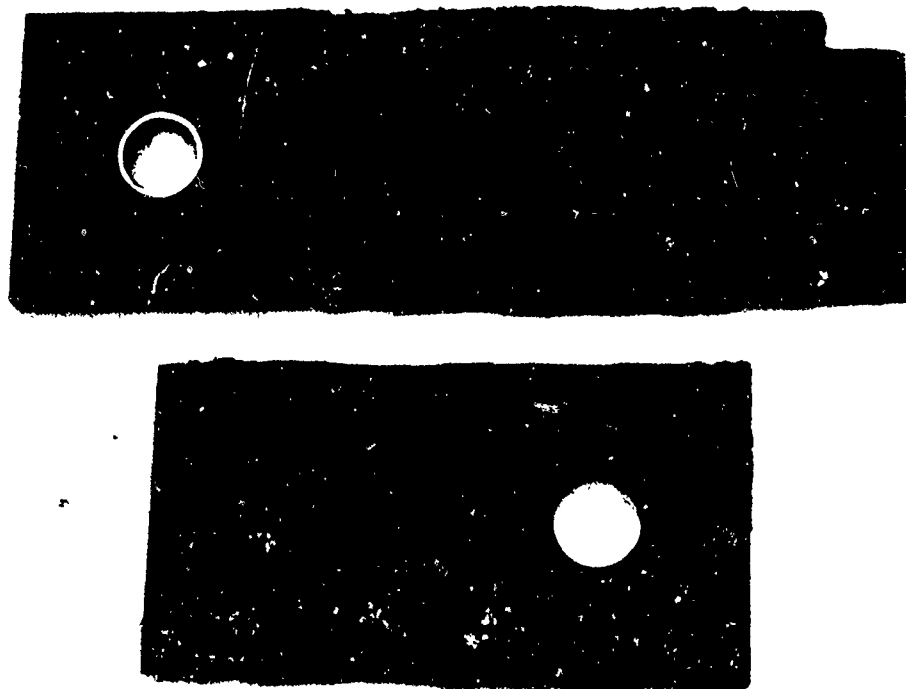


Figure 78 Constant Amplitude (Tension-Compression) Fatigue Test:  
One-Fifth Scale Specimen K900442



Figure 79 Constant Amplitude (Tension-Compression) Fatigue Test:  
One-Fifth Scale Specimen K994568

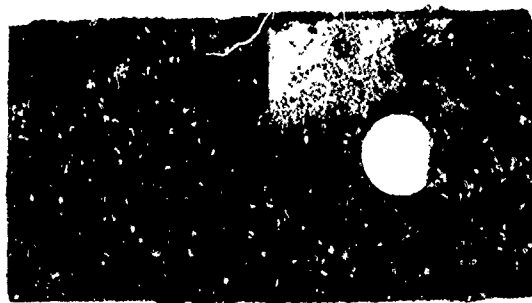


Figure 80 Random Loading (1% Lifetime) Test: One-Fifth Scale  
Specimen K900441



Figure 81 Random Loading (1% Lifetime) Test: One-Fifth Scale  
Specimen K900448



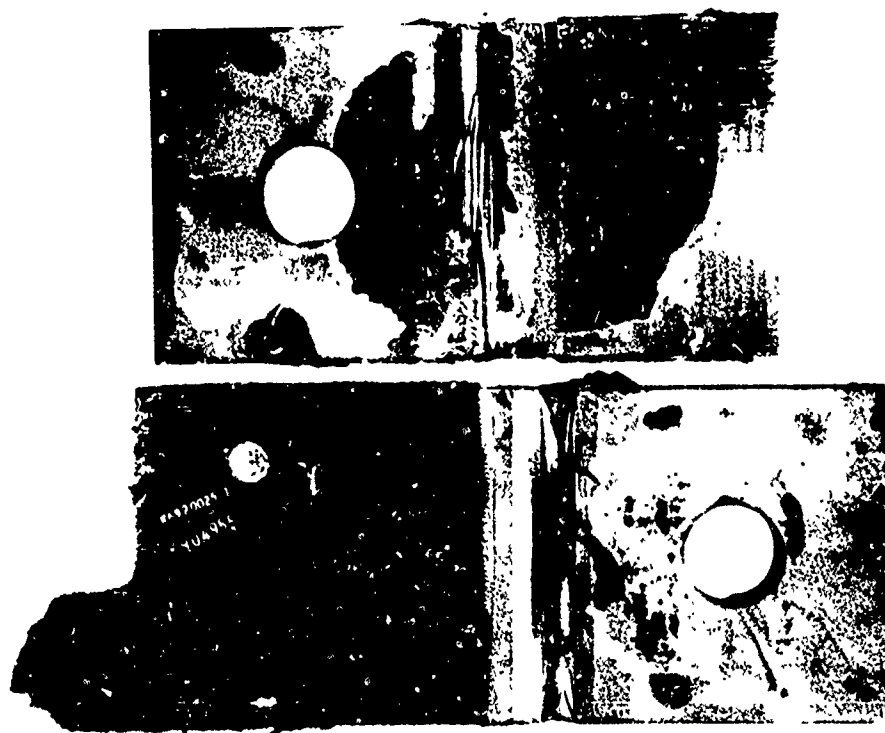


Figure 82 Random Loading (1% Lifetime) Test: One-Fifth Scale Specimen K904955

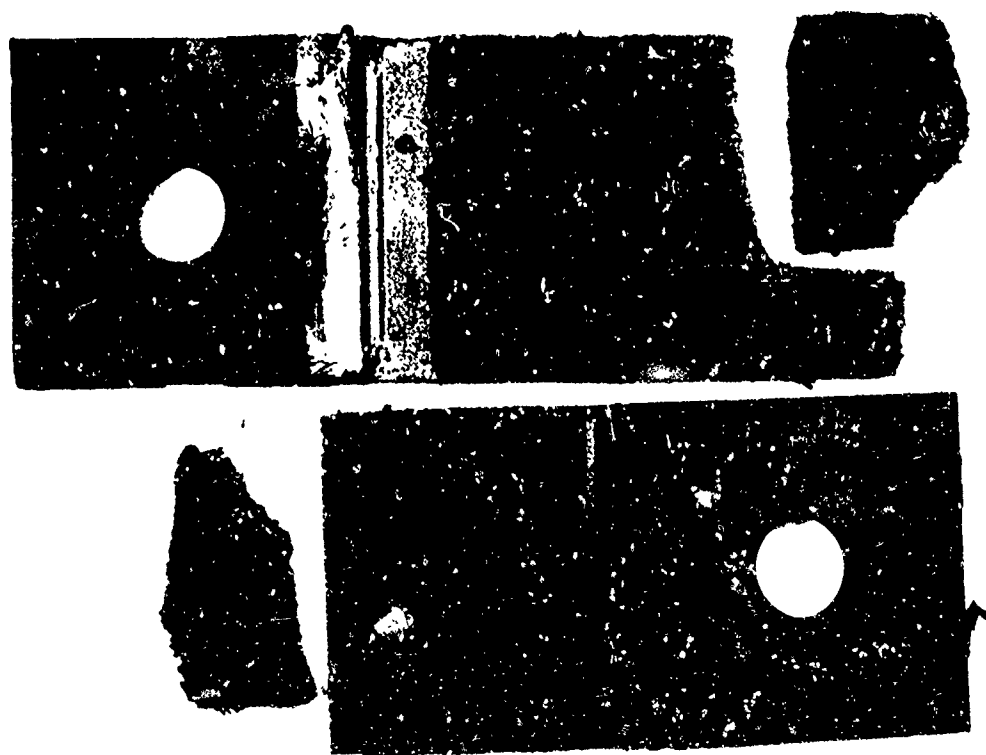


Figure 83 Random Loading (1% Lifetime) Test: One-Fifth Scale Specimen K904958

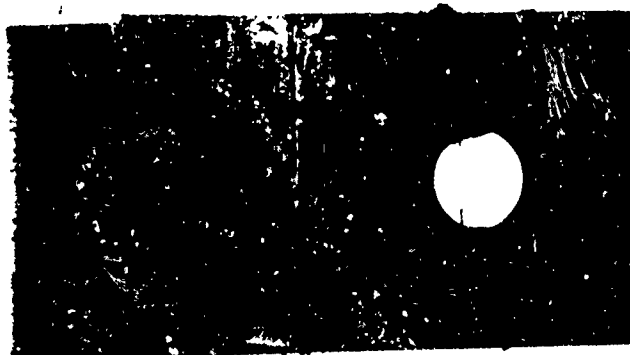
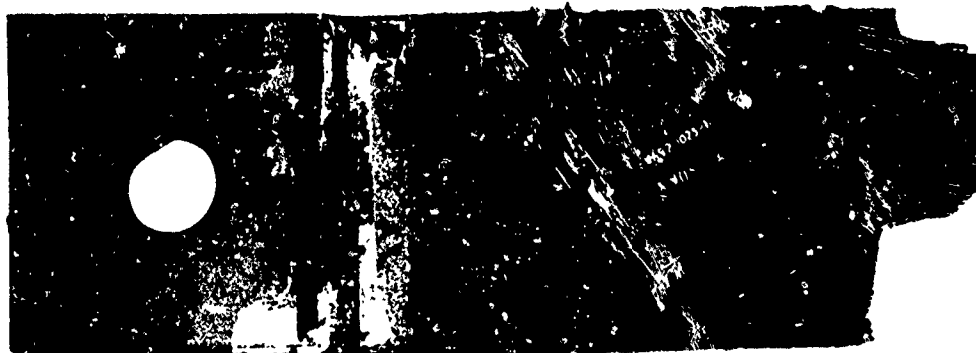


Figure 84 Random Loading (1% Lifetime) Test: One-Fifth Scale Specimen K905016

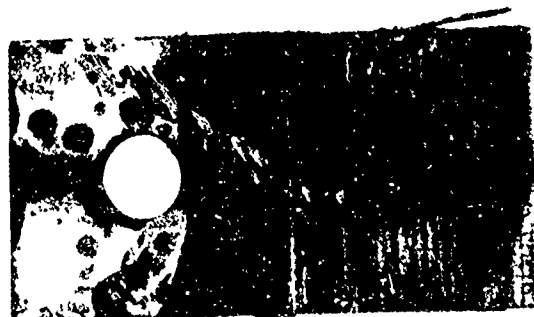


Figure 85 Random Loading (10% Lifetime) Test: One-Fifth Scale Specimen K900441



Figure 86 Random Loading (10% Lifetime) Test: One-Fifth Scale Specimen K904950

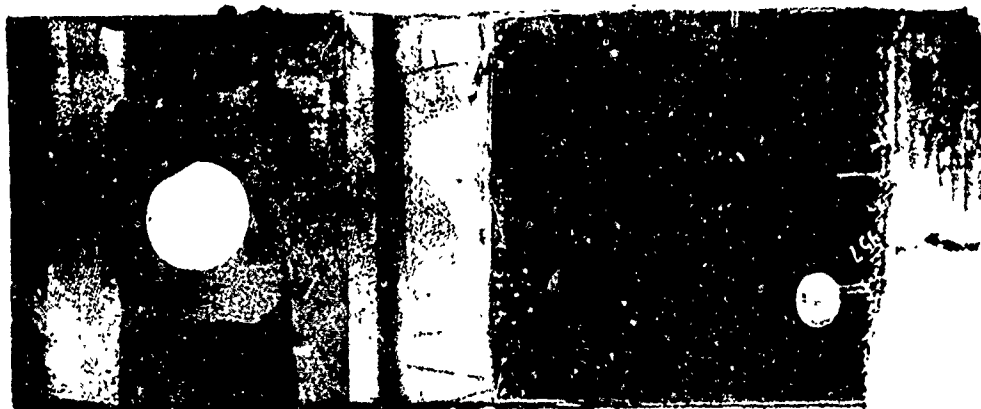


Figure 87 Random Loading (10% Lifetime) Test: One-Fifth Scale Specimen K904957

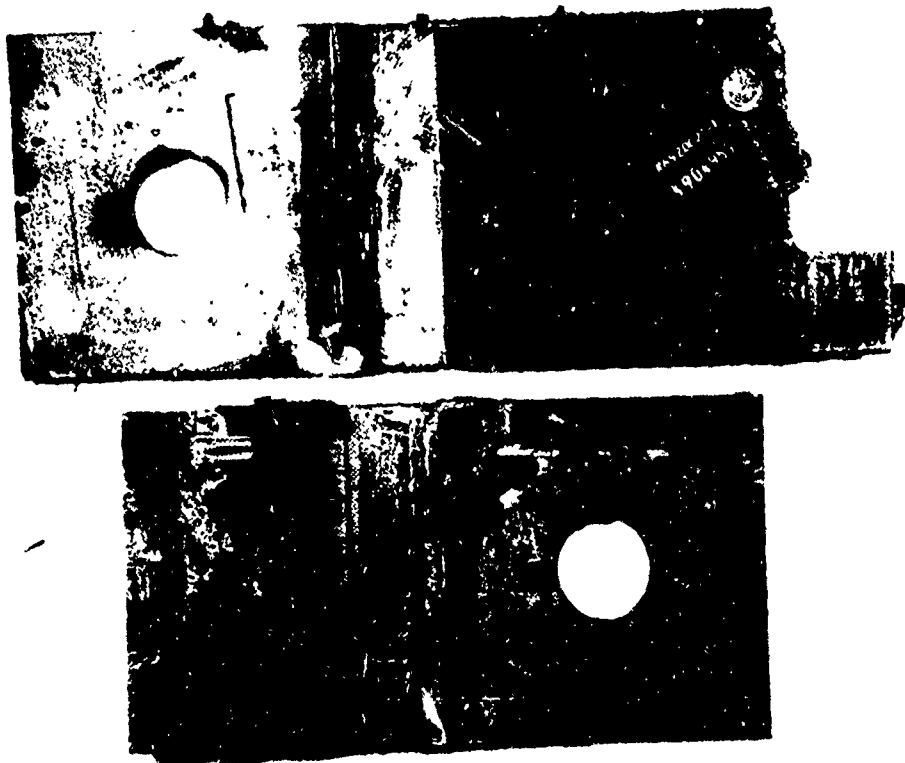


Figure 88 Random Loading (10% Lifetime) Test: One-Fifth Scale  
Specimen K904959

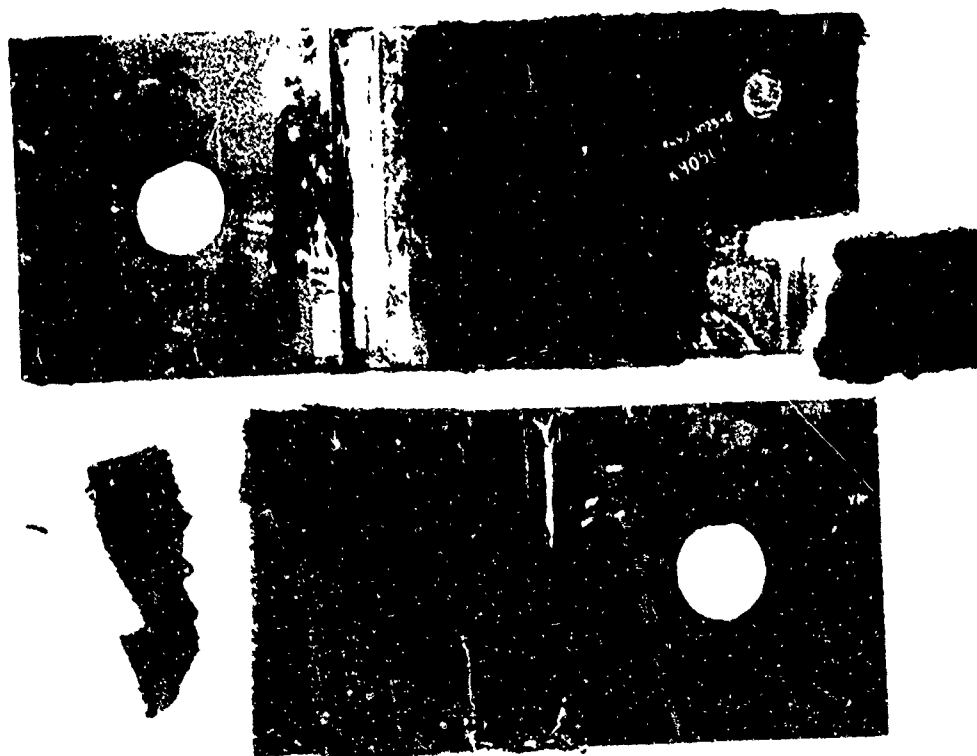


Figure 89 Random Loading (10% Lifetime) Test: One-Fifth Scale  
Specimen K905017



Figure 90 Random Loading (50% Lifetime) Test: One-Fifth Scale  
Specimen K900449



Figure 91 Random Loading (50% Lifetime) Test: One-Fifth Scale  
Specimen K900450

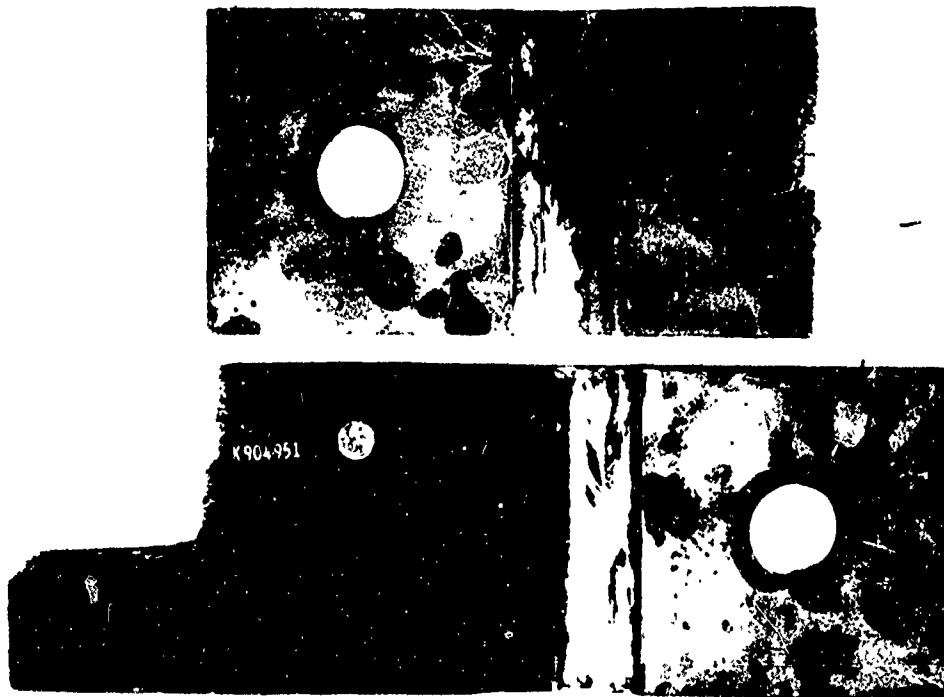


Figure 92 Random Loading (50% Lifetime) Test: One-Fifth Scale Specimen K904951

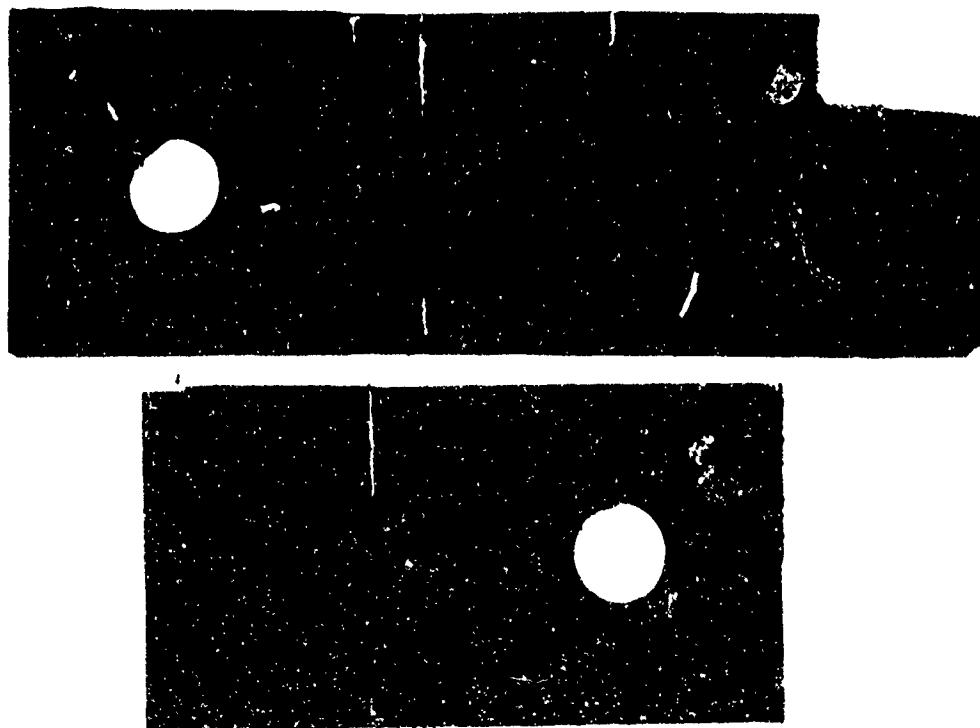


Figure 93 Random Loading (50% Lifetime) Test: One-Fifth Scale Specimen K904952



Figure 94 Random Loading (50% Lifetime) Test: One-Fifth Scale Specimen K904953



Figure 95 Random Loading (50% Lifetime) Test: One-Fifth Scale Specimen K904954



Figure 96 Random Loading (50% Lifetime) Test:  
One-Fifth Scale Specimen K904956

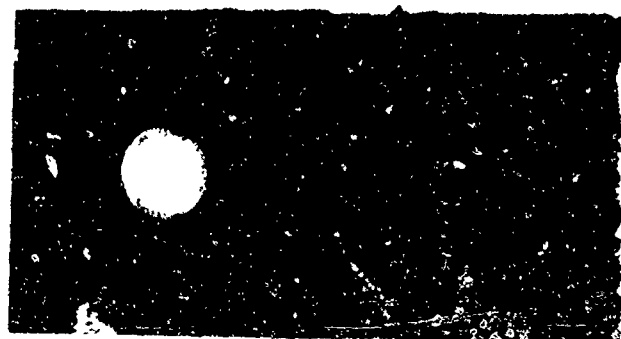
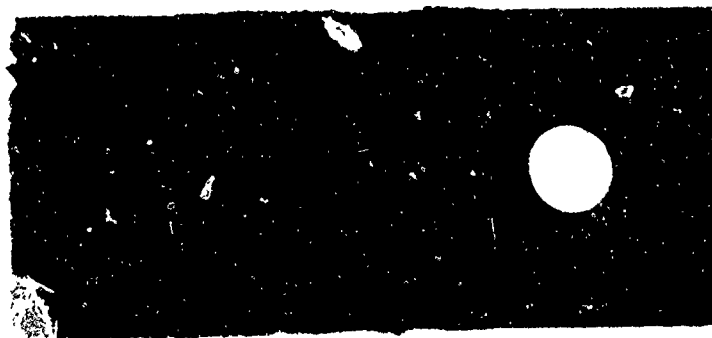


Figure 97 Random Loading (50% Lifetime) Test:  
One-Fifth Scale Specimen K905015





Figure 98 Random Loading (50% Lifetime) Test:  
One-Fifth Scale Specimen K905018



Figure 99 Random Loading (50% Lifetime) Test:  
One-Fifth Scale Specimen K905022



Figure 100 Random Loading (50% Lifetime) Test:  
One-Fifth Scale Specimen K905023



Figure 101 Fatigue-to-Failure Tests: One-Fifth Scale  
Specimen K012443

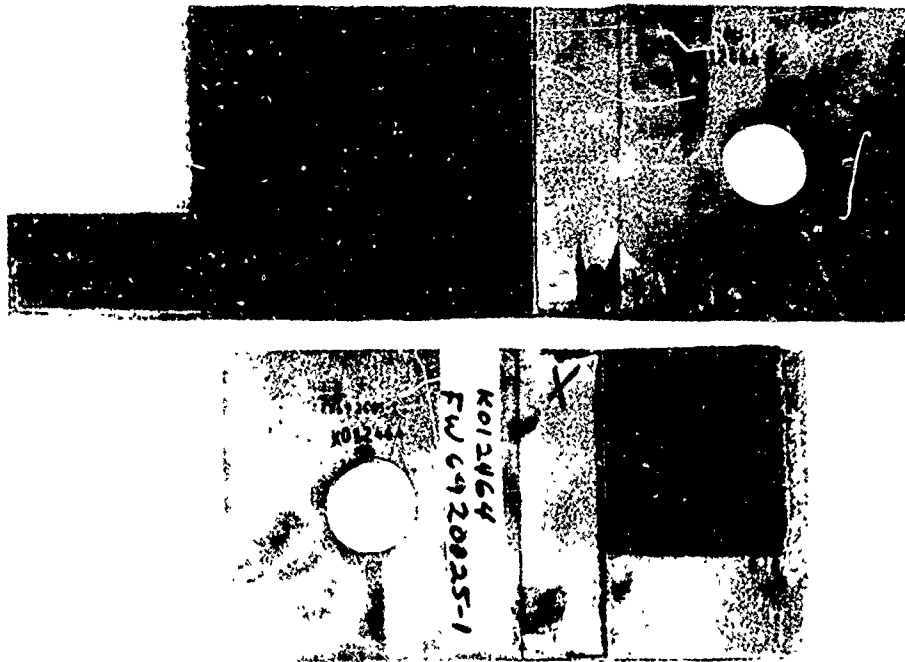


Figure 102 Fatigue-to-Failure Tests: One-Fifth Scale  
Specimen K012464



Figure 103 Fatigue-to-Failure Tests: One-Fifth Scale  
Specimen K012479



Figure 104 Fatigue-to-Failure Tests: One-Fifth Scale  
Specimen K012480



Figure 105 Fatigue-to-Failure Tests: One-Fifth Scale  
Specimen K012481



Figure 106 Fatigue-to-Failure Tests: One-Fifth Scale Specimen K012484

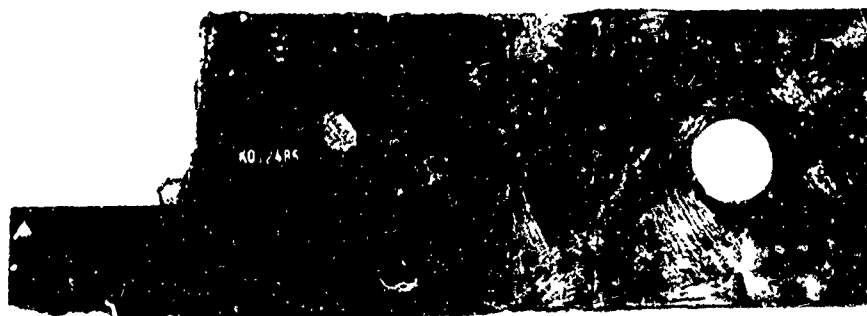


Figure 107 Fatigue-to-Failure Tests: One-Fifth Scale Specimen K012485

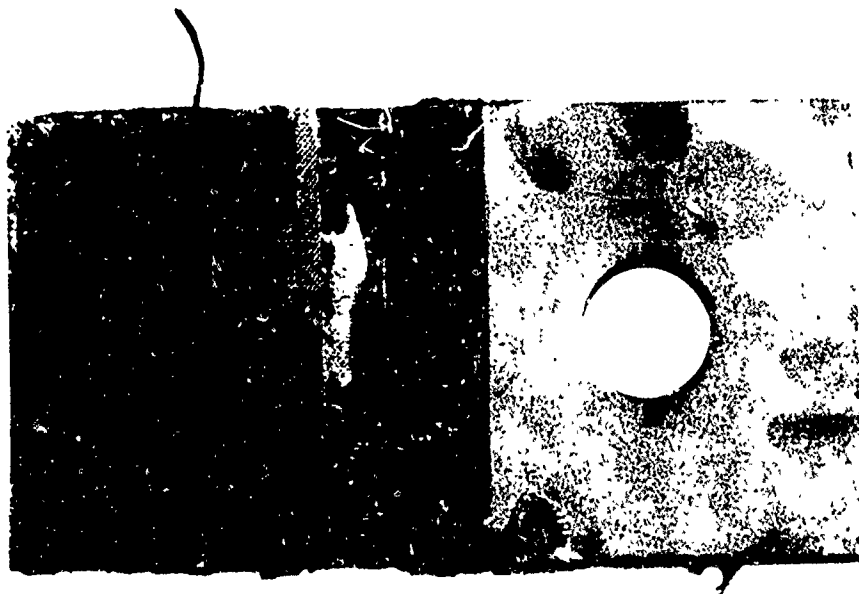
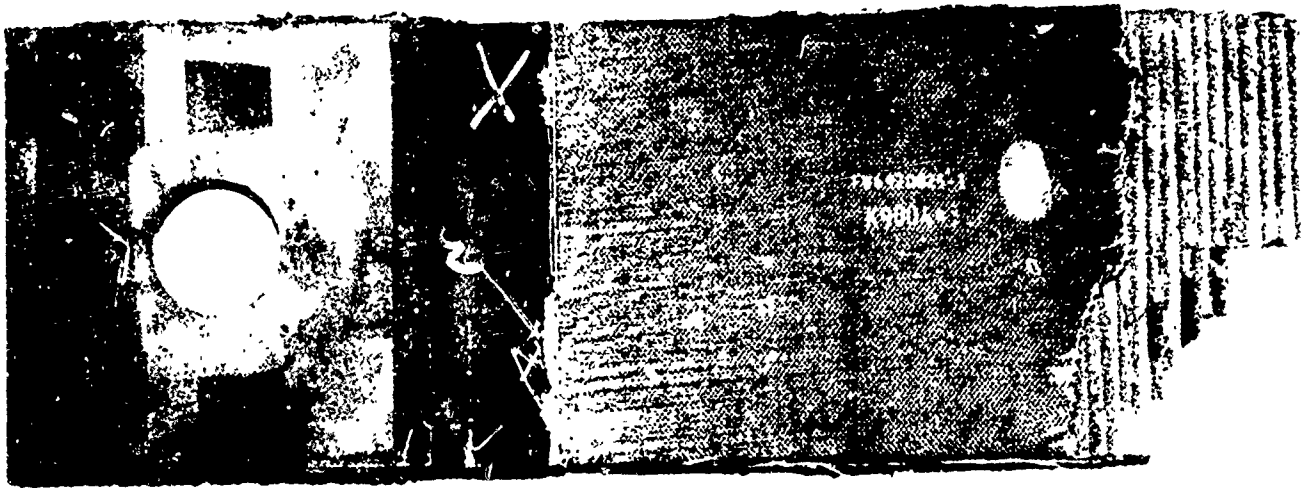


Figure 108 Fatigue-to-Failure Tests: One-Fifth Scale  
Specimen K900443

A P P E N D I X    V  
P H O T O G R A P H S    O F    1 / 2 - S C A L E  
S P E C I M E N    F A I L U R E S

Photographs of 1/2-scale specimens are given in this section for the 10% lifetime tests and the fatigue-to-failure tests. Failure modes are discussed in subsection 6.7.



Figure 109 Random Loading (10% Lifetime) Test: Group of One-Half Scale Specimens (Front Side)

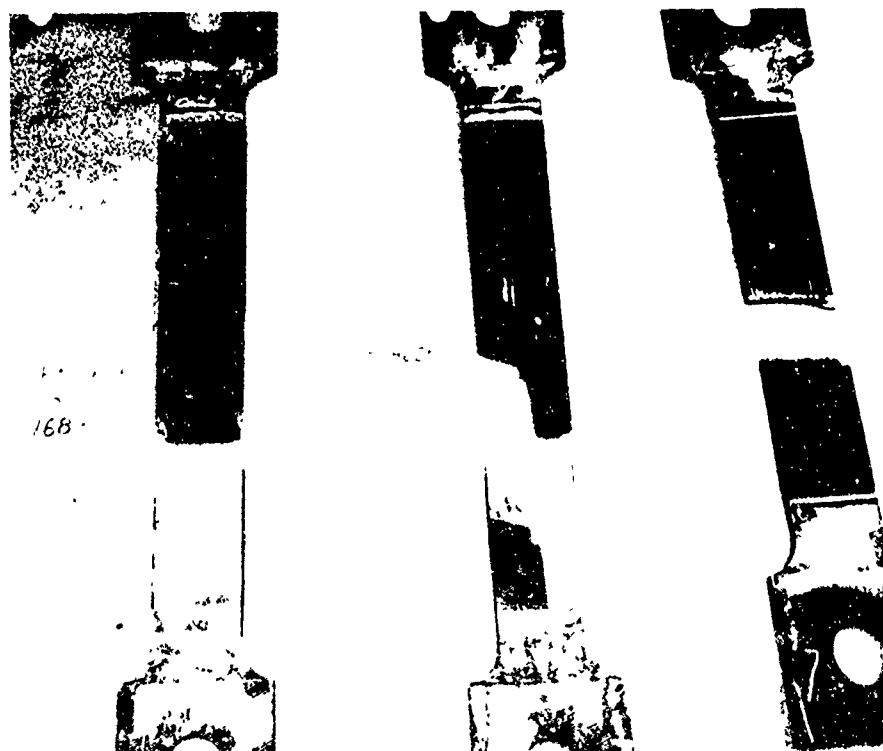


Figure 110 Random Loading (10% Lifetime) Test: Group of One-Half Scale Specimens (Back Side)



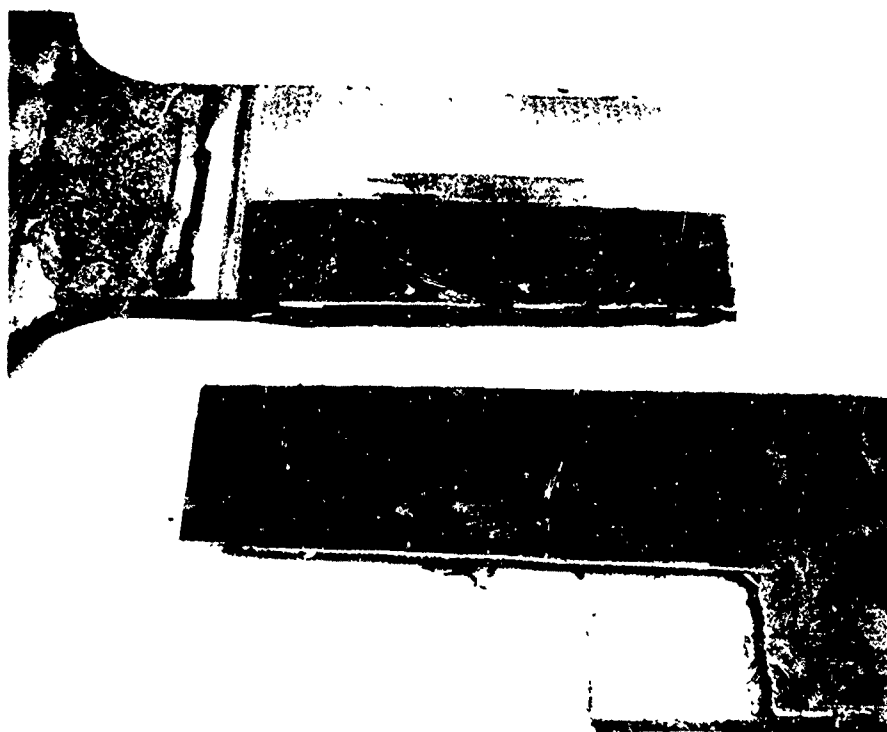


Figure 111 Fatigue-to-Failure Test: One-Half Scale  
Specimen F504619 (Front Side)

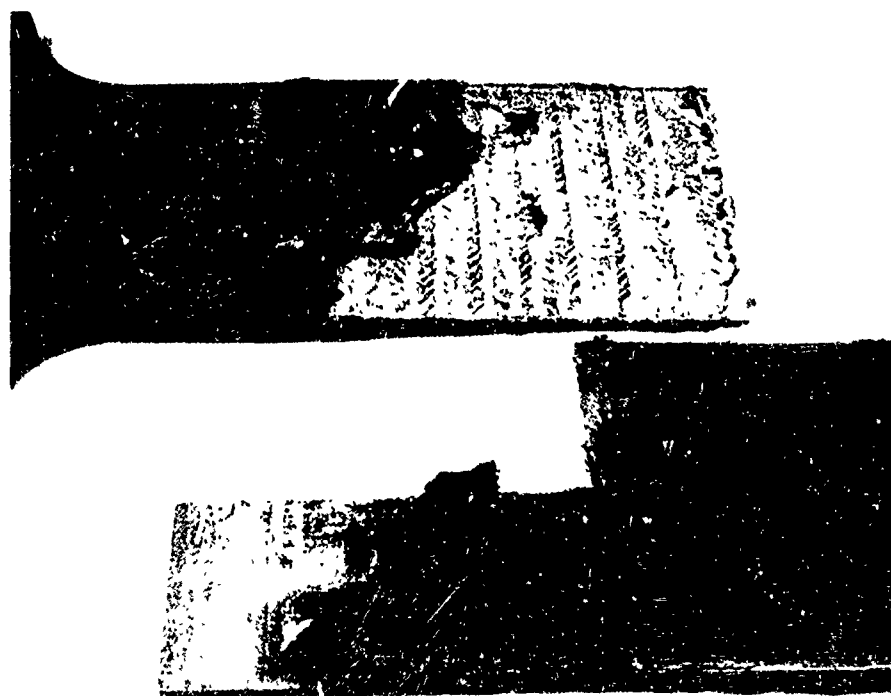


Figure 112 Fatigue-to-Failure Test: One-Half Scale  
Specimen F504619 (Back Side)



Figure 113 Fatigue-to-Failure Test: One-Half Scale Specimen F504621 (Front Side)



Figure 114 Fatigue-to-Failure Test: One-Half Scale Specimen F504621 (Back Side)

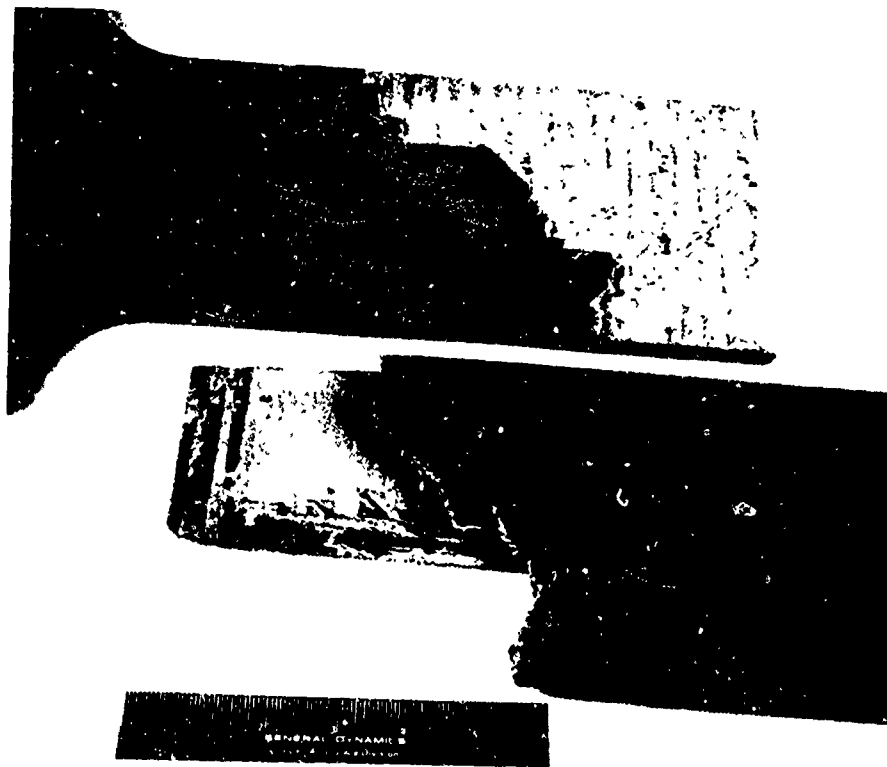


Figure 115 Fatigue-to-Failure Test: One-Half Scale Specimen F504622 (Front Side)

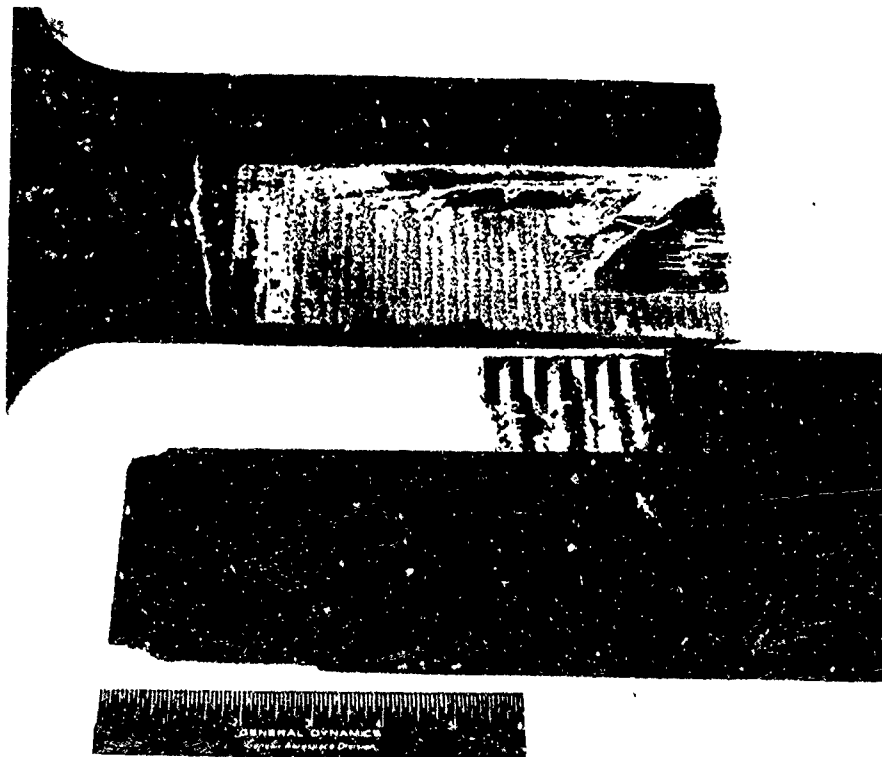


Figure 116 Fatigue-to-Failure Test: One-Half Scale Specimen F504622 (Back Side)

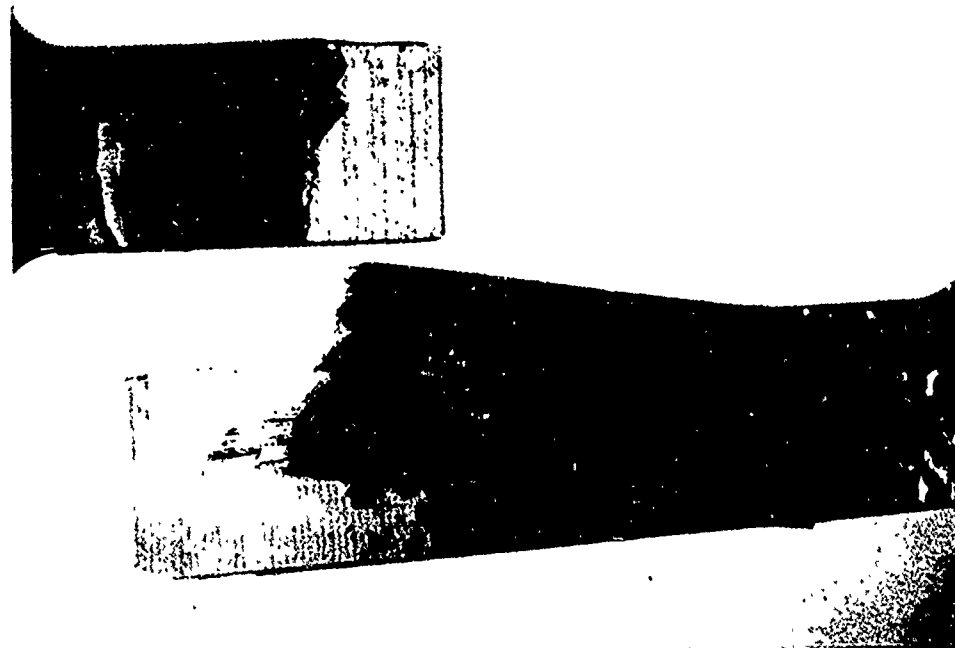


Figure 117 Fatigue-to-Failure Test: One-Half Scale  
Specimen F504623 (Front Side)

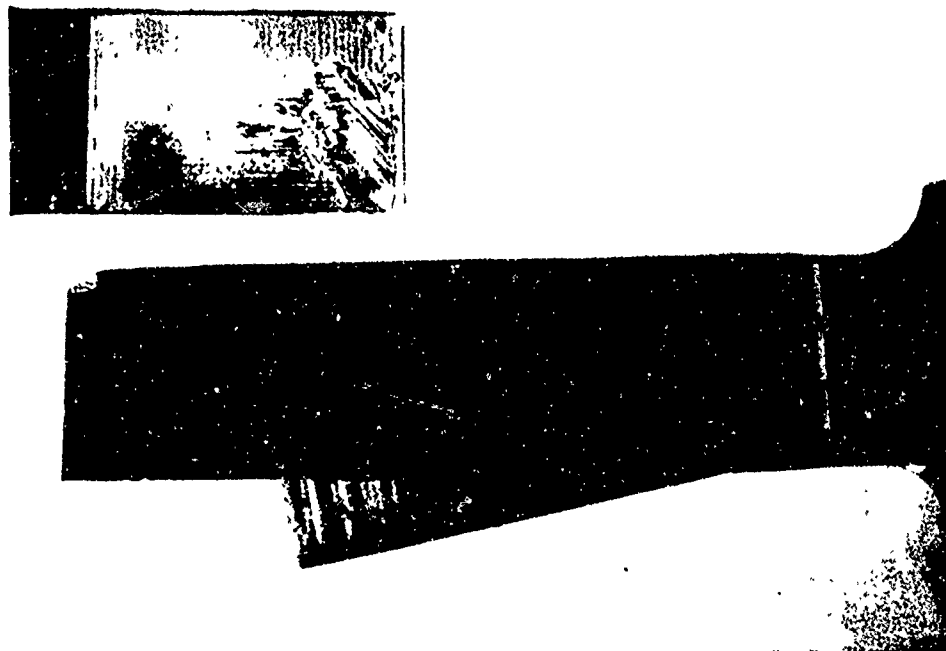


Figure 118 Fatigue-to-Failure Test: One-Half Scale  
Specimen F504623 (Back Side)

# A P P E N D I X   V I S T A T I S T I C A L   P R O P E R T I E S   O F T H E   W E I B U L L   D I S T R I B U T I O N

The Weibull cumulative probability distribution function is represented mathematically as follows.

$$F(t|a,b) = 1 - \exp\left(-\left(\frac{t}{b}\right)^a\right), \quad (44)$$

where  $a$  and  $b$  are parameters greater than zero to be determined from test data, and where  $t$  is the random variable involved, e.g., time to failure, cycles to failure. The Weibull probability density function is obtained by differentiating Equation (44)

$$f(t|a,b) = \frac{a}{b} \left(\frac{t}{b}\right)^{a-1} \exp\left(-\left(\frac{t}{b}\right)^a\right). \quad (45)$$

This function is plotted in Figures 119 and 120 for various values of  $a$  and  $b$ . The failure rate function defined by

$$R(t|a,b) = \frac{f(t|a,b)}{1 - F(t|a,b)} \quad (46)$$

becomes

$$R(t|a,b) = \frac{a}{b} \left(\frac{t}{b}\right)^{a-1}. \quad (47)$$

This function increases with time for most fatigue situations since in these situations the parameter  $a$  is greater than one. Equation (47) is plotted in Figure 121 for various values of the shape parameter  $a$ .

The  $k$ -th moment of the distribution is given by

$$E(t^k) = b^k \Gamma\left(\frac{k}{a} + 1\right). \quad (48)$$

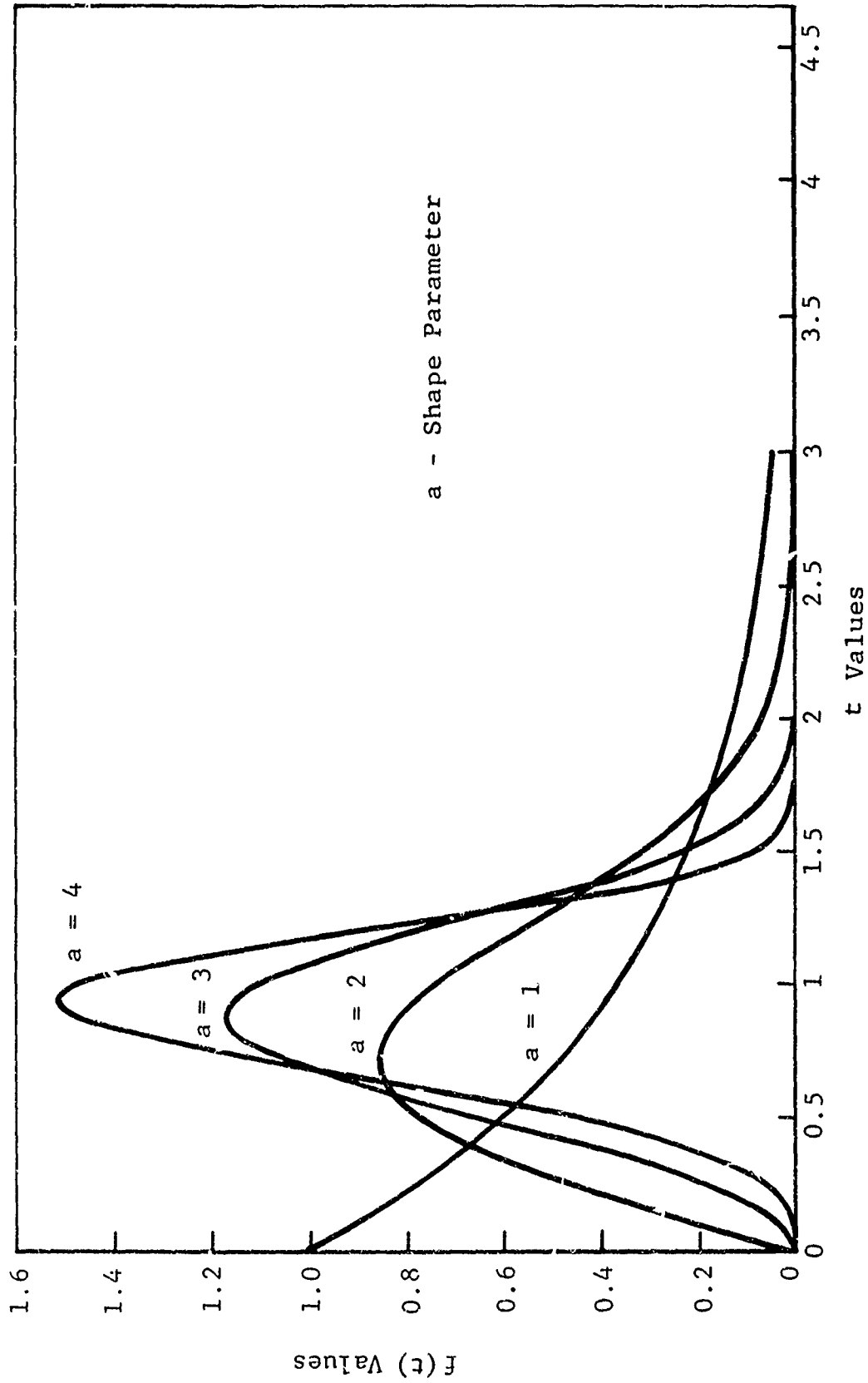


Figure 119 Weibull Density Function - Scale Parameter Fixed  $\eta = 1$  to One

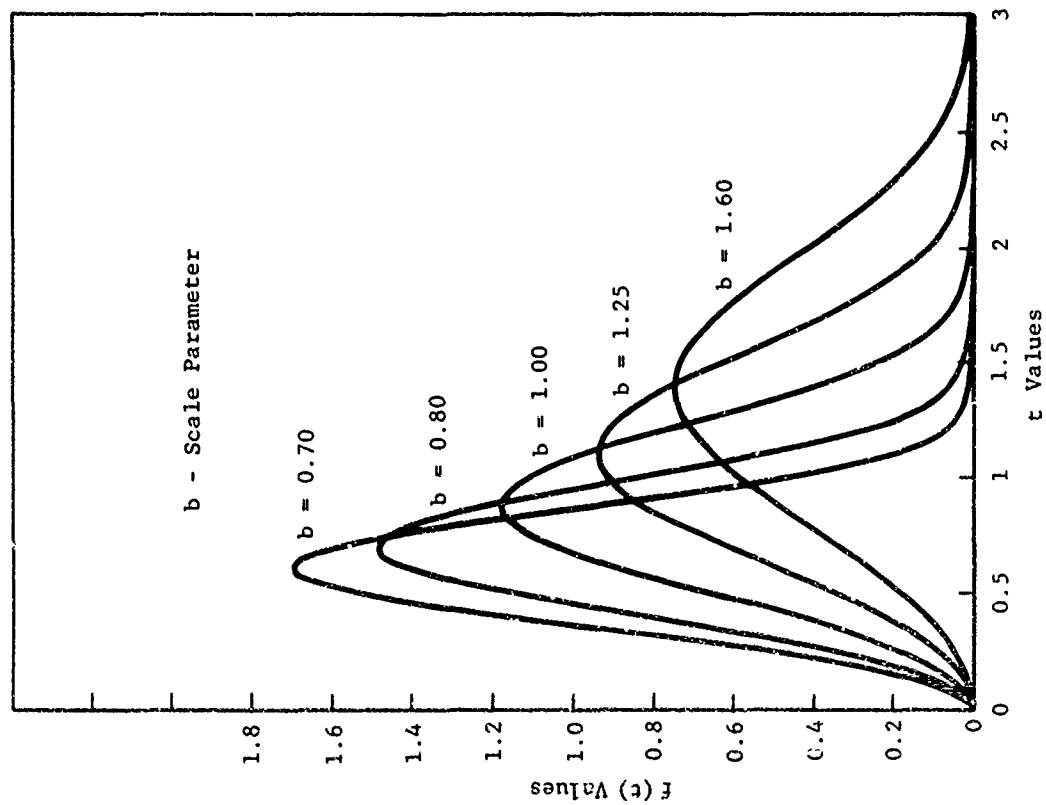


Figure 120 Weibull Density Function - Shape Parameter Fixed Equal to Three

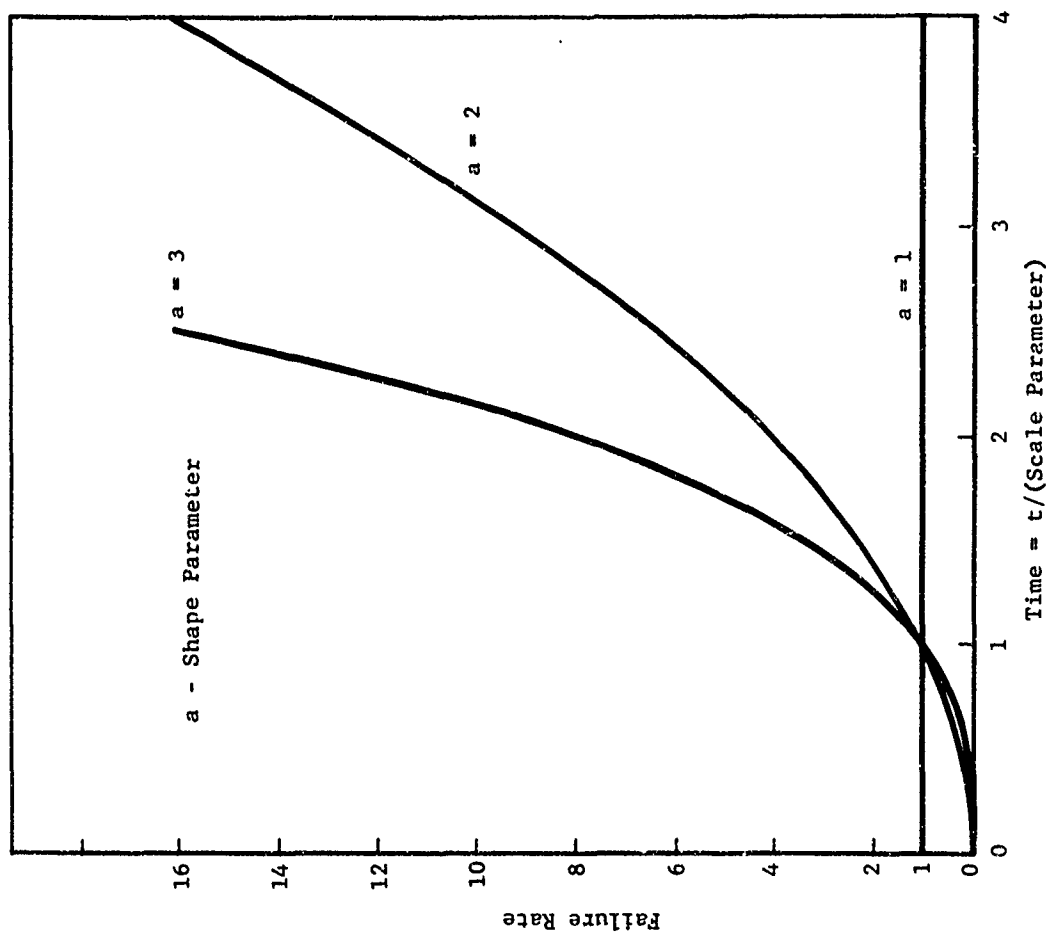


Figure 121 Weibull Failure Rate Function

where  $\Gamma$  is the standard gamma function. Thus, the mean and variance of the distribution are

$$E(t) = b \Gamma\left(\frac{1}{a} + 1\right), \quad (49)$$

and

$$\text{Var}(t) = b^2 \left[ \Gamma\left(\frac{2}{a} + 1\right) - \Gamma^2\left(\frac{1}{a} + 1\right) \right]. \quad (50)$$

In Equation 44 if  $t = b$  then  $F(t=b|a,b) = 1 - \exp(-1) = .632$ , which is constant regardless of the value of the parameter  $a$ . Thus  $t = b$  is called the characteristic value of the random variable. The parameter  $b$  determines the location of the distribution and the parameter  $a$  being inversely proportional to the variance of the random variable  $t$  (see Equation (50)) is called the shape parameter of the distribution. The Weibull distribution is positively skewed for values of the shape parameter  $a$  less than 3.57, and is negatively skewed for values of the shape parameter greater than 3.57.

A very useful parameter of the Weibull distribution is the coefficient of variation which is defined by

$$CV(t) = \frac{\sqrt{\text{Var}(t)}}{E(t)} \quad (51)$$

Thus using equations (49) and (50) equation (51) becomes

$$CV(a) = \frac{\left[ \Gamma\left(\frac{2}{a} + 1\right) - \Gamma^2\left(\frac{1}{a} + 1\right) \right]^{1/2}}{\Gamma\left(\frac{1}{a} + 1\right)} \quad (52)$$

The coefficient of variation is only a function of the shape parameter  $a$  and reflects relative variation independent of the underlying scale parameter of the distribution. A plot of Equation (52) is given in Figure 40.



## APPENDIX VII

### LEAST - OF - TWO STATISTICAL ANALYSIS

The test specimens used for this program had two nominally identical sides (Figures 5 and 6). Due to symmetry, one side of the specimen fails before the other side when fatigue tested. The service life of symmetric specimens may be thought of as the time to first failure of two nominally identical specimens or the time to failure is the least-of-two (Reference 54).

The service life distribution parameters may be determined by estimating the service life variability parameter from small element tests, and estimating the central location parameter of the service life distribution from full-scale fatigue tests. Thus the major part of least-of-two statistical analysis is being able to relate the distribution of the least-of-two variate and its parameters to the distribution of a single variate and its parameters.

A least-of-two statistical analysis is developed in the following paragraphs for the log-normal and Weibull distributions.

#### LOG-NORMAL LEAST-OF-TWO STATISTICAL ANALYSIS

Based on the fact that the logarithm of the number of cycles to failure for a single component is normally distributed, the probability distribution for the log life of a full scale symmetric component made up of two nominally identical halves is the least-of-two normal variates.

Let  $F(x|\mu, \sigma^2)$  and  $f(x|\mu, \sigma^2)$  denote the cumulative distribution and density function respectively for a normally distributed variable with mean  $\mu$  and variance  $\sigma^2$ . Then the logarithm of the least-of-two log-normal variables has the same distribution as the least-of-two normal variables which each have distribution  $F(x|\mu, \sigma^2)$ .

If  $y$  denotes the least-of-two normal variables, then the probability density,  $g(y|\mu, \sigma^2)$ , of  $y$  is given in terms of  $F(x|\mu, \sigma^2)$  and  $f(x|\mu, \sigma^2)$  by

$$g(y|\mu, \sigma^2) = 2f(y|\mu, \sigma^2) (1 - F(y|\mu, \sigma^2)) \quad (53)$$

and the cumulative distribution,  $G(y|\mu, \sigma^2)$ , of  $y$  is given by

$$\begin{aligned} G(y|\mu, \sigma^2) &= \int_{-\infty}^y g(y|\mu, \sigma^2) dy \\ &= 2F(y|\mu, \sigma^2) - F^2(y|\mu, \sigma^2) \end{aligned} \quad (54)$$

Equations (53) and (54) are easily derivable from the Theory of Order Statistics (see Reference 55).

The mean and variance of  $y$  are derived to be

$$E(y) = \mu - \frac{\sigma}{(\pi)^{1/2}} \quad (55)$$

$$\text{Var}(y) = \sigma^2 \left( \frac{\pi - 1}{\pi} \right) \quad (56)$$

Equations (55) and (56) allow estimates of the mean and variance of  $y$  to be transformed into estimates of the mean and variance of the single normal variable and vice versa.

With the properties derived here, standard statistical techniques can be applied to the least-of-two distribution for making inferences regarding service life characteristics of the least-of-two log-normally distributed variables.

#### WEIBULL LEAST-OF-TWO STATISTICAL ANALYSIS

In this section the Weibull distribution with the shape parameter  $a$  and scale parameter  $b$  is assumed to be the parent distribution. The cumulative distribution function in this case is given by

$$F(x|a, b) = 1 - \exp\left(-\left(\frac{x}{b}\right)^a\right) \quad (57)$$

The cumulative distribution,  $G(y|a, b)$ , of the least-of-two Weibull variates is given in terms of  $F(x|a, b)$  by

$$G(y|a, b) = 2F(y|a, b) - F^2(y|a, b) \quad (58)$$

Equation (58) is easily derivable using Theory of Order Statistics (see Reference 51). Equation (58) can be rewritten as

$$F(y|a,b) = F(y|a,b) (2 - F(y|a,b)) . \quad (59)$$

Then substituting Equation (57) into (59) and simplifying, the distribution of  $y$  becomes

$$G(y|a,b) = 1 - \exp(-2(\frac{y}{b})^a) , \quad (60)$$

which is a Weibull distribution with shape  $a$  and scale parameter  $b(2^{-\frac{1}{a}})$ . That is

$$G(y|a,b) = F(y|a,b(2^{-\frac{1}{a}})) . \quad (61)$$

Thus the only difference between the distribution of the least-of-two Weibull variables and a single Weibull variable is the scale parameter.

Statistical inference about the least-of-two Weibull variates can be based on existing statistical techniques for making inferences about the Weibull distribution.

## REFERENCES

1. Halpin, J. C., Private Communication to M. E. Waddoups, Convair Aerospace Division of General Dynamics, 1970.
2. Whittaker, I. C. and P. M. Besuner, "A Reliability Analysis Approach to Fatigue Life Variability of Aircraft Structures," Technical Report AFML-TR-69-65, April 1969.
3. Whittaker, I. C. and J. J. Gerharz, "A Feasibility Study for Verification of Fatigue Reliability Analysis," AFML-TR-70, to be published.
4. Freudenthal, A. M., "Reliability Analysis Based on Time to First Failure," Technical Report AFML-TR-67-149, May 1967.
5. Halpin, J. C., J. R. Kopf, and W. Goldberg, "Time Dependent Static Strength and Reliability for Composites," Journal of Composite Materials, Vol. 4, October 1970.
6. Breyan, William, "Effects of Block Size, Stress Level, and Loading Sequence on Fatigue Characteristics of Aluminum-Alloy Box Beams," ASTM STP 462, January 1970, p. 127.
7. Clevenson, Sherman A. and Roy Steiner, "Fatigue Life Under Various Random Loading Spectra," The Shock and Vibration Bulletin 35, Part 2, U. S. Naval Research Laboratory, Washington, D. C., January 1966, pp. 21-31.
8. Jacoby, G. H., "Comparison of Fatigue Lives Under Conventional Program Loading and Digital Random Loading," ASTM STP 462, January 1970, pp. 184-202.
9. Jacoby, G., "Fatigue Life Estimation Processes Under Conditions of Irregularly Varying Loads," AFML-TR-67-215, Wright-Patterson Air Force Base, August 1967.
10. Lowcock, M. T. and T. R. G. Williams, "Effect of Random Loading on the Fatigue Life of Aluminum Alloy L. 73," A. A. S. U. Report No. 225, University of Southampton, Hampshire, England, July 1962.

11. Naumann, E. C., "Evaluation of the Influence of Load Randomization and of Ground-Air-Ground Cycles on Fatigue Life," NASA TN D-1584, Langley Research Center, Langley Station, Hampton, Virginia, October 1964.
12. Schijve, J. et al., "Fatigue Tests with Random and Programmed Load Sequences, With and Without Ground-to-Air Cycles: A Comparative Study on Full-Scale Wing Center Section," Technical Report AFFDL-TR-66-143, Wright-Patterson Air Force Base, 1966.
13. Osgood, Carl C., Fatigue Design. New York: Wiley-Interscience, A Division of John Wiley & Sons, Inc., 1970.
14. Swanson, S. R., "Load Fatigue Testing: State of the Art Survey," Materials Research and Standards, April 1968, page 15.
15. Plunkett, R., and N. Viswanathan, "Fatigue-Crack-Propagation Rates Under Random Excitation," Transactions of ASME, Journal of Basic Engineering, March 1967, pp. 55-68.
16. Wheeler, O. E., "Crack Growth Under Spectrum Loading," General Dynamics Report FZM-5602, 30 June 1970.
17. Manning, S. D. "Parametric Study for Correlating the Predicted Crack Growth Rate in D6ac Steel Under Spectrum Loading With Test Results," MRS-70-006, General Dynamics Report MRS-70-006, 20 August 1970.
18. Boller, K. H., "Effect of Single Stress Change in Stress on Fatigue Life of Plastic Laminates Reinforced with Unwoven "E" Glass Fibers," Technical Report No. AFML-TR-66-202, December 1966.
19. Hofer, K. E. and E. M. Olsen, "An Investigation of the Fatigue and Creep Properties of Glass Reinforced Plastics for Primary Aircraft Structures," IIT Research Institute, Chicago, Illinois, AD-652415, April 1967.
20. Broutman, L. J. and S. Sahu, "A New Theory to Predict Cumulative Fatigue Damage in Fiber Reinforced Plastics," Paper Presented at the Second SSTM Conference on Composite Materials: Testing and Design, April 20-22, 1971, Anaheim, California.

21. Shockey, P. D., J. D. Anderson, and K. E. Hofer, "Structural Airframe Application of Advanced Composite Materials, Volume V, Mechanical Properties - Fatigue," AFML-TR-69-101, March 1970.
22. Shockey, P. D., and K. E. Hofer, "Development of Engineering Data for Advanced Composite Materials, Volume II, Fatigue and Load Rate Characteristics," (to be published).
23. Advanced Composites Design Guide, Volume 1, Design, Third Edition, November 1971.
24. McKague, E. L., and R. J. Stout, "Some Physical, Environmental, and Mechanical Properties of Graphite-Epoxy Composites," General Dynamics Report SMD-047, April 1970.
25. McKague, E. L., "Graphite-Epoxy Composite Constant Amplitude Fatigue Study," General Dynamics Report SMD-048, April 1969.
26. Paul, E. R. and S. D. Manning, "Instructions to Customer, IBM 360, Procedure BY4 (Random Load Generation Program)," Convair Aerospace Division of General Dynamics, 8 July 1971.
27. Leonhardt, J. L., P. D. Shockey, and V. J. Studer, "Advanced Development of Boron Composite Wing Structural Components," Technical Report AFML-TR-70-261, December 1970.
28. Composite Handbook, General Dynamics Report FZM-12-13016, 24 March 1970.
29. Press, H., M. T. Meadows, and I. Hadlock, "A Reevaluation of Data on Atmospheric Turbulence and Airplane Gust Loads for Application in Spectral Calculations," NACA Report 1272, 1956.
30. Celata, R. T., et al., F-111 A/E/D, "Mission Analysis to Determine Maneuver Load Factor Exceedence Spectra," General Dynamics Report FZM-12-10783, 27 June 1969, Contract AF33(657)-13403.
31. Thompson, O. N., Private Communication to S. D. Manning, Convair Aerospace Division of General Dynamics, April 1971.

32. Mood, A. M. and F. A. Grayhill, Introduction to Theory of Statistics, Second Edition, McGraw-Hill, New York 1963.
33. Kaminski, B. E., G. H. Lemon, and E. L. McKague, Development of Engineering Data For Advanced Composite Materials, Volume I, "Static and Thermophysical Properties," AFML-TR-70-108, Vol. 1, October 1972.
34. Halpin, J. C. and M. E. Waddoups, "Fatigue and Fracture of Composite Structures," Presented at National Symposium at George Washington University, 28 March 1972 (to be published).
35. Rivlin, R. S., and A. G. Thomas, "Rupture of Rubber, I. Characteristic Energy for Tearing," Journal of Polymer Science, Vol. X., No. 3, 1952.
36. Irwin, G. R., "Fracture Dynamics Fracturing of Metals," ASM, Cleveland, 1948.
37. Weibull, W., "A Statistical Representation of Fatigue Failure in Solids," Transactions of the Royal Institute of Technology, Stockholm, No. 27, 1949.
38. Fletcher, R. and M. J. P. Powell, "A Rapidly Convergent Descent Method for Minimization," Computer Journal (British), Vol. 6, pp. 163-168, 1963.
39. Paris, P. D. and F. Erdogan, "A Critical Analysis of Crack Propagation Laws," Transactions of the ASME, Volume 85, December 1963.
40. Averback, B. L., et al. (Editors), Fracture, New York: John Wiley and Sons, Inc., 1959, pp. 337-353.
41. Jaroslav, Nemec, Rigidity and Strength of Steel Parts, Prague: Publishing House of the Czechoslovak Academy of Sciences, 1966, pp. 768, 785, and 800.
42. Mann, J. Y., Fatigue of Materials, Melbourne: Melbourne University Press, 1967, pp. 126-127.
43. Fatigue Design Handbook, Vol. 4, New York: Society of Automotive Engineers, Inc., 1968, pp. 28, 29, and 90.

44. Thoman, D. R., L. J. Bain, and C. E. Amtel, "Influences on the Parameters of the Weibull Distribution," *Technometrics*, Vol. 11, No. 3, August 1969, pp. 445-460.
45. Clevenston, S. A. and R. Steiner, "Fatigue Life Under Various Random Loading Spectra," Proceedings of the 35th Symposium on Shock and Vibration, Volume 85, December 1963.
46. Rice, S. O., "Mathematical Analysis of Random Noise," Parts I and II, Bell System Technical Journal, Volume XXIII No. 3, July 1944, and Parts III and IV, Volume XXIV No. 1, January 1945.
47. Cetala, R. T., et al., F-111A/E/D, "Mission Analysis to Determine Maneuver Load Factor Exceedance Spectra," General Dynamics Report FZM-12-10783, 27 June 1969, Contract AF33(657)-13403.
48. Bendat, Julius S., "Probability Functions for Random Responses: Prediction of Peaks, Fatigue Damage, and Catastrophic Failures," NASA CR-33, April 1964.
49. Kowalewski, J., "Veber die Beziehung der Lebensdauer von Bauteilen bei Unregel Maessig Schwankenden und Geordnetan Belastungsfolgen," DVL-Bericht 249 Deutsche Versuchsanstalt für Luft und Raumfahrt, Porz-Wahn, 1963.
50. Hillberry, B. M., "Fatigue Life of 2024-T3 Aluminum Alloy Under Narrow and Broad-Band Random Loading," ASTM STP 462, January 1970, pp. 167-182.
51. McMaster, M. V., "Random Number Subroutine," CF 608, Convair Aerospace Division of General Dynamics, 30 June 1968.
52. Bendat, Julius S. and Allan G. Piersol, Measurement and Analysis of Random Data, New York: John Wiley & Sons, Inc, 1966.
53. Bendat, Julius S., "Probability Functions for Random Responses: Prediction of Peak, Fatigue Damage, and Catastrophic Failures," NASA CR-33, April 1964, p. 39.
54. Lemon, G. H., "Service Life Distribution Characteristics of Structural Components," General Dynamics Report ERR-FW-1056, December 1970.



55. Lemon, G. H., "Service Life Distribution Characteristics of Structural Components," General Dynamics Report ERR-FW-1056, December 1970.